VISCOUS FLOW THROUGH SUDDEN CONTRACTIONS

By

VERUSCHA PIENAAR
NH Dipl (Chem Eng), MTech (Chem Eng) (Cape Technikon)

Dissertation submitted in fulfilment of the degree
DOCTOR TECHNOLOGIAE
in the Faculty of Engineering
Cape Technikon

February 2004

VISCOUS FLOW THROUGH SUDDEN CONTRACTIONS

Veruscha Pienaar

Flow Process Research Centre, Cape Technikon,
PO Box 652, Cape Town, 8000, South Africa.
February, 2004.

ABSTRACT

Despite efforts since the 1950s, laminar flow through pipe fittings is still a topic that needs investigation (Jacobs, 1993). Most experimental studies on this topic include fittings such as contractions, expansions, elbows, valves and orifices (Edwards *et al.*, 1985; Turian *et al.*, 1998; Pal & Hwang, 1999). Although sudden contractions are not often found in industry, most researchers included these fittings as part of their experimental investigation.

The volume of work done on flow through sudden contractions over the last 50 years (e.g. Bogue, 1959; Christian *et al.*, 1972; Vrentas & Duda, 1973; Boger, 1987; Bullen *et al.*, 1996; Sisavath *et al.*, 2002), establishes its place of importance in the fundamental understanding of fluid flow and fluid mechanics.

There are inconsistent reports on the status of the study of Newtonian fluids flowing through sudden contractions, i.e., that "it is a solved problem" (Boger, 1987) and "that it is far from being resolved" (Sisavath *et al.*, 2002). One reason for this apparent contradiction is the fact that most experimental studies do not agree with one another or with analytical and numerical studies. A state-of-the-art literature review by Pienaar *et al.* (2001) confirmed this and that further investigation of this topic is required.

To explore these contradictions, it was necessary for one study to do both an experimental and numerical investigation and compare the results with existing literature. It was also important to find some basis for agreement of experimental work and not just add another data set to the existing scattered database.

A test facility was built for testing three contraction ratios, i.e., $\beta = 0.22$, 0.50 and 0.85. A range of Newtonian and non-Newtonian fluids was tested over a wide range of Reynolds number ($Re = 0.01 - 100\,000$).

A numerical study of this problem was performed using the general-purpose, commercially available software, CFX. Good agreement was found with similar studies in literature, but not with the experimental results in terms of overall pressure drop. However, this work was very useful in determining the detail of the flow phenomena required for the conical approximation developed in this work.

It was demonstrated how different results could be obtained by evaluating the two methods used in literature i.e., the extrapolation of the pressure grade line to the contraction plane and the total pressure drop approach. These methods both involved the application of Bernoulli (energy balance equation), but it was further

shown that different results could be obtained, depending on the friction loss calculation method used and the length of straight pipe included in the total pressure drop. In the pressure grade line method, it was demonstrated that the selection of points used for determining the fully developed friction gradient had an effect on the results obtained. It is argued that these different approaches can explain the discrepancies found in the literature and that a sound basis for further experimental investigation has been provided.

An approximation was also obtained for the pressure drop in the contraction based on the flow phenomena upstream of the sudden contraction plane, assuming a conical boundary. Excellent agreement was obtained between this model and the semi-empirical model of McNeil and Morris (1995) for contraction ratio $\beta = 0.22$. It was demonstrated that there is potential for the extrapolation of this model to larger contraction ratios.

In conclusion, a sudden pipe contraction – arguably geometrically the simplest pipe fitting – has been used to establish and validate a protocol for the experimental method and analysis of results for the determination of fitting losses in laminar flow. The main contribution of this work is in the experimental method, analysis of results, modelling of flow through sudden contractions and actual values for C_{con} for three contraction ratios.

DECLARATION

I, Veruscha Pienaar, hereby declare that the contents of this dissertation/thesis represent my own unaided work, and that the dissertation/thesis has not previously been submitted for academic examination towards any qualification. Furthermore, it represents my own opinions and not necessarily those of the Cape Technikon.

Veruscha Pienaar

February 2004

DEDICATION

To my dad Johnny, my mom Shirley and my brothers Zachery, Ashwin and Ormund.

To my great grandmother Catherine Van Turha, who lived her life gracefully and in thankfulness for 94 years.

"For wisdom will enter your heart, and knowledge will be pleasant to your soul, discretion will protect you and understanding will guard you"

Proverbs 2:10-11

ACKNOWLEDGEMENTS

I wish to thank:

- My supervisor, Prof. Paul Slatter, for his guidance, encouragement and tremendous support not only with my studies but also in my personal development.
- My family, friends and colleagues who have been so supportive over the many years of studies.
- Prof Liz van Aswegen for linguistic revision and Marion Davids for Internet and library assistance.
- All the students in the slurry and rheology laboratories who assisted with test work.
- The Council of the Cape Technikon and the National Research Foundation for financial assistance towards this research. Opinions expressed in this dissertation and the conclusions arrived at, are those of the author and are not necessarily to be attributed to the Cape Technikon or the National Research Foundation.

TABLE OF CONTENTS

LIST OF FIGURES

LIST OF TABLES

REFERENCES

APPENDICES

NOMENCLATURE

Symbol	Description	Unit
A	cross sectional area	m^2
C_{con}	laminar flow loss coefficient constant	-
C_v	solids volumetric concentration	%
C_w	solids concentration by weight	%
c_{et}	kinetic energy correction at the throat	-
c_{mt}	momentum correction at the throat	-
d	particle diameter	m
D	internal pipe diameter	m
E	sum of mean error squared	
F	force	N
f	Fanning friction factor	
G_N	geometry factor	
g	gravitational acceleration	m/s^2
H	head	m
K	fluid consistency index	$Pa.s^n$
K'	apparent fluid consistency index	$Pa.s^{n'}$
k	hydraulic roughness	m
L	pipe length	m
L_e	entry length after contraction plane	m
L_{ex}	new exit length prior to contraction plane	m
L_v	Boger exit length prior to contraction plane	m
M	mass	kg
m	slope	-
N	number of data points	-
n	flow behaviour index	-
n'	apparent flow behaviour index	-
p	pressure	Pa
p_s	static pressure	Pa

Q	volumetric flow rate	m^3/s
R	radius	m
Re	Reynolds number	-
Re_{crit}	critical Reynolds number at onset of transition	-
Re_{MR}	Metzner&Reed Reynolds number (Power law)	-
Re_3	Slatter Reynolds number (Yield pseudoplastic)	-
Re_r	roughness Reynolds number	-
r	correlation coefficient	-
r	radius from the centerline of the pipe	m
t	time	s
u	point velocity	m/s
V	average velocity	m/s
z	elevation from datum	m
α	kinetic energy correction factor	-
α_t	core-area fraction at throat	-
β	contraction ratio, D_d/D_u	-
$\dot{\gamma}$	shear rate	s^{-1}
δ	viscous sub-layer thickness	m
Δ	increment	
λ_t	throat friction-factor coefficient	-
μ	dynamic viscosity	Pa.s
ρ	fluid or slurry density	$kg.m^{-3}$
ρ_w	density of water	$kg.m^{-3}$
τ	shear stress	Pa
τ_o	wall shear stress	Pa
τ_y	yield stress	Pa
ϕ	shape function for conical approximation	-

Subscripts

85	85^{th} percentile of particles passing
0	at the wall of the pipe
3	reference to Slatter Reynolds number
ann	annulus
con	contraction
crit	critical
calc	calculated
d	downstream
fitt	fitting
l	loss
m	mixture (slurry)
obs	observed (experimental)
r	roughness
s	solids
u	upstream
v	volumetric
w	water

CHAPTER 1

CHAPTER 1
INTRODUCTION

1.1 INTRODUCTION

Although efforts have been made since the 1950s, laminar flow through pipe fittings is still a topic that needs investigation (Jacobs, 1993). Most experimental studies on this topic included fittings such as contractions, expansions, elbows, valves and orifices (Edwards *et al.*, 1985; Turian *et al.*, 1998; Pal & Hwang, 1999). Although sudden contractions are not often found in industry, most researchers included these fittings as part of their experimental investigation. McNeil and Morris (1995) *investigated flow through sudden contractions and expansions because* understanding flow behaviour through these geometrically simple fittings could enhance the understanding of flow through more complex fittings such as valves, which are a combination of contracting and expanding flows.

Judging from the volume of work done on flow through sudden contractions over the last 50 years (e.g. Bogue, 1959; Christian *et al.*, 1972; Vrentas & Duda, 1973; Boger, 1987; Bullen *et al.*, 1996; Sisavath *et al.*, 2002), it must definitely have a place of importance in the fundamental understanding of fluid flow and fluid mechanics. Much of the early work was done to understand entry flow phenomena, concentrating on downstream flow phenomena and turbulent flow (Boger & Ramamurthy, 1970; Bullen *et al.*, 1987; White *et al.*, 1987).

In 1987 Boger stated that laminar flow of Newtonian fluids through sudden contractions "is a solved problem". Sisavath *et al.* (2002) indicated that several studies were done on laminar flow of non-Newtonian fluids through sudden contractions, but that less was done on Newtonian fluids. He stated that the determination of additional pressure drop for laminar flow of Newtonian fluids through sudden contractions "is far from being resolved". The reason for this apparent contradiction was the fact that most experimental studies did not agree with one another or with analytical and numerical studies. A state-of-the-art literature review by Pienaar *et al.* (2001) confirmed this yet again and therefore further investigation of this topic is required.

To investigate these contradictions, it is necessary for one project to do both an experimental and numerical study and compare it to existing literature. Not only that, but also to find agreement of results and not just add another data set to the existing scattered database.

Contractions are geometrically simple, eliminating the debate of whether the physical length of the fitting should be included or excluded in the analysis. If some agreement could be found between this study and others, either experimental, numerical or analytical, it would lay the foundation for investigating additional losses for flow through various other industrial fittings, ensuring that the same repeatable procedure will be followed by researchers who wish to make a contribution to creating a database of loss coefficient data, especially for viscous laminar flow where the discrepancies are most obvious. Until these discrepancies

have been resolved, it is meaningless to generate any more data. Agreement between a CFD study and an experimental study would be especially useful because doing these studies on CFD will save both time and money, but CFD is only as good as the set of experimental results that it is compared to, if such experimental results exist.

This study was therefore carried out on sudden contractions to:

- investigate the possible reasons for variations in experimental results obtained by various experimental researchers;
- find out why analytical and numerical studies and experimental studies did not yield the same results; and
- to provide definitive data for design purposes.

1.2 STATEMENT OF THE PROBLEM

There are no reliable experimentally determined loss coefficient data available for predicting additional losses through sudden contractions that agree with theoretical predictions or other experimental studies, especially for laminar flow.

1.3 OBJECTIVES

The objectives of this thesis are to:

1. Experimentally determine loss coefficient data for 3 contraction ratios between 0.1 and 0.9.

2. Evaluate the reason why different results may be obtained by scrutinising the existing experimental procedure and analysis of experimental results.
3. Use commercially available CFD software to investigate the flow through sudden contractions concurrently with the experimental investigation.
4. To develop a more reliable model to predict losses through sudden contractions based on the macro (experimental investigations) and micro (from CFD investigation) energy views.

The emphasis in these objectives will be in the low Reynolds number laminar flow region, i.e., $0.01 < Re < 100$, since $Re = 100$ is often indicated in the literature as the starting point of laminar flow breakdown or where the data starts to deviate from the laminar flow line.

1.4 METHODOLOGY

The methodology used to investigate this problem will be as follows:

- Building a test loop facility with 3 contractions ranging between 0.1 and 0.9.
- Test rheologically different fluids both in straight pipes (to determine rheological parameters) and in contractions (to determine loss coefficient data).
- The results will be analysed using the energy balance (Bernoulli) equation to calculate the losses in the fitting. These will be correlated to the appropriate Reynolds number in laminar flow to determine the loss coefficient constants (C_{con}) for contraction ratios between 0.1 and 0.9.

- The results will be evaluated to determine the effect of rheology on fitting losses, the role of the Reynolds number, the micro and macro energy view and models to predict fitting losses.
- Results from experiments and CFD will be used to develop a model for the prediction of these fitting losses that will be acceptable and will agree with other numerical or experimental studies.

1.5 SCOPE

This work will evaluate losses in sudden contractions using Newtonian and time independent homogeneous non-Newtonian fluids, with the emphasis on laminar flow. However, experimental work will include laminar, transitional and turbulent flow for completeness of the study.

1.6 IMPORTANCE AND BENEFITS

This study will not only derive a method for predicting losses through sudden contractions, but also emphasise what may be going wrong in the experimental investigations and in the analyses of results, which have lead to the discrepancies experienced at present. These analogies can then be extrapolated to investigating other fittings (e.g. valves, bends, etc.) reliably.

CHAPTER 2

CHAPTER 2
THEORY AND LITERATURE REVIEW

2.1 INTRODUCTION

This chapter provides a review of the literature on pressure losses through pipe fittings, with the emphasis on flow through sudden contractions. It will review the literature and theory that is relevant to the understanding of the losses that occur as a fluid passes through a sudden contraction.

The flow phenomena will be described for both laminar and turbulent flow. The techniques for determining loss coefficient data will be reviewed. The analysis of results will include straight pipe flow, and friction factors used will be described for both Newtonian and non-Newtonian fluids. Loss coefficient data is generally correlated to the Reynolds number; therefore the various Reynolds numbers used for Newtonian and non-Newtonian fluids will be discussed. The fundamental theory reviewed will therefore include flow through straight pipes, laminar and turbulent flow, head losses due to friction, total head and pressure losses and minor losses in piping systems.

Since this work will review both Newtonian and non-Newtonian fluids, the fundamental theory and the application of viscometry and rheology will be reviewed. The investigation of contractions has been of a theoretical and experimental nature. Both the theoretical and experimental studies will be reviewed.

This chapter will conclude with the research topics identified based on the literature reviewed as well as a presentation of the expected outcomes of this study. This present study will focus on obtaining reliable experimental results that can be compared with various theoretical models and experimental results found in literature.

2.2 FLOW IN STRAIGHT PIPES

The determination of the frictional pressure drop in straight pipes is very important in the analysis of losses due to sudden contractions since a contraction is essentially two straight pipes that are connected. The determination of the losses contributed by any fitting requires that the frictional losses in the straight pipes be deducted from the total pressure loss across the system (Miller, 1978). The theory available for determining frictional pressure drop in straight pipes will therefore be reviewed.

2.2.1 Shear Stress Distribution in Straight Pipes

To demonstrate the shear stress distribution in a pipe (Figure 2.1) one can consider a coaxial cylindrical element of length L and radius R over which a pressure difference Δp exists (Massey, 1970). The shear stress, τ, acts uniformly on the curved surface of this cylinder to provide the retarding force, F_3. A force balance over the cylinder where will yield the shear stress within the pipe radius r (Massey, 1970)

$$\tau = \frac{\Delta p r}{2L} \tag{2.1}$$

and also the shear stress at the pipe wall where $r = \frac{D}{2}$

$$\tau_o = \frac{D\Delta p}{4L}. \qquad (2.2)$$

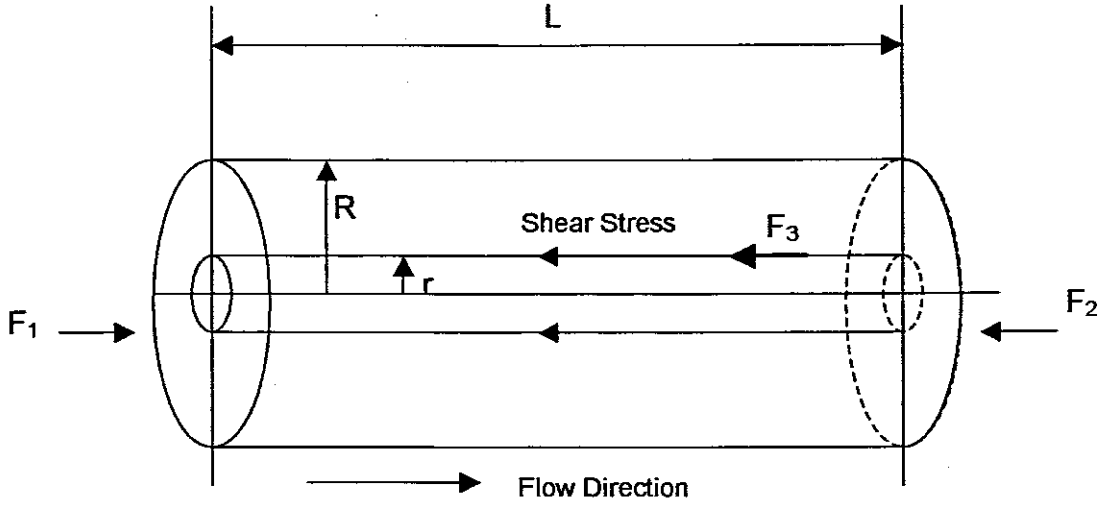

Figure 2.1: Shear stress distribution in a pipe

In the experimental procedure it is possible to measure the pressure drop across a known length of straight pipe and Eq. (2.2) can be used to calculate the shear stress at the pipe wall. These fundamental relationships are based on a force balance and the assumption that the fluid is homogeneous; it does not rely on any assumptions regarding the viscous nature of the fluid (Slatter, 1994).

2.2.2 Energy Losses and Friction Factors for Newtonian Fluids

When a fluid flows through a pipe, there is a dissipation of energy. Energy is expended in overcoming viscous friction or in causing turbulent mixing to occur. When flow occurs in a horizontal straight pipe of uniform diameter, this energy loss manifests itself as a head loss ΔH, that can be detected by appropriately connected manometer tubes. The pressure loss can be calculated from (Massey, 1970)

$$\Delta p = \rho g \Delta H . \tag{2.3}$$

The head loss, or loss of energy per unit weight, is given directly by the head difference, ΔH, measured in metres of fluid, which can be calculated using the Darcy formula (Massey, 1970)

$$\Delta H = \frac{4fL}{D}\left[\frac{V^2}{2g}\right] \tag{2.4}$$

where f is the Fanning friction factor defined as (Massey, 1970),

$$f = \frac{\tau_0}{\frac{1}{2}\rho V^2} \tag{2.5}$$

and

$$\tau_o = \frac{D\Delta p}{4L}. \tag{2.2}$$

The basic equation from which the frictional pressure drop may be calculated can be obtained by rearranging Eq. (2.2), (2.4) and (2.5) which yields

$$\Delta p = \frac{2 f L \rho V^2}{D}. \tag{2.6}$$

Equation 2.6 is very useful because it is valid for all types of fluids and for both laminar and turbulent flow, provided that the appropriate value of f is used (Holland & Bragg, 1995).

For Newtonian laminar flow, the Fanning friction factor is a function of the Reynolds number (Re) and is given by (Holland & Bragg, 1995)

$$f = \frac{16}{Re}. \tag{2.7}$$

For Newtonian turbulent flow, the friction factor dependence on the Reynolds number decreases gradually with increasing Reynolds number and is a function of the relative roughness of the pipe (Holland & Bragg, 1995). The greater the roughness, the higher the value of f for a given Reynolds number (Re). At very high values of Re, the friction factor becomes independent of Re. The simplest expression for calculating the friction factor in turbulent flow is the Blasius equation, which is valid for Reynolds numbers between 3000 and 100 000 for hydraulically smooth pipes (Holland & Bragg, 1995),

$$f = \frac{0.079}{Re^{0.25}}. \tag{2.8}$$

Based on the experimental work of Nikuradse in 1930 on rough pipes, Von Kármán and Prandtl combined this work with their boundary layer theory and derived the semi-empirical rough pipe flow laws (Chadwick & Morfett, 1993).

$$\frac{1}{\sqrt{f}} = -4\log\left(\frac{k}{3.7D}\right) \tag{2.9}$$

From 1937 to 1939 Colebrook and White investigated randomly rough commercial pipes opposed to the uniform sand roughened pipes of Nikuradse and proposed the well-known and applied Colebrook & White equation (Chadwick & Morfett, 1993)

$$\frac{1}{\sqrt{f}} = -4\log\left[\left(\frac{k}{3.7D}\right) + \frac{1.26}{Re\sqrt{f}}\right]. \tag{2.10}$$

2.2.3 Laminar Flow of Newtonian Fluids

When a fluid flows, shear deformation will take place. Laminar flow is characterised by the fact that individual fluid particle paths do not cross those of neighbouring particles in the adjacent laminae. The rate of deformation is known as the shear rate, $\dot{\gamma}$. Viscous stresses are set up when there is relative movement between adjacent particles. At low velocities, viscous forces dominate inertia forces and restrain any particles from moving from their path. Newton postulated the basic law of viscous resistance in 1687 as

$$\tau = \mu \frac{du}{dy}. \tag{2.11a}$$

The term $\frac{du}{dy}$ is the rate at which the velocity u increases with the co-ordinate y perpendicular to the velocity, μ is the coefficient of viscosity and τ is the resulting shear stress on a surface perpendicular to and in the direction of increasing y (Massey, 1970). For the axially symmetric flow of a fluid in a pipe, the relationship becomes

$$\tau = \mu\left(-\frac{du}{dr}\right). \tag{2.11b}$$

By integrating Eq. (2.11), one can obtain the velocity at any point in the pipe by applying a boundary condition that the velocity is zero at the pipe wall, hence assuming no-slip,

$$u = \frac{\tau_0}{2\mu R}\left(R^2 - r^2\right). \tag{2.12}$$

The total flow in the pipe can therefore be determined by integrating Eq. (2.12) resulting in the Hagen-Poiseuille equation (Holland & Bragg, 1995) where

$$Q = \frac{\pi R^4}{32\mu}\left(\frac{\Delta p}{L}\right) \tag{2.13}$$

and the average velocity can be found from

$$V = \frac{Q}{A}. \tag{2.14}$$

The velocity profile can be written as

$$u = u_{max}\left(1-\left(\frac{r}{R}\right)^2\right) \tag{2.15}$$

where $u_{max} = 2V$.

From Eq. (2.12) and Eq. (2.13) it can be demonstrated that

$$\tau_0 = \mu\frac{8V}{D}. \tag{2.16}$$

In a pipe, Eq. (2.11) can be written as

$$\tau_0 = \mu\left[-\frac{du}{dr}\right]_0, \tag{2.17}$$

therefore

$$\frac{8V}{D} = \left[-\frac{du}{dr}\right]_0. \tag{2.18}$$

From this equation the very important correlation between shear rate and pseudo shear rate can be established that forms the basis of tube viscometry.

2.2.4 Non-Newtonian Fluids

Non-Newtonian fluids exhibit an apparent viscosity that varies with shear rate, unlike Newtonian fluids where the viscosity does not vary with shear rate (Holland & Bragg, 1995). These fluids may therefore be classified according to either their response to externally applied pressure or according to the effects produced under

the action of shear stress (Chhabra & Richardson, 1999). The behaviour of these fluids can be classified as:

(a) Time-independent fluid behaviour (Shear thinning, Viscoplastic and Shear thickening fluid behaviour).

(b) Time-dependent fluid behaviour (Thixotropy and Rheopexy).

(c) Viscoelastic fluid behaviour.

The focus of this study is essentially on time-independent fluids.

2.2.5 Rheological Characterisation

The determination of the flow behaviour of a fluid involves the measurement of shear stress in a fluid at various shear rates (Holland & Bragg, 1995). A plot of shear stress versus shear rate for a particular fluid sample is called a flow curve and it would normally consist of a collection of experimentally determined points through which a curve may be drawn (Alderman, 1996). If an equation can be fitted to the curve, it facilitates calculation of the behaviour of the fluid. Only the data in laminar flow are used for curve fitting to determine the rheological constants (Alderman, 1996). The rheological model that best fits the data points defines the fluid's rheological character. The data are used to determine the yield stress parameter in the model, τ_y, if appropriate, the fluid consistency index, K, and the flow behaviour index, n, for the particular fluid (Alderman, 1996).

These flow models are approximations to the actual behaviour of the fluid and should not be used outside the range of conditions, especially shear rates, for which they are determined (Coulson & Richardson, 1990).

The most common relationships of shear stress versus shear rate are shown in Figure 2.2.

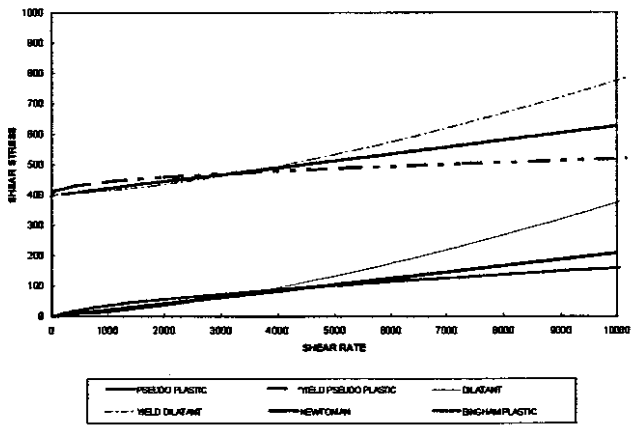

Figure 2.2: Idealised flow curves of time-independent fluids

2.2.6 Laminar Flow of Time-Independent Non-Newtonian Fluids in Straight Pipes

Several rheological models exist that can be used to model the laminar flow behaviour of non-Newtonian fluids, but the Herschel-Bulkley model is able to accommodate most other models as explained below.

The equations for laminar pipe flow can be derived as follows as described by Govier and Aziz (1972). The velocity gradient is given by

$$\frac{du}{dr} = \left[\frac{1}{K}\right]^{\frac{1}{n}} \left[\frac{r\Delta p}{2L} - \tau_y\right]^{\frac{1}{n}}. \qquad (2.19)$$

In this case it is clear that, when $\tau = \frac{r\Delta p}{2L} \leq \tau_y$, the fluid does not shear and adjacent laminae are stationary relative to one another. This occurs for values of $r \leq r_{plug}$ where

$$r_{plug} = \frac{R\tau_y}{\tau_0}. \tag{2.20}$$

The situation is shown graphically in Figure 2.3.

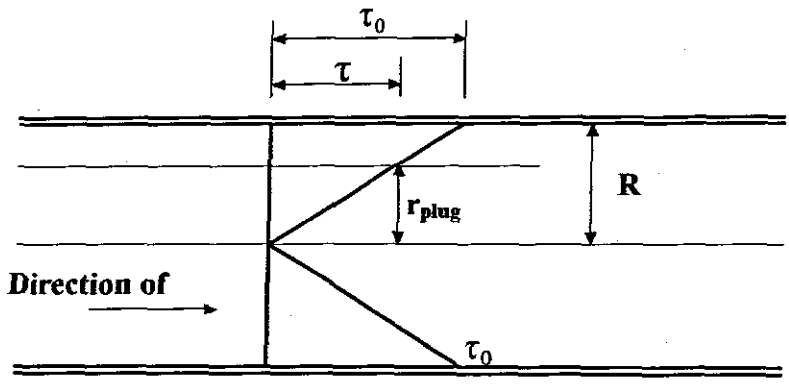

Figure 2.3: Shear stress distribution in a pipe showing unsheared plug radius

For $R > r > r_{plug}$ the fluid shears and Eq. (2.19) can be integrated to yield

$$u = \frac{\left[\frac{1}{K}\right]^{\frac{1}{n}}}{\left[\frac{\Delta p}{2L}\right]} \frac{n}{n+1}\left[\left(\tau_0 - \tau_y\right)^{\frac{n+1}{n}} - \left(\tau - \tau_y\right)^{\frac{n+1}{n}}\right]. \tag{2.21}$$

When $0 < r < r_{plug}$ the fluid moves as a plug at a uniform plug velocity u_{plug} and after integration the full relationship can be written as

$$\frac{32Q}{\pi D^3} = \frac{8V}{D} = \frac{4n}{K^{\frac{1}{n}}\tau_0^3}\left(\tau_0 - \tau_y\right)^{\frac{1+n}{n}}\left[\frac{\left(\tau_0 - \tau_y\right)^2}{1+3n} + \frac{2\tau_y\left(\tau_0 - \tau_y\right)}{1+2n} + \frac{\tau_y^2}{1+n}\right], \tag{2.22}$$

where $\tau_0 = \frac{D\Delta p}{4L}$ and $V = \frac{Q}{A}$.

The following rheological relationships can be accommodated in the yield pseudoplastic model:

Yield dilatant ($\tau_y > 0$ and $n > 1$)

Bingham plastic ($\tau_y > 0$ and $n = 1$)

Yield pseudoplastic ($\tau_y > 0$ and $n < 1$)

Dilatant ($\tau_y = 0$ and $n > 1$)

Newtonian ($\tau_y = 0$ and $n = 1$)

Pseudoplastic ($\tau_y = 0$ and $n < 1$).

It was demonstrated in Eq. (2.18) that the shear rate at the pipe wall for Newtonian fluids is $\frac{8V}{D}$. For non-Newtonian flow, this is not the case (Wilson *et al.*, 1992) and the quantity $\frac{8V}{D}$ is called pseudo shear rate, flow characteristic or bulk shear rate. The plot of τ_0 versus $\frac{8V}{D}$ is called a pseudo shear diagram. The pseudo shear rate is of great importance in non-Newtonian flow, and can be related to the true shear rate by the Rabinowitsch-Mooney relation (Chhabra & Richardson, 1999),

$$\left[-\frac{du}{dr}\right]_0 = \frac{8V}{D}\left[\frac{3n'+1}{4n'}\right] \tag{2.23}$$

where

$$n' = \frac{d(\ln \tau_0)}{d\left(\ln \frac{8V}{D}\right)}. \tag{2.24}$$

The most commonly used models to describe laminar flow in straight pipes are the pseudoplastic and yield pseudoplastic models and the Metzner and Reed generalised approach (Slatter, 1994).

2.2.7 Metzner-Reed Generalised Approach

Metzner and Reed (1955) developed a general technique for expressing the laminar flow rheological properties of many non-Newtonian fluids in circular pipe flow by considering the wall shear stress, $\tau_0 = D\Delta p/4L$, as a function of the pseudo shear rate 8V/D. This relationship is

$$\tau_0 = K'\left(\frac{8V}{D}\right)^{n'}, \tag{2.25}$$

and n' is the tangent to the double logarithmic plot of τ_0 versus 8V/D at any particular value of τ_0 or 8V/D and K' is the intercept on the y axis. This relationship can be used directly for design purposes in laminar flow. It has been found experimentally that for many fluids K' and n' are constant over wide ranges of τ_0 or 8V/D. For some fluids, this is not the case (the log-log plot is not a straight line) and care must be taken to ensure that the range of application is narrow, i.e., that the particular values of K' and n' used are valid for the actual values of 8V/D or τ_0 in a given design problem. In some cases, different values of K' and n' would have to be used for every value of 8V/D (Slatter, 1994).

The relationships between K' and K and n' and n for a power–law fluid are given below:

$n' = n$

and

$$K' = K\left(\frac{1+3n}{4n}\right)^{n}. \tag{2.26}$$

For a Newtonian fluid, $n' = 1$ and $K' = \mu$.

2.2.8 General Approach

One of the primary objectives of rheometry is the establishment of the relationship between the shear stress and the shear rate – often referred to as a rheogram or a flow curve and can be cast in the form developed by Weissenberg in 1929 (Tanner & Walters, 1998)

$$\dot{\gamma} = f(\tau). \tag{2.27}$$

For laminar tube flow the relationship between the bulk shear rate 8V/D, the wall shear stress τ_0 and the volumetric flow rate Q is (Tanner & Walters, 1998)

$$\frac{8V}{D} = \frac{32Q}{\pi D^3} = \frac{4}{\tau_0^3}\int_0^{\tau_0} \tau^2 \dot{\gamma}(\tau) d\tau . \tag{2.28}$$

This relationship is of fundamental importance for several reasons:

A plot of 8V/D vs τ_0 will give a unique line for a given material for all values of D (Chhabra & Richardson, 1999). This means that in general the bulk shear rate (8V/D) is a unique function of the rheogram $\dot{\gamma} = f(\tau)$ and the wall shear stress (τ_0), provided that there is no time dependency or slip at the wall and the flow is laminar.

Being a definite integral, Eq. (2.28) shows that the relationship between 8V/D and τ_0 can be obtained by numerical integration using data directly from a rheometer, without using a conventional rheological model.

Since (8V/D) is a unique function of the rheogram and the wall shear stress, Eq. (2.28) is independent of pipe diameter, and can be used for scale-up and design.

It provides the link or pathway between the rheogram and the pseudo shear diagram, i.e., given a rheogram, Eq. (2.28) can be used to construct a pseudo shear diagram (8V/D vs τ_0), which can be used for design in laminar flow. Conversely, the process can be reversed by differentiating Eq. (2.28). This provides the link or pathway between the pseudo shear diagram and the rheogram. This approach is used to derive the Rabinowitsch-Mooney relationship, which enables us to construct a rheogram if we have a pseudo shear diagram. The main problem with tube viscometry is that 8V/D is not true shear rate but the wall shear rate for a Newtonian fluid, therefore the bulk shear rate has to be transformed to the true shear rate, ($\dot{\gamma}$).

Differentiation of Eq. (2.28) after some manipulation will yield the following, known as the Rabinowitsch-Mooney equation:

$$\dot{\gamma}_0 = \left(-\frac{du}{dr}\right)_0 = \frac{8V}{D}\left(\frac{3n'+1}{4n'}\right) \tag{2.23}$$

If one plots a log-log pseudo shear diagram with τ_0 versus 8V/D for the laminar flow region, then n' is the slope of the tangent of the graph. The slope will only be approximately constant if the fluid is a power-law fluid (Chhabra & Richardson, 1999).

2.3 REYNOLDS NUMBERS

The Reynolds number can be used to determine what flow regime exists under given conditions (Holland & Bragg, 1995).

2.3.1 Newtonian Reynolds Number

The famous dye experiment carried out by Osborne Reynolds in 1883 (from Coulson & Richardson, 1990), in his study of the head losses associated with the flow of water through pipes, showed clearly the distinction between laminar and turbulent flow. He stated the transition between the two regimes was characterised by a dimensionless group,

$$\mathrm{Re} = \frac{\rho V D}{\mu}, \tag{2.29}$$

called the Reynolds number, in his honour (Coulson & Richardson, 1990). The Reynolds number is the ratio between the inertial forces and viscous forces. Stable laminar flow ends at Re = 2100 and turbulent flow ensues (Metzner & Reed, 1955; Govier & Aziz, 1972; Coulson & Richardson, 1990). This Reynolds number is used to describe the ratio of forces that exists in Newtonian fluids (Holland & Bragg, 1995).

Non-Newtonian fluids are more complex and many Reynolds numbers have been formulated to accommodate them. Not all of them will be discussed, only the ones that will be used in this thesis, which is the Metzner and Reed Reynolds number (Re_{MR}) and the Slatter Reynolds number (Re_3). The Reynolds number correlating the loss coefficient should account for the complete non-Newtonian characteristics of the fluid. The Reynolds numbers selected each describe different types of non-Newtonian behaviour.

2.3.2 Metzner and Reed Generalised Reynolds Number

Metzner and Reed (1955) developed a generalised Reynolds number for non-Newtonian flow:

$$Re_{MR} = \frac{8\rho V^2}{K'\left(\frac{8V}{D}\right)^{n'}}, \tag{2.30}$$

where

$$K' = K\left(\frac{3n+1}{4n}\right)^n \tag{2.26}$$

and n = n'.

Hence, for a power law fluid, Eq. (2.30) can be rewritten in terms of K and n as

$$Re_{MR} = \frac{8\rho V^2}{K\left(\frac{8V}{D}\right)^n}\left(\frac{4n}{3n+1}\right)^n. \tag{2.31}$$

2.3.3 Slatter Reynolds Number

Slatter (1994) developed a Reynolds number that places emphasis on the yield stress. Using the fundamental definition that Re ∝ inertial / viscous forces, the final formulation is

$$Re_3 = \frac{8\rho V_{ann}^{\ 2}}{\tau_y + K\left(\frac{8V_{ann}}{D_{shear}}\right)^n}. \tag{2.32}$$

The development of this Reynolds number is presented below, starting with the fact that in the presence of a yield stress the central core of the fluid moves as a solid plug. The unsheared plug is treated as a solid body in the centre of the pipe; the flow that the plug represents must be subtracted, as it is no longer being treated as part of

the fluid flow. The corrected mean velocity in the annulus V_{ann} is then obtained as follows,

$$V_{ann} = \frac{Q_{ann}}{A_{ann}}, \tag{2.33}$$

where

$$Q_{ann} = Q - Q_{plug} \tag{2.34}$$

and

$$Q_{plug} = u_{plug} A_{plug}. \tag{2.35}$$

The constitutive rheological equation can be integrated to obtain the plug velocity u_{plug},

$$u_{plug} = \frac{D}{2K^{\frac{1}{n}}\tau_0}\frac{n}{n+1}\left[\left(\tau_0 - \tau_y\right)^{\frac{n+1}{n}}\right]. \tag{2.36}$$

The radius of the plug is

$$r_{plug} = \frac{\tau_y}{\tau_0}R. \tag{2.37}$$

The area of the annulus is

$$A_{ann} = \pi\left(R^2 - r_{plug}^2\right). \tag{2.38}$$

The sheared diameter, D_{shear}, is taken as the characteristic dimension because this represents the zone in which shearing of the fluid actually takes place, and it is defined as

$$D_{shear} = D - D_{plug}, \tag{2.39}$$

where

$$D_{plug} = 2r_{plug}. \tag{2.40}$$

This expression can be used to represent both Herschel-Bulkley and Bingham plastic behaviour (Slatter & Wasp, 2000).

2.3.4 Friction Factors for Non-Newtonian Fluids

Various correlations exist for the calculation of τ_0 and f for non-Newtonian fluids (Heywood, 1984) and will not be reproduced here.

For inelastic non-Newtonian fluids, the Fanning friction factor in laminar flow becomes (Holland & Bragg, 1995)

$$f = \frac{16}{Re_{MR}}. \tag{2.41}$$

Slatter (1999) developed a friction factor for fluids with a yield stress

$$f_{ann} = \frac{2\tau_0}{V_{ann}^2}. \tag{2.42}$$

For smooth wall turbulent flow, the friction factor can be correlated by the generalised form of the Von Kármán equation as given by Dodge and Metzner (1959)

$$\frac{1}{\sqrt{f}} = \frac{4}{n'^{0.75}} \log\left(f^{\left(1-\frac{n'}{2}\right)} Re_{MR} \right) - \frac{0.4}{n'^{\frac{1}{2}}}. \tag{2.43}$$

Slatter (1994) developed a friction factor for non-Newtonian slurries based on particle roughness, where d_{85} is the representative particle size.

- For smooth wall turbulent flow (where Re_r is the roughness Reynolds number)

$$\frac{V}{V_*} = 2.5\ln\left(\frac{R}{d_{85}}\right) + 2.5\ln Re_r + 1.75. \tag{2.44}$$

- For fully developed rough wall turbulent flow

$$\frac{1}{\sqrt{f}} = 4\log\left(\frac{3.34D}{d_{85}}\right). \qquad (2.45)$$

2.4 PHYSICAL MODELLING PRINCIPLES

Experiments are often required to determine the way in which one variable depends on another because complete analytical solution of engineering problems involving the flow of real fluids is seldom attainable. Experimental investigation may require testing in several sizes, and it is necessary to understand the relationship between models of different size in order to correctly interpret the qualitative and quantitative data obtained from such experiments. The concepts of dimensional analysis and physical, geometric, kinematic and dynamic similarity are introduced as they apply to the specific problem of modelling and data interpretation of fittings of different size.

Dimensional analysis enables the reduction of individual quantities relevant to a physical problem to be assembled into dimensionless groups, often referred to by name (Massey, 1970). These groups assist in the interpretation of model studies by ensuring that the conditions under which tests and observations take place at one size fitting are the same as those at the other size fitting.

Physical similarity, like dimensional analysis, helps to ensure that the conditions under which tests and observations take place at one scale are the same as those on another scale (Massey, 1970). The models at different scale are said to be physically similar in respect of specified physical quantities (e.g. velocity), when the ratio of

corresponding magnitudes of these quantities between the two systems is the same everywhere. For any comparison between models, the sets of conditions associated with each must be physically similar.

Geometric similarity is the similarity of shape (Massey, 1970). The requirement is that any ratio of length in one model to the corresponding length in another model is the same. This ratio is referred to as the scale factor. Geometric similarity is the first requirement of physical similarity.

Kinematic similarity is similarity of motion and requires similarity of both length and time interval (Massey, 1970). When flows are kinematically similar, the patterns formed by streamlines are geometrically similar at the same time. Geometric similarity alone does not imply kinematically similar flows.

Dynamic similarity is similarity of forces (Massey, 1970). Since there may be several kinds of forces acting on a fluid particle, it is usually impossible to satisfy dynamic similarity of them all simultaneously. The justification for comparing observations from one model flow system with those in another are that the fluid behaviour is similar in the two systems, implying kinematic similarity. Geometric similarity alone does not imply dynamic similarity. The requirements for kinematic similarity are both geometric and dynamic similarity. This produces geometric similarity of flow patterns, and is of prime importance in this study.

The forces that control the behaviour of fluids could be due to the differences in piezometric pressure or pressure forces, the action of viscosity, gravity, surface tension, elasticity or inertia. Of primary concern in this work is the ratio of viscous to inertial forces; the dimensionless group of specific interest in this study is therefore the Reynolds number.

2.5 MINOR LOSSES IN PIPES

Head losses, in addition to those due to straight pipe friction, are always incurred at pipe bends, junctions and valves. These additional losses are due to eddy formation generated in the fluid at the fitting and must be taken into account. In the case of long pipelines of several kilometres, these local losses may be negligible, but for short pipelines they may be greater than the straight pipe frictional losses (Chadwick & Morfett, 1993). A general theoretical treatment for local head losses is not available, but it is usual to assume rough turbulence (where the friction factor is independent of the Reynolds number) since it leads to the simple equation (Chadwick & Morfett, 1993):

$$h_{fitt} = k_{fitt} \frac{V^2}{2g} \tag{2.46}$$

h_{fitt} = local head loss

k_{fitt} = fitting loss coefficient.

The two methodologies for the prediction of losses in pipe fittings are based on the following assumptions (King, 2002):

a) The fitting will contribute to the energy dissipation an amount equivalent to an additional length of pipe that is calculated as a multiple of the pipe diameter.

b) Kinetic energy is dissipated as the fluid flows through the fitting and the loss is calculated in terms of the number of velocity heads that are lost.

The loss coefficient is related to the upstream Reynolds number of the flow through the fitting

$$k_{tot} = \frac{C_{fitt}}{Re} + k_{fitt}\left(1 + \frac{0.0254}{D}\right) \tag{2.47}$$

and C_{fitt} and k_{fitt} are determined experimentally (King, 2002).

2.6 CALCULATING LOSS COEFFICIENTS

The energy losses across a fluid-conveying conduit in a fluid are normally accounted for using the energy balance or Bernoulli equation:

$$z_1 + \frac{\alpha_1 V_1^2}{2g} + \frac{p_1}{\rho g} = z_2 + \frac{\alpha_2 V_2^2}{2g} + \frac{p_2}{\rho g} + \sum_{i=1}^{N} h_{loss}, \tag{2.48}$$

where subscripts 1 and 2 refer to the upstream and downstream conditions respectively, V is the mean flow velocity, z is the elevation from the datum, α is the kinetic energy correction factor, p is the static pressure and where there are N sources of energy loss (Edwards *et al.*, 1985). Each term in the expression represents energy per unit weight of fluid, known as energy head or head loss, and is a statement of the law of conservation of energy as applied to fluid flow. The head

loss is in units of metres. For the case of a head loss in a fitting, the Bernoulli equation may be rewritten as:

$$z_1 + \frac{\alpha_1 V_1^2}{2g} + \frac{p_1}{\rho g} = z_2 + \frac{\alpha_2 V_2^2}{2g} + \frac{p_2}{\rho g} + h_1 + h_{fitt} + h_2, \qquad (2.49)$$

where h_1 and h_2 refer to the friction head loss in the straight pipe upstream and downstream of the fitting and h_{fitt} refers to the head loss in the fitting. The head loss, h, in the straight pipe can be calculated from Eq. (2.4).

The assumption of uniform velocity profiles is not always acceptable for all problems (Potter & Wiggert, 1997) as in the case of the analysis of losses across contractions where the upstream and downstream diameters are different. The control-surface integral must then be taken into consideration with the proper expression for the velocity distribution. The distribution can be accounted for by introducing the kinetic-energy correction factor, α, defined by

$$\left| \alpha = \frac{\int u^3 dA}{\bar{V}^3 A} \right|. \qquad (2.50)$$

For a flow with a parabolic profile in a pipe $\alpha = 2$. For most internal turbulent flows the profile is nearly uniform with $\alpha \approx 1.05$. Since this value is so close to unity it is often taken as $\alpha = 1$ (Potter & Wiggert, 1997).

For pseudoplastic fluids α becomes (Jadallah, 1980)

$$\alpha = \frac{3(1+3n)^2}{(1+2n)(3+5n)}. \qquad (2.51)$$

For yield pseudoplastic fluids α becomes (Baudouin, 2003)

$$\alpha = 2\tau_0^4 \frac{M(\tau_0-\tau_y)^2 + B\tau_Y(\tau_0-\tau_y) + Y\tau_y^2}{\left[\frac{(\tau_0-\tau_y)^2}{1+3n} + \frac{2\tau_y(\tau_0-\tau_y)}{1+2n} + \frac{\tau_y^2}{1+n}\right]^3}, \tag{2.52}$$

where

$$M = \frac{3}{(3n+1)(4n+2)(5n+3)},$$

$$B = \frac{6}{(2n+1)(3n+2)(4n+3)},$$

$$Y = \frac{1}{2(n+1)^3}.$$

On dimensional grounds, the head loss in a fitting will depend upon the fluid velocity, fluid properties and the geometry of the fitting as follows (Edwards *et al.*, 1985):

$$\frac{2gh_{fitt}}{V^2} = \text{fn}(\text{Reynolds number, geometry}) \tag{2.53}$$

and can be expressed as a function of the velocity energy head and is usually taken as a direct proportionality:

$$h_{fitt} = k_{fitt}\frac{V^2}{2g}. \tag{2.54}$$

Hence, the loss coefficient of the fitting is given by

$$k_{fitt} = h_{fitt}\frac{2g}{V^2}. \tag{2.55}$$

This can also be expressed in terms of pressure drop because $\Delta p = \rho g \Delta h$ and then Eq. (2.55) becomes

$$k_{fitt} = \frac{\Delta p_{fitt}}{\frac{1}{2}\rho V^2} \tag{2.56}$$

where:

(1) k_{fitt} is the non-dimensionalised difference in overall pressure between the ends of two long straight pipes when there is no fitting and when the real fitting is installed (Miller, 1978). This is shown in Figure 2.4 below.

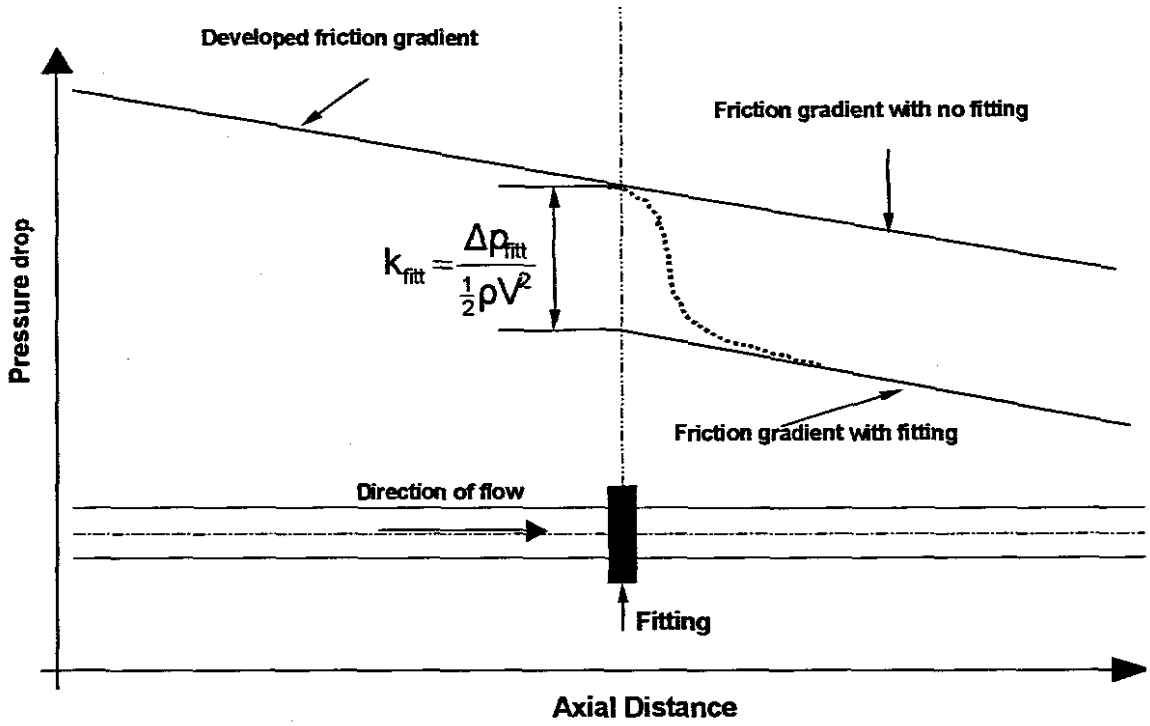

Figure 2.4: Definition of the loss coefficient (Miller, 1978)

(2) Δp_{fitt} is the pressure loss across the fitting. The flow lengths over which pressure losses occur start from a few diameters upstream to several pipe diameters downstream of the actual length of the fitting. This is known as the region of influence or interference. Δp_{fitt} should be measured across this region. It can be the measured static pressure drop (Δp_s) or the total pressure that is $\Delta p_{tot} = \Delta p_s + \frac{1}{2}\rho V^2$. It is therefore important to state whether k_{fitt} is based on the static or total pressure (Miller, 1978).

(3) ρ is the density of the fluid. In the case of settling slurries it can be based on either the *in situ* or delivered concentration and this also needs to be specified.

(4) V is the mean flow velocity in the pipe. If there is a change in pipe diameter, the convention is to use the higher mean flow velocity of either the upstream or the downstream pipe.

Equation (2.56) is based on the static pressure only. In the case of contractions where the upstream and downstream velocities are different, the total pressure should be used to account for changes in kinetic energy. Therefore, for a sudden contraction, Eq. (2.56) becomes:

$$k_{con} = \frac{\left[\frac{\Delta p_{con}}{\rho g} + \frac{\left(\alpha_1 V_1^2 - \alpha_2 V_2^2\right)}{2g}\right]}{\frac{V_2^2}{2g}} \qquad (2.57)$$

With the exception of abrupt contractions and expansions, all other fittings have a physical length. There are three distinct conventions for estimating the length of the straight pipe in the test section (Perry & Chilton, 1973):

1. the actual length of the centreline of the entire system is taken;
2. the lengths of the individual pieces of pipe that are actually straight are summed up; and
3. the distances between the intersections of the extended centrelines of the successive straight pipes are added.

2.7 FLOW PHENOMENA IN SUDDEN CONTRACTION

Flow patterns within contractions have been observed and used to gain an understanding and calculate pressure losses in the contraction. Several good reviews exist on this topic (e.g. Shah & London, 1978), and only the important aspects pertaining to this work will be highlighted in this section.

2.7.1 Turbulent Flow

Turbulent flows through sudden contractions are well described in most texts on fluid mechanics. Some of the literature has been reviewed and there is general agreement about the form of the flow patterns and the reason for the pressure drop (Massey, 1970; Chadwick & Morfett, 1994; Holland & Bragg, 1995; Finnemore & Franzini, 2002).

In turbulent flow there is a marked drop in pressure as the fluid passes through the contraction. The pressure loss is due to an increase in velocity and the loss of energy in turbulence. There is a rise in pressure at the upstream corner of the contraction due to streamline curvature so that the centrifugal action causes the pressure at the pipe wall to be greater than in the centre of the stream. The streamlines continue to curve downstream of the contraction to form a cross section where a minimum pressure and maximum velocity are obtained. This is known as the *vena contracta*. The contracted flowing stream is surrounded by fluid that is in a state of turbulence but has very little forward motion. Downstream of the *vena contracta* the flow stream expands, the velocity decreases and the pressure rises. Between points D and E the fluid is in a very disturbed condition because the stream

expands and the velocity decreases while the pressure rises. After this expansion, the flow is normal. This is shown in Figure 2.5.

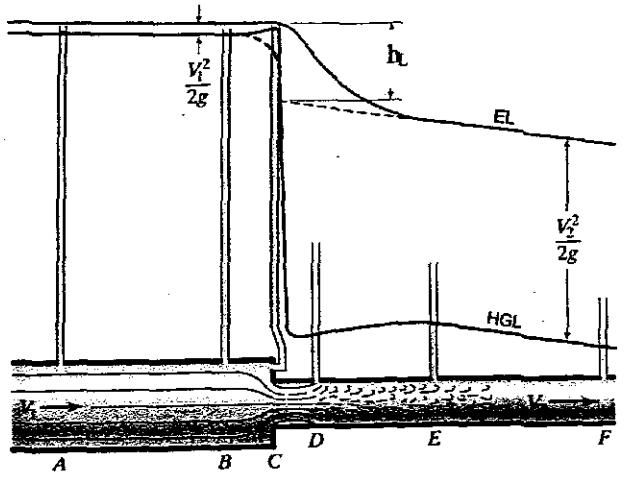

Figure 2.5: Local head loss at a sudden contraction (from Finnemore & Franzini, 1997)

2.7.2 Laminar Flow

When a fluid flows through a sudden contraction, the flow progresses from being fully developed at a plane some distance upstream from the contraction to being fully developed in the downstream tube at a distance L_e from the contraction (Boger, 1987). A stationary flow vortex is present in the corner of the upstream tube and the contraction plane and detaches from the wall at a distance L_v. It reduces the available flow area and the fluid accelerates and results in a partially developed velocity profile at the entrance of the downstream tube. After the contraction plane, the centreline velocity continues to develop until it reaches 99% of its fully developed value. This distance is known as the entry length, L_e.

A diagram illustrating these phenomena is shown in Figure 2.6.

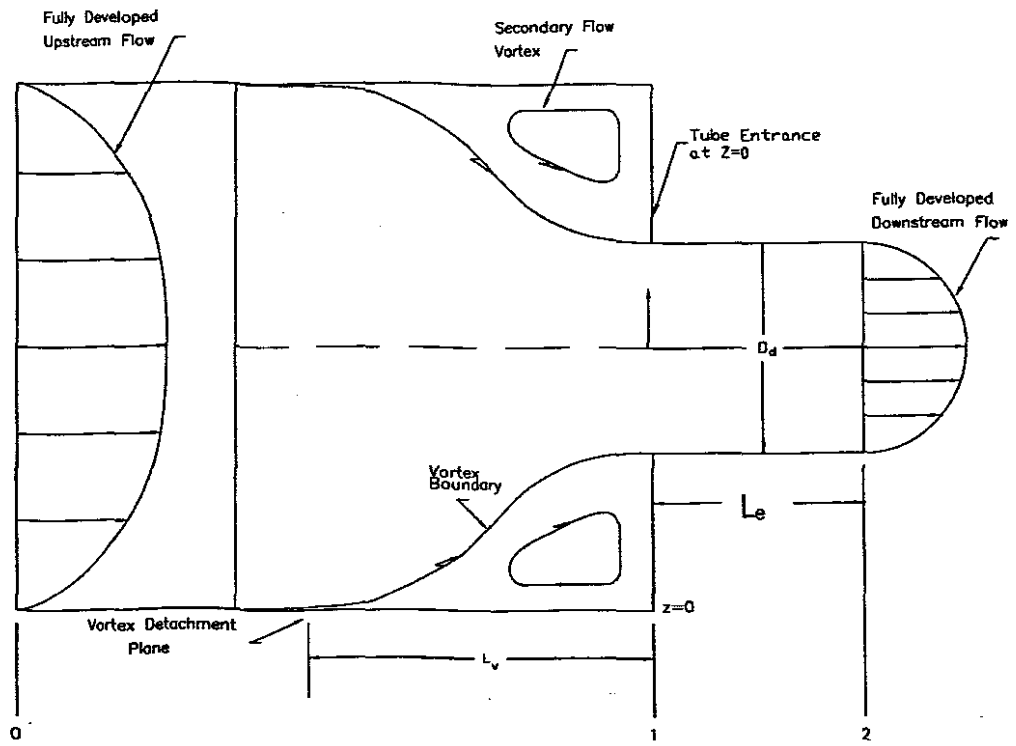

Figure 2.6: Basic elements of laminar flow through a contraction (From Boger, 1987)

The vortex size decreases as the fluid velocity increases and the velocity profile changes from being partially developed to being uniform (flat) at the entrance of the downstream tube (Ramamurthy & Boger, 1971).

2.7.2.1 Creeping Flow

At $Re \leq 1$, creeping flow exists (Boger, 1987). The velocity profile development is only slightly distorted from being fully developed as it enters the smaller pipe and the profile is independent of the Reynolds number. The vortex reattachment length is independent of the Reynolds number and

$$L_v = 0.17 D_u, \tag{2.58}$$

and the entry length is constant and

$$L_e = \frac{0.49D_d}{2} \tag{2.59}$$

where D_u and D_d are the upstream and downstream diameters respectively.

2.7.2.2 Inertial Flow

At $Re \geq 1$, fluid inertia becomes important. The stationary vortex decreases in size as Re increases and at $Re = 100$, $L_v = 0.05D_u$. The entry length becomes Reynolds number dependent (Boger, 1987), but at a given Reynolds number, it is a weak function of the contraction ratio, β_{con}, (Vrentas & Duda, 1973). Later investigations reported that inertia only starts to dominate at $Re > 50$ (McNeil *et al.*, 1999).

2.7.2.3 Effect of Rheology on Flow Patterns

The rheology of the fluid has the following effect on the upstream flow vortex:

- Shear thinning decreases the size of the flow vortex (Kim-E *et al.*, 1983).
- Visco-elastic properties increase the size of the flow vortex (White *et al.*, 1987).
- Low yield numbers ($Y = \frac{\tau_y R_u}{\eta U}$) are sufficient to eliminate the upstream flow vortex for Bingham plastic fluids (Hammad & Vradis, 1996), where R_u is the radius of the upstream pipe, η is the plastic viscosity and U is the inlet streamwise velocity.

Understanding the effect of flow patterns through contractions can assist in solving problems in extrusion processes (Hammad & Vradis, 1996).

2.7.2.4 The Effects of Rheology on the Entry Length

The effects of rheology on the entry length are summarised below.

The entry length can be expressed as a function of the flow behaviour index, n (Collins & Schowalter, 1963; Ramamurthy & Boger, 1971). The entry length increases as the flow behaviour index decreases from 1 to 0.1 (Collins & Schowalter, 1963). Philippoff and Gaskins (1958) have reported a number of experiments indicating an extremely short entry length for viscoelastic fluids. Kim-E *et al.*, (1983) found that the entry length results for highly shear thinning fluids is identical to Newtonian results and that the relationship established by Boger (1987) was applicable for Re = 0 to 100 and this is shown in Figure 2.7.

$$L_e = 0.0709\mathrm{Re} + 0.589 \qquad (2.60)$$

The velocity profile at the entrance of an abrupt 2 to 1 contraction is uniform for Newtonian and inelastic power-law fluids when $0.585 \leq n \leq 1$ and $20 \leq \mathrm{Re} \leq 1942$ (Ramamurthy & Boger, 1971).

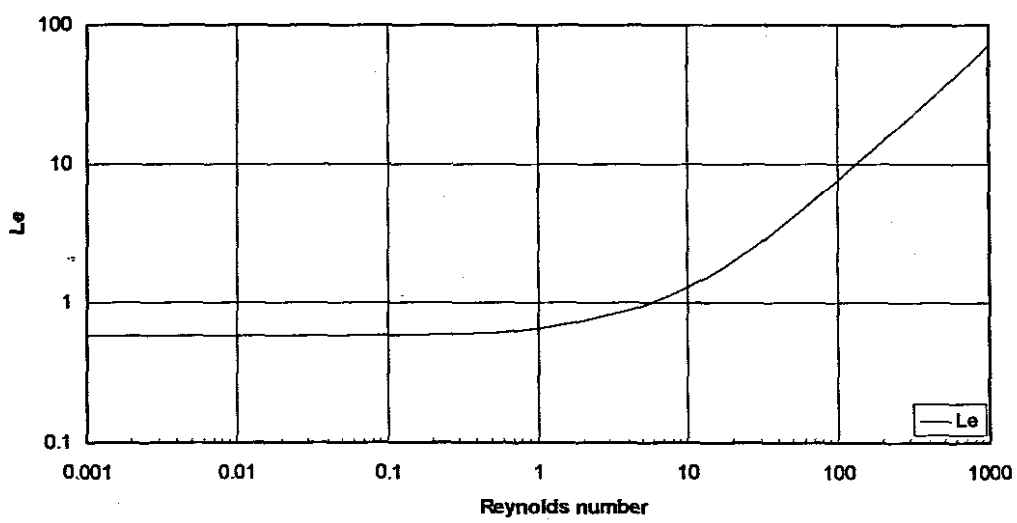

Figure 2.7: Dependence of the entry length on Reynolds number (Eq. 2.60)

2.7.2.5 Velocity Overshoots

At Reynolds numbers between 50 and 200, a concavity exists in the entrance-velocity profile also known as velocity overshoots. Off-centre maxima or velocity overshoots were reported to exist at Re = 100 by Boger (1982), Re = 100 and 200 by Vrentas and Duda (1973) and Re = 50 by Christiansen *et al.* (1972). The depth of the concavity increases with β_{con} and Re (Christiansen *et al.*, 1972). Figure 2.8 shows the dependence of axial velocities at the tube entrance and an example of velocity overshoots. For Bingham fluids velocity overshoots are evident at lower Reynolds numbers (Hammad & Vradis, 1996), but this is not obtained with shear thinning fluids (Kim-E *et al*, 1983).

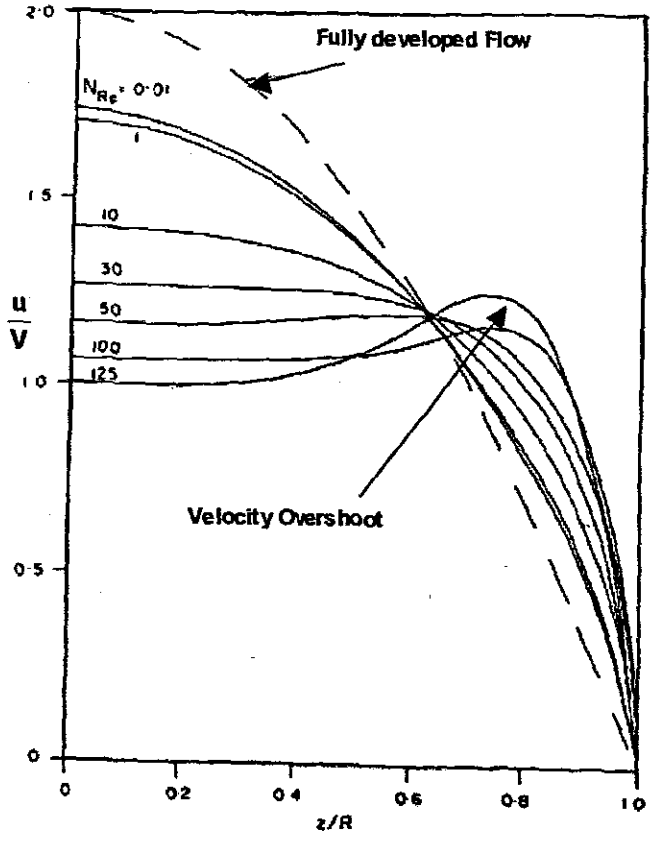

Figure 2.8: Effect of Reynolds number on the entrance velocity profile (from Boger, 1982)

2.7.3 Pressure Losses

The accurate prediction of pipe contraction pressure loss is important in the design of pipe systems where close control of the flow distribution in a network of pipes is required, such as heat exchangers, in the extrusion of polymer melts and other sludges encountered in the oil and gas production industries (Hammad & Vradis, 1996). The pressure loss through sudden contractions is associated with the development of the velocity profile as the fluid enters the smaller tube. The investigation and determination of the entry length therefore forms a basis for the work done to determine pressure losses in contractions.

This work often excluded the flow phenomena in the upstream tube as the assumption was that the flow was fully developed as it entered the smaller tube. Bogue (1959) was the first to suggest that this was not the case for viscous fluids and that a stationary vortex is formed upstream that could contribute considerably to the total pressure loss across the contraction. Durst and Loy (1985) recognised the importance of both upstream and downstream flow phenomena and although detailed measurements were made of these quantities both experimentally and computationally, they did not develop a predictive method for the calculation of pressure drop due to sudden contractions. Although some pressure drop results were reported for $\beta = 0.25$, the change in velocity components has also not been accounted for as required for the determination of head losses using Eq. (2.57), since the upstream and downstream diameters are not the same.

2.7.4 Turbulent Loss Coefficients k_{con} for Sudden Contraction

As stated earlier, a general theoretical treatment is not yet available for the losses through sudden contractions (Chadwick & Morfett, 1993), but some derivations exist based on the application of the Bernoulli equation and the momentum equation. This approach is very reliable for sudden expansions but in the case of a sudden contraction, the analysis can only be applied after the *vena contracta* and it is necessary to have experimental values of the contraction ratio [β_{con}] (Holland & Bragg, 1995).

The following Reynolds numbers were reported at which the *vena contracta* exists for Newtonian fluids as shown in Table 2.1.

Table 2.1: Re at which vena contracta exist

Re	β_{con}	REFERENCE
186 for very viscous fluids	0.16	Astarita and Greco, 1968
200	0.44,0.16, 0.0625	Vrentas and Duda, 1973
> 400	0.09	La Nieve, 1968
>1000	0.125	Sylvester and Rosen
1346 for water	0.16	Astarita and Greco, 1968
2100 for water	0.25	Ramamurthy and Boger, 1971

Although Chadwick and Morfett (1993) stated that experiments indicate that the contraction of the flow area is approximately 40% and give an approximation, loss coefficients for sudden contractions from the literature (Franzini & Finnemore, 2002) are often tabulated and are given below for a range of contraction ratios between 0 and 1 as shown in Table 2.2.

Table 2.2: Loss coefficients for sudden contraction (From Chadwick & Morfett, 1993)

β_{con}	0	0.1	0.2	0.3	0.4	0.5	0.6	0.7	0.8	0.9	1.0
k_{con}	0.50	0.45	0.42	0.39	0.36	0.33	0.28	0.22	0.15	0.06	0.00

Table 2.3 shows data from Hwang and Houghtalen (1996). In this case, the loss coefficient is dependent on the velocity in the smaller pipe for each contraction ratio.

Table 2.3: Loss coefficients for sudden contractions (From Hwang & Houghtalen, 1996)

VELOCITY IN SMALLER PIPE (m/s)	RATIO OF SMALLER TO LARGER PIPE DIAMETERS, D_2/D_1									
	0	**0.1**	**0.2**	**0.3**	**0.4**	**0.5**	**0.6**	**0.7**	**0.8**	**0.9**
1	0.49	0.49	0.48	0.45	0.42	0.38	0.28	0.18	0.07	0.03
2	0.48	0.48	0.47	0.44	0.41	0.37	0.28	0.18	0.09	0.04
3	0.47	0.46	0.45	0.43	0.40	0.36	0.28	0.18	0.10	0.04
6	0.44	0.43	0.42	0.40	0.37	0.33	0.27	0.19	0.11	0.05
12	0.38	0.36	0.35	0.33	0.31	0.29	0.25	0.20	0.13	0.06

Miller (1978) produced a graph of loss coefficient versus contraction ratio and this is shown in Figure 2.9.

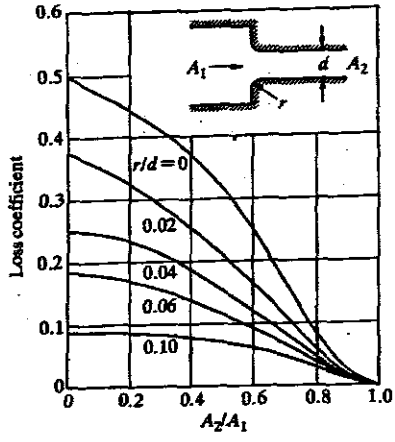

Figure 2.9: Loss coefficients for sudden contractions (From Miller, 1978)

Values obtained in Miller are slightly higher than those quoted in Hwang & Houghtalen (1996). There is no mention of velocity dependence of the loss coefficient in Miller (1978) and Finnemore & Franzini, (1997) whereas Hwang & Houghtalen (1996) listed values at different velocities.

2.7.5 Laminar Flow Loss Coefficient Constant C_{con} for Sudden Contraction

For laminar flow, the loss coefficient is inversely proportional to the Reynolds number (Edwards *et al.*, 1985; Ma, 1987; Slatter *et al.*, 1997; Pienaar, 1998) and the data loci present as a straight line of slope –1.:

$$k_{con} = \frac{C_{con}}{Re}. \qquad (2.61)$$

For Newtonian fluids, the Newtonian Reynolds number given by Re_N will apply. For non-Newtonian fluids the Metzner & Reed Reynolds number given by Re_{MR} or the Slatter Reynolds number given by Re_3 will be applicable. These Reynolds numbers are described in detail in Section 2.3.

Loss coefficient data determined experimentally are given in Table 2.4. The laminar flow loss coefficient constant is denoted by C_{con} and for turbulent flow by k_{con}.

Table 2.4: Loss coefficient data for Newtonian and non-Newtonian fluid flow through sudden contractions

REFERENCE	FLUID	β_{con}	C_{con}	k_{con}
Hooper, 1981	-	-	160	-
Edwards *et al.*, 1985	50% Glycerol/water lubricating oil	0.198	110	0.45
Edwards *et al.*, 1985	50% Glycerol/water lubricating oil, CMC, china clay	0.436	59	0.33
Ma, 1987	Laterite & gypsum slurries	0.5	900	0.23
Pienaar, 1998	100% Glycerol, kaolin, CMC	0.463	640	0.42
Pienaar, 1998	100% Glycerol, kaolin, CMC	0.205	1300	0.44
Pal & Hwang, 1999	Oil-in-water emulsions	0.244	-	0.43

It is not understood why the results from different researchers vary so much. The sharpness of the contraction has a significance influence on the loss coefficient and any deviation from a sharp edged contraction will result in a lower loss coefficient value (Bullen *et al.*, 1996) and this may be the reason. The experimental data are insufficient to draw any conclusions. The experimental procedure for determining loss coefficient data will therefore be reviewed to facilitate an understanding of the discrepancies.

2.8 EXPERIMENTAL DETERMINATION OF LOSS COEFFICIENTS

This section will review the experimental practices when measuring losses through sudden contractions and other fittings to establish if a consistent practice exists. It

will focus on the placement of pressure tappings before and after the contraction plane and the analysis of results.

Experimental determination of the loss coefficient can be done by directly measuring the pressure drop across the fitting including the sections upstream and downstream that are not fully developed and by calculating the head loss Eq. (2.49) and hence the loss coefficient (Pienaar, 1998), or by measuring the pressure gradient along the length of the upstream and downstream pipes (Edwards *et al.*, 1985).

It is, however, very difficult in practice to distinguish between the incompletely developed and the fully-developed flow region prior to and after the fitting, hence making it difficult to measure the pressure drop due to the fitting only (Ward-Smith, 1976). Experimental determination of fitting losses is therefore carried out by measuring the overall friction loss in a system made up of two lengths of straight pipe connected in series by a fitting or valve. To obtain the loss due to a fitting or valve, the friction loss in the straight pipe is subtracted from the total friction loss measured (Perry & Chilton, 1973). The total length of straight pipe can either include or exclude the physical length of the fitting resulting in the k_{gross} only if the straight pipe losses are subtracted

$$k_{gross} = \frac{1}{\frac{1}{2}\rho V^2}\left[-\Delta p - \frac{1}{2}\rho V^2 \frac{4f}{D}(L_u + L_d)\right], \qquad (2.62)$$

or k_{nett} if the length of the fitting is included as a length of straight pipe (ESDU, 1989)

$$k_{nett} = \frac{1}{\frac{1}{2}\rho V^2}\left[-\Delta p - \frac{1}{2}\rho V^2 \frac{4f}{D}(L_u + L_{fitt} + L_d)\right]. \qquad (2.63)$$

Ma (1987) has done a significant amount of work analysing loss coefficient data by excluding and including the physical length of the fitting. He has concluded that the values of k_{fitt}, excluding the physical length of the fitting as a piece of straight pipe, have lower scatter than those including the physical length of the fitting. In the case of determining losses in contractions, this should not be an issue since a contraction does not have a physical length.

It was not always clear from the work reviewed which method was used. Definitions of fitting loss and the total length given by various researchers are given in Table 2.5.

Clearly, direct comparison of experimental results is not possible where physical straight pipe length, overall length, and fully developed flow length are used by different researchers.

Table 2.5: Definition of fitting losses and total length given by various authors

RESEARCHER	DEFINITION OF Δp_{fitt}
Steffe *et al.* (1984)	The total length of flow included that contributed by the valve, fitting or elbow. The pressure tap downstream of the fitting (p_2) was 20.8 diameters from the fitting. The straight pipe friction losses was correlated as $f = 14.14\ Re_{MR}^{-1.048}$ instead of the usual $f = 16/Re_{MR}$.
Edwards *et al.* (1985)	The total head loss is the sum of the head losses for all straight pipe sections and all fittings.
Das *et al.* (1991)	The pressure drop due to the bend is obtained from the difference between the static pressure of the upstream, fully developed flow and the static pressure of the downstream, fully developed flow regions across the bend.
Mukhtar *et al.* (1995)	Measured the pressure drop across a bend one pipe diameter upstream of the bend and two pipe diameters downstream of the bend.

Bojcic *et al.* (1997)	The total length of pipe is the sum of the lengths of straight pipe sections and the lengths of fittings measured on the centrelines of the fittings.
Pal and Hwang (1999)	Δp for expansions, contractions and valves is defined as a sudden pressure change in the transitional section for an assumed fully developed flow and can be determined by extrapolating the pressure profiles of both the upstream and downstream pipes to the expansion plane. Pressure taps were located 5, 10 and 25 diameters upstream and downstream of the fitting and the pressure differential taken as the difference between the pressures at the tappings 25 diameters upstream and downstream.

The dependence of the laminar entrance loss coefficient on the contraction ratio was correlated by Kaye and Rosen (1971) and serves as the basis for many other correlations widely used today (ESDU, 1989). In this experimental study, a minor adjustment was made from previous work, that is, to increase the tapping distance to the entrance of the contraction to at least 2 diameters. The entrance losses were obtained from the equilibrium pressure gradient in the downstream test section $(dp/dz)_T$ and a pressure measurement p_{ES} taken 2 diameters prior to the contraction plane. The pressure loss due to the contraction was then determined as follows:

$$\Delta p_{ent} = p_{ES} - \left|\left(\frac{dp}{dz}\right)_E \Delta l\right| - \left|\left(\frac{dp}{dz}\right)_T L_T\right|. \qquad (2.64)$$

The equilibrium pressure gradient in the entrance was calculated from the equilibrium test section downstream using the contraction ratio

$$\left(\frac{dp}{dz}\right)_E = \beta^2 \left(\frac{dp}{dz}\right)_T. \qquad (2.65)$$

It was found that the correction for the friction losses in the entrance tube was significant only for the three largest contraction ratios, in this case being 0.636, 0.411 and 0.213. Reanalysis of previous data resulted in a higher value of C_{con} and

was said to be due to the fact that the entrance section was not long enough to permit fully developed flow before reaching the contraction. Also concluded is that an upstream diameter greater than twice the diameter of the downstream tube may be considered an infinite reservoir. Reynolds numbers as low as 5 were obtained.

Boger and Ramamurthy (1970) placed the tapping only on the downstream test section at 2 feet (608 mm) intervals along the downstream test section, with the first tap only 1 diameter from the contraction plane when measuring loss coefficients for viscous power-law fluids.

Jadallah (1980) measured the axial pressure gradients upstream and downstream of the contraction and extrapolated the fully developed pressure gradient to the contraction plane to determine the pressure drop across the contraction.

Ma (1987) also measured the axial pressure gradients along the upstream as well as the downstream tangent lines. He used the total pressure drop method by selecting one point upstream and one point downstream. He however measured the pressure gradient for the straight pipe sections as well, and did not have to calculate the friction factor from pipe flow theory.

Pienaar (1998) measured the pressure 50 diameters upstream and downstream of the contraction and calculated the friction loss from the wall shear stress for Newtonian fluids

$$\tau_0 = \mu \frac{8V}{D} \tag{2.16}$$

and for non-Newtonian fluids

$$\frac{32Q}{\pi D^3} = \frac{8V}{D} = \frac{4n}{K^{\frac{1}{n}} \tau^3_0} (\tau_0 - \tau_y)^{\frac{1+n}{n}} \left[\frac{(\tau_0 - \tau_y)^2}{1+3n} + \frac{2\tau_y(\tau_0 - \tau_y)}{1+2n} + \frac{\tau^2_y}{1+n} \right]. \tag{2.22}$$

It is clear that various different methods have been used for the determination of loss coefficient data. A systematic experimental procedure is required to determine loss coefficient data that are in agreement with one another and with numerical and analytical results.

2.9 LAMINAR TO TURBULENT TRANSITION

Experimental results for laminar/turbulent transition in contractions are given in Table 2.6. These results are taken only from experimental results that were presented in the form of loss coefficient (k_{con}) versus Reynolds number. The Reynolds number for the laminar/turbulent transition is denoted by Re_{crit}. The critical Reynolds number can be taken as the intersection of the lines for laminar and turbulent flow. If determined in this way, the critical Reynolds number often lies somewhere between the lower and upper critical Reynolds number because the data start to deviate from the laminar line at Re ≈ 200, after which the flow will be very unstable until it reaches fully developed flow at approximately Re ≈ 10^4. McNeil *et al.* (1999) reported that for Reynolds numbers up to 50, only the viscous forces are important. The sudden change in the area will cause the flow to expand gradually into the smaller pipe. At Reynolds numbers above 200, the flow is laminar, but the sudden change in area will cause the flow to enter the pipe jet-like and inertia forces

must be considered. This behaviour is similar to turbulent flows. Work done on non-Newtonian fluids often included Newtonian fluids as the data fell on the same line. For Newtonian fluids, Re_N is used whereas for non-Newtonian fluids Re_{MR} or Re_3 is used.

Table 2.6: Laminar/turbulent transition for contractions

CONTRACTION RATIO, β_{con}	Re_{crit}	REFERENCE
0.205	200	Pienaar, 1998
0.445	200	Edwards *et al.*, 1985
0.463	200 - 1800	Pienaar, 1998
0.500	3913	Ma, 1987
0.660	200	Edwards *et al.*, 1985

The reason for the discrepancy in the results of Ma (1987) compared with those of Pienaar (1998) and Edwards *et al.* (1985) is possibly due to the fact that the lowest Reynolds number that was tested was 500, already in the transition region. Edwards *et al.* (1985) tested up to Reynolds numbers of 500, just enough to show that the loss coefficient starts to deviate from the laminar line at $Re \approx 200$.

2.10 PREDICTION OF LOSS COEFFICIENTS AND COMPARISON WITH EXPERIMENTAL DATA

2.10.1 Laminar Flow

Edwards *et al.* (1985) correlated their results for $\beta_{con} = 0.445$ and $\beta_{con} = 0.660$ as

$$k_{con} = \frac{110}{Re} \tag{2.66}$$

and

$$k_{con} = \frac{59}{Re} \tag{2.67}$$

respectively, using Re_N for Newtonian fluids and Re_{MR} for fluids with pseudoplastic behaviour.

Ma (1987) correlated the results for $\beta_{con} = 0.5$ as

$$k_{con} = \frac{900}{Re} \tag{2.68}$$

using Re_N for Newtonian fluids and Re_{MR} for fluids with pseudoplastic behaviour and those fluids exhibiting a yield stress.

Pienaar (1998) correlated the results for $\beta_{con} = 0.205$ and $\beta_{con} = 0.463$ as

$$k_{con} = \frac{1300}{Re} \tag{2.69}$$

and

$$k_{con} = \frac{640}{Re} \tag{2.70}$$

respectively, using Re_N for Newtonian fluids and Re_{MR} for fluids with pseudoplastic behaviour and Re_3 for fluids with a yield stress.

Rao (1986) suggested the following equation to calculate k_{con} for $Re < 250$ both Newtonian and non-Newtonian fluids, provided that the appropriate Reynolds number is being used,

$$k_{con} = 1.32 + \frac{159(1-\beta_{con}^2)}{Re}. \tag{2.71}$$

ESDU (1989) suggested a similar expression for the prediction of the loss coefficient in laminar flow for Newtonian fluids that is valid for $Re < 10^4$,

$$k_{con} = \left(0.32 + \frac{159}{Re}\right)(1-\beta_{con}). \tag{2.72}$$

McNeil and Morris (1995) used a semi-empirical mechanistic approach to develop a one-dimensional flow model for predictions of frictional losses through expansions and extended this approach to contractions. The procedure for calculating the loss coefficient involves the following:

- Determine the diameter ratio, β, and the geometry factor, G_N

$$G_N = 0.127\,(1-\beta^2) \tag{2.73}$$

- Determine the throat Reynolds number, Re_t

$$Re_t = \frac{Re_u}{\beta} \tag{2.74}$$

- Determine the core-area fraction, α_t

$$\alpha_t = 0.5 + \gamma\left(1 - \exp(-B)(G_N Re_t)^{1/3}\right) \tag{2.75}$$

where

$$\gamma = 0.23\left(1-\beta^{10}\right)\left(1-\exp\left(-10\left(1-\beta^{1.04}\right)\right)\right) \tag{2.76}$$

$$B = 0.04 + 0.001\exp\left(6\beta^{3.5}\right) \tag{2.77}$$

- Determine the throat momentum (c_{mt}) and kinetic energy correction (c_{et}) factors

where

$$c_{mt} = \frac{0.6220}{\alpha_t} + \frac{0.04466}{(1-\alpha_t)} \tag{2.78}$$

$$c_{et} = \frac{0.4906}{\alpha_t^2} + \frac{0.009437}{(1-\alpha_t)^2} \tag{2.79}$$

- Determine the throat friction-factor coefficent, λ_t

$$\lambda_t = 16 + 22.27\left[\frac{(\alpha_t - 0.5)}{(0.75-\alpha_t)}\right]^{0.858} \tag{2.80}$$

- Determine the loss coefficient, k_N

$$k_N = (1+\beta^2)(c_{mt} - c_{mu}\beta^2) + \beta^4 c_{eu} - c_{et} + \frac{4}{3}\frac{(1-\beta)}{3(1+\beta)Re_t G_N}\left[\lambda_t(1+2\beta) + \beta^2\lambda_u(2-2\beta-3\beta^2)\right] \quad (2.81)$$

The deficiencies highlighted by McNeil and Morris (1995) were that not all the data was modelled because the data available did not give enough insight into the flow behaviour of the fluid through the contraction, and more experimentation is needed. Another concern was the use of the unproven two-stream model in interpreting the data. The determination of the flow mechanisms is essential and more fundamental measurements are needed to develop and validate the approach.

A comparison of Eq. (2.66), (2.68) and (2.70) with experimental results is shown in Figure 2.10 as well as a comparison of the correlations obtained by Edwards *et al.* (1985), Ma (1987) and Pienaar (1998). The expression suggested by Rao (1986) is based on the experimental work done by Edwards *et al.* (1985). The correlation and the experimental data of Ma (1987) fell within the experimental scatter of the experimental loss coefficient data of Pienaar (1998). The experimental data represents Newtonian fluids as well as fluids with pseudoplastic and yield pseudoplastic behaviour. It is not clear why the experimental results of Pienaar (1998) and Ma (1987) are different from the experimental results of Edwards *et al.* (1985). Both Ma and Edwards measured the pressure gradient upstream and downstream, while Pienaar measured the total pressure drop across the entire system. One would therefore expect the work of Edwards *et al.* and Ma to correlate better because a similar methodology was applied compared with that of Pienaar.

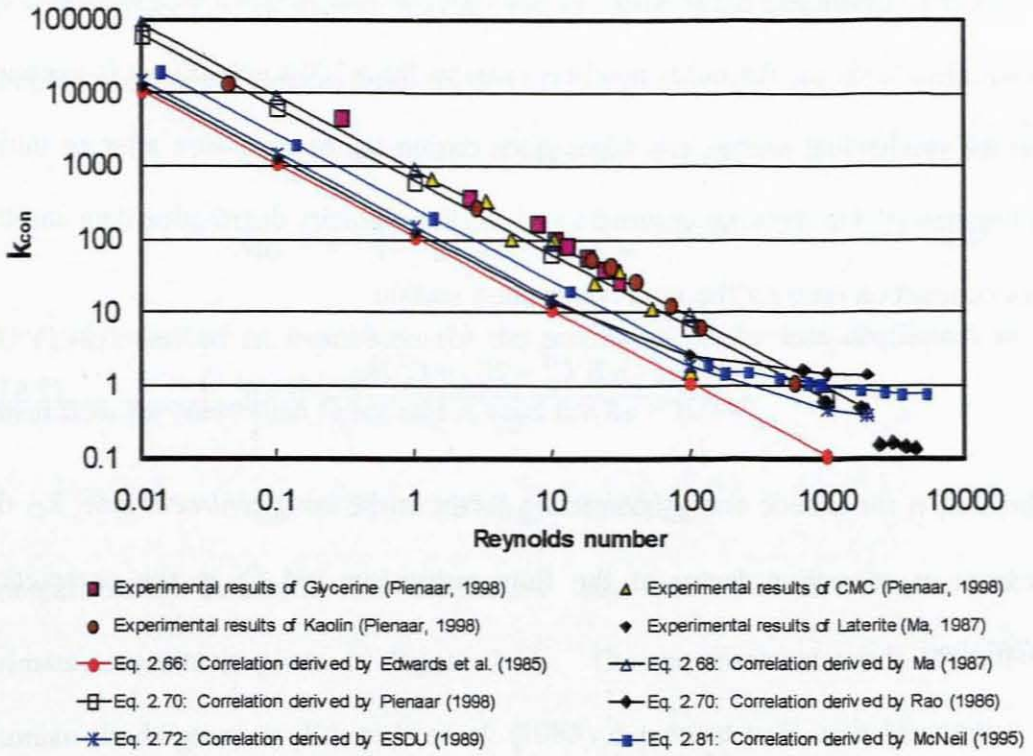

Figure 2.10: Comparison of correlations for laminar flow with experimental data for a contraction ratio $\beta \approx 0.5$

2.10.2 Turbulent Flow

Miller (1978), ESDU (1989) and Idelchik (1986) presented design methods to predict pressure losses through pipe contractions based on experimentally determined pressure loss coefficients.

The static pressure drop due to the contraction is given by ESDU (1989) as

$$\Delta p = \tfrac{1}{2}\rho V_2^2\left(k_{con} + \alpha_3 - \alpha_0\beta_{con}^2\right) \qquad (2.82)$$

where α_3 and α_0 are the kinetic energy correction factors which allow for non-uniform velocity profiles and β_{con} is the contraction ratio expressed as the area ratio of the smaller to the larger pipe.

Kays (1950) developed a theory for the prediction of contraction loss coefficients for Newtonian fluids for Reynolds numbers ranging from 500 to 10000. It is assumed that the mechanical energy loss takes place during the re-expansion after an initial contraction (C_c) to the *vena contracta* and requires velocity distribution data and the area contraction ratio for the *vena contraction* section.

$$k_{con} = \frac{1-\alpha_1\beta^2C_c^2-2C_c+C_c^2 2k_{d3}}{C_c^{\,2}} - \left(1-\beta_{con}^2\right), \qquad (2.83)$$

where α_1 is the kinetic energy correction factor at the *vena contracta* side, k_{d3} the momentum correction factor at the flow expansion and C_c is the contraction coefficient.

Although the literature suggests that the loss coefficient is independent of the Reynolds number at high velocities, Bullen *et al.* (1987) suggest a Reynolds number dependence at high velocities and present another method of prediction. The work was an extension to that of Kays (1950), which now included the losses due to recirculation at the contraction plane and at the *vena contracta*, while taking into account the recoverable and non-recoverable pressure losses. Also presented in this work was the dependence of the loss coefficient on the inlet sharpness of the contraction plane

$$k_{con} = \frac{2g\overline{A_2^{-2}}h_A}{Q} - \left[1-\beta_{con}^2\right] \qquad (2.84)$$

where h_A is the actual head loss consisting of a recoverable and non-recoverable pressure loss.

Holland and Bragg (1995) presents an equation to calculate the loss coefficient k_{con} for turbulent flow of Newtonian fluids

$$k_{con} = 0.4[1.25 - \beta_{con}] \text{ when } \beta_{con} < 0.715 \quad (2.85)$$

$$k_{con} = 0.75[1.0 - \beta_{con}] \text{ when } \beta_{con} > 0.715. \quad (2.86)$$

ESDU (1989) derived an expression for the prediction of the loss coefficient in turbulent flow for Newtonian fluids that is valid for $Re > 10^4$

$$k_{con} = 0.539 - 0.374\beta_{con} - 0.165\beta_{con}^2. \quad (2.87)$$

A comparison of turbulent loss coefficient data from various sources with experimental results is given in Figure 2.11. The experimental work of non-Newtonian fluids given by Edwards *et al.* (1985) compared well with Newtonian data given by Perry and Chilton (1973).

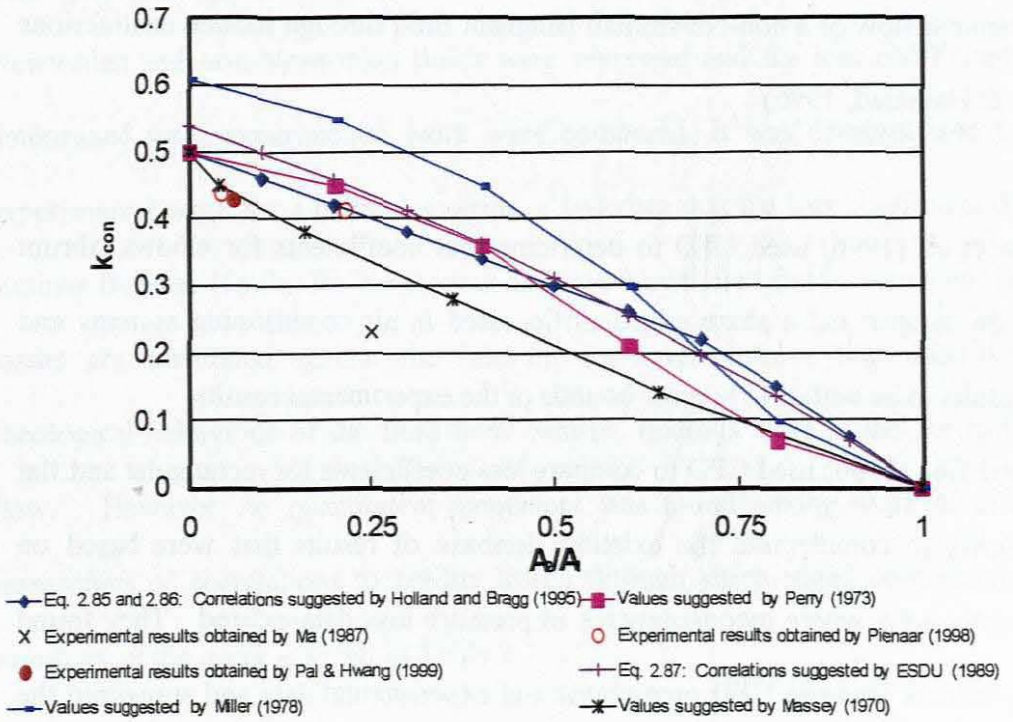

Figure 2.11: Comparison of turbulent loss coefficient data for sudden contractions

2.11 CFD ANALYSIS TO EXTEND EXPERIMENTAL DATA

The sudden contraction, due to its geometrical simplicity and hydrodynamic complexity, has been used as a benchmark problem in computational fluid mechanics. It is used to test various numerical methods as well as to validate the constitutive equations used to characterise the rheology of non-Newtonian fluids. The sudden contraction geometry has often been used to study the entry length and the prediction of the pressure drop in the entrance region and this work has often been associated with flows and pressure losses through contractions. This work in many cases paints only half the picture, because for viscous fluids the upstream developments may add considerably to the overall pressure loss especially in laminar flow where an upstream vortex is present (Bogue, 1959). Other numerical studies were the investigation on the effect of moderate and high Reynolds numbers on the laminar flow of a non-Newtonian Bingham fluid through sudden contractions (Vradis & Hammad, 1996).

Mumma *et al.* (1996) used CFD to determine loss coefficients for elbows, abrupt exits, gate damper and a sharp-edged orifice used in air conditioning systems and found results to be within 15% error bounds of the experimental results.

Riffat and Gan (1996) used CFD to compare loss coefficients for rectangular and flat oval elbows to complement the existing database of results that were based on experiments only, where inconsistencies in pressure loss data existed. They found good agreement between CFD predictions and experimental data and supported the use of CFD to expand the experimental studies that are expensive, laborious and time- consuming.

Only one study was found that derived an approximation for the excess pressure drop using the finite-element code FLUIDITY based on a solution obtained by Sampson to the problem of flow through a sudden contraction (Sisavath *et al.*, 2002). An approximation was derived for the loss coefficient constant as shown in Eq.(2.88)

$$C_{con} = 6\pi\left(1-\frac{R_1^2}{R_2^2}\right). \tag{2.88}$$

This work was, however, limited to creeping flow, but at a Reynolds number of 10, it approximates that of ESDU as shown in Eq. (2.72).

2.12 SUMMARY

The equations to determine loss coefficients for laminar and turbulent flow for both Newtonian and non-Newtonian fluids were reviewed and the loss coefficient data determined from experimental work were compared. It was demonstrated by the experimental work for a particular series of test data that the loss coefficient data in laminar flow are similar for Newtonian and non-Newtonian fluids, provided that the losses are correlated against the relevant Reynolds number that describes the rheological behaviour of the fluid best. Similar findings were found for turbulent flow. However, no quantitative agreement was found among work of different researchers or correlations to predict losses through sharp-edged contractions. A summary of the work is given in Table 2.7.

Table 2.7: Conclusions and equations on loss coefficient data for sudden contractions

	LAMINAR	TURBULENT
NEWTONIAN	The loss coefficient becomes inversely proportional to the Reynolds number at low Reynolds numbers (Miller, 1978).	The loss coefficient is independent of the Reynolds number. It increases as the contraction ratio decreases.
Equations for Newtonian fluids	$k_{con} = \frac{C_{con}}{Re}$ **(Eq. 2.61)** $k_{contr} = 1.32 + \frac{159(1-\beta_{con})}{Re}$ **(Eq. 2.71)** **(Eq. 2.81)**[1]	$k_{con} = 0.4[1.25-\beta_{con}]$ when $\beta_{con} < 0.71$ **(Eq. 2.85)** $k_{con} = 0.75[1.0-\beta_{con}]$ when $\beta_{con} > 0.715$ **(Eq. 2.86)** $k_{con} = 0.539 - 0.374\beta_{con} - 0.165\beta_{con}^2$ **(Eq. 2.87)** **(Eq. 2.81)**
NON-NEWTONIAN	C_{con} is similar as for Newtonian fluids. Non-Newtonian behaviour can be accounted for by using the Reynolds number best describing the rheology of the fluid. This is based on work done by Edwards *et al.*(1985), Rao (1986), Ma (1987), Pienaar (1998) and Pal and Hwang (1999).	Most experimental work suggests that the loss coefficients are similar to those for Newtonian fluids.
Equations for non-Newtonian fluids	$k_{con} = \left(0.32 + \frac{159}{Re}\right)\left(1-\beta_{con}^2\right)$	-
CFD	$C_{con} = 6\pi(1-R_1^2/R_2^2)$ **(Eq. 2.88)**	-

[1] *This Equation is too long to fit in space provided and can be looked up in the text on page* 52. It is valid for both laminar and turbulent flow.

2.13 CONCLUSIONS

The flow behaviour through straight pipes for both Newtonian and non-Newtonian fluids has been described as it plays an important role in the analysis of fitting losses. The various Reynolds numbers used for Newtonian and non-Newtonian fluids were introduced and described. For Newtonian fluids, the Newtonian Reynolds number Re_{Newt} was used, for fluids exhibiting pseudoplastic and yield pseudoplastic behaviour the generalised Metzner & Reed Reynolds number Re_{MR} and the Slatter Reynolds number Re_3 were used respectively.

A summary of work done on the flow behaviour of Newtonian and non-Newtonian fluids through contractions as well as the experimental investigations and the predictive correlation derived from these experiments was presented and discussed and the main conclusions are as follows:

1. General agreement among the work of researchers exists for turbulent flow through contractions.
2. The prediction of the laminar flow loss coefficient constant, C_{con}, is based on experimental data except for one case where it was found by an analytical method based on Sampson's rule. Good agreement was found between the model and CFD. This work was, however, not verified by experiment.
3. There is still little agreement between experimental work and numerical and theoretical studies. Theoretical and numerical investigators question the reliability of the experimental work to explain these discrepancies and vice versa for experimentalist.

4. The flow of a Newtonian fluid through a sudden contraction is not a solved problem owing to what has been found in the available literature.

2.14 RESEARCH ASPECTS IDENTIFIED

It is evident from the literature review that there are certain aspects that need to be researched. These are as follows:

- There is a lack of experimental data for flow through sudden contractions, especially at low Reynolds numbers for both Newtonian and non-Newtonian fluids.
- The data that is available from various researchers do not agree and this issue needs to be addressed and resolved before any further experimental studies can be done for any other fittings.
- Comparison between experimental data and theoretical modelling is not good and this issue needs to be addressed.
- There is a need to establish dynamic similarity for geometrically similar contractions.
- Experimental studies are very time consuming and the use of CFD to extend the existing database of knowledge (especially for pressure drop determination) for the investigation of flow through sudden contractions should be validated.
- Most investigations on sudden contractions have concentrated on the losses associated with developing flow in the entry length downstream of the contraction plane. However, for low Reynolds numbers laminar flow, the opposite is true, and the losses associated with flow phenomena upstream of the contraction plane need further qualitative and quantitative investigation.
- Using a contraction bypasses any debate regarding whether the length of the fitting should be included or excluded.
- It is fundamentally important to formulate experimental and analytical protocols to eliminate discrepancies in the final loss coefficient values because the literature contains several divergent approaches.

CHAPTER 3

CHAPTER 3
EXPERIMENTAL INVESTIGATION

3.1 INTRODUCTION

The flow phenomena through sudden contractions were investigated in the Flow Process Research Centre (FPRC) at the Cape Technikon with the objectives of both scrutinising, formulating and validating the experimental procedures for determining loss coefficient data for pipe fittings and to produce loss coefficient data for design purposes. Sudden contractions were used for this study because of their geometric simplicity.

A study was previously conducted at the FPRC using a versatile research instrument, the Balanced Beam Tube Viscometer (BBTV) (Slatter *et al.*, 1997; Pienaar, 1998). The results were compared with similar experimental studies in the literature. The results Jadallah (1980) obtained were lower than that of Pienaar (1998) and those obtained by Ma (1987) were higher than those of Pienaar. The difference in results was especially evident in the laminar region. It was clear from a state-of-the-art literature review (Pienaar *et al.*, 2001), that the deviations in results for what is perceived as a relatively simple problem were unacceptable. It is therefore critically important that some light be shed on the discrepancy of published results before any further work can be undertaken for all types of pipe fittings. An experimental rig was designed, constructed and commissioned to investigate this problem and to extend the work done on non-Newtonian fluids flowing through

contractions to three diameter ratios. Jadallah (1980) tested two contraction ratios and Ma (1987) tested one.

In this chapter the following aspects will be discussed:

- The experimental apparatus.
- The experimental procedure.
- The error analysis.
- Water results in straight pipes.
- Properties of fluids.

3.2 DESCRIPTION OF THE EXPERIMENTAL RIG

The experimental apparatus consisted of a 50mm progressive cavity positive displacement pump, two flow meters (a magnetic flow meter and a mass flow meter), a 42.26mm internal diameter upstream straight pipe section and a specially machined contraction union allowing for fitting straight pipe sections of various diameters downstream. A schematic diagram of the apparatus is given in Figure 3.1.

The 200-litre storage tank was fitted with a mixer driven by a motor of 1.5 kW to ensure that solids were kept in suspension during the experiments with slurries. The pump was fitted with a variable speed drive to enable tests at different flow rates. A three-way valve was located at the pump outlet to allow a by-pass of fluid back to the storage tank to enable the measurement of low flow rates in the contractions. The fluid passed through a heat exchanger followed by a surge damper 50mm in

diameter and 0.4m high. The fluid then passed through the two flow meters in series.

Two flow meters were used to ensure accurate flow measurements.

- A Krohne IFC 010D electromagnetic flow meter of 42mm internal diameter was mounted vertically.
- A mass flow meter (Massflo® by Danfoss Instrumentation) with an internal diameter of 21mm was installed horizontally. The flow meter is made of stainless steel and measures flow directly in kg/h, as well as density, temperature and sugar concentration (Brix). The signal converter MASS 6000 has a current output of 4 - 20 mA, a load less than 800 ohm and an adjustable 0 - 30 seconds time constant. The low-flow cut-off is 0 - 9.9% of the maximum flow rate.

The flow meters were calibrated using the "bucket and stopwatch" method.

The upstream and downstream straight pipe sections were each 5m long to ensure fully developed flow at the inlet and redevelopment downstream of the contraction. The pipes were fitted with pressure tappings to measure the pressure grade line across the contractions. The distance between the tappings was decreased and increased logarithmically towards and after the contraction. The tappings were constructed by machining solid PVC rods of 30mm diameter. A 12mm bore was also drilled half way and threaded for the valves to be screwed in. These sections were glued at the specified distances. The tappings of 3mm were drilled carefully in the pipe walls with length to diameter ratios greater than four to ensure accurate readings (Hanks, 1975; Goldstein, 1983). All burrs were carefully removed from the

inside edge of each tapping. All threads were assembled with thread tape to prevent any leakages. After this, the pipe internal diameter was measured before the pipe was mounted on the rig. The pipes and tappings were mounted horizontally using a spirit level.

All pressure tappings were connected to 3mm Nylon tube pressure lines filled with water. The pressure from the test point was transmitted to the pressure transducers by opening the valve that connects the tapping to the pressure line. The valves as well as the pressure tappings were numbered from 1 to 24.

Solids pods were installed between the pressure tap and the pressure line to collect any solid particles coming from the test fluid, preventing it from entering the pressure lines and the transducers. Each pod was fitted with a valve on top for flushing away any air bubbles and at the bottom for flushing away the solid particles or viscous fluids to the collecting gutter. Four valves on the main pressure line allowed isolation of lines 1, 2, 3 or 4 so that the differential pressure could be measured between different tappings. A schematic diagram of this is given in Figure 3.2.

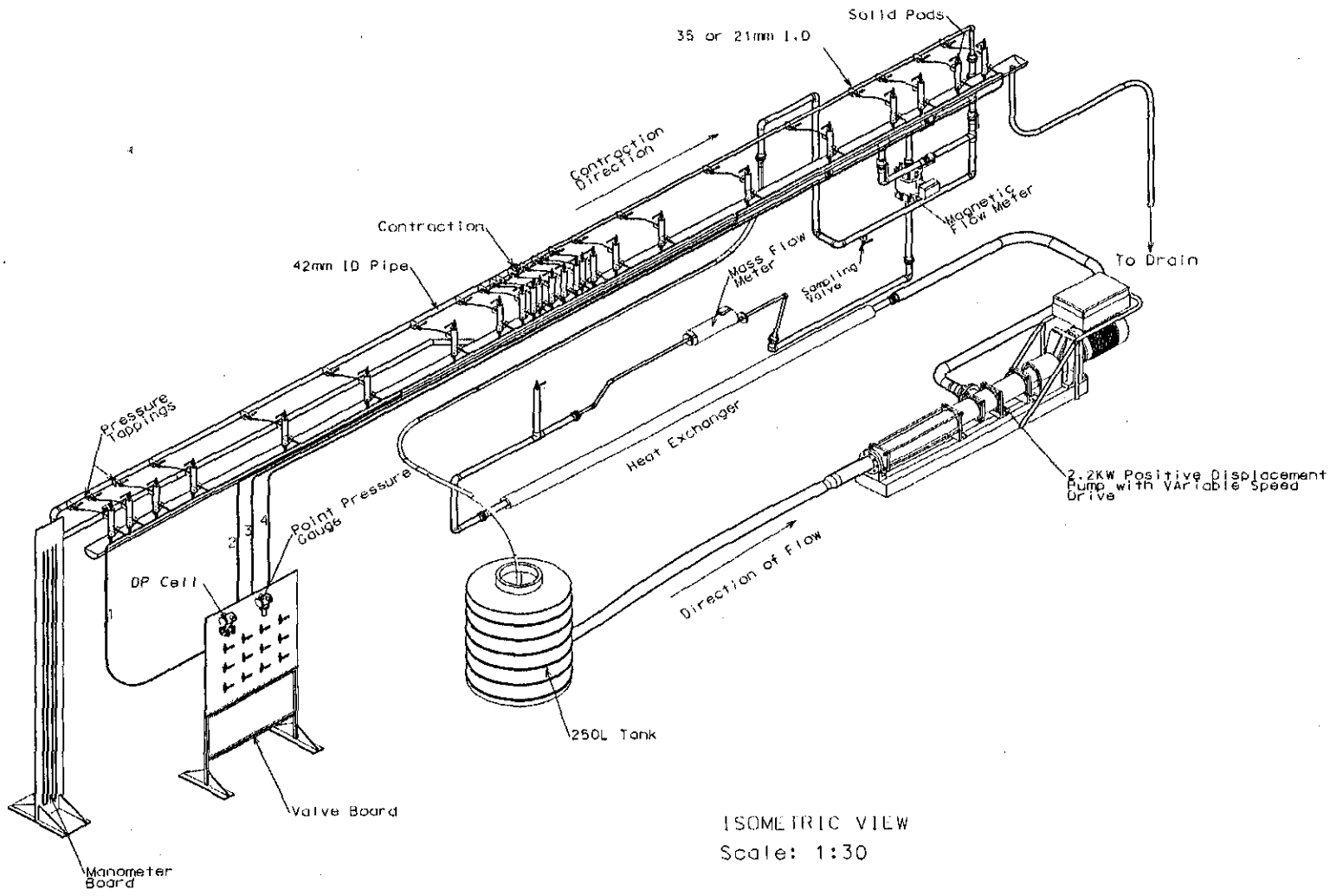

Figure 3.1: Schematic diagram of experimental apparatus

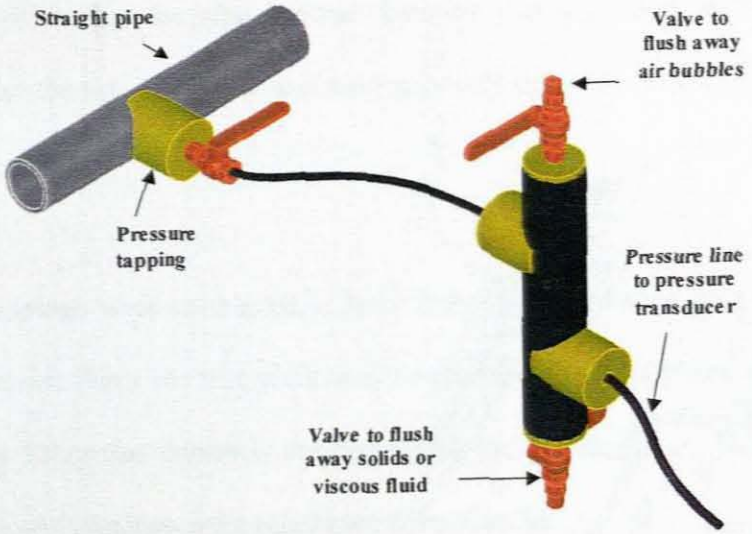

Figure 3.2: Pressure tapping, solids pod and connection to pressure transducer

Two types of pressure transducers were used for measuring the pressure grade line and the differential pressure difference across the straight pipe:

- A Fuji Electric point pressure transducer (PPT) type FHPWO2V1-AKCYY OY [GP] serial number A1K15295 version 25.0. It has a maximum range of 130 kPa with an accuracy of 0.25%. The output of this instrument is a DC current ranging from 4 to 20 mA, which is proportional to the applied pressure. The ranges and span are adjustable electronically with a Hand Held Communicator (HHC) to a turndown ratio of 10.
- A Fuji Electric differential pressure transducer (DP cell) type FKKW35V1-AKCYY AA [DP] serial number A1F1026T version 25.0 was used to measure differential pressure between two points. It has the same characteristics as the

PPT, i.e., maximum range of 130 kPa turned down to a minimum of 13kPa with an accuracy of 0.25%, using the HHC.

The hand-held communicator [HHC] used was a Fuji Electric type FXW 10 AY1-A3. This portable instrument allowed communication with both DP cell and PPT. It has some interesting features such as data display, range, span, time constant, unit, calibration, etc. It was used mainly to change the ranges and to check the data display with the logged values on the test program.

Two U-tube manometers were used for calibration of the pressure transducers:

- a mercury-water manometer was used for calibration in the higher pressure range ($\geq$ 20 kPa);
- a water- air manometer was used to calibrate in the lower pressure range ($\leq$ 20 kPa).

A data acquisition system was used to collate the data. It consisted of an HP 34970A data acquisition / switch unit equipped with various channels to convert analogue signals from the pressure transducers and flow meters to digital signals that are logged to the computer. The 4 – 20 mA transducer outputs are converted to 0.4 – 2 V using a precision 250 Ω resistor. The computer used with the DAU was a Celeron 300 that captured and processed all the data. Test programs were written in Visual Basic 6. The data analysis was done using a programmed Microsoft Excel spreadsheet.

The rheology of the test fluids was also obtained from a Paar Physica MCR 300 rotational rheometer. This instrument was used in cases where the fluids were less viscous and for which sufficient laminar flow could not be achieved on the straight pipes of the Fitting Rig. Those fluids were tested in the rheometer over the same range of shear rates and temperatures encountered during the HGL test.

3.3 STRAIGHT PIPES

The internal pipe diameter (D) was determined by measuring the mass of water (M_w) required to fill a known length of pipe (L). The diameter was then calculated from Eq. (3.1).

$$D = \sqrt{\frac{4M_w}{\pi \rho_w L}} \tag{3.1}$$

The diameter was measured between various tapping distances for each pipe.

The same procedure was followed for each pipe and the average internal diameter for each pipe is given in Table 3.1.

Table 3.1: Nominal diameter and internal diameter of pipes used

NOMINAL DIAMETER [mm]	INTERNAL DIAMETER [mm]
13	9.28
25	21.0
40	36.0
50	42.3

3.4 CONTRACTING UNION

The upstream pipe diameter was kept constant while the downstream pipe was replaced by one of different diameter. A specially machined union was used to construct the sudden contraction. The pipes were mounted flush leaving no gaps that would influence the flow patterns. The upstream and downstream pipe diameters and the resulting contraction ratio in both diameter and area ratio of downstream to upstream pipes are shown in Table 3.2.

Table 3.2: Contraction ratios obtained for upstream and downstream pipes

UPSTREAM DIAMETER [mm]	DOWNSTREAM DIAMETERS [mm]	DIAMETER RATIO, β [D_D/D_U]	AREA RATIO, β^2 [A_D/A_U]
42. 3	9.28	0.219	0.0480
42. 3	21.0	0.496	0.246
42. 3	36.0	0.851	0.724

3.5 EXPERIMENTAL PROCEDURE

This section will describe the experimental procedure used to obtain the measured variables, i.e., velocity and pressure drop. The experimental procedure consists of calibrating the instruments, measuring the pressure drop in the straight pipe sections to determine the viscous properties of the fluid, and to measuring the pressure grade line across the contraction.

3.5.1 Calibration

Prior to any experimental study it is important to ensure that the instruments give reliable results. This is achieved by means of calibration.

3.5.1.1 Differential Pressure Transducer

The differential pressure transducer was calibrated for ranges ranging from 0 to 130 kPa using a U-tube manometer. The procedure is described below.

1. Air bubbles and solids are flushed from all lines using the main water supply connected to the pressure line.
2. The differential pressure transducer is connected to the manometer so that the high and low-pressure sides are connected to the high and low-pressure sides of the U-tube manometer.
3. A differential head, corresponding to the upper bound of the range, is set up in the glass tubes of the U-tube manometer.
4. The differential head is physically measured with a fixed tape measure within ± 1 mm accuracy while at the same time the DP cell output is logged.
5. The differential head is then decreased uniformly in 10 parts and step 4 repeated, until the equilibrium is attained.

The calibration equation is obtained by performing a linear regression on the pressure based on the differential heads and the transducer DC voltage output. The coefficient of correlation R^2 should be at least 0.9999, as shown in Figure 3.3.

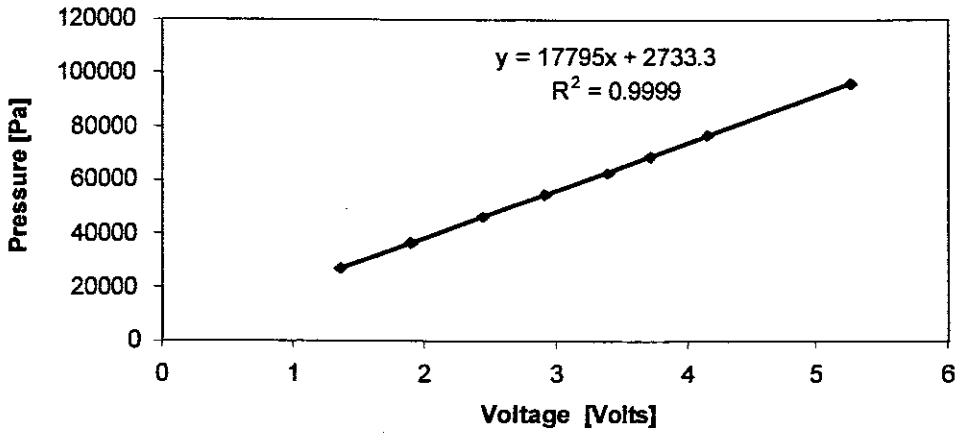

Figure 3.3: Typical calibration curve for differential pressure transducer

3.5.1.2 Flow meter

The two flow meters work on two different basic principles, i.e., gravimetric and magnetic; they were mounted in series to measure the same flow rate. Having the two flow meters in series was particularly useful when non-conductive materials such as the Newtonian viscous oil was tested, in which case the magnetic flow meter did not work. The flow meters were calibrated using the bucket and stopwatch method. Care was taken that the flow readings from the two instruments were always the same to within ±0.001 l/s. When the discrepancies were significant between the two instruments (especially at very low flow rates), the flow rate was measured using the bucket and stopwatch method. The minimum flow rates that could be measured accurately by the magnetic and mass flow meter were 0.05 and 0.02 l/s respectively.

3.5.2 The Test Procedure

The final product of a test is the plot of k_{con} versus Reynolds number. To achieve this, the following steps were followed and will be described in detail in following sections:

- The fluids are loaded in the rig and circulated for approximately thirty minutes to ensure a consistent and homogeneous mixture so that a representative sample can be taken.
- A sample is taken from a sampling tap to measure the relative density.
- A straight pipe test is done for the rheological characterisation as described in Section 3.5.4. A sample is sent to the rheometer for comparison.
- The pressure grade line is measured (PGL test) from tap 5 up to 20 as described in Section 3.5.3.
- The pump speed is increased, the pressure grade line is measured and k_{con} computed as shown in Eq. (2.58).
- This is done until the maximum output of the pump or pressure transducers is reached.
- Plot k_{con} versus Reynolds numbers.
- The overall procedure is repeated for other fluids. The loss coefficient constant is calculated from all the data in the laminar region below the transitional Reynolds number of 200 as described in Chapter 4.

3.5.3 Pressure Grade Line Test

The measurement of the pressure grade line was very tedious and care had to be taken to ensure the right operating conditions to obtain the best pressure drop results. Because only one transducer was used to take the readings at 16 pressure tappings (as shown in Figure 3.4), it was important to ensure that the flow was steady before pressure drop readings could be taken. An operator was required to open the valves to each pressure pod at exact intervals to reduce variability of results. The procedures are described in detail below.

3.5.3.1 Obtaining Steady Flow

The pressure grade line test required two operators. The pump is switched on, and the fluid is left to run for a while to obtain steady flow. All pods must be flushed and filled with water beforehand.

Valve number 5 (Fig. 3.4) is opened to the pressure line. Readings are taken on the same point to ensure that the flow is steady. To ascertain this, the pressure was measured at the same flow rate and the pressure was logged and a plot of pressure versus time was constructed. Typical plots of unsteady flow, either increasing or decreasing, are shown in Figure 3.5 and steady flow is shown in Figure 3.6.

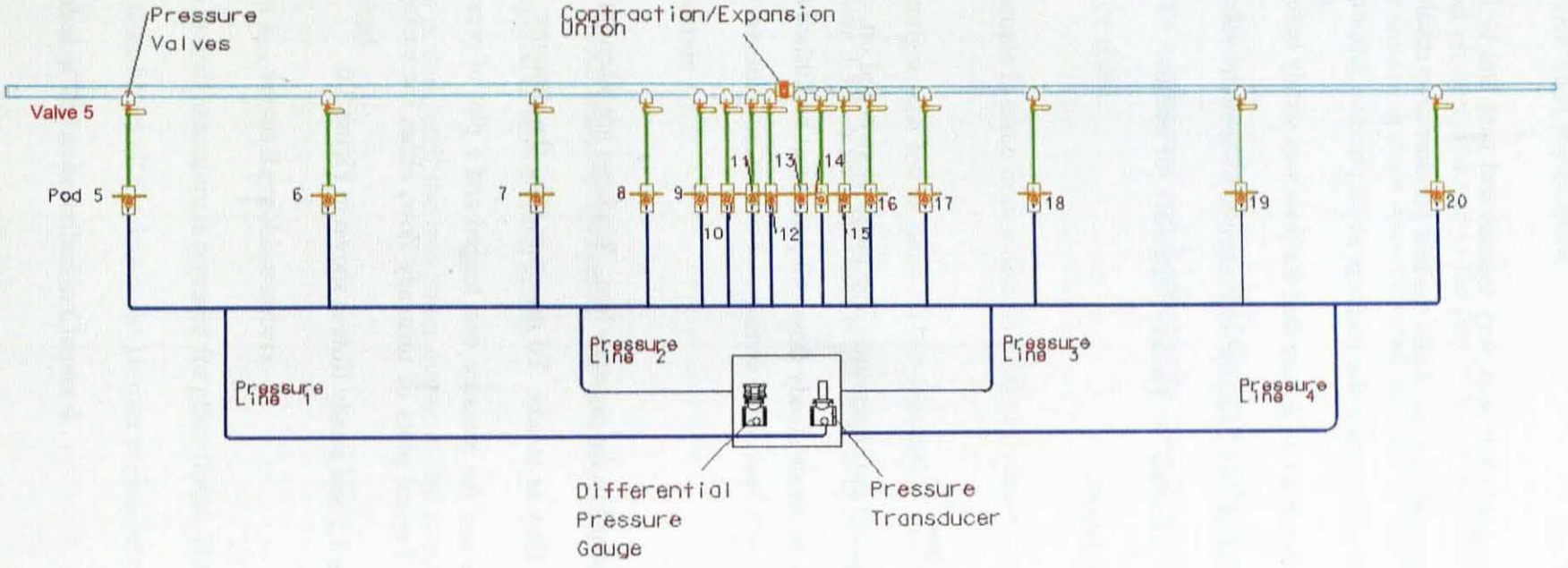

Figure 3.4: Layout of test rig before automation with only one point pressure transducers

It was observed that the pressure stabilizes after about five seconds after opening and closing a valve to a pressure pod. This elapse of time is necessary to damp the transient effects generated by the difference of pressure between pressure taps.

Figure 3.5: "Unsteady" decreasing or increasing of flow with time

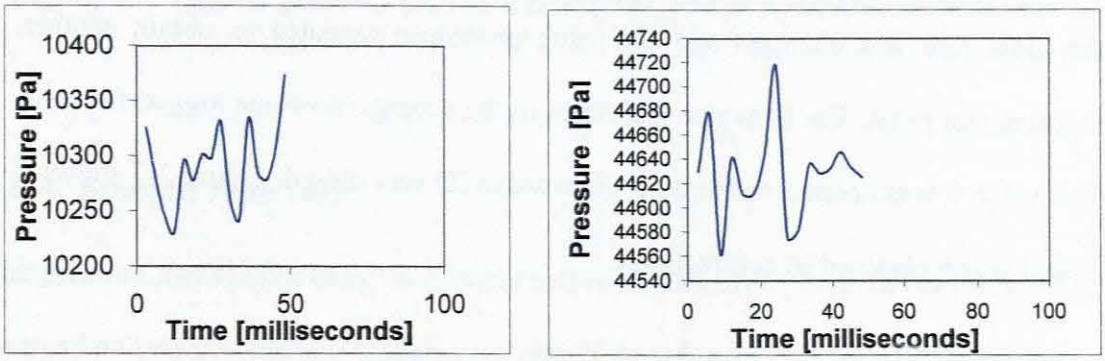

Figure 3.6: "Steady flow" pressure fluctuates evenly with time

3.5.3.2 Contraction Test

When the pressure became stable as shown in Figure 3.6, the test could start. The test was carried out as follows:

- Operator (A) on the computer logs the appropriate information such as: date, test type, material type, relative density, transducer range.

- Operator (A) takes the first pressure reading, on tapping 5.
- Operator (B) closes valve 5 and opens valve 6.
- Operator (A) waits five seconds and than takes the second pressure reading, on tapping 6.
- Operator (B) closes valve 6 and opens valve 7.
- Operator (A) wait five seconds and than takes the third pressure reading, on tapping 7.
- Operator (B) closes valve 7 and opens valve 8.

The same process was repeated until the sixteenth pressure reading was taken, on valve 20. This test run yielded one point on the graph k_{con} versus Reynolds numbers. The flow rate was changed and the same procedure repeated to obtain another experimental point. The flow rate was taken as the average flow rate logged from the time valve 5 was opened to the time when valve 20 was closed. Figure 3.7 shows a typical graph obtained in contractions.

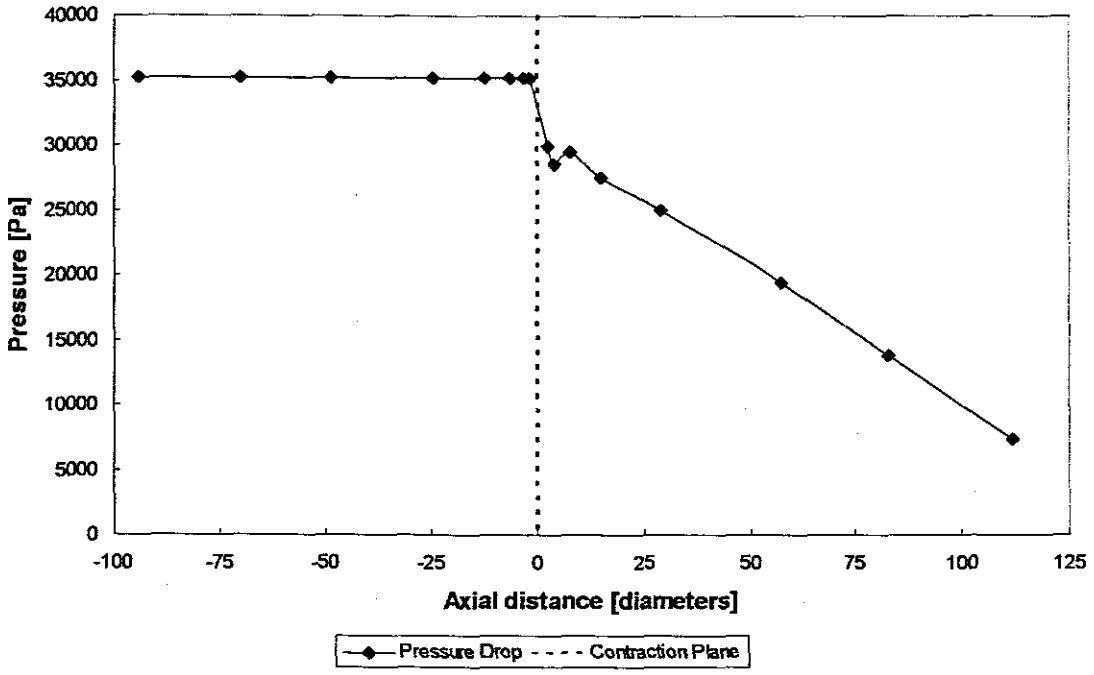

Figure 3.7: Typical graph of pressure grade line test in a sudden contraction

3.5.4 Straight Pipe Test

The pressure line is divided in two parts by closing one of the four valves provided on this line between the two tappings for which the pressure drop will be measured. One half is connected to the high side of the DP cell and the other half to the lower side. The operator increases (or decreases) the flow rates smoothly and takes pressure and flow rate readings at the same time. The same procedure is repeated until the maximum (minimum) flow is reached. One reading yields one point on the graph of shear stress versus pseudo-shear rate.

This test is performed on both pipes. The graphs obtained must be co-linear in the laminar region as shown in Figure 3.8. The rheological constants are then calculated. A sample is also sent for rheological testing on an MCR300 rheometer for

comparison and to be used in cases where unsatisfactory results are obtained in the straight pipes or when the viscosity is sensitive to small changes in temperature. In this case, the relationship between the viscosity and temperature is determined by measuring the viscosity over a range of different temperatures (also known as a temperature sweep) on the rheometer. This enabled the calculation of the viscosity at the specific temperature measured for each test. This procedure was used for the oil tests.

3.6 AUTOMATION OF TEST RIG

The test procedure described above (Section 3.5.3) was time consuming, having an operator opening and closing 16 valves to obtain one value of the k_{con} versus Reynolds number chart. Operators had to be extremely careful in opening and closing the valves to avoid discrepancies in pressure reading from one tap to another tap, which often resulted in errors and discarding of results. It was therefore decided to automate the rig by installing nine point pressure transducers, four prior to and five after the contraction. This would allow measuring the complete pressure grade line at once. Four point pressure transducers (PPT) were installed upstream of the contraction and five downstream of the contraction. The only concern was that the number of pressure points measured was reduced to 9 compared to 16 previously. The effect of reducing the number of points for extrapolation of the fully developed friction gradient to the contraction plane had to be evaluated carefully. The position of the point pressure transducers is shown in Figure 3.9.

3.6.1 Contraction Test

This test required one operator only as opposed to the manual operation that required two operators. The procedure is as follows:

1. The pressures lines must be flushed beforehand to ensure that all the lines and pods are free of any air and are full of water.
2. All the pressure valves leading to the PPT must be opened.
3. The appropriate information (date, material, density, etc.) is logged.
4. A check is conducted (Section 3.5.3.1) to ensure that steady flow is obtained.
5. The appropriate range for each PPT is selected.
6. The pressure and flow readings is taken (this operation is repeated twice at the same settings).
7. The flow rate is changed and steps 5, 6 and 7 repeated until the maximum flow rate is attained on the pump or the maximum pressure on the point pressure transducers is reached.

Note: all the experimental measurements are automatically logged by the PC via the DAU. The data are automatically processed by a spreadsheet, which calculates the Reynolds numbers and the loss coefficients.

3.6.2 Straight Pipe Test

Another advantage of the automated system was that straight pipe data could be obtained as a difference between the pressure measurements of two point pressure transducers. As the length between those two point pressure transducers is known,

the wall shear stress is obtained using Eq. (2.2), $\tau_0=D\Delta P/4L$. A typical graph of the data is shown in Figure 3.8. Only laminar data were used to obtain rheological parameters (see Figure 3.9).

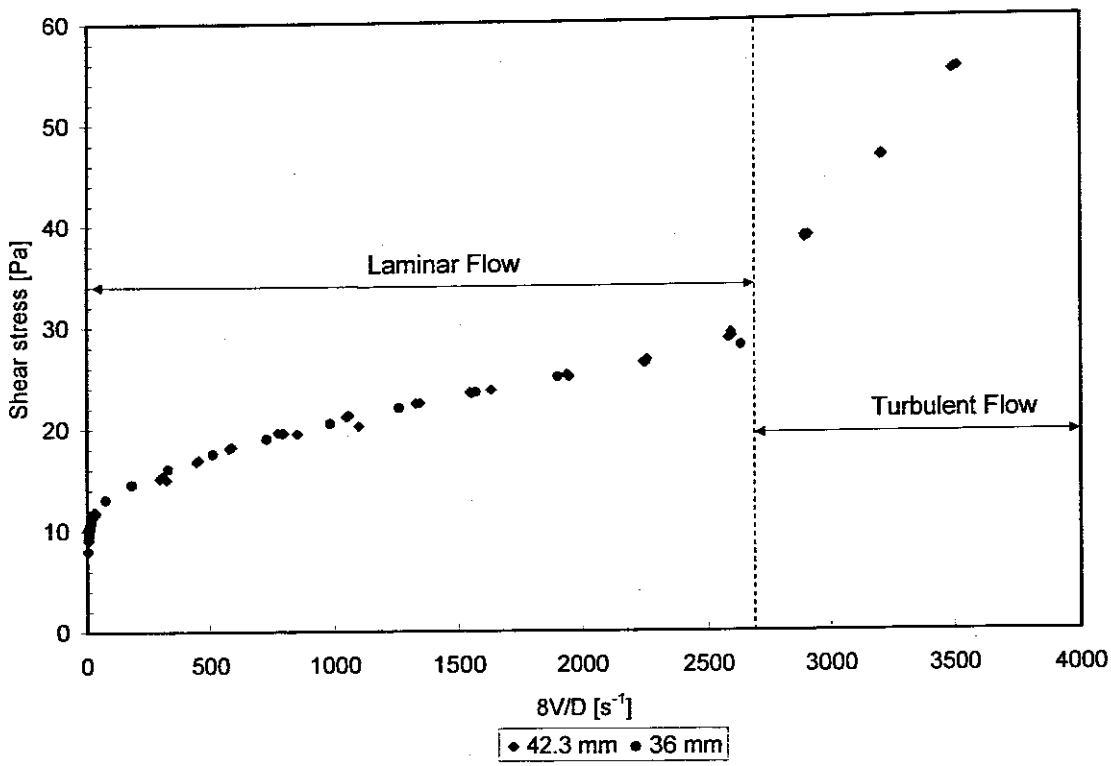

Figure 3.8: Pseudo-shear diagram obtained from the automated rig

3.7 Comparison of the Manual and the Automated System

In the manual system, the pressure distribution could be evaluated with 16 points, whereas in the automated system only 9 points were used. Besides this, the automated system has many advantages:

- A test run is completed in a relatively short elapse of time; the loss coefficient is not biased by any changes in the flow rate which could occur in the long time taken to complete one test on the manual system, considering the time to take the readings at 16 points one after the other.

- A better statistical analysis may be performed as the number of data points is increased.
- This system alleviate the operators exhaustion of opening and closing sixteen valves to obtain one experimental data point or the miscommunication between the two operators which could lead to the loss of experimental data.

3.8 EXPERIMENTAL ERRORS

When experimental work is carried out, it is important to evaluate the magnitude of uncertainty associated with the measured and computed variables.

3.8.1 Errors in Measured Variables

3.8.1.1 Axial Distance

The axial distances of pipes was measured with a tape measure graduated in mm. The absolute error on measurement is ± 0.001 m. The average tapping distance was 0.533 m resulting in a relative error in length of ± 0.2%.

3.8.1.2 Weight

All samples were measured with an electronic balance, accurate to ±0.001 g. Thus a sample of say 50 g would give rise to a relative error of ± 0.002 %.

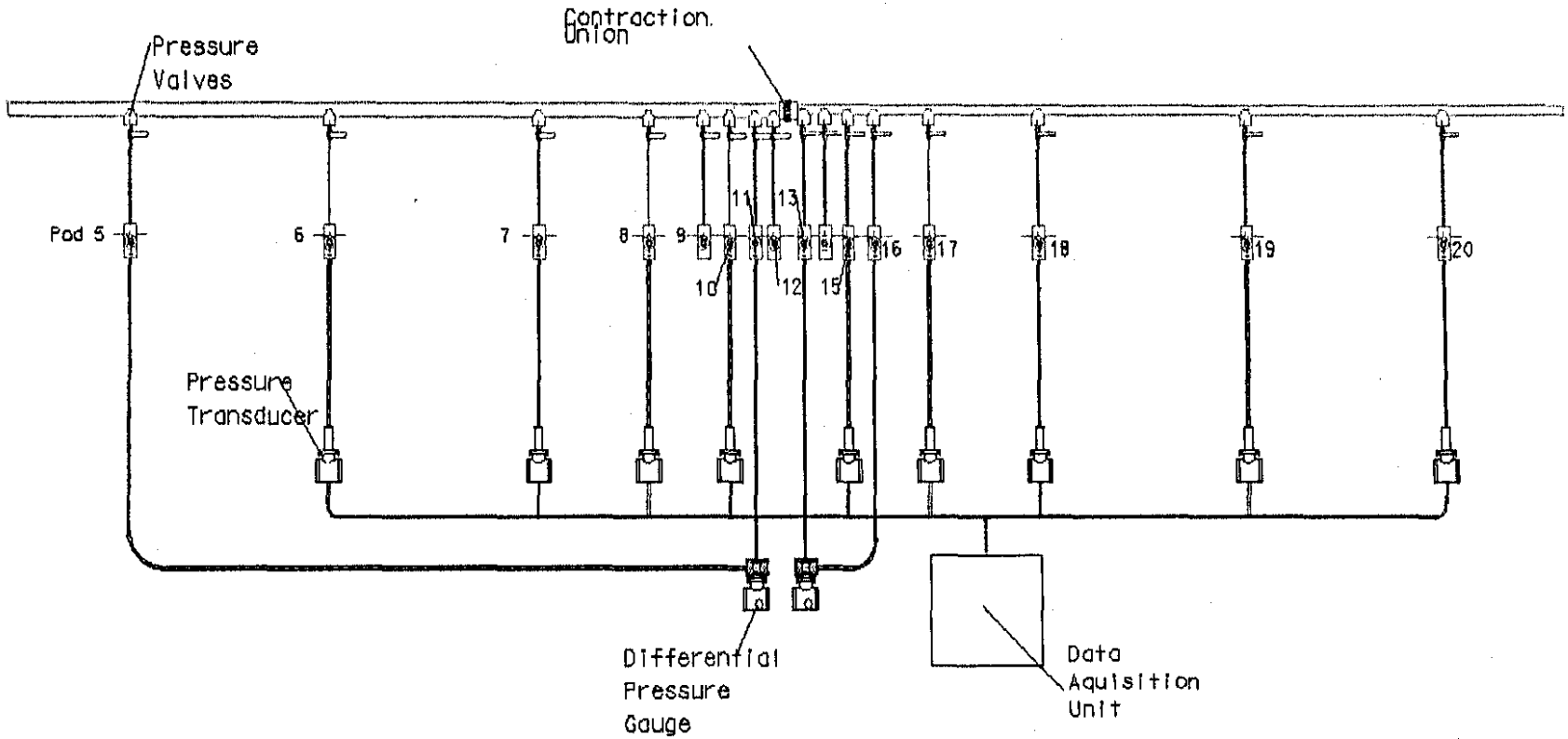

Figure 3.9: Layout of automated test rig with individual point pressure transducers

3.8.1.3 Flow Rate

Flow meters used for measurement of flow rate were accurate at ± 0.001 l/s, which can be assumed as the absolute error. The average of the two instruments was taken as long as they were within ± 1 % difference. However the repeated measurement of both instruments displayed absolute errors not exceeding 0.5 % at 99.9 % confidence level, thus the overall error can be assumed as 0.71 % (quadratic mean). A cut-off flow rate of 0.02 l/s was established for the mass flow meter and 0.05 l/s for the magnetic flow meter. Below the value of 0.02 l/s, the bucket and stopwatch method was used to measure the flow rate and sufficient time was taken to fill the bucket so that errors were negligible.

3.8.1.4 Pressure

The pressure transducers used were accurate at 0.25 % of the full range. Care was taken in calibrating the transducers so that a correlation coefficient of 0.9999 was attained. Such calibration gave rise to an average error of 0.24 %. Thus the overall error in pressure measurement was 0.35 % (quadratic mean).

3.8.2 Calculated and Combined Errors

When a quantity involves more than one independent measurement, then the errors will combine in the following way. Errors are usually assumed to be randomly distributed following the Gaussian distribution and can be quantified using the procedure recommended by Brinkworth (1968). The highest expected error can be determined using a root mean square approach.

If the quantity X is a function of N other quantities i.e, $X = \phi(a, b, c, \ldots N)$,

the highest expected error ΔX can be calculated from Eq. (3.2)

$$\left(\frac{\Delta X}{X}\right)^2 = \sum\left(\frac{\partial X}{\partial N}\right)^2\left(\frac{N}{X}\right)^2\left(\frac{\Delta N}{N}\right)^2. \qquad (3.2)$$

This error analysis has been used to quantify the errors for pipe diameter, wall shear stress, pseudo-shear rate and Reynolds numbers. In this section the equations used in the evaluation of the accuracy of principal derived variables are presented. Although typical numerical values are given, true values of accuracy depend on actual measured values.

3.8.2.1 Pipe Internal Diameter

The pipe internal diameter is a calculated variable. It is obtained from Eq. (3.1), where the measured parameters are the mass of water (M_w) and the length (L). The highest expected error in calculating the diameter is given by Eq.(3.3), which is the combination of Eq. (3.1)and Eq. (3.2):

$$\left(\frac{\Delta D}{D}\right)^2 = \left(\frac{1}{2}\sqrt{\frac{4}{\pi\rho_w M_w L}}\right)^2\left(\frac{M_w}{D}\right)^2\left(\frac{\Delta M_w}{M_w}\right)^2 + \left(-\frac{1}{2}\sqrt{\frac{4M_w}{\pi\rho_w L^3}}\right)^2\left(\frac{L}{D}\right)^2\left(\frac{\Delta L}{L}\right)^2. \qquad (3.3)$$

Eq. (3.3) can be further simplified as

$$\left(\frac{\Delta D}{D}\right)^2 = \frac{1}{4}\left(\frac{\Delta M_w}{M_w}\right)^2 + \frac{1}{4}\left(\frac{\Delta L}{L}\right)^2. \qquad (3.4)$$

The highest expected error is

$$\frac{\Delta D}{D} = \pm\frac{1}{2}\sqrt{\left(\frac{\Delta M_w}{M_w}\right)^2 + \left(\frac{\Delta L}{L}\right)^2}. \qquad (3.5)$$

3.8.2.2 Velocity

The velocity is derived from

$$V = \frac{Q}{A} = \frac{Q}{\left(\pi \frac{D^2}{4}\right)}. \tag{2.14}$$

Application of Eq. (3.2) to the above equation gives

$$\left(\frac{\Delta V}{V}\right)^2 = \left(\frac{\Delta Q}{Q}\right)^2 + 4\left(\frac{\Delta D}{D}\right)^2. \tag{3.6}$$

The velocity expected highest error is then given by

$$\frac{\Delta V}{V} = \pm\sqrt{\left(\frac{\Delta Q}{Q}\right)^2 + 4\left(\frac{\Delta D}{D}\right)^2} \tag{3.7}$$

3.8.2.3 Pseudo-Shear Rate

The pseudo-shear rate is calculated as

$$\gamma = \frac{8V}{D}. \tag{3.8}$$

Application of Eq. (3.2) to the above equation gives

$$\left(\frac{\Delta \gamma}{\gamma}\right)^2 = \left(\frac{\Delta V}{V}\right)^2 + \left(\frac{\Delta D}{D}\right)^2. \tag{3.9}$$

The expected highest error of the pseudo-shear rate in terms of measured variables can be expressed as follows:

$$\frac{\Delta \gamma}{\gamma} = \pm\sqrt{\left(\frac{\Delta Q}{Q}\right)^2 + 5\left(\frac{\Delta D}{D}\right)^2}. \tag{3.10}$$

3.8.2.4 Shear Stress

Shear stress is obtained from the relation

$$\tau_0 = \frac{D\Delta p}{4L}. \tag{2.2}$$

Application of Eq. (3.2) to the above equation gives

$$\left(\frac{\Delta\tau_0}{\tau_0}\right)^2 = \left(\frac{\Delta(\Delta p)}{\Delta p}\right)^2 + \left(\frac{\Delta D}{D}\right)^2 + \left(\frac{\Delta L}{L}\right)^2. \tag{3.11}$$

The shear stress expected highest error is then given as

$$\frac{\Delta\tau_0}{\tau_0} = \pm\sqrt{\left(\frac{\Delta(\Delta p)}{\Delta p}\right)^2 + \left(\frac{\Delta D}{D}\right)^2 + \left(\frac{\Delta L}{L}\right)^2}. \tag{3.12}$$

3.8.2.5 Reynolds Number

The Reynolds number errors are evaluated based on the Newtonian Reynolds number error as follows:

$$\mathrm{Re} = \frac{\rho V D}{\mu}. \tag{2.29}$$

Application of Eq. (3.2) to the above equation gives

$$\left(\frac{\Delta \mathrm{Re}}{\mathrm{Re}}\right)^2 = \left(\frac{\Delta\rho}{\rho}\right)^2 + \left(\frac{\Delta V}{V}\right)^2 + \left(\frac{\Delta D}{D}\right)^2 + \left(\frac{\Delta\mu}{\mu}\right)^2. \tag{3.13}$$

Equation (3.17) gives the Reynolds numbers expected highest error in terms of measured variables as

$$\frac{\Delta \mathrm{Re}}{\mathrm{Re}} = \pm\sqrt{\left(\frac{\Delta\rho}{\rho}\right)^2 + \left(\frac{\Delta Q}{Q}\right)^2 + 5\left(\frac{\Delta D}{D}\right)^2 + \left(\frac{\Delta\mu}{\mu}\right)^2}. \tag{3.14}$$

3.8.2.6 The Loss Coefficient

The loss coefficient is determined from Eq. (2.57) as

$$k_{fitt} = \frac{\frac{\Delta p_{fitt}}{\rho g} + \frac{\alpha_1 V_1^2 - \alpha_2 V_2^2}{2g}}{\left(\frac{V_2^2}{2g}\right)}. \qquad (2.57)$$

As V_1 and V_2 are linked by the area ratio β^2, the above equation can be rewritten as

$$k_{fitt} = \left(\frac{2\Delta p_{fitt}}{\rho V_2^2}\right) + \theta, \qquad (3.15)$$

where

$$\theta = \alpha_1 \beta^4 - \alpha_2. \qquad (3.16)$$

Application of Eq. (3.2) to Eq. (3.15) gives

$$\left(\frac{\Delta k_{fitt}}{k_{fitt}}\right)^2 = \left(1 - \frac{\theta}{k_{fitt}}\right)^2 \left[\left(\frac{\Delta(\Delta p_{fitt})}{\Delta p_{fitt}}\right)^2 + \left(\frac{\Delta \rho}{\rho}\right)^2 + 4\left(\frac{\Delta V}{V}\right)^2\right]. \qquad (3.17)$$

The loss coefficient expected highest error in term of measured variables could then be given as

$$\frac{\Delta k_{fitt}}{k_{fitt}} = \pm\left(1 - \frac{\theta}{k_{fitt}}\right)\sqrt{\left(\frac{\Delta(\Delta p_{fitt})}{\Delta p_{fitt}}\right)^2 + \left(\frac{\Delta \rho}{\rho}\right)^2 + 4\left(\frac{\Delta Q}{Q}\right)^2 + 16\left(\frac{\Delta D}{D}\right)^2}. \qquad (3.18)$$

Equation (3.18) suggests that the error in k_{fitt} increases as k_{fitt} becomes smaller, and conversely the error decreases, as k_{fitt} is higher. The factor θ highlights both the influence of the velocity profile and the diameter ratio on k_{fitt}. The highest expected errors on the computed variables are shown in Table 3.3.

Table 3.3: Errors of principal computed variables

PIPE DIAMETER [mm]	EXPECTED HIGHEST ERROR (± %)				
	Internal Diameter	Velocity	Pseudo-shear rate	Shear stress	Reynolds numbers
9.28	0.43	1.12	1.2	0.37	1.01
21.0	0.18	0.8	0.82	0.56	1.30
36.0	0.67	1.52	1.66	0.78	1.94
42.3	0.63	1.45	1.58	0.73	1.87

It can be shown that θ is the highest when the pipes run both in laminar flow and for the Newtonian fluids it takes the limiting values presented in Table 3.4.

Table 3.4: Newtonian values of θ for fittings tested

CONTRACTION, β	θ
0.22	-2.00
0.50	-1.88
0.85	-0.95

3.9 WATER RESULTS IN STRAIGHT PIPES

Water was tested in the straight pipes to establish credibility, accuracy and precision of the experimental apparatus, the Fitting Rig.

The pipe roughness was determined by measuring the pressure drop across a known length of pipe and by comparing it with the Colebrook-White Equation, Eq. (2.10), (King, 2002). The comparison of the experimentally obtained shear stresses (τ_0) with that of the calculated shear stresses using Colebrook-White is shown in Figure 3.10 - Figure 3.13. The values of k determined are given in Table 3.5.

Table 3.5: Pipe roughness obtained for the straight pipes

NOMINAL DIAMETER [mm]	INTERNAL DIAMETER [mm]	PIPE ROUGHNESS [μm]
13	9.28	0
25	21.0	4.4
40	36.0	0
50	42.3	19

Figure 3.10 shows results obtained for the 9.28 mm pipe. It also demonstrates how more accurate results can be obtained in the lower pressure ranges by adjusting the range of the pressure transducer by means of the hand-held communicator. It also demonstrates the repeatability of the results at higher ranges using various lengths of pipe (tapping distances L) and the same transducer set to various pressure ranges. The graph is shown on logarithmic scale so that the data obtained at lower velocities can be seen clearly.

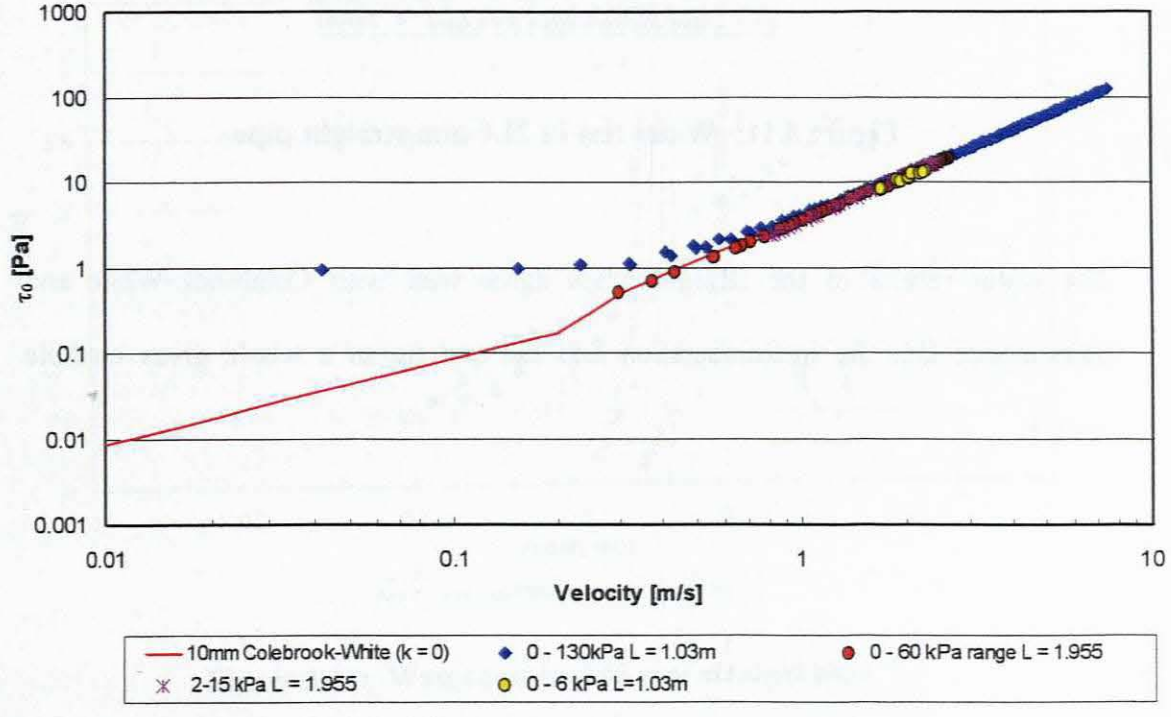

Figure 3.10: Water test in 9.28 mm straight pipe

Figure 3.11 - Figure 3.13 show the water test results in the 21 mm, 36 mm and 42.3 mm pipes. A significant scatter of the results can be seen for data obtained in the 42.3 mm pipe in comparison with the other pipes. The reason for this is that the pressure losses in this pipe are very small.

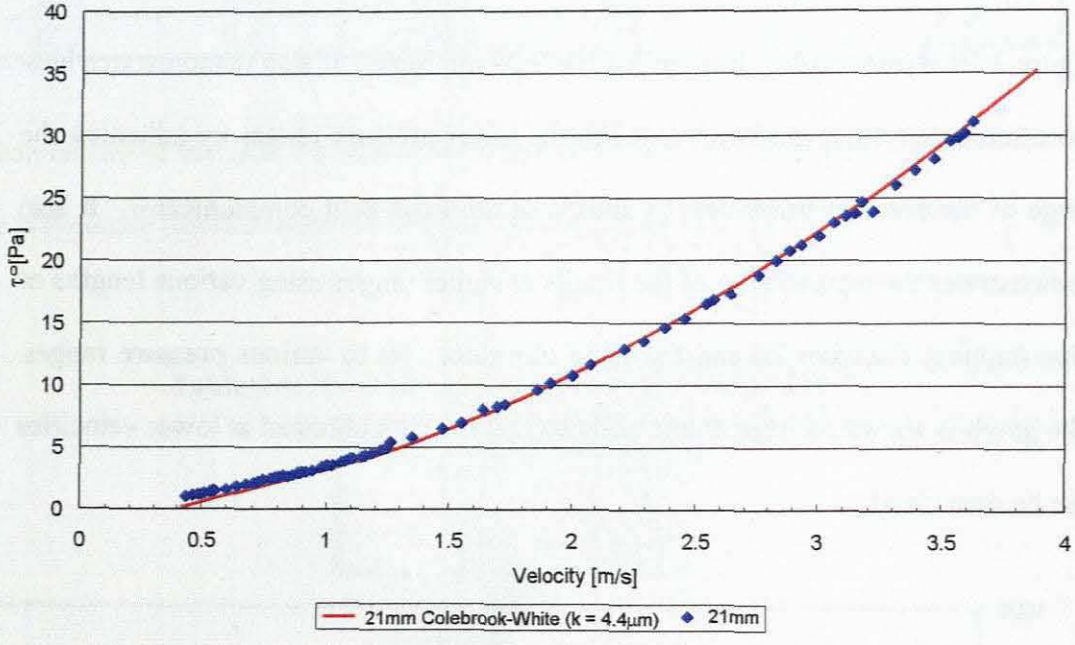

Figure 3.11: Water test in 21.0 mm straight pipe

The water results in the straight pipes agree well with Colebrook-White and demonstrate that the instrumentation and the test rig as a whole gives credible results.

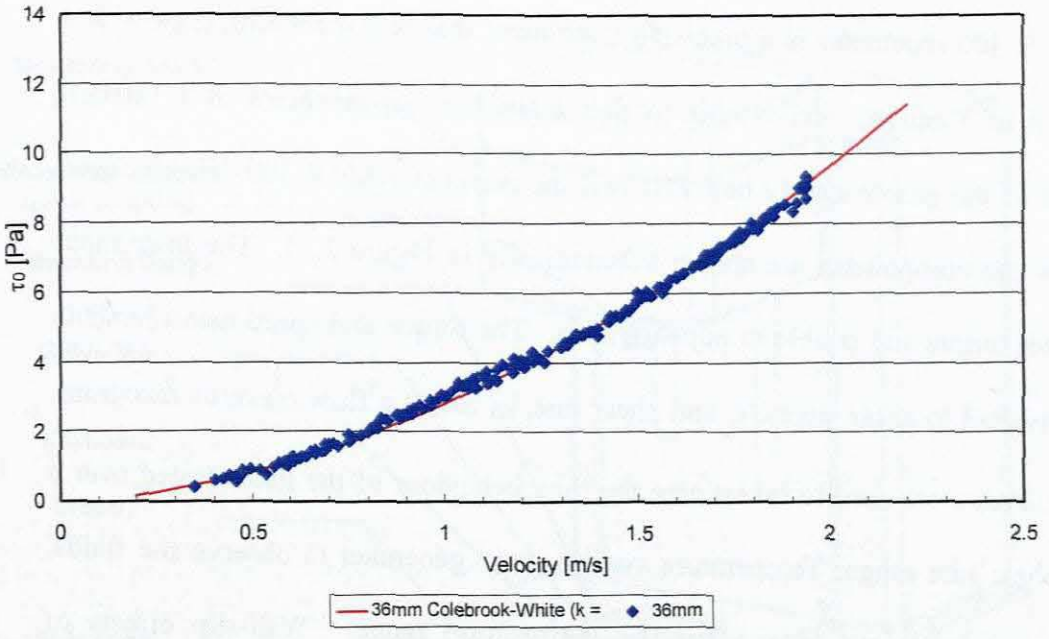

Figure 3.12: Water test in 36.0 mm straight pipe

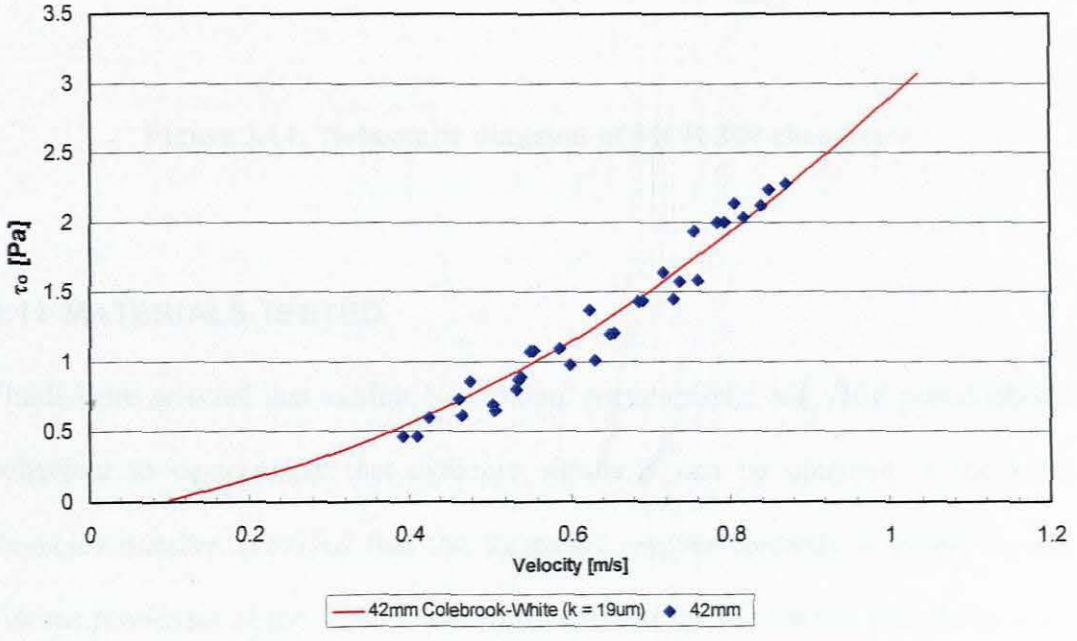

Figure 3.13: Water test in 42.3 mm straight pipe

3.10 PAAR-PHYSICA MCR 300 RHEOMETER

The MCR 300 rheometer is a precision instrument that sets measuring gaps with a precision of 1 micron and is able to detect angular displacements of 1 μrad; it consists of the power supply unit PS1 and the rheometer MCR 300. The function controls and components are shown schematically in Figure 3.14. The instrument generates torque and is able to adjust speeds. The torque and speed measurements are converted to shear stress, τ, and shear rate, $\dot{\gamma}$, called a flow curve or rheogram. Flow curves were used to investigate the flow behaviour of the fluids tested over a wide shear rate range. Temperature sweeps were generated to observe the fluids' rheological behaviour over a specific temperature range. Wall-slip effects of smooth-walled geometries have been reported when testing suspensions at high concentration (Chhabra & Richardson, 1999). A sandblasted bob was used to minimise slip effects when testing kaolin slurries for this work.

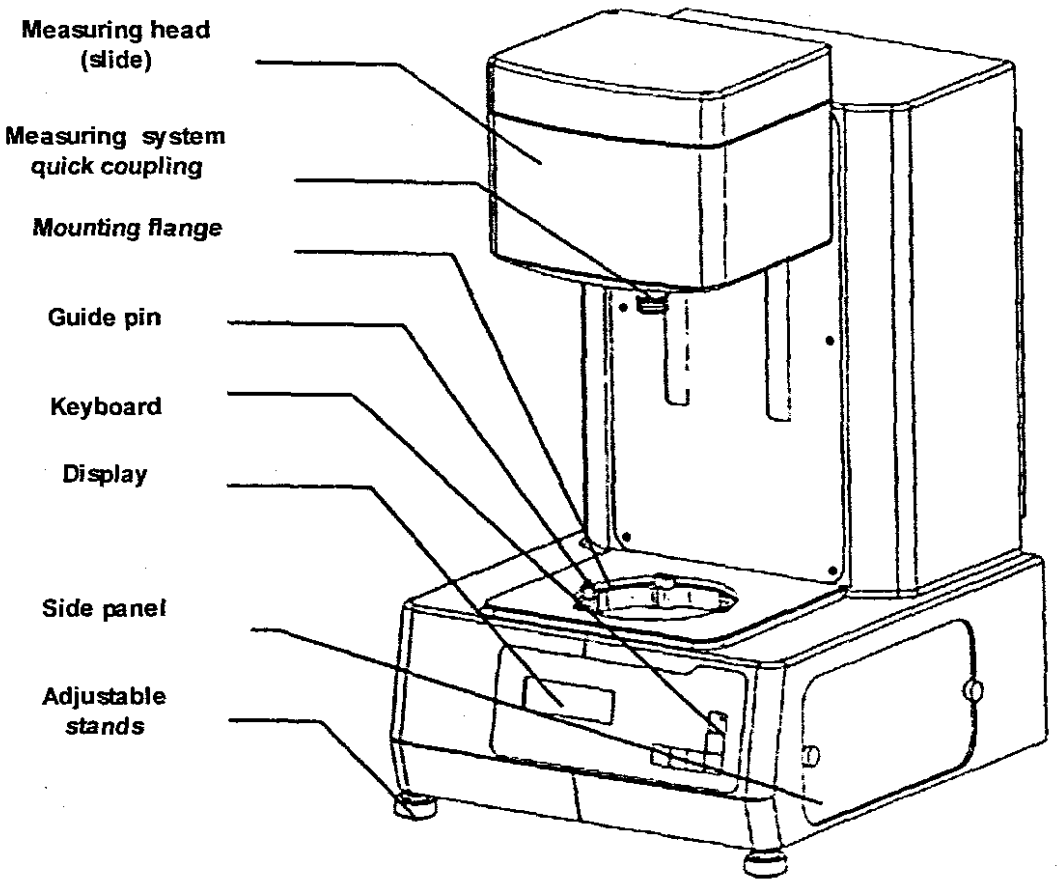

Figure 3.14: Schematic diagram of MCR 300 rheometer

3.11 MATERIALS TESTED

Fluids were selected that exhibit Newtonian, pseudoplastic and yield pseudoplastic behaviour to demonstrate that dynamic similarity can be obtained at the same Reynolds number, provided that the Reynolds number correctly accounts for the viscous properties of the fluid. The fluids selected for the tests in this thesis were water, glycerol solutions, SAE Oil (Newtonian behaviour), Carboxy Methyl Cellulose (CMC) (pseudoplastic behaviour) and kaolin slurries (yield pseudoplastic

behaviour) as previously shown in literature (Edwards *et al.*, 1985; Slatter & Pienaar, 1998). Glycerol solutions were used initially as the Newtonian fluid, but owing to excessive air entrainment that occurred during pumping, it was decided to replace them with lubricating oil, SAE. A detailed description of these fluids is given in the sections below.

The objective of this thesis is not about rheological characterisation methods of fluids as this is a science on its own. Standard rheological equipment (Paar-Physica MCR 300) and standard methods of rheological characterisation were used to characterise the fluids and to compare them with straight pipe results. Where possible, straight pipe results were used. Results from the rheometer were only used when insufficient laminar flow data were obtained in the tubes.

3.11.1 Glycerol

Pure glycerol was diluted with tap water to obtain 75 % and 90 % concentrations. The viscosity of these solutions was sensitive to temperature variation and care was taken to record the temperature of each test to ensure that the appropriate viscosity is applied to calculate the Reynolds number. A sample of the glycerol purchased for the tests was tested before dilution with the rheometer to obtain the viscosity at 25 °C. The relative density was determined to be 1.258 and the viscosity 0.682 Pa.s as shown in Figure 3.15.

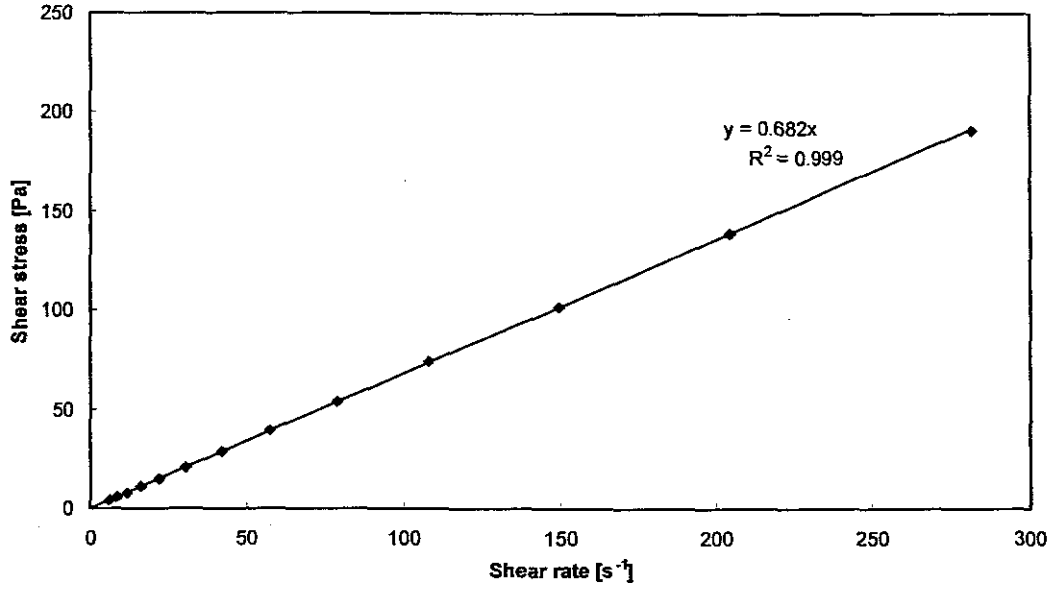

Figure 3.15: Laboratory test of glycerol at 25°C and relative density of 1.2583

Densities and viscosities of glycerol solutions (Perry, 1984) are presented below in Table 3.6. Interpolation of the relative densities and viscosities from this table yield a viscosity of 0.685 Pa.s that is comparable to what was obtained from the rheology laboratory.

Table 3.6: Viscosity of glycerol solutions (Perry, 1984)

AQUEOUS GLYCEROL SOLUTIONS					
			Viscosity, mN.s.m^{-2}		
% Weight glycerol	Grams per Liter	Relative density 25°/25°C	20°C	25°C	30°C
100	1261	1.262 01	1 495	942	622
99	1246	1.259 45	1 194	772	509
98	1231	1.256 85	971	627	423
97	1216	1.254 25	802	521	353
96	1201	1.251 65	659	434	296
95	1186	1.249 10	543.5	365	248
80	996.8	1.209 25	61.8	45.72	34.81
50	563.2	1.127 20	6.032	5.024	4.233
25	265.0	1.061 15	2.089	1.805	1.586
10	102.2	1.023 70	1.307	1.149	1.021

The pure glycerol was not tested in the rig because of the hydroscopic nature of the glycerol, which might have led to changes in the viscosity due to absorption of small amounts of water.

The viscosity for the 90 % glycerol solution with a relative density of 1.236 was obtained from the straight pipe tests as shown in Figure 3.16. The viscosity obtained was 0.124 Pa.s.

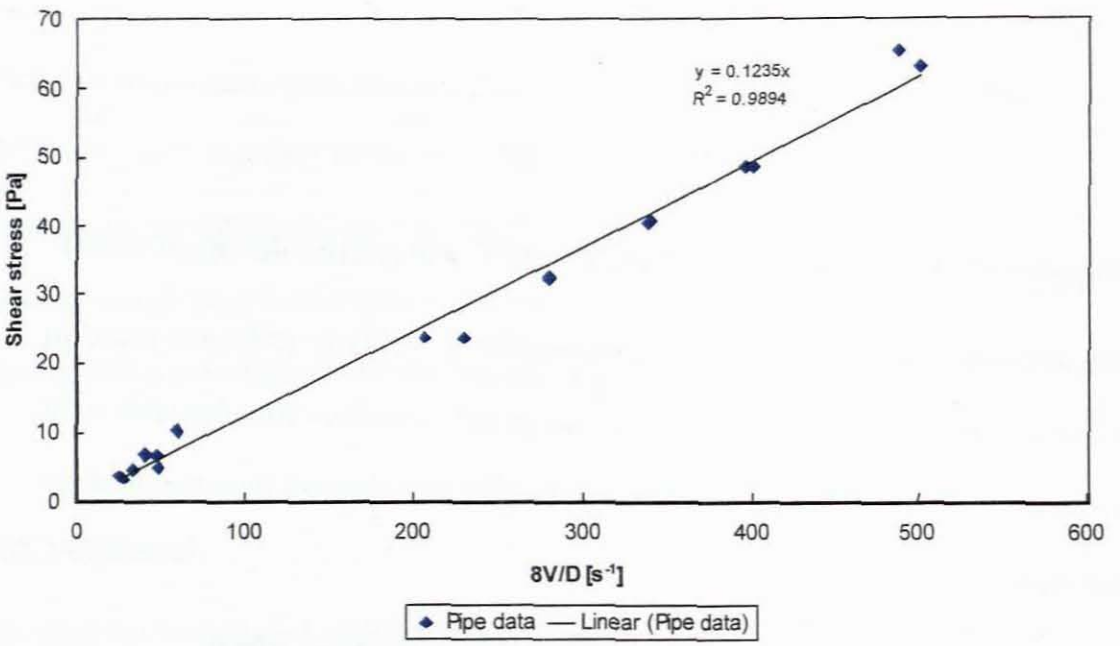

Figure 3.16: *Flow curve from pipe tests for 90 % glycerol solution*

3.11.2 Sugar Solution

Sugar solution was prepared from bags of Huletts sugar mixed with tap water. A weight concentration of 50 % was prepared. The relative density was 1.199 and the viscosity determined from the pipe tests as 0.008 Pa.s as shown in Figure 3.17. There was good agreement between the rheometer and pipe tests.

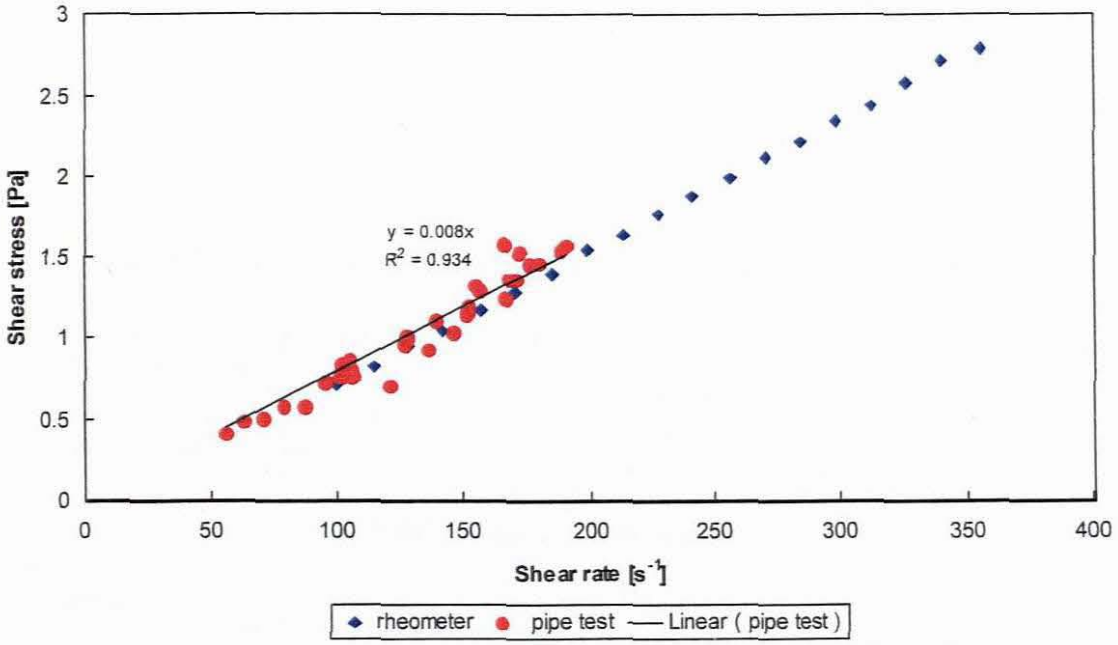

Figure 3.17: Flow curve from pipe tests and rheometer for 50 % sugar solution

3.11.3 Oil

Shell Helix lubricant oil was used as the viscous Newtonian fluid. The lubricant oil is based on a blend of high viscosity index mineral oils and additives. The oil was very sensitive to changes in temperature and straight pipe tests were not used to determine the viscosity, as the temperature was not always constant for each test. A temperature sweep was therefore conducted on the MCR 300 rheometer over the range of temperatures measured on the Fittings Rig, the viscosity was calculated for each test point based on the rheometer results and the temperature measured on the rig. The viscosity versus temperature results is shown in Figure 3.18.

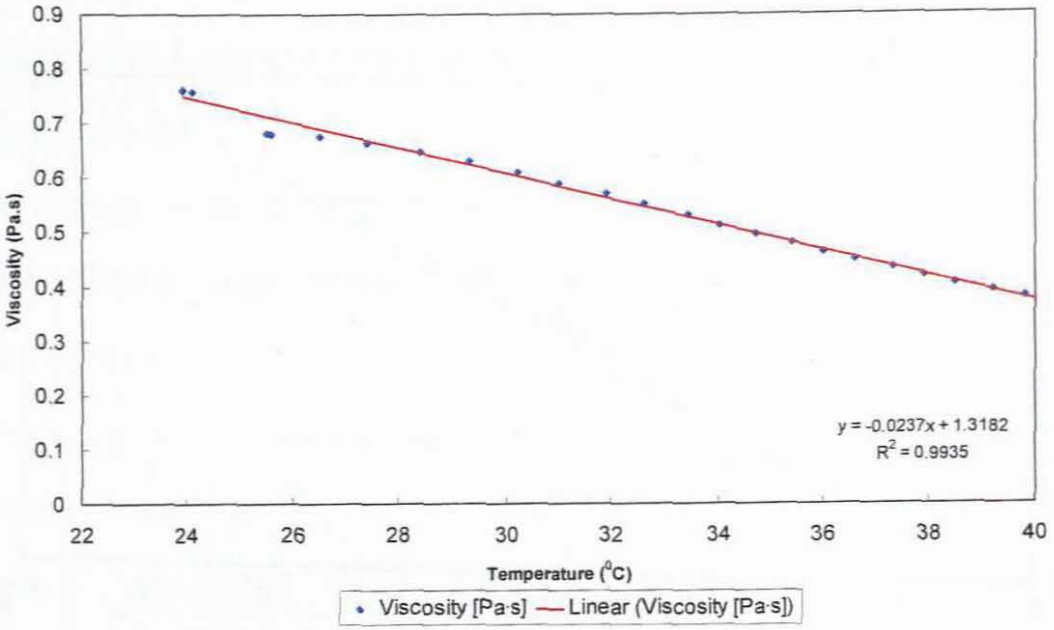

Figure 3.18: Temperature sweep for SAE 20W-50 oil

3.11.4 Carboxyl Methyl Cellulose (CMC)

CMC is a versatile material used widely in industries, e.g., paper glue, drilling mud, protective colloid, resin emulsion, paints, etc. The CMC was supplied originally in a powder form. The CMC solutions were made up in a 1 m^3 storage tank by adding the powder into water slowly and agitating the solution with a mechanical mixer. Care was taken to avoid the formation of large lumps. The solution was thoroughly mixed over 48 hours before being transferred into the rig. The rheology of the material was monitored daily to check any variation in the rheological parameters. Concentrations by weight of 3 %, 5 %, 8 % and 10 % were prepared. Although it was attempted to make up the same solution for tests in each contraction, it was not possible and small variations existed in the final concentration. These variations were, however, accounted for by detailed rheological characterisation of the fluid.

3.11.4.1 Contraction Ratio β = 0.22

The rheological results obtained for the CMC solutions that were tested in the contraction with β = 0.22 are given in Table 3.7 and Figure 3.19. The actual concentrations were 3.66% and 4.41% by mass.

Table 3.7: Fluid properties of CMC tested in contraction β = 0.22

SAMPLE	DENSITY [kg/m^3]	K' [Pa.s^n]	n'
CMC 3%	1021	0.182	0.744
CMC 5%	1025	0.718	0.672

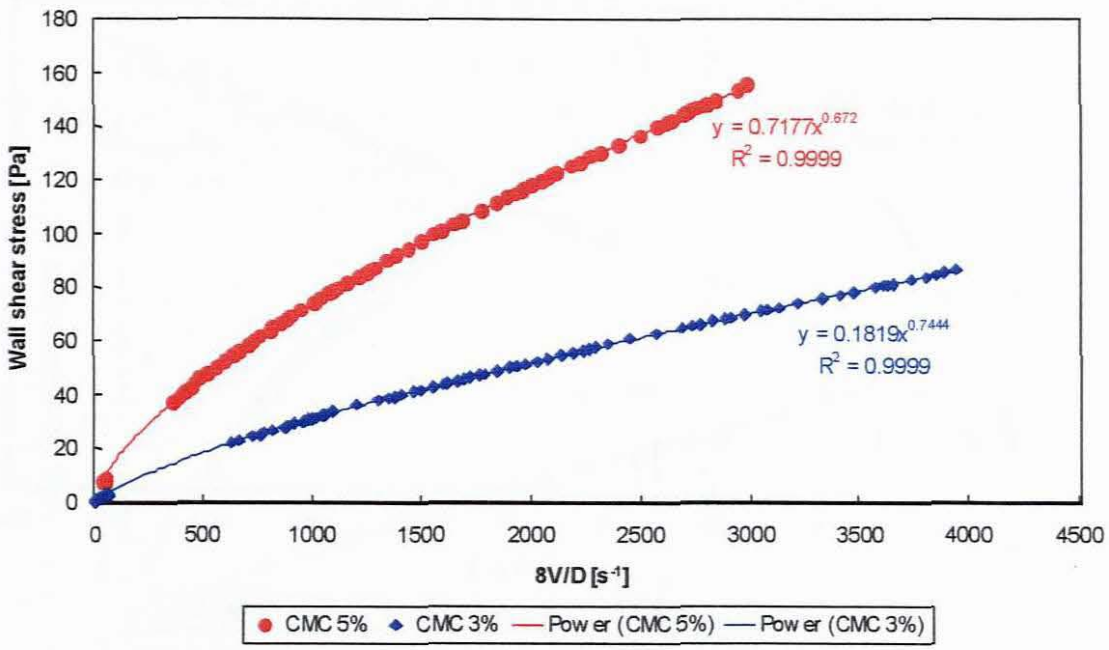

Figure 3.19: Flow curves for CMC tested in contraction β = 0.22

3.11.4.2 Contraction Ratio β = 0.5

The rheological results obtained for the CMC solutions that were tested in the contraction with β = 0.5 are given in Table 3.8 and Figure 3.20. The actual concentrations were 4.59% and 7.89% by mass.

Table 3.8: Fluid properties of CMC tested in contraction β = 0.5

SAMPLE	DENSITY [kg/m^3]	K' [Pa.s^n]	n'
CMC 5%	1026	0.756	0.694
CMC 8%	1045	2.82	0.550

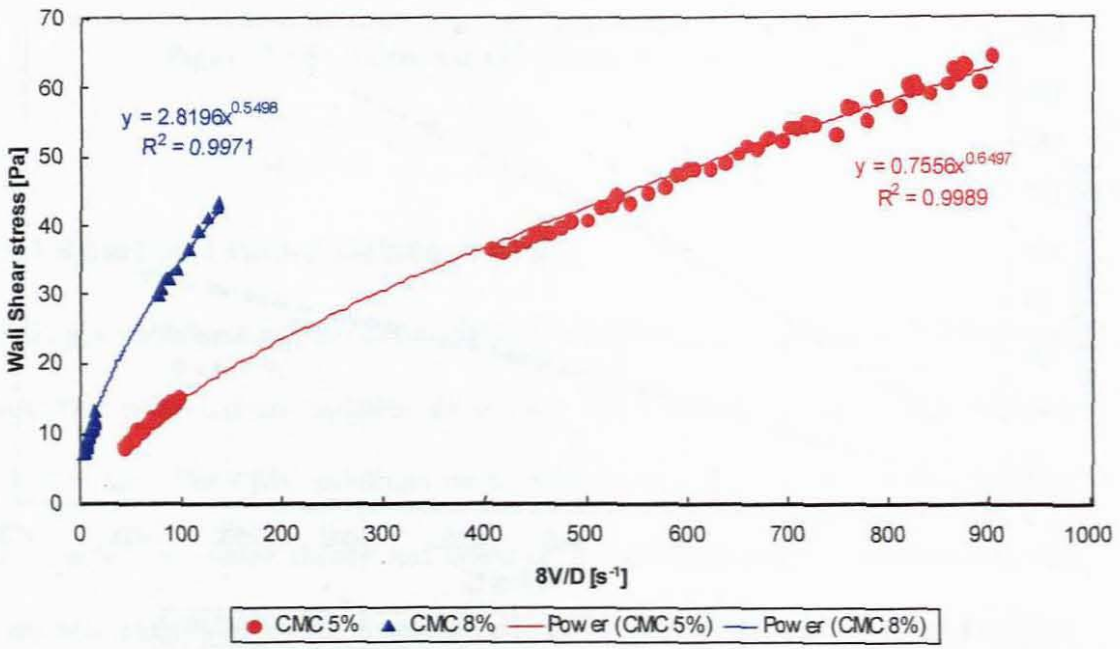

Figure 3.20: Flow curves for CMC tested in contraction β = 0.5

The results in Figure 3.20 were carried out in a 42.3 mm pipe and 21 mm pipe and the results obtained in each pipe are restricted either by the maximum pressure drop that can be measured with the DP cell or the minimum flow rate that can be measured by the flow meter.

3.11.4.3 Contraction Ratio β = 0.85

The rheological results obtained for CMC solutions tested in the contraction with β = 0.85 are given in Table 3.9 and Figure 3.21. The actual concentrations were 5.33% and 7.89% by mass.

Table 3.9: Fluid properties of CMC tested in contraction β = 0.85

SAMPLE	DENSITY [kg/m^3]	K' [Pa.s^n]	n'
CMC 5%	1030	0.300	0.683
CMC 8%	1045	1.49	0.579

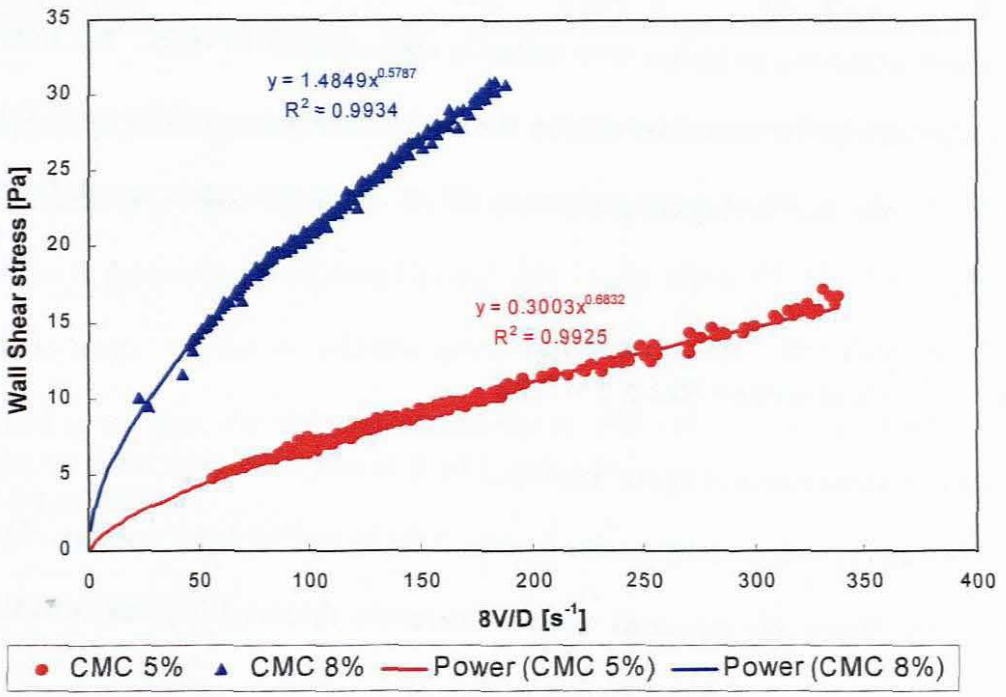

Figure 3.21: Flow curves for CMC tested in contraction β = 0.85

3.11.5 Kaolin

The kaolin used for this work was obtained from the Fish Hoek area in the Western Cape Province and primarily results from *in situ* weathering of Cape granite. The refining process consists of wet milling, screening and hydro cyclone beneficiation followed by mechanical-thermal drying. The mineralogical composition of kaolin is basically kaolinite with trace mica and quartz.

Kaolin slurry was prepared from dry kaolin powder and tap water. The mixture was left to stand for at a few days to allow for full hydration. It was then transferred into the rig. Because the particles settle slowly, the mixer was always running in the storage tank to keep the solution homogeneous.

Different concentrations of kaolin were tested in each contraction ratio. The flow curves obtained with the rheometer and the rheological parameters will be given for each $\beta = 0.22$ and the rheological parameters for all contraction ratios are given in Table 3.12.

3.11.5.1 Contraction Ratio $\beta = 0.22$

Volumetric concentrations of approximately 5 %, 8 % and 10 % were made up and tested. The actual concentrations were 4.06 %, 8.24 % and 10 % by volume. The density of the fluids was measured using a volumetric flask and is given with the rheological parameters in Table 3.10 and Table 3.11.

Rheological parameters were obtained from both the straight pipe tests and the rheometer for comparison. The values of these parameters are given in Table 3.10 and in Table 3.11 respectively.

Table 3.10: Rheological parameters obtained from pipe tests for kaolin tested in contraction β = 0.22

SAMPLE	DENSITY [kg/m^3]	τ_Y [Pa]	K [Pa.s^n]	n
Kaolin 5%	1067	0.38	0.062	0.634
Kaolin 8%	1136	10.17	0.088	0.645
Kaolin 10%	1165	18.50	0.37	0.511

Table 3.11: Rheological parameters obtained from rheometer for kaolin tested in contraction β = 0.22

SAMPLE	τ_Y [Pa]	K [Pa.s^n]	n	$\dot{\gamma}$ region (s^{-1})
Kaolin 5%	1.23	0.147	0.514	10 - 632
Kaolin 8%	6.85	0.884	0.386	10 - 1262
Kaolin 10%	12.1	3.30	0.267	10 - 1262

A comparison of the results shows excellent agreement between the rheometer and the tubes and is given in Figure 3.22. The reason for this comparison was to ensure that even if there was insufficient laminar data in the pipes, the rheometer results could be used. As far as possible when sufficient laminar flow data could be obtained in the pipe, the rheological parameters obtained from the pipe tests were used for calculations.

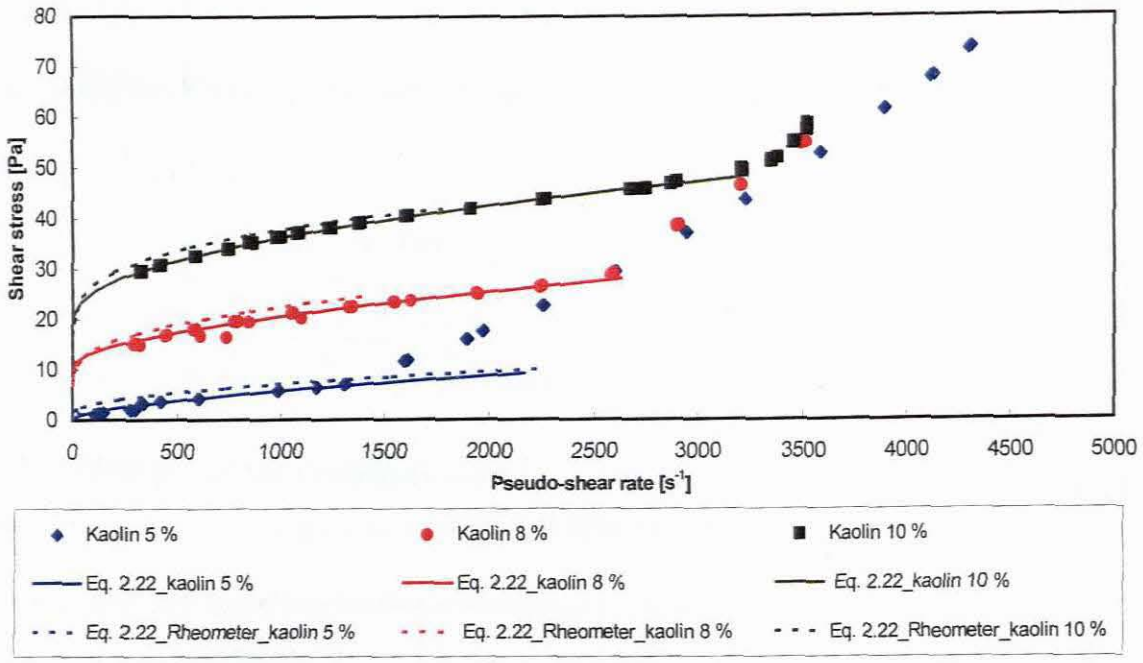

Figure 3.22: Comparison of rheological parameters obtained in pipe loop and rheometer for kaolin tested in contraction β = 0.22

Rheological parameters for kaolin tested in the contractions with β = 0.5 and 0.85 are given in Table 3.12. The actual concentrations were 9.64 %, 11.82 %, 8.48 %, and 13.15 % by volume.

Table 3.12: Rheological parameters obtained from pipe tests for kaolin tested in other contractions

CONTRACTION	SAMPLE	DENSITY [kg/m^3]	τ_Y [Pa]	K [Pa.s^n]	n
β = 0.5	Kaolin 10%	1159	16.0	1.12	0.422
β = 0.5	Kaolin 12%	1195	16.5	13.2	0.164
β = 0.85	Kaolin 9%	1140	7.99	10.1	0.183
β = 0.85	Kaolin 13%	1217	33.0	1.55	0.506

The fluid viscous property range is summarised in Figure 3.23 as a plot of apparent viscosity and shear rate. Apparent viscosities of the fluids tested ranged from 0.01 – 20000 Pa.s over the shear rate range $0.001 < \dot{\gamma} < 10000\ s^{-1}$.

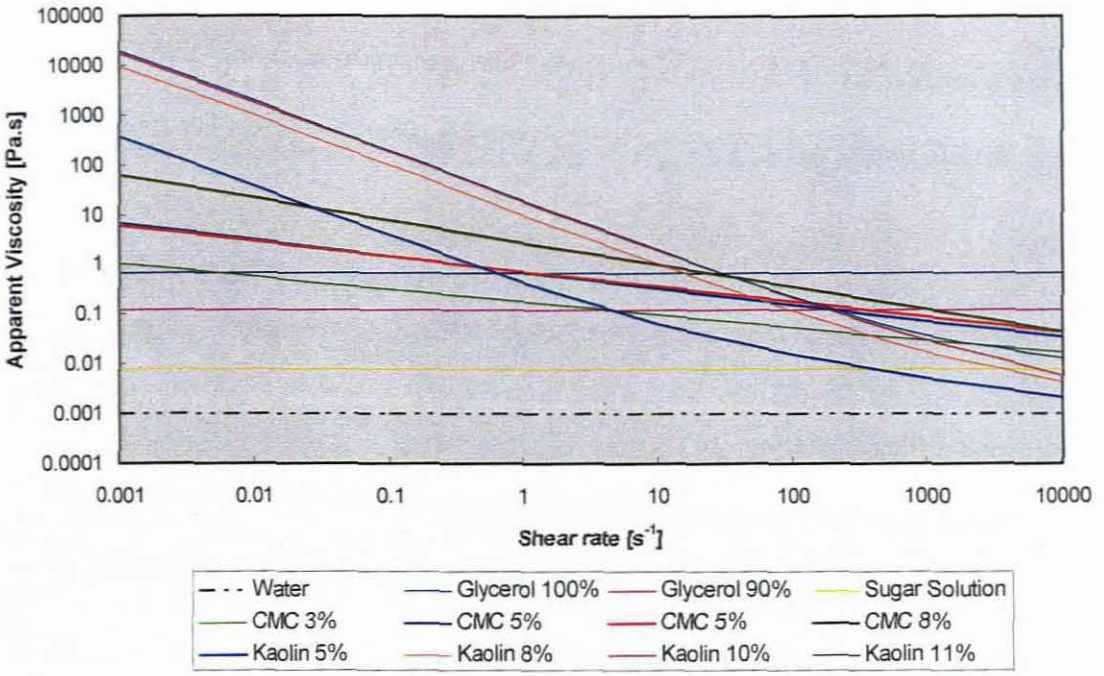

Figure 3.23: Apparent viscosity for all fluids tested

3.12 CONCLUSIONS

The conclusions from this work are summarised below.

1. A test rig has been constructed for measuring losses in straight pipes and losses due to sudden contractions using a range of Newtonian and non-Newtonian materials.
2. The rig has been commissioned using clear water tests.
3. The operation of the fitting rig used to collate pressure drop results for losses through sudden contractions has been described.
4. The calibration and test procedures for the collection of accurate data were described.

5. The automation of the rig has been described and the advantages and disadvantages given.
6. The experimental errors have been quantified and are within acceptable limits.
7. The materials tested were described and an explanation was given for material choice.
8. Water was tested in straight pipes to establish the credibility, accuracy and precision of the test equipment. Straight pipe results correlated well with the Colebrook-White equation.
9. The straight pipe tests were verified with a rheometer and the determination of fluid properties was described and discussed. The apparent viscosities of materials tested ranged from 0.001 – 20 000 Pa.s.
10. Data were gathered for the evaluation of losses due to sudden contractions using three contraction ratios i.e., $\beta = 0.22$, 0.50 and 0.85.

CHAPTER 4

CHAPTER 4

ANALYSIS OF EXPERIMENTAL RESULTS

4.1 INTRODUCTION

In this chapter the analysis of the test results is explained in detail. The experimental data were analysed in various ways to evaluate the effect of these analyses on the loss coefficient, k_{con} and the loss coefficient constant, C_{con}. This was deemed necessary owing to the differences in results obtained by various researchers (Ma, 1980; Edwards *et al.*, 1985; Pienaar, 1998). The results can be analysed by using two methods. The first method is to extrapolate the fully developed pressure gradient to the contraction plane if the pressure is measured along the length of the two pipes. The second method is to measure the total pressure drop across the system by using two pressure taps only. This is experimentally a cheaper method, as only one pressure transducer is required. The two methods both have challenges in the evaluation of the results that will be discussed later in this chapter. The layout of this chapter is as follows:

- Analysis of experimental results using pressure grade line approach.
- Presentation of k_{con} versus Re plots for diameter ratios

  $\Rightarrow \beta = 0.22$

  $\Rightarrow \beta = 0.50$

  $\Rightarrow \beta = 0.85.$
- Comparison with previous results.

- Discussion of results obtained and comparison with previous results
- Effect of various methods of analysis on the loss coefficient
  - ⇒ Effect of number of points used for extrapolation
  - ⇒ Total pressure drop approach
  - ⇒ Effect of length of pipe.
- Effect of rheology on the loss coefficient.
- Selection of data for determination of C_{con}.
- Conclusions.

4.2 ANALYSIS OF RESULTS USING THE PRESSURE GRADELINE APPROACH

The static pressure is measured along the length of the pipes, both upstream and downstream by means of eight pressure taps initially and after automation of the rig four and five either side of the contraction. The convention is to extrapolate the fully developed pressure gradient to the contraction plane, but in practice it is often difficult to determine where the fully developed region is. For the evaluation of the results obtained in this work, points close to the contraction plane were excluded. This is shown in Figure 4.1. The point closest to the contraction plane upstream was 24.4 diameters to avoid distorted flow close to the contraction and downstream more than 100 diameters to allow for fully developed flow after the contraction. This was based on the trends observed from the pressure grade line versus axial distance plots for several fluids.

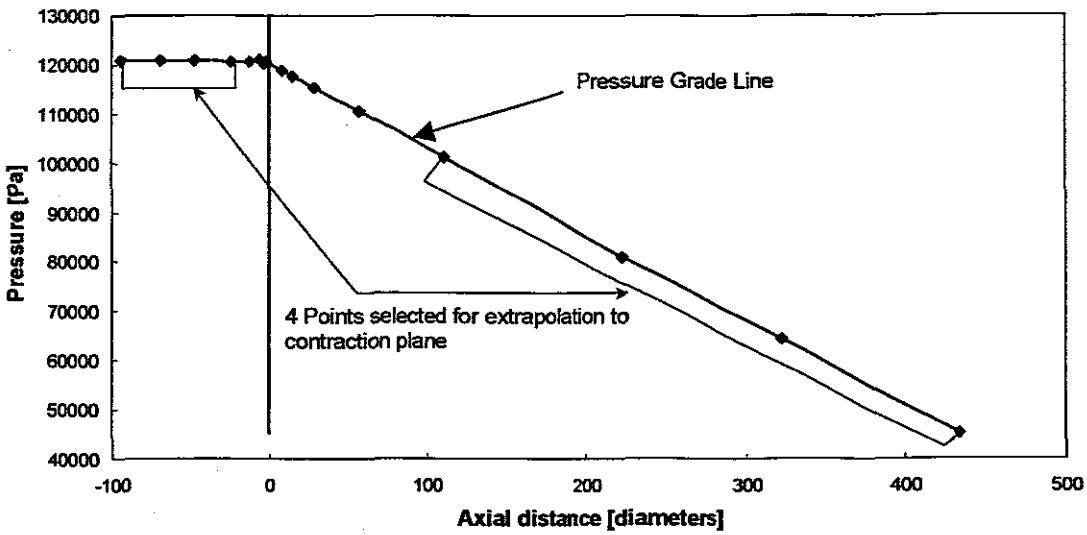

Figure 4.1: Selection of data points for extrapolation

The steps in calculating the loss coefficient were as follows:

- The slope and intercept were determined upstream and downstream using the selected data points as shown in Figure 4.1. These data points were used for all tests.
- The pressure was calculated at the contraction plane both upstream and downstream.
- The pressure drop at the contraction (Δp_{con}) was determined by subtracting the downstream pressure from the upstream pressure at the contraction plane.
- The loss coefficient, k_{con}, was then calculated as:

$$k_{con} = \frac{\left[\frac{\Delta p_{con}}{\rho g} + \frac{\left(\alpha_1 V_1^2 - \alpha_2 V_2^2\right)}{2g}\right]}{\frac{V_2^2}{2g}} \qquad (2.57)$$

For Newtonian fluids, α was taken as 2 for laminar flow, for pseudoplastic

$$\alpha = \frac{3(3n+1)^2}{(2n+1)(5n+3)}, \tag{2.51}$$

and for yield pseudoplastic fluids (Baudouin, 2003)

$$\alpha = 2\tau_0^4 \frac{M(\tau_0-\tau_y)^2 + B\tau_Y(\tau_0-\tau_y) + Y\tau_y^2}{\left[\frac{(\tau_0-\tau_y)^2}{1+3n} + \frac{2\tau_y(\tau_0-\tau_y)}{1+2n} + \frac{\tau_y^2}{1+n}\right]^3} \tag{2.52}$$

where $M = \frac{3}{(3n+1)(4n+2)(5n+3)}$

$$B = \frac{6}{(2n+1)(3n+2)(4n+3)}$$

$$Y = \frac{1}{2(n+1)^3}.$$

The loss coefficient constant, C_{con}, is defined as the hyperbolic constant

$$k_{con} = \frac{C_{con}}{Re}. \tag{2.61}$$

The loss coefficients were evaluated using the logarithmic least square error.

$$E = \sum\left(\ln\frac{C_{con}}{Re} - \ln k_{con\ obs}\right)^2. \tag{4.1}$$

C_{con} is obtained by minimising E for each contraction ratio.

4.3 LOSS COEFICIENT DATA OBTAINED FOR THIS WORK

The loss coefficient data obtained for this work are presented below as plots of k_{con} versus Reynolds number. For Newtonian fluids the Newtonian Reynolds number [Re_N] Eq. (2.29) has been used, for pseudoplastic fluids the Metzner-Reed Reynolds number [Re_{MR}] Eq. (2.32) and for yield pseudoplastic fluids the Slatter Reynolds

number [Re_3] Eq. (2.33) (Pienaar, 1998). The effect of the rheology of the fluid and the Reynolds number will be demonstrated in Section 4.6.

4.3.1 Contraction $\beta = 0.22$

Water, Newtonian oil, CMC (3% and 5% by mass) and kaolin (8% and 10% by volume) were tested in the contraction of $\beta = 0.22$. The laminar loss coefficient constant, C_{con}, was obtained by Eq. (4.1) using k_{con} results at Reynolds numbers less than 10. Turbulent results were obtained at Reynolds numbers between 6000 and 70 000. An average was calculated to obtain the turbulent loss coefficient for this contraction ratio. The results obtained are given in Table 4.1 and Figure 4.2. The detailed results of the pressure drop along the axial distance across the contraction for all the fluids as well as the calculated variables are given in Appendix A.

Table 4.1: Loss coefficient data for $\beta = 0.22$

DIAMETER RATIO $[D_D/D_U]$	AREA RATIO $[A_D/A_U]$	C_{con}	k_{con}
0.22	0.048	364	1.003

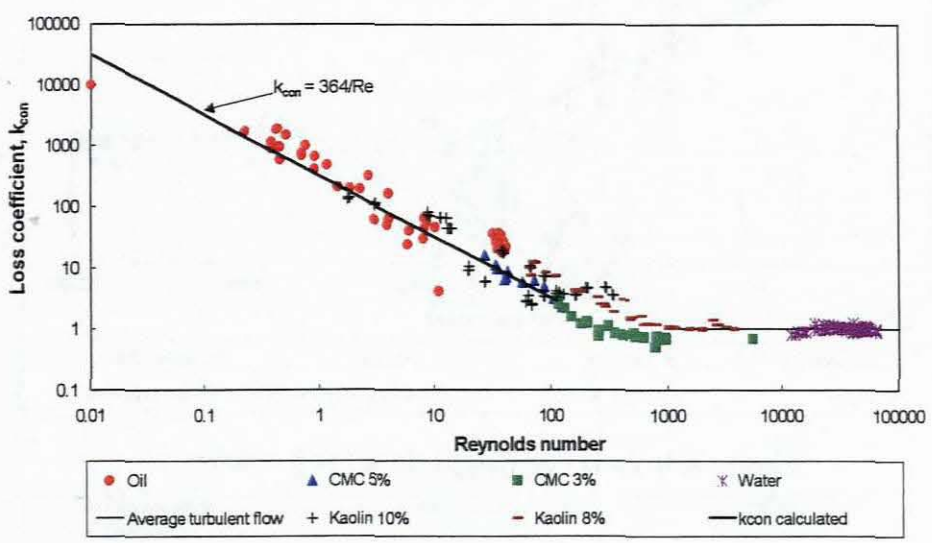

Figure 4.2: Loss coefficient data for $\beta = 0.22$

4.3.2 Contraction $\beta = 0.5$

Water, glycerol solutions, sugar solution, CMC at concentrations of 5% and 8% by mass, and kaolin at a volumetric concentration of 13% were tested in the contraction of $\beta = 0.5$. The laminar loss coefficient constant, C_{con}, was obtained by Eq. (4.1) using k_{con} results at Reynolds numbers less than 10. Turbulent results were obtained at Reynolds numbers between 6000 and 70 000. An average was calculated to obtain the turbulent loss coefficient for this contraction ratio. The results obtained are given in Table 4.2 and Figure 4.3. The detailed results of the pressure drop along the axial distance across the contraction for all the different fluids as well as the calculated variables are given in Appendix B.

Table 4.2: Loss coefficient data for $\beta = 0.5$

DIAMETER RATIO $[D_D/D_U]$	AREA RATIO $[A_D/A_U]$	C_{con}	k_{con}
0.50	0.25	288	0.346

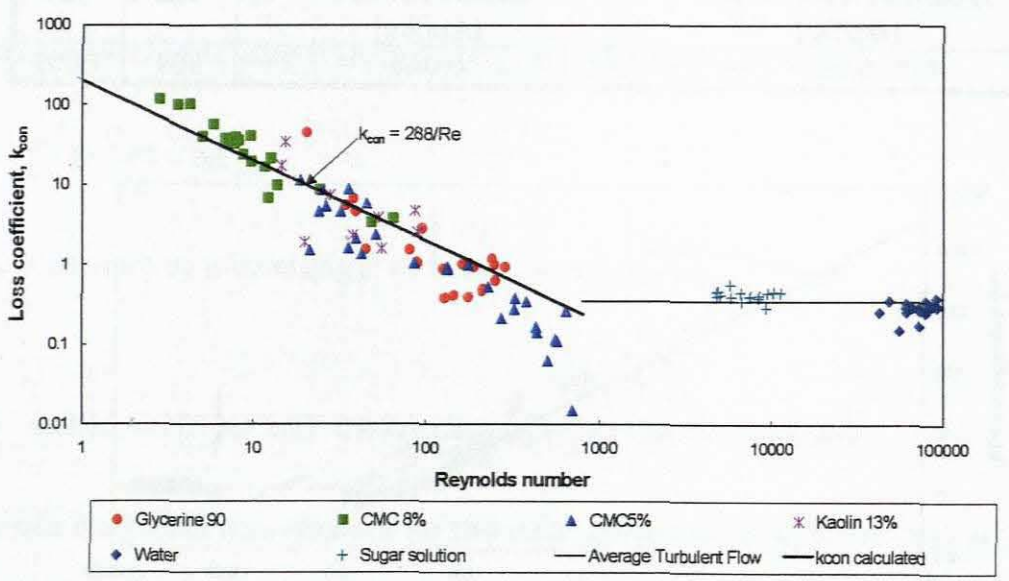

Figure 4.3: Loss coefficient data for $\beta = 0.5$

4.3.3 *Contraction* $\beta = 0.85$

Water, glycerol 100% and glycerol solution of 75%, sugar solution, CMC at concentrations of 5% and 8% by mass and kaolin at a volumetric concentration of 13% were tested in the contraction of $\beta = 0.85$. The laminar loss coefficient constant, C_{con}, was obtained by Eq. (4.1) using k_{con} results at Reynolds numbers less than 10. Turbulent results were obtained at Reynolds numbers between 6000 and 70 000. An average was calculated to obtain the turbulent loss coefficient for this contraction ratio. The results obtained are given in Table 4.3 and Figure 4.4. The detailed results of the pressure drop along the axial distance across the contraction for all the different fluids as well as the calculated variables are given in Appendix C.

Table 4.3: Loss coefficient data for $\beta = 0.85$

DIAMETER RATIO $[D_D/D_U]$	AREA RATIO $[A_D/A_U]$	C_{con}	k_{con}
0.85	0.72	155	0.145

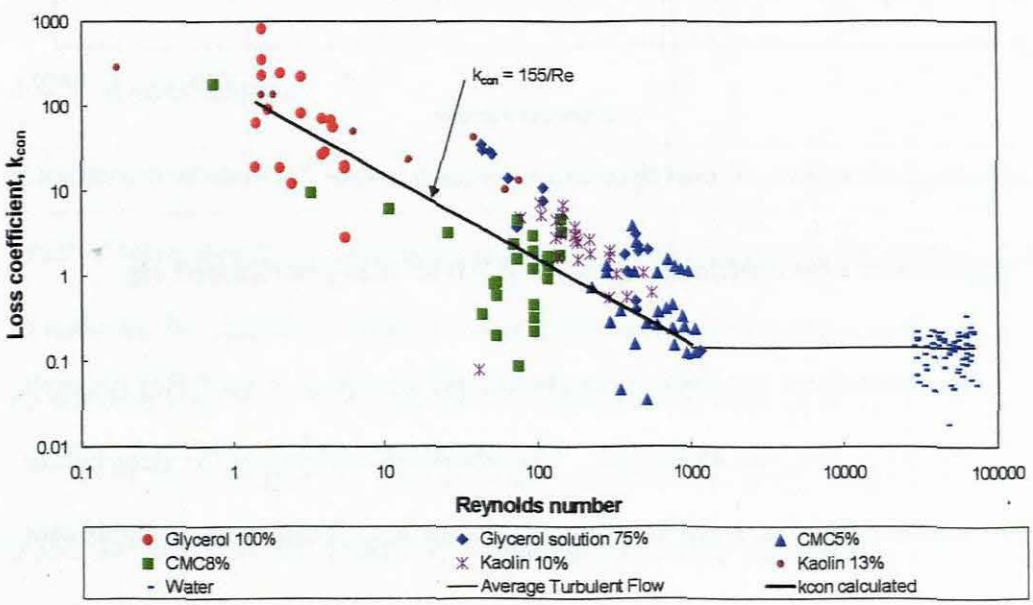

Figure 4.4: Loss coefficient data for $\beta = 0.85$

After the automation of the rig, tests were repeated in the contraction with $\beta = 0.85$ and the results are presented in Figure 4.5. The results were compared with those obtained previously (Figure 4.4), by plotting the results on the same trend line ($k_{con} = 155/Re$) as shown in Figure 4.5. The scatter of results was reduced significantly. This means that similar results were obtained using a new rig almost one year later. This validated the results obtained previously. The advantage of the automated rig was that the scatter was reduced at larger contraction ratios and that the data in Figure 4.5 were measured in one week, compared with that in Figure 4.4 that took almost four months.

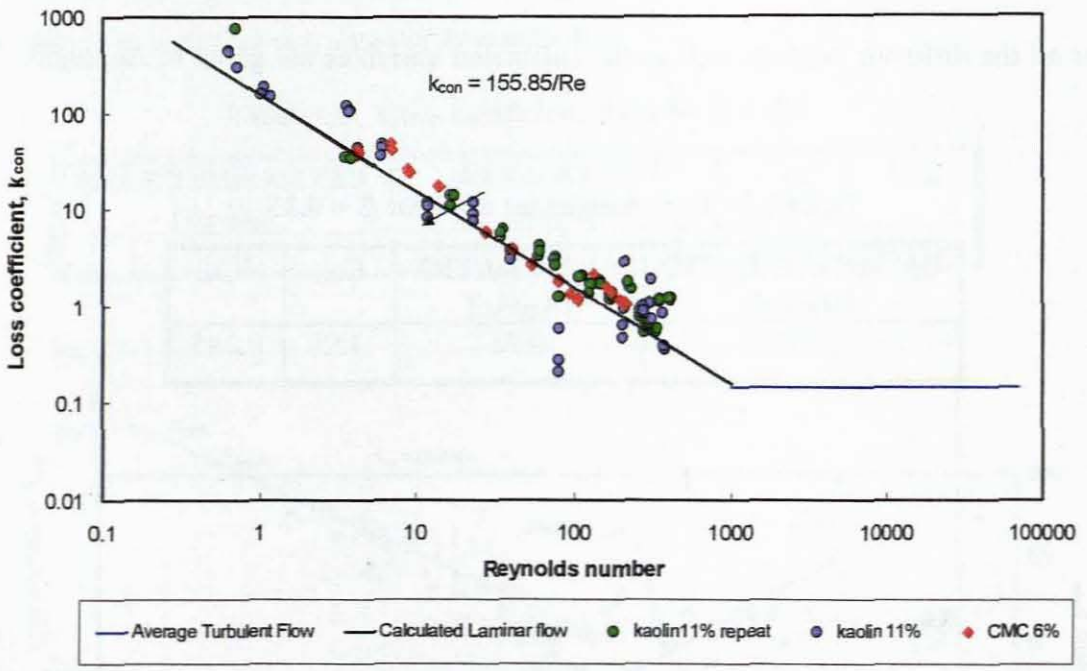

Figure 4.5: Loss coefficient data for $\beta = 0.85$ using automated rig

In order to compare these two sets of results, the product ($C_{con} = k_{con} * Re$) for each data point for $Re < 100$ was examined. The statistical analysis of the data before and after automation of the rig is given in Table 4.4. There was a significant

reduction in the standard error and standard deviation. The 95% confidence level improved from 87 to 21.

Table 4.4:Statistical analysis of data ($C_{con} = k_{con}$* Re) obtained in contraction $\beta = 0.85$ before and after automation

	BEFORE	AFTER
Mean	223.8	215.1
Standard Error	43.40	10.95
Median	116.5	197.9
Standard Deviation	294.4	100.4
Sample Variance	86647	10074
Kurtosis	9.46	1.21
Skewness	2.89	1.00
Range	1396	517.5
Minimum	3.24	16.6
Maximum	1399	534.1
Sum	10297	18071
Count	46.00	84.00
Confidence Level (95.0%)	87.41	21.78

4.4 COMPARISON WITH PREVIOUS RESULTS

A comparison of results will be discussed in this section.

4.4.1 Experimental

Comparison of this work with experimental data in literature is given in Table 4.5 in order of increasing β. Contractions are geometrically simple, but it remains difficult to make up fittings with exactly the same contraction ratio, because one has to rely on standard pipe sizes. So although it is attempted to make up a contraction ratio of 0.5, when the true internal diameters are measured, it might range from 0.445 to 0.550 as found in the literature. This makes direct comparison very difficult.

Although β values are not identical, some broad comparisons can be made and no visible trend was found for work done by various researchers.

Table 4.5: Comparison of experimentally determined C_{con} and k_{con} with previous results

INVESTIGATOR	β	C_{con}	k_{con}
Sylvester & Rosen (1970)	0.125	295	2.400
Pienaar (1998)	0.204	1298	1.650
This work	0.228	364	1.003
Astarita & Graco (1968)	0.402	795	5.480
Jadallah (1980)	0.445	110	0.450
Pienaar (1998)	0.463	641	0.414
This work	0.496	240	0.346
Ma (1987)	0.550	900	0.230
Jadallah (1980)	0.660	59	0.330
This work	0.851	155	0.145

4.4.2 Empirical and Semi-Empirical Models

The experimental data were compared with other models (ESDU, 1989; McNeil & Morris, 1995) and are given in Figure 4.6 - Figure 4.8. Various aspects of the presented results will be discussed in the following section.

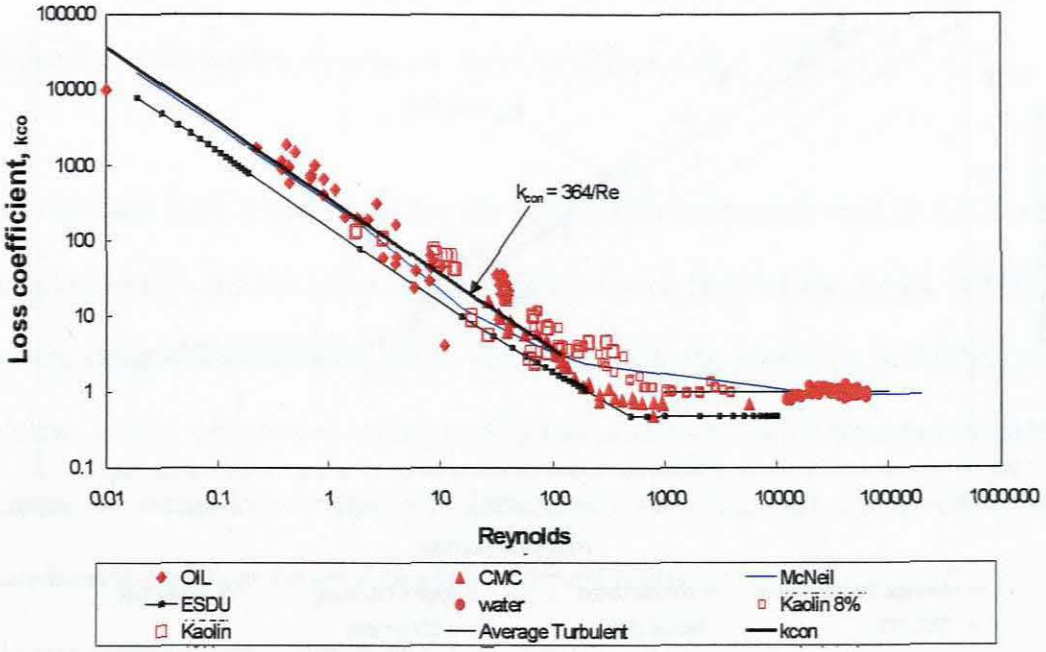

Figure 4.6: β = 0.22 comparison with ESDU (1989) and McNeil & Morris (1995)

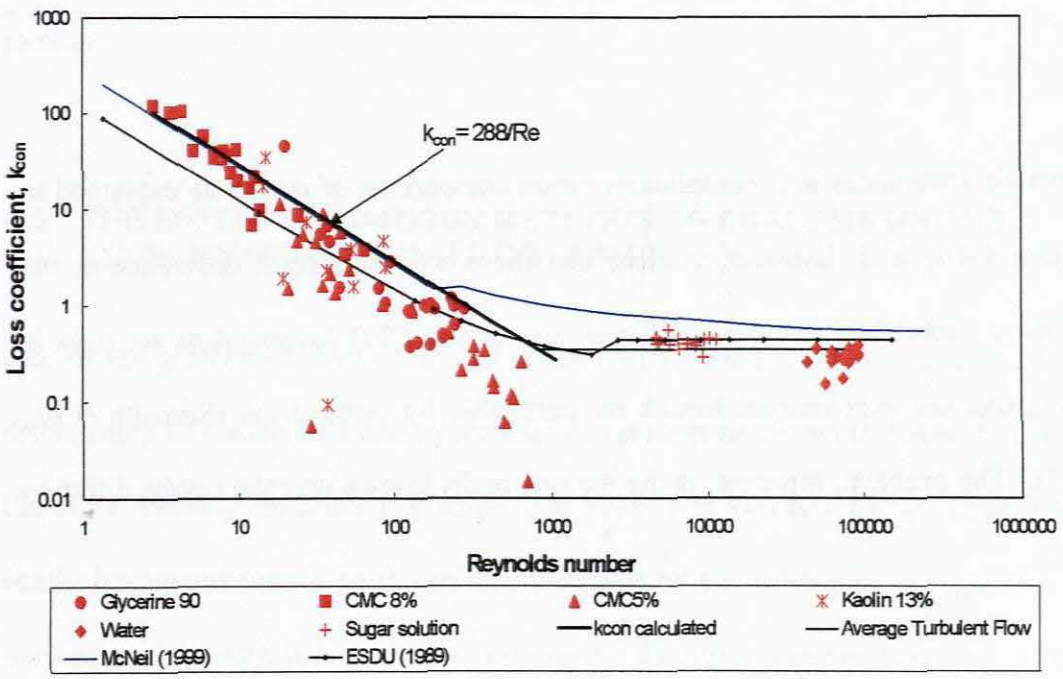

Figure 4.7: β = 0.5 comparison with ESDU (1989) and McNeil & Morris (1995)

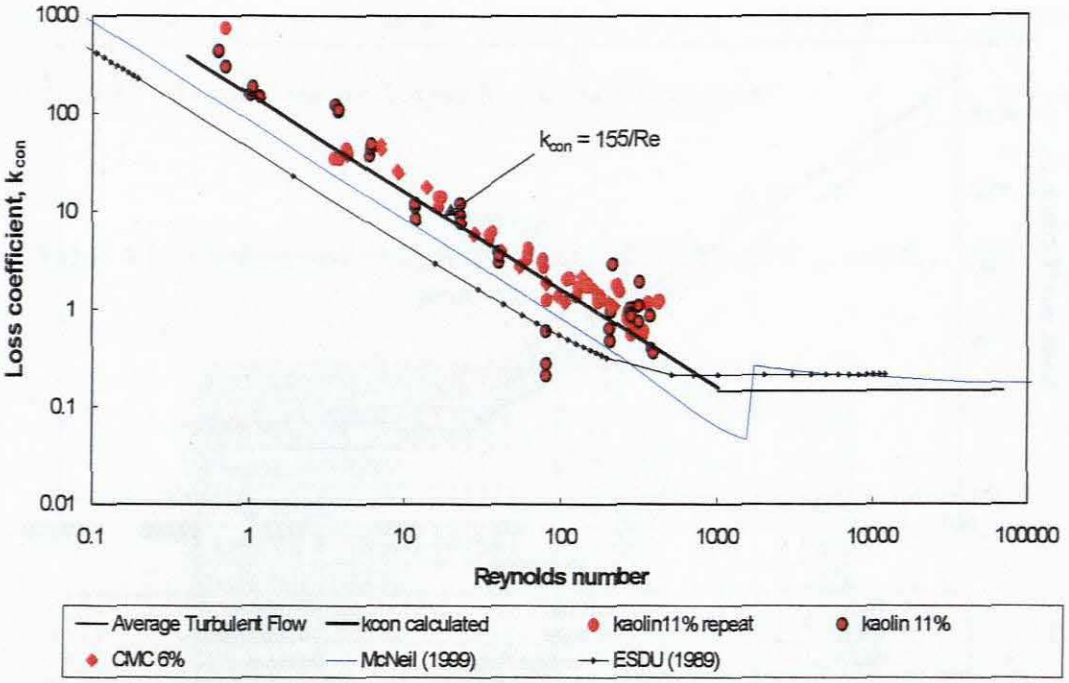

Figure 4.8: β = 0.85 comparison with ESDU (1989) and McNeil & Morris (1995)

Although differences in β complicates direct comparison of results as explained in Section 4.4.1, it is, however, evident that there is a significant difference in the results as shown in Table 4.5 and it may appear that CFD investigators are right in saying that the experimental results are unreliable for comparison (Sisavath *et al.*, 2002). The problem, however, is that no one really knows why the results differ so much.

Using correlations developed for predicting losses through sudden contractions, good correlation was found between the experimental results of this work with that

of McNeil and Morris (1995). The prediction from ESDU (1989) agreed with the higher Reynolds number results, i.e., Re > 10 (Figure 4.6).

For turbulent flow, it was found that for the smallest contraction ratio, $\beta = 0.22$, the turbulent results did not agree with the prediction of Holland and Bragg (1995) as for the other two contraction ratios, but rather with the prediction of McNeil and Morris (1995). McNeil and Morris (1995) also predicts an earlier transition from the viscous to inertia driven range with decreasing contraction ratio and a very abrupt transition to turbulent flow for larger contraction ratios.

Having once again confirmed the variation in experimental results obtained, the methods of analysis were evaluated and the results of this are presented in the next section.

4.5 THE EFFECT OF VARIOUS METHODS OF ANALYSIS ON THE LOSS COEFFICIENT DATA OBTAINED

One of the greatest concerns that this study tries to understand and address is the discrepancy in results obtained by various researchers as shown in Table 4.5. It is therefore critically important that some light be shed on the discrepancy of published results before any further work can be undertaken on any other pipe fittings. One of the reasons investigated, as being responsible for discrepancies obtained, is the method of analysis.

The first method is to extrapolate the fully developed pressure gradient to the contraction plane if the pressure is measured along the length of the two pipes. The second method is to measure the total pressure drop across the system by using two pressure taps only. This is experimentally a cheaper method, as only one pressure transducer is required. There are difficulties associated with both methods that could influence the results obtained to some extent. For the pressure gradient to be determined, it is required to select the points that are in the fully developed friction gradient region, but this is not always an easy task, as the distance of interference changes with Reynolds number (Pal & Hwang, 1999). For the total pressure drop method on the other hand, one needs to ensure that the additional losses are accounted for by ensuring that there is significant length of straight pipe. The difficulty is often encountered that to determine the loss in the fitting, two large numbers are being subtracted to obtain a very small number, resulting in significant errors or negative results (Sisavath, 2002). In this study the pressure gradient was measured as described in Chapter 3, but results can also be analysed using both methods. In both cases the Bernoulli equation is applied and it should result in the same answer, provided everything else is the same.

In the following section the data obtained for Newtonian lubrication oil flowing through a sudden contraction of $\beta = 0.22$ will be re-analysed using the pressure grade line approach as well as the total pressure drop approach to obtain values of k_{con} and C_{con} based on Newtonian flow. The results will be presented in plots of k_{con} versus Reynolds number.

4.5.1 Pressure Grade Line Approach

The sensitivity of the pressure drop and k_{con} on the selection of the data points used for extrapolation of the fully developed friction gradient to the contraction plane were evaluated by excluding some data points and evaluating the results to see the effect of the number of points used for extrapolation. This is illustrated in Figure 4.1. In addition to the earlier analysis where 4 points were used for extrapolation, all the data, 3 and 5 points, will be used to obtain k_{con} as described above. In all cases the slope and intercept were determined upstream and downstream, the pressure was calculated at the contraction plane and the pressure drop in the contraction (Δp_{con}) determined by subtracting the downstream pressure drop from the upstream pressure drop. The results are shown in Table 4.6.

Table 4.6: Results obtained when using various numbers of points selected for extrapolation to contraction plane

RANGE NAME	NO OF POINTS	SLOPE UPSTREAM	PRESSURE UPSTREAM [Pa]	SLOPE DOWNSTREAM	PRESSURE DOWNSTREAM [Pa]	Δp_{con}	k_{con}
All data	8points	-2.61	416277	-741	413236	3041	17.06
Range 4	5points	-3.13	416241	-735	411282	4959	29.08
Selected data	4points	-4.75	416121	-731	409893	6228	37.04
Range 3	3points	-3.51	416218	-722	406726	9492	57.50
Calculated		-1.83		-787			

It was found that for a single test run, using the same experimental data, the pressure drop across the fitting could change by as much as 67 % depending on the range of data points selected. ΔP_{con} is therefore very sensitive to the slope obtained for the extrapolated friction gradient.

The same analysis was done on all the data to obtain the loss coefficient constant, C_{con}. The results are shown in Table 4.7.

Table 4.7: Values obtained for C_{con} when using various numbers of points selected for extrapolation to the contraction plane

RANGE	NO OF POINTS	C_{con}
All data	8points	301.1
Range 4	5points	385.85
Selected data	4points	390.45
Range 3	3points	666.24

The results obtained for C_{con} for all sets of data are shown in Figure 4.9 below. Severe scatter was obtained with range 4, although it gave comparable values of C_{con} to that of selected data. At low Reynolds number range Re < 1, k_{con} was very sensitive to the slopes obtained for range 4.

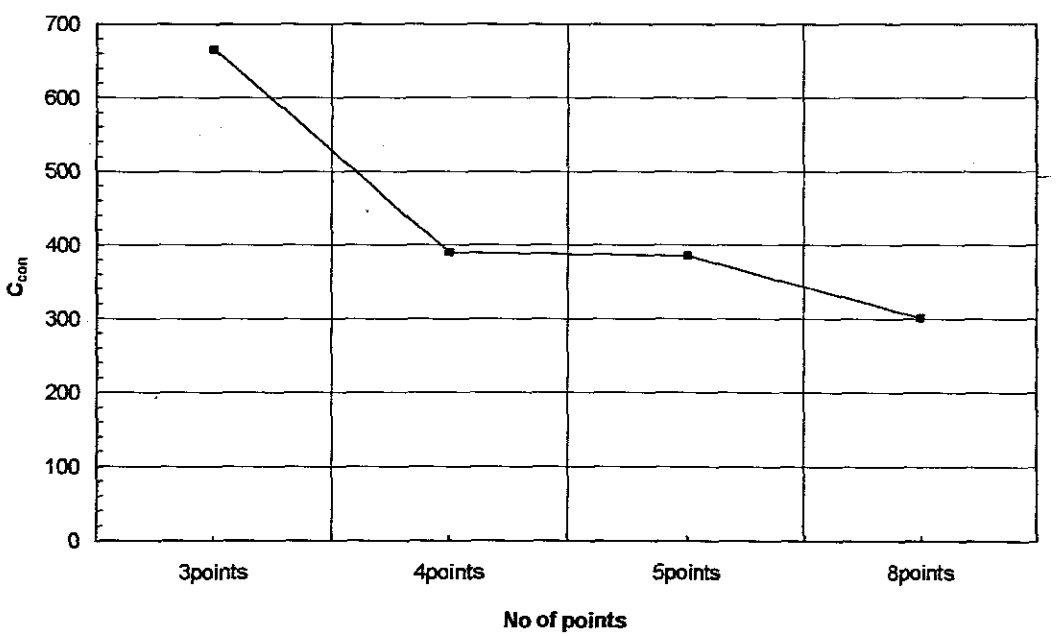

Figure 4.9: C_{con} obtained for various number of points used for extrapolation of fully developed pressure gradient

The above analysis indicates the need to be careful when selecting the data for extrapolation to the contraction plane as it could lead to significant errors.

4.5.2 Total Pressure Drop Approach

The same results were then analysed using the total pressure drop approach. In this case only two points were used - one upstream and one downstream. The procedure to calculate the loss coefficient using an energy balance was as follows:

$$\frac{p_1}{\rho g}+\alpha_1\frac{V_1^2}{2g}+z_1=\frac{p_2}{\rho g}+\alpha_2\frac{V_2^2}{2g}+z_2+\sum h_L, \qquad (2.48)$$

where

$$\sum h_L = h_{upstream}+h_{downstream}+h_{fitting}. \qquad (4.2)$$

To obtain the loss due to the fitting itself, the friction loss in the straight pipe is subtracted from the overall friction loss (Perry, 1984). The above equation then changes to

$$h_{fitt}=(z_1-z_2)+\frac{(p_1-p_2)}{\rho g}+\frac{(\alpha_1 V_1^2-\alpha_2 V_2^2)}{2g}-h_{upstream}-h_{downstream}. \qquad (4.3)$$

In this study the total pressure drop is taken between the upstream and downstream pressure taps that contain the test fitting. To calculate the loss coefficient for each contraction, the following steps are required.

- Calculate τ_0 for upstream and downstream pipes.

  For Newtonian fluids from pipe flow theory,

$$\tau_0 = \frac{f\rho V^2}{2} \tag{2.5}$$

or from experimental data

$$\tau_0 = \frac{D\Delta p}{4L}. \tag{2.2}$$

- Calculate the head loss due to friction in both pipes using

$$h_{con} = \frac{4L\tau_0}{D\rho g}. \tag{4.4}$$

- Calculate the head loss in fitting (h_{con}) using Eq. (4.3).
- Calculate the loss coefficient (k_{con})

$$k_{con} = \frac{h_{con}}{\frac{V_2^2}{2g}}. \tag{4.5}$$

Because the test rig was fitted with multiple pressure taps, this method could be applied using tappings at various distances, i.e., shorter or longer pipe lengths upstream or downstream of the contraction. In this case, the total length of the pipe was used, 50 diameters (50D) upstream and downstream and 25D upstream and downstream as shown in Figure 4.10 below.

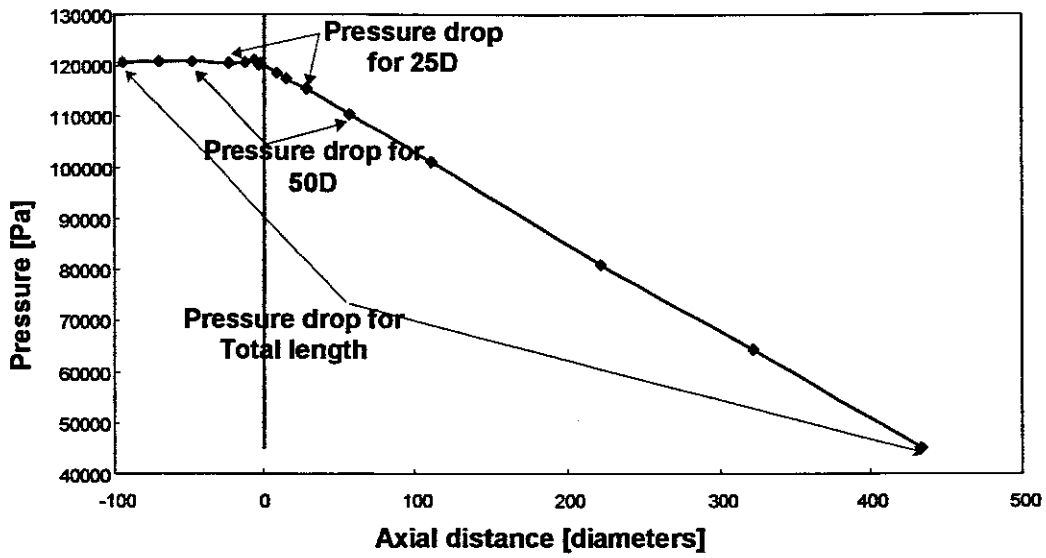

Figure 4.10: Points selected for total pressure drop approach

By reducing the length of straight pipe to 50D upstream and downstream resulted in C_{con} being similar to that obtained by using selected data from the pressure grade line approach for oil in a contraction with $\beta = 0.22$. The results are shown in Table 4.8.

Table 4.8: C_{con} obtained using total pressure drop approach

RANGE	LENGTH UPSTREAM	LENGTH DOWNSTREAM	C_{con}
Full length	100D	400D	1184.30
50D	50D	50D	393.66
25D	25D	25D	207.75

Glycerol solution results obtained from contraction $\beta = 0.5$ were analysed using the various methods and the results are shown in Figure 4.11 as a plot of k_{con} versus Reynolds number. The methods used were the pressure grade line method using all data and selected data as well as the total pressure drop approach using three

different lengths of straight pipe as well as using two methods for obtaining τ_0. The results obtained from the total pressure drop method were significantly higher than those obtained from the pressure grade line method using selected data.

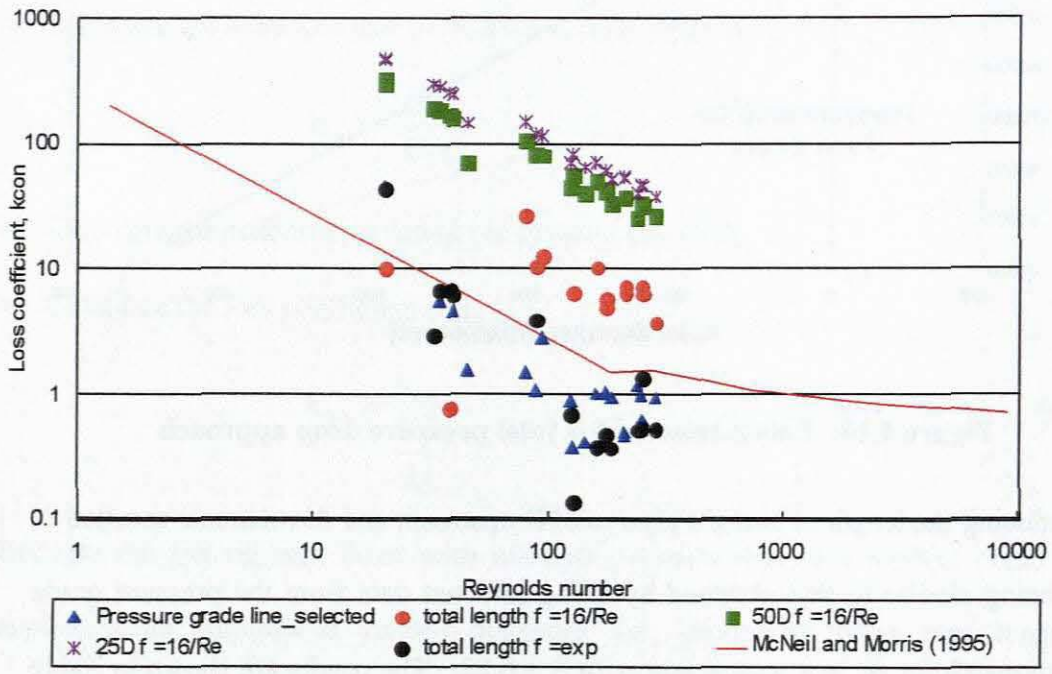

Figure 4.11: Analysis of glycerol results using various methods of analysis

When the total length of pipe was used, almost half of the k_{con} values obtained were negative as a result of two large numbers being subtracted from each other. When the measured friction factor was used, however, the results obtained correlated well with the pressure grade line approach. This clearly indicates that differences in calculated and measured friction factors are magnified when a long section of pipe is used.

With this information at hand, a comparison was done using data from the literature. Various analysis techniques were applied to see if any agreement could be found and whether this is indeed a possible reason for the discrepancies found. The contraction ratio tested most frequently in literature is $\beta = 0.5$ and it was used for comparative purposes in the following section.

A comparison of all results is given in Figure 4.12. In this graph the results are shown for test data analysed in the following ways:

1. Results obtained using the pressure gradient approach, but using selected data for extrapolation [◆].
2. Results obtained using the pressure gradient approach, but using all data for extrapolation [▲].
3. Results obtained using the total pressure drop approach for the total length of pipe using the theoretical friction factor [■;▪].
4. Results obtained using the total pressure drop approach for the total length of pipe using the experimental friction factor [▲;●].

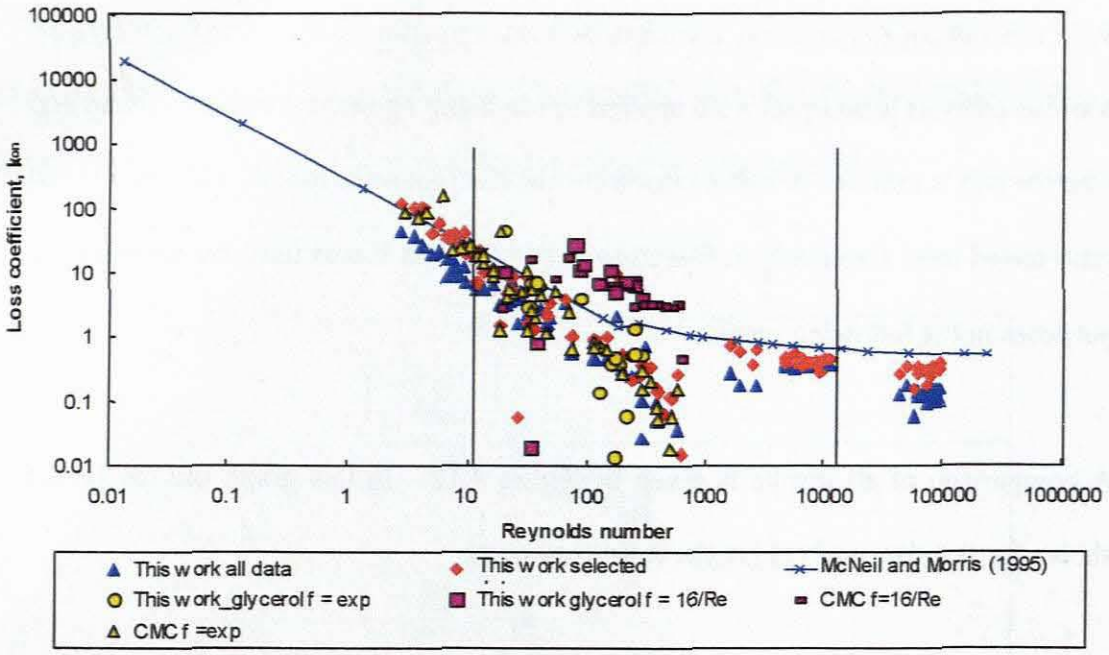

Figure 4.12: Results from various methods of analysis

The results obtained and shown in Figure 4.12 were compared with available models. These results are shown in Figure 4.13.

1. Data and results obtained by Jadallah (1980) [●].
2. Data and results obtained by Ma (1987) [-].
3. Results obtained using the BBTV by Pienaar (1998) [■;●].
4. This work analysed using total pressure drop approach with theoretical friction factor [■].
5. This work analysed using total pressure drop approach with experimental friction factor [●].
6. Comparison with McNeil and Morris approximation (1995) [-x-].
7. Comparison with ESDU correlation (1989) [-x-].
8. Turbulent approximation of Holland (1990) [---◦---]
9. Turbulent approximation of Hwang (1999) [-□-]

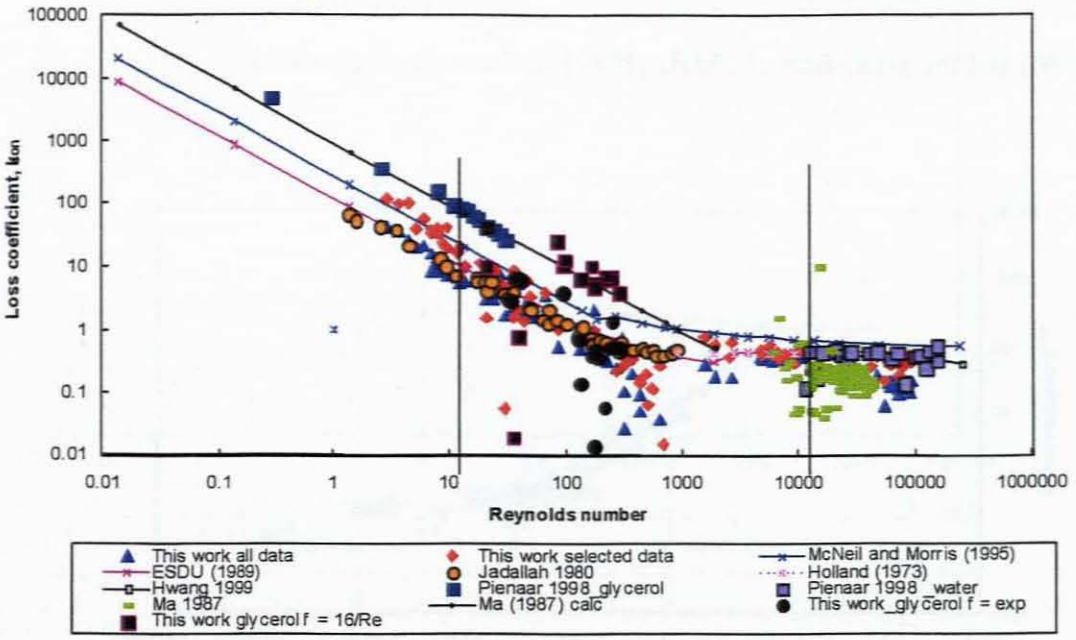

Figure 4.13: Comparison of results from this work and literature

4.5.3 Discussion of the Comparison (Figure 4.13)

By using various methods of analysis, results from the same raw data could be obtained that agreed either with Jadallah (1980), Ma (1987), Pienaar (1998) or McNeil and Morris (1995) as shown in Figure 4.13. The importance of the analysis and interpretation of the experimental results are demonstrated in this graph and the important points are listed below.

4.5.3.1 Re = 10 –10000

Between Re = 10 – 10 000, the fact that all the data points are used for extrapolation or that some data are selected gives little difference in the loss coefficient calculated. It is clear that the range of data selected for analysis of results has a significant effect at Reynolds numbers less than 10 and greater than 10 000.

Good agreement was found between this work using all data and that of Jadallah (1980) and the prediction of ESDU (1989) as shown in Figure 4.14.

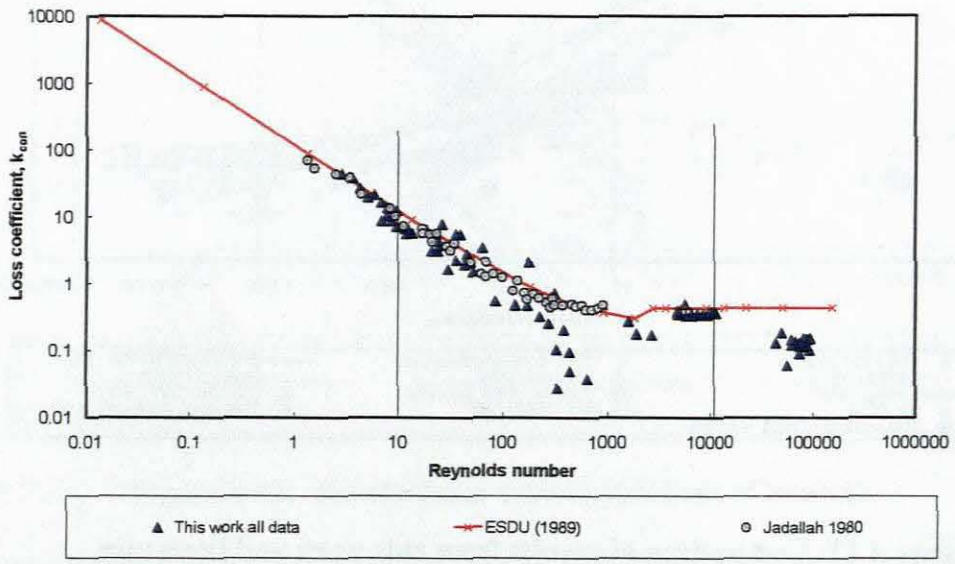

Figure 4.14: Comparison of results for Re = 10 – 10 000

4.5.3.2 Re > 10 000

At Re > 10 000, the results were significantly lower than predicted results and it was obvious that in this range the data closed to the contraction plane had to be excluded from the pressure gradient analysis.

4.5.3.3 Re < 10

At Re < 10, good agreement was found between this work using selected data and the prediction of McNeil and Morris (1995) as shown in **Figure 4.15**.

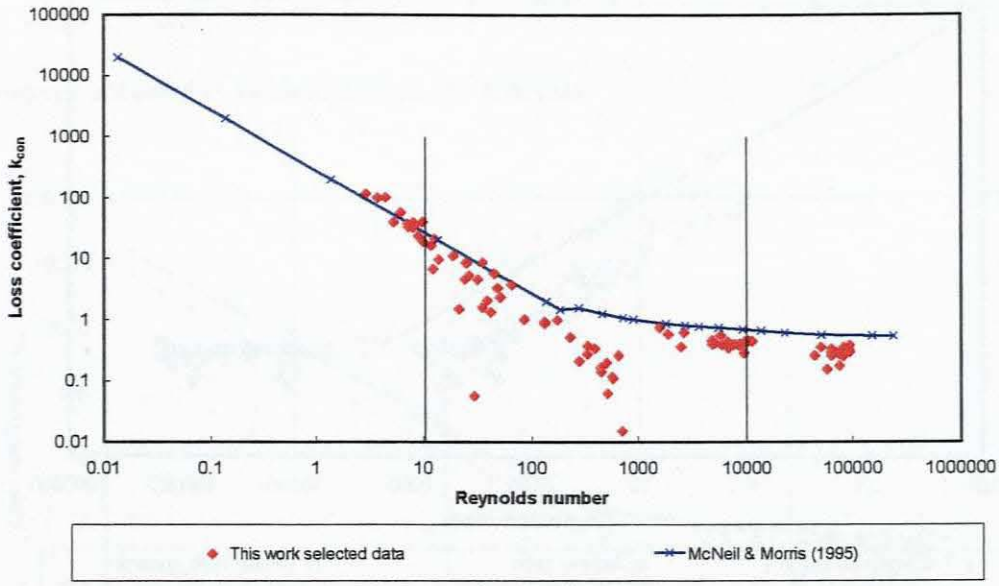

Figure 4.15: Comparison of results for Re < 10

4.5.3.4 Reaching Agreement by Using a Different Method of Analysis

In laminar flow, the results obtained from the BBTV using the total pressure drop approach were six times greater than results obtained in this study and those of others. This result was, however, in agreement with that of Ma (1987). Using the results obtained on the Fitting Rig, similar results were obtained when the total pressure drop approach was used by calculating the total pressure drop as the difference between the furthest tapping upstream and downstream. In this case, the friction factor was calculated as $f = 16/Re$. If, however, the same data are analysed using the experimentally determined friction factor, the loss coefficients reduce to agree well with the results obtained using either all data or selected data. The reason that they agree with both data sets is because they fall within the Reynolds number range where the loss coefficient obtained is independent of the range of data selected. This is shown in Figure 4.16.

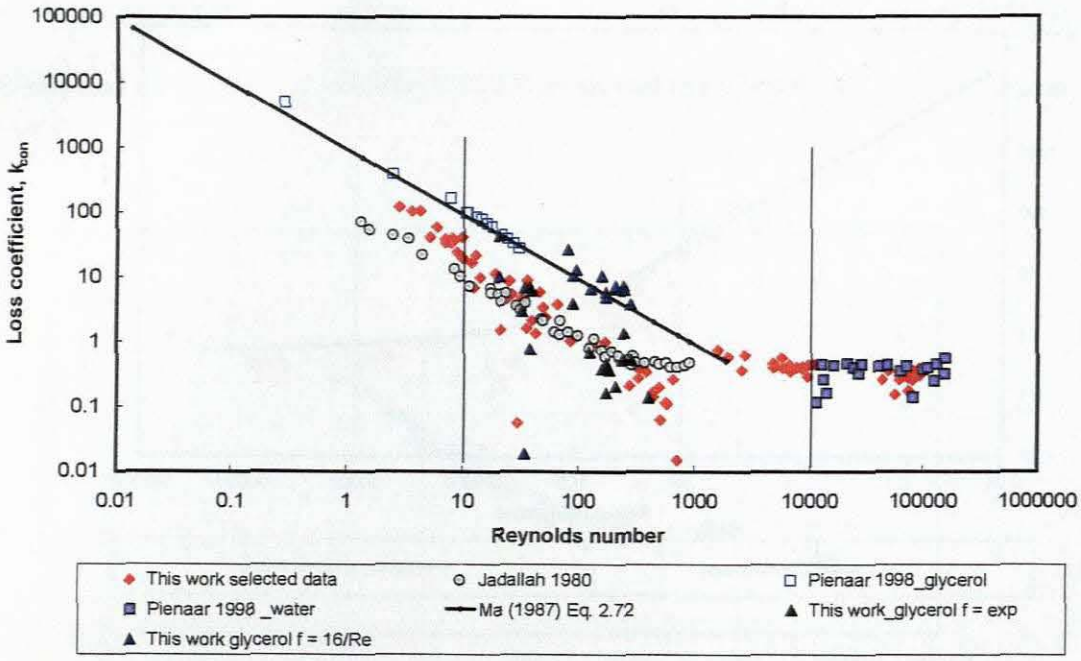

Figure 4.16: Comparison when using different methods of analysis

Another reason for discrepancies

The reason why Ma's work resulted in high values of C_{con}, is because he did not test at Reynolds numbers lower than Re = 100. It was demonstrated that results should be extrapolated from low Reynolds numbers to higher Reynolds numbers. This phenomenon is discussed later in this chapter.

Turbulent flow

For turbulent flow, good agreement was found between the results from the Fitting Rig and the Balanced Beam Tube Viscometer (BBTV) (Pienaar, 1998). The prediction of McNeil and Morris (1995) for turbulent flow did not agree with the experimental results or the prediction of others for $\beta = 0.5$ as demonstrated in Figure 4.17.

It was clear that in the determination of loss coefficient data for pipe fittings, the answer obtained is as important as the analysis.

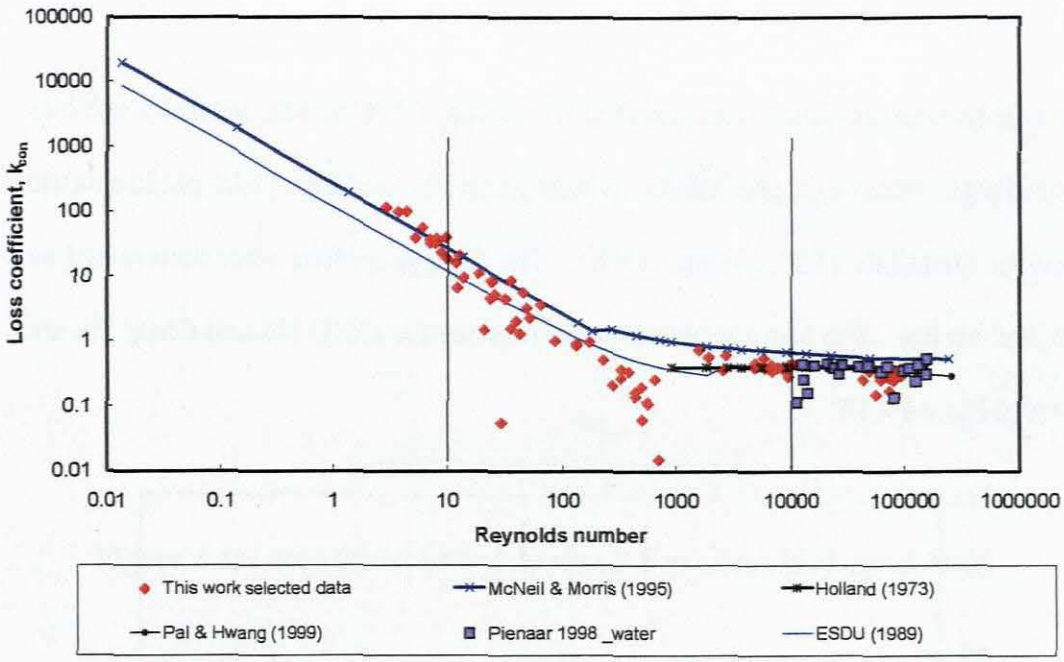

Figure 4.17: Comparison of turbulent flow results

4.6 EFFECT OF RHEOLOGY ON THE LOSS COEFFICIENT

The loss coefficient is correlated with the Reynolds number, which is the ratio between viscous and inertial forces. It is therefore ideal to establish dynamic similarity within the fittings and the Reynolds number is the appropriate way to establish this. It was shown previously that the Metzner-Reed Reynolds number could be used to model fluids with pseudoplastic behaviour (Edwards *et al.*, 1985) and that the Slatter Reynolds number could be used to model fluids with yield pseudoplastic behaviour (Slatter & Pienaar, 1999).

By ensuring that the rheology is accounted for by the Reynolds number used to model the data the same loss coefficient can be used for both Newtonian and non-Newtonian behaviour.

Two non-Newtonian fluids were selected for testing, CMC which generally exhibits pseudoplastic behaviour and kaolin, which generally exhibits yield pseudoplastic behaviour (Jadallah, 1980; Pienaar 1998). The fluid properties were determined as described earlier. The loss coefficient data obtained for CMC 3% and CMC 5% are shown in Figure 4.18.

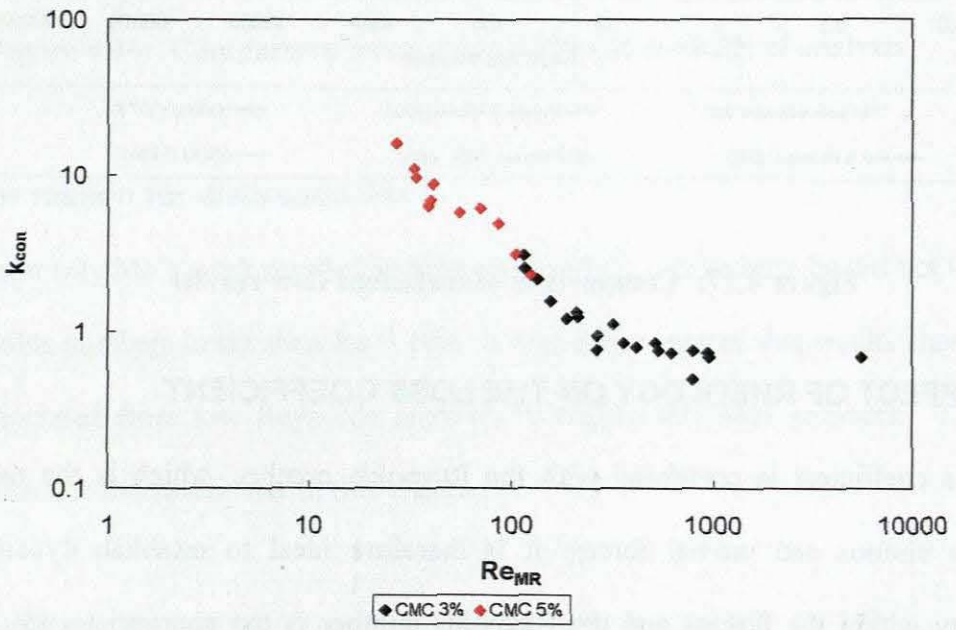

Figure 4.18: Loss coefficient data for CMC

The effect of rheology is demonstrated in Figure 4.19 where the results are compared with those when using the Newtonian Reynolds number and the apparent viscosity at the wall, rather than those Reynolds numbers that account more appropriately for the rheology of the fluid.

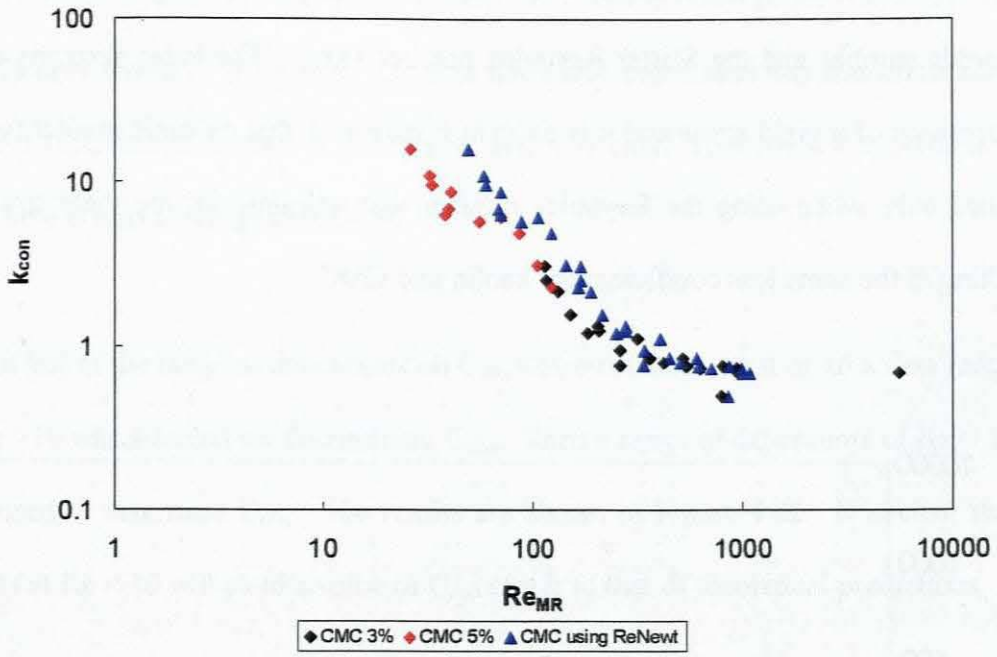

Figure 4.19: Sensitivity of loss coefficient data to rheology of fluid

Figure 4.20 clearly demonstrates that by careful analysis of results (by selecting the right range for extrapolation to the contraction plane) and by accounting for fluid properties, one value of the loss coefficient constant C_{con}, can be obtained.

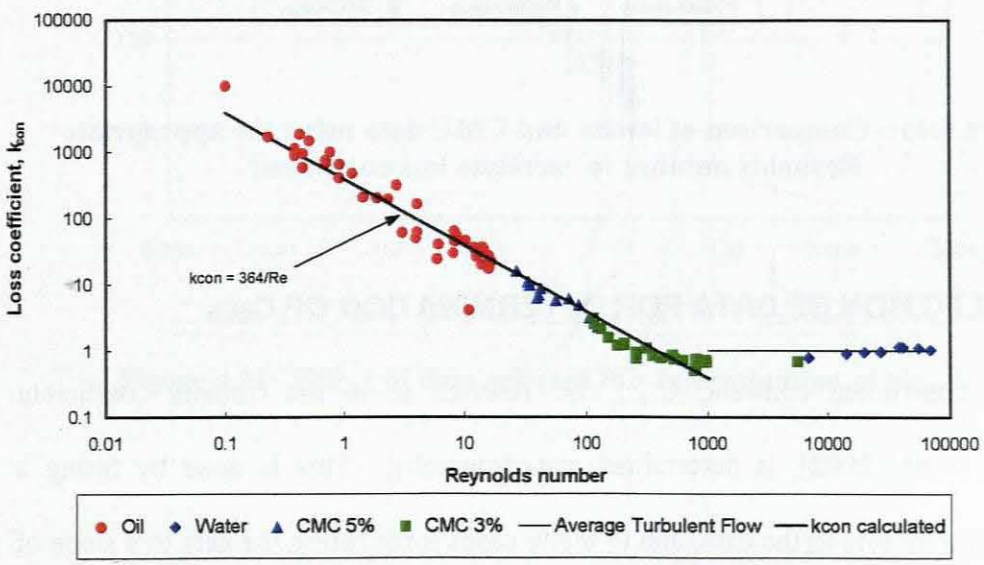

Figure 4.20: Comparison of oil and CMC data using the appropriate Reynolds number to correlate loss coefficient

The same procedure was followed for a kaolin sample using the Metzner-Reed Reynolds number and the Slatter Reynolds number (Re_3). The latter accounts for the presence of a yield stress and it is clear in Figure 4.21 that dynamic similarity is attained only when using the Reynolds number that accounts for the yield stress, resulting in the same loss coefficient for kaolin and CMC.

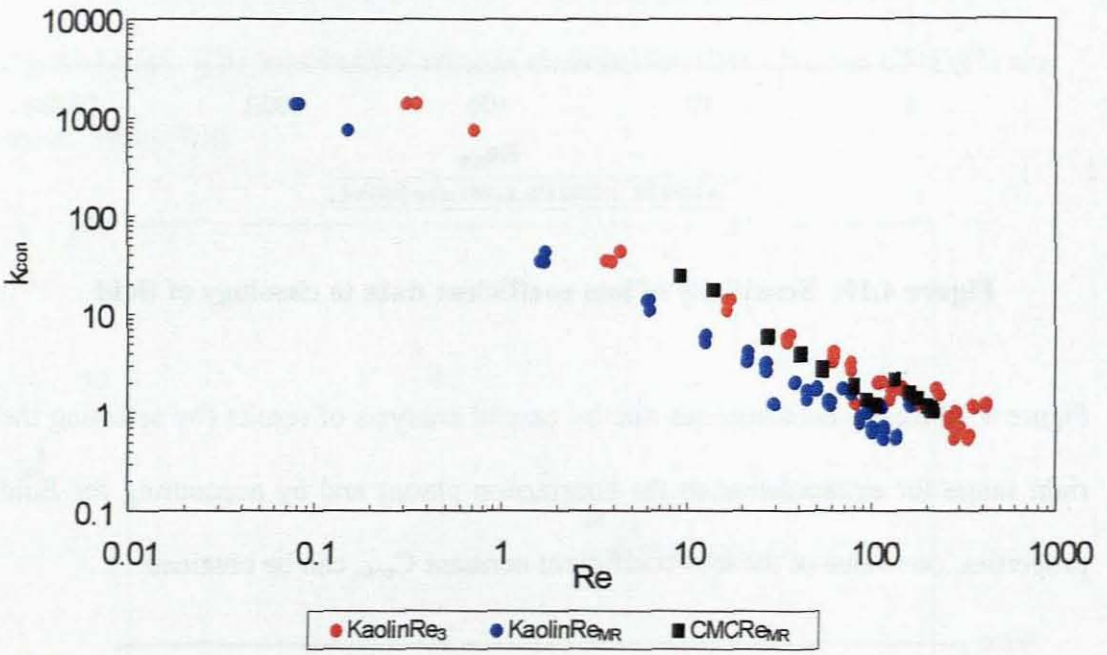

Figure 4.21: Comparison of kaolin and CMC data using the appropriate Reynolds number to correlate loss coefficient

4.7 SELECTION OF DATA FOR DETERMINATION OF C_{CON}

The loss coefficient constant, C_{con}, also referred to as the Couette coefficient (Sisavath *et al.*, 2002), is determined experimentally. This is done by fitting a power-law trendline to the data, and in many cases force fitting the data to a slope of –1. The value of C_{con} is therefore based on the range of data available. Jadallah

(1980) tested to as low as Re = 1, Pienaar (1998) tested down to Re = 0.1, but Ma (1987) only tested to Re =100. There is definitely more than one transition zone when a fluid flows through a contraction and it is clear from McNeil's prediction that there is also a change at Re = 10.

The effect of the range of data points on C_{con} was evaluated. First of all a data range at Re >10 was selected for determining C_{con}. Then a range of data points of Re < 10 was used to determine C_{con}. The results are shown in Figure 4.22. It is clear that results at Re < 10 will yield a value of C_{con} closer to that of theoretical predictions.

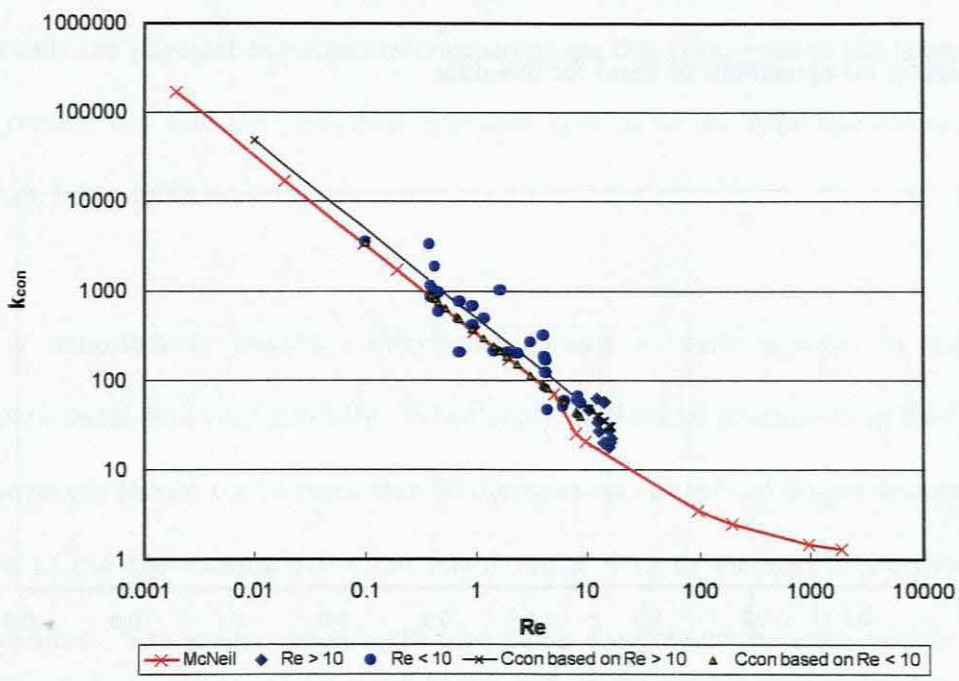

Figure 4.22: Effect of data selected for determination of C_{con}

4.8 C_{CON} VERSUS CONTRACTION RATIO

A comparison of C_{con} obtained for this work with that summarised in Jadallah (1980) is given in Table 4.9 and Figure 4.23 below.

Table 4.9: C_{con} obtained by various researchers

β	C_{con}	INVESTIGATOR
0.125	295	Sylvester & Rosen (1970)
0.228	385	This work
0.402	795	Astarita & Graco (1968)
0.445	110	Jadallah (1980)
0.496	288	This work
0.5	900	Ma (1987)
0.660	59	Jadallah (1980)
0.851	155	This work

There is clearly no agreement or trend for this data.

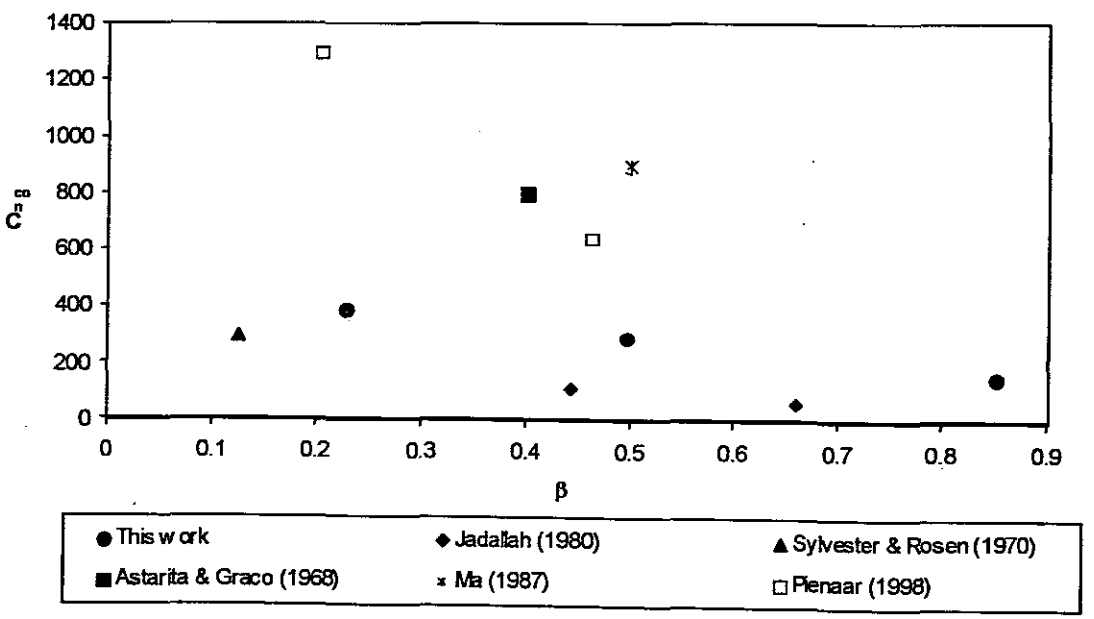

Figure 4.23: C_{con} versus contraction ratio for various researchers

4.9 CONCLUSIONS

In this chapter, the analysis and the results obtained for three contraction ratios have been presented for both laminar, transitional and turbulent flow. Comparison with previous work showed discrepancies as found in literature. This has been investigated by applying various methods to analyse the same set of raw data and results were obtained that agreed with every other set of data obtained in literature.

Although previous workers (Jadallah, 1980; Ma, 1987; Pienaar, 1998) presented similar plots, this is a study to demonstrate how various results could be obtained for the loss coefficient constant C_{con}, as was done in this section. It is evident that it is not only the physical experimental measurements that contribute to the large scatter of results, but also the analytical approach applied to the experimental results to obtain loss coefficients.

It is important to analyse experimental results in various ways by assessing experimental data very carefully. When applying the total pressure drop method, the pipe length should not be more than 50 diameters upstream and downstream and it is best to use the measured friction factor rather than to estimate it by theoretical equations. The longer the straight pipe used, the greater the error will be in the estimated friction factor, often resulting in negative values for k_{con}.

Furthermore, this is the first study to offer a plausible explanation for the discrepancies exposed in the literature. This issue is of fundamental relevance to

this entire field of study because, until it is resolved, there is no basis of credibility for extending similar studies to the more complex geometries found in industrial applications such as valves, bends, etc. This study therefore initiates a credible study of industrial urgency and importance.

CHAPTER 5

CHAPTER 5
APPLICATION OF CFD TO INVESTIGATE THE FLOW BEHAVIOUR THROUGH A SUDDEN CONTRACTION

5.1 INTRODUCTION

To investigate the flow behaviour through a sudden contraction, a commercially available software package for fluid flow calculations, CFX, was used. The objective of this work was to determine the pressure drop across the sudden contraction using the fluid properties of a Newtonian fluid tested in the experimental rig and evaluate the results in exactly the same way as the real experimental results.

This study is important to determine the applicability of Computational Fluid Dynamics (CFD) studies to determine loss coefficient data for fittings. Sisavath *et al.* (2001) investigated creeping flow through a sudden contraction and obtained a correlation C_{con} based on Sampson's rule as discussed in Chapter 2. They did, however, not compare their results with experimental data because of the discrepancies that existed between the experimental data obtained by various researchers.

In this work it was attempted to do both an experimental and numerical investigation simultaneously and to compare the results obtained. The experimental results were presented in Chapter 4. In this chapter, a description and the operation of the program will be given as well as the pressure drop results and loss coefficient data

obtained for the geometry constructed. It was decided to use CFX only for laminar flow of Newtonian fluids to eliminate any debate regarding the ability of the software to handle non-Newtonian fluids and turbulence. As shown in the previous chapters, it is possible to obtain dynamic similarity for Newtonian and non-Newtonian fluids by using the appropriate Reynolds number that best accounts for its viscous behaviour.

5.2 DESCRIPTION OF CFX PROGRAM OPERATION

CFX-4 solver is a program for the prediction of laminar and turbulent flow, and heat transfer, together with additional models such as multiphase flows, combustion and particle transport. The first version of the code (originally FLOW3D) was limited to simple Cartesian and cylindrical geometries. The second release of the software overcame this limitation through the use of a body-fitted coordinate system. The third release and the current CFX-4 extend the geometric capabilities of the code by using the facility of multi-block or block-unstructured grids; i.e., the grid may now be constructed by gluing together an arbitrary number of topologically-rectangular grids or blocks.

The suite of CFX-4 programs comprises the following modules:

- the Pre-process Module or Geometry and Grid Generators.
- the Front End Module of the CFX-4 Solver.
- the Solution Module of the CFX-4 Solver.
- the Post-processing or Graphics Modules.

5.2.1 The Geometry and Grid Generators

These may be used to define both the geometrical domain of the calculation and the finite difference grid. Details of the topology and the grid coordinates are written to disk in a form readable by the Front End of the solver. The Geometry and Grid Generators include the interactive grid generators, CFX-Meshbuild and CFX-Build, which may also be used to specify some of the topological features of the geometry, and the finite element to multi-block grid converter, CFX-Meshimport.

5.2.2 The Front End

This takes the input specification of the problem and converts it from a form convenient for the design into a form for efficient execution. At the same time, detailed error checking is performed. The Front End also provides simple utilities to help the user specify the problem; for example, a database is provided which provides the physical properties of some common Newtonian fluids. The problem is specified in a single data file using the Command Language. The command language is a set of English-like commands, subcommands and associated keywords. In the Interactive Front End, CFX-Setup, this data file is constructed automatically via a graphical user interface. User-defined Fortran routines may be included for features that are too complex to be described using the command language.

5.2.3 The Solution Module

This solves the discretised representation of the problem. It receives the information in a form that permits maximum efficiency to be obtained from different types of computers, including vector and parallel processors. The Solution Module has only a few output facilities; for example, for printing the solution and dumping the solution to disk files.

5.2.4 The Graphics Modules

These modules produce the main graphics output. Essentially, the Solution Module writes the results to disk files, and these are then read by the Graphics Modules. Interfaces to other post-processing packages have been constructed, and there are a number of post-processing options available for various workstations.

5.2.5 The Governing Equations

The flow calculations in the software are based on the solution of the Navier-Stokes equations with various extensions. The equations solved in laminar flows in CFX-4 are as follows:

The equations for conservation of mass and momentum

$$\frac{\partial \rho}{\partial t} + \nabla.(\rho \mathbf{u}) = 0. \tag{5.1}$$

$$\frac{\partial \rho \mathbf{u}}{\partial t} + \nabla.(\rho \mathbf{u} \otimes \mathbf{u}) - \nabla.\tau = -\nabla p + \mathbf{B} \tag{5.2}$$

Transient advection diffusion where the shear stress tensor is given by

$$\tau = \mu\left[\nabla u + (\nabla u)^T\right], \tag{5.3}$$

and possibly other scalar equations such as, in a non-isothermal flow, an equation for conservation of energy where ρ is the fluid density, u is the fluid velocity, p is the pressure, t is the time, μ is the molecular viscosity and B is a body force. The most common type of body force is the gravitational term where $B = \rho g$ and is only explicitly included for buoyant flows. The tensor product is defined by

$$(a \otimes b)_{ij} = a_i b_j. \tag{5.4}$$

The equations for laminar flow are:

$$\frac{\partial \rho}{\partial t} + \frac{\partial}{\partial x^i}\left(\rho u^i\right) = 0 \tag{5.5}$$

and

$$\frac{\partial \rho U^k}{\partial t} + \frac{\partial}{\partial x^i}\left(\rho u^i u^k\right) - \frac{\partial \tau^{ik}}{\partial x^i} = -\frac{\partial p}{\partial x^k} + B^k \tag{5.6}$$

where

$$\tau^{ik} = \mu\left(\frac{\partial u^k}{\partial x^i} + \frac{\partial u^i}{\partial x^k}\right). \tag{5.7}$$

The summation convention is used where repeated indices are summed over.

5.3 CFD INVESTIGATION

The details of the CFD investigation such as the geometry, grid and grid optimisation will be presented in this section.

5.3.1 Geometry

A two-dimensional model was created of a 42.26 mm pipe upstream connected to a 9.28 mm pipe downstream. The upstream length was 100 mm (approximately 2.5D) and the downstream length 150 mm (approximately 15D). These distances were indicated from initial CFX tests done on longer test sections as being sufficient for investigating the distance of interference. Three solid blocks were created by means of extrusion. A 10-degree wedge was specified and is shown in Figure 5.1. Inlet, outlet and symmetry planes were specified. A fully developed velocity profile was specified at the inlet of the upstream pipe. This was done to avoid a long upstream section that would only consume solution time when solved and not give more information about what happens in the region near the contraction plane.

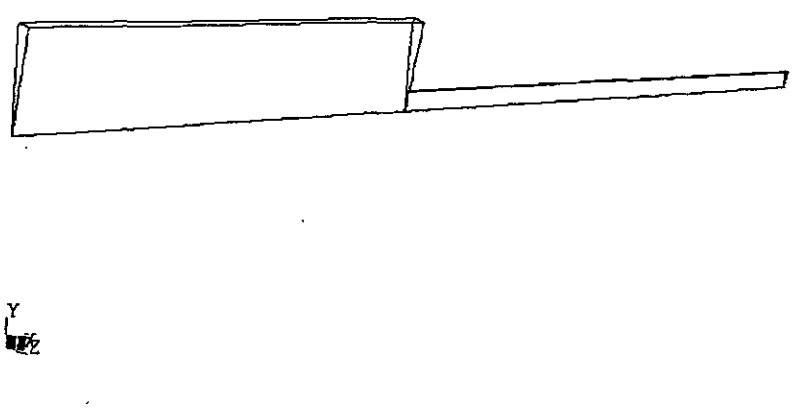

Figure 5.1: Geometry of sharp-edged contraction using CFX (not to scale)

5.3.2 Boundary Conditions

Mass flow boundaries were specified at the inlet and outlet. Mass flow boundaries are used to model inflow and outflow boundaries where the total mass flow rate into or out of the domain is known. This is done by applying a nominal Neumann boundary condition to the velocity field, $\frac{\partial u^i}{\partial n} = 0$. The discrepancy between the actual mass flow rate out of the domain and the desired flow rate M is computed. An increment is added to u^i on the boundary in the direction of the outward going unit normal to n^i to force the outward mass flow rate to the desired value. This is equivalent to

$$\frac{\partial u^i}{\partial n} = \lambda n^i, \tag{5.8}$$

where λ is chosen to force the desired mass flow rates.

5.3.3 Grid and Mesh

A one-way biased, body-fitted grid was chosen, concentrating the grid at the outlet of the upstream pipe and the inlet of the downstream pipe as shown in Figure 5.2, where the maximum changes in the pressure gradient were expected owing to changes in the velocity profile.

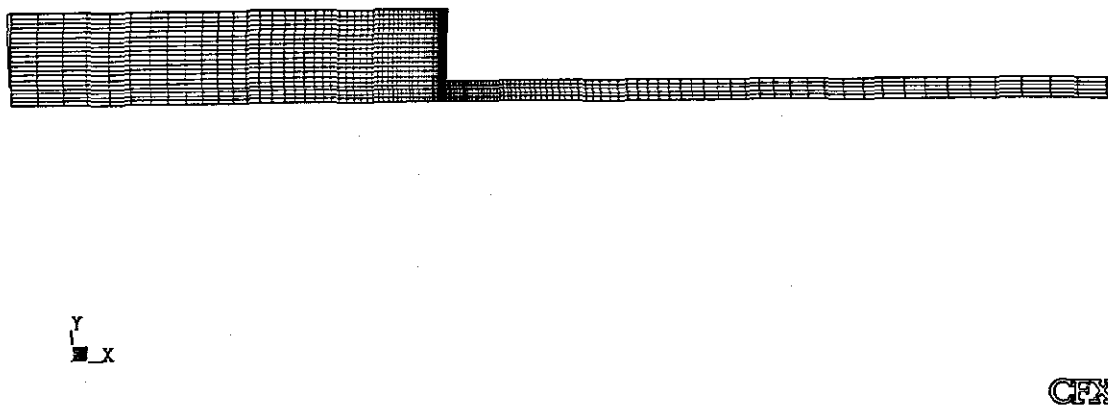

Figure 5.2: Illustration of one-way biased grid spacing (not actual grid used)

5.3.4 Grid Sensitivity and Optimisation Study

Three grids were constructed to investigate grid dependency. The results of the study are shown in Table 5.1. Grid 2 was selected for all investigations to obtain more detail in the 270 and 90-degree corners of the contraction. In Table 5.1, the results from Grid 3 are taken as the reference pressure from which the difference of the other three grids was calculated. The difference between the total pressure drop obtained from grids 1 – 2 were less than 2 % and for Grid 4 less than 0.1 %, an indication that the solution is grid independent.

Table 5.1: Grid optimisation

GRID	NO. OF ELEMENTS	P_{tot} [Pa]	DIFFERENCE [%]
Grid1	10 200	8.552	1.90
Grid2	20 000	8.570	1.70
Grid3	51 600	8.718	0
Grid4	68 000	8.713	0.057

5.3.5 Fluid

The physical properties of lubrication oil at 25°C were specified as per specimen tested in the Flow Process Research Centre and are as shown in Table 5.2.

Table 5.2: Fluid properties of lubrication oil used in CFX simulations

FLUID PROPERTY	RESULTS OBTAINED IN THE FLOW PROCESS RESEARCH CENTRE
Density [kg/m^3]	887
Viscosity [Pa.s]	0.353

5.3.6 Simulations

The objective was to determine the pressure drop due to the contraction for Reynolds numbers of 100, 10, 1, 0.1 and 0.01. This was done by specifying the mass flow into the boundary based on the Reynolds number as shown in Table 5.3.

Table 5.3: Mass flow rate at various Reynolds numbers

REYNOLDS NUMBER	MASS FLOW [kg/s]
0.01	7.17E-07
0.1	7.17E-06
1	7.17E-05
10	7.17E-04
100	7.17E-03

5.4 ANALYSIS OF RESULTS OBTAINED FROM CFX

From the outset of this work it was decided to analyse the data in exactly the same way one would for physical experiments of this nature, i.e., the evaluation of the pressure grade line (Edwards *et al.*, 1985; Pal & Hwang, 1999). One of the advantages of numerical studies is that more detail can be extracted from the areas of interest – at the exit from the upstream pipe and the entrance of the downstream pipe – because of the fine grid spacing compared with actual pressure tappings mounted around this area. A diagram presented by Boger (1987) shows the factors that influence the pressure drop across the sudden contraction very clearly. This drawing is shown in Figure 2.6 in an attempt to draw a correlation between the flow phenomena and the pressure gradient.

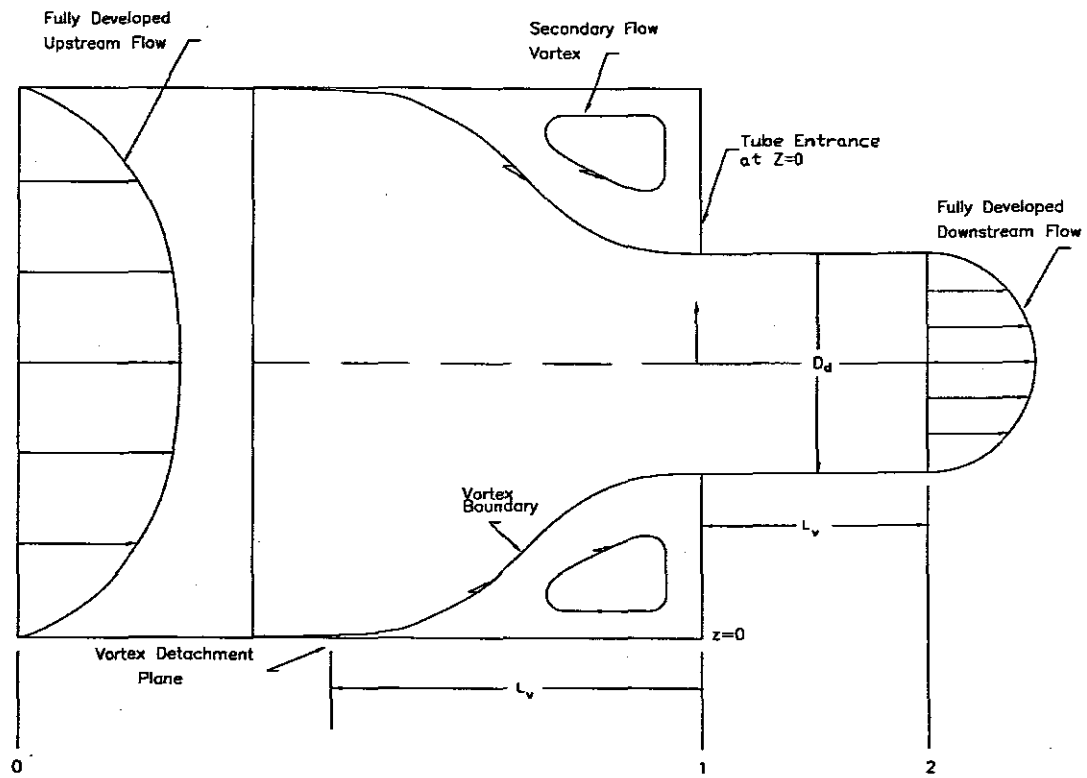

Figure 2.6: Basic elements of laminar flow through a contraction (Boger, 1987)

The fully developed upstream and downstream flow should have a constant pressure gradient. At the vortex detachment plane (as shown in Figure 2.6), the pressure gradient upstream should change significantly, and similarly for the downstream section. The length from the detachment plane to the contraction plane will be referred to as L_{ex} in this work. The entry length in the smaller tube will be referred to as L_e.

- L_{ex} is defined as the length upstream from the contraction plane to where the pressure grade line starts to deviate from that of the fully developed pressure grade line as shown in Figure 5.3.

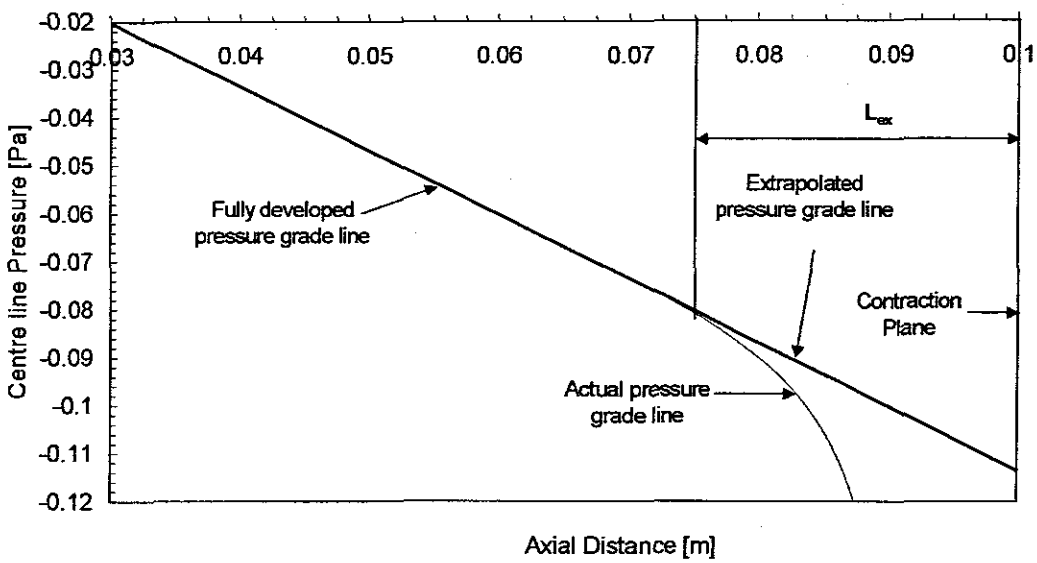

Figure 5.3: Definition of L_{ex}

- L_e is defined as the length downstream from the contraction plane to where the actual pressure grade line coincides with the fully developed pressure grade line as shown in Figure 5.4.

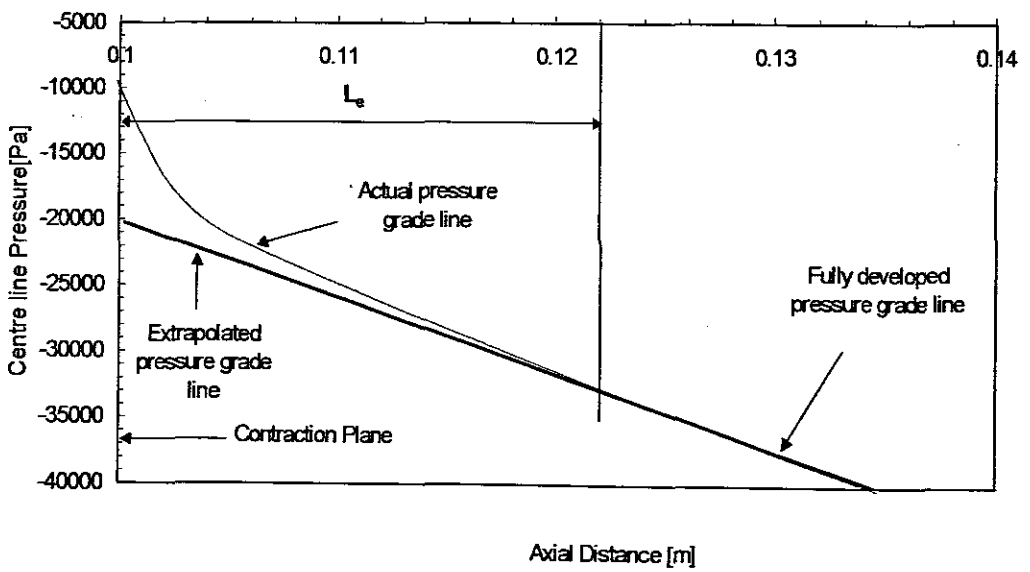

Figure 5.4: Definition of L_e

The values of L_{ex} and L_e are presented in Table 5.4 and Figure 5.5. It is clear that L_e tends to zero for Re < 1 and that L_{ex} decreases for Re > 1. The average value of L_{ex} presented for this work exclude L_{ex} obtained at Re = 100.

Table 5.4: Values of L_{ex} and L_e

Re	L_{ex} [m]	Le [m]
0.01	0.0248	0.000402
0.1	0.0246	0.000402
1	0.0246	0.000402
10	0.0232	0.602
100	0.0173	3.63

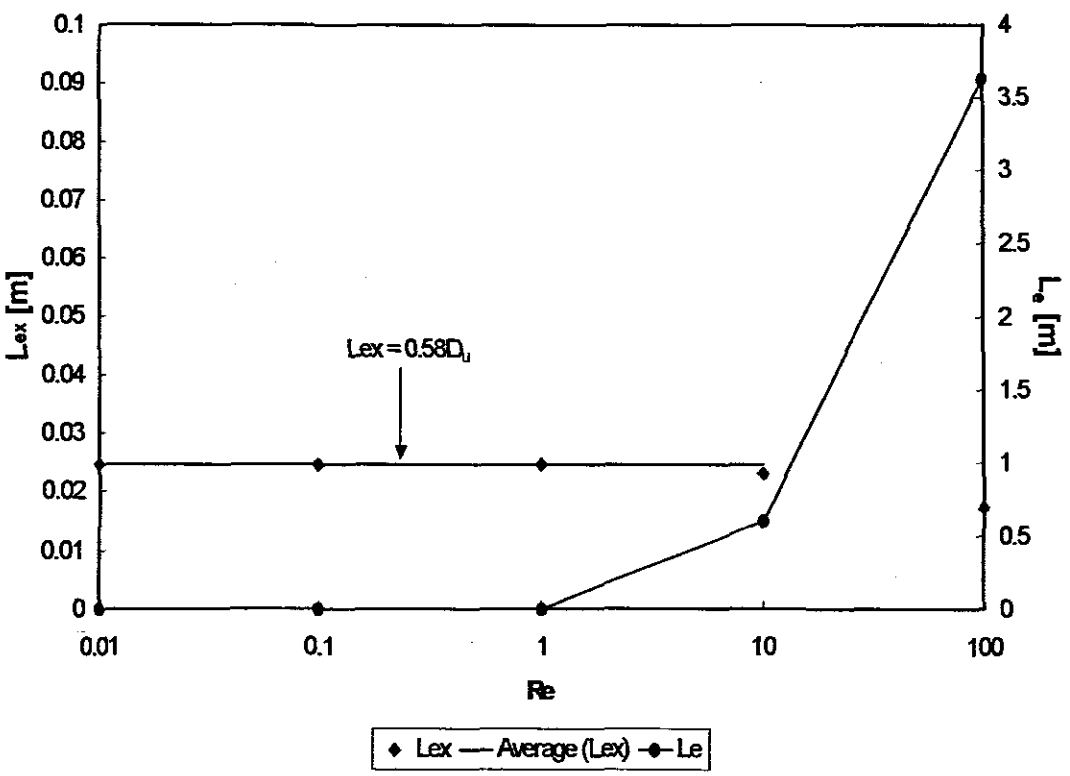

Figure 5.5 Values of L_{ex} and L_e

The exit length has previously been defined as $L_v = 0.17D$ (Boger, 1987). This is also shown in Figure 5.6. In the present work it was found that $L_{ex} = 0.58D$. This difference deserves comment. Two different techniques and phenomena were used. Boger used streak photography to determine the value of L_v. In the present work the pressure grade line was used to determine L_{ex}. It is clear that the present work identifies the earliest point where steeper centre line pressure gradients are observed than in the fully developed region upstream as shown in Figure 5.6 from the plot of dp/dx versus axial distance. The pressure gradient at the wall is increasing and peaks due to the secondary flow vortex. This increase is not observed at the centre line. This agrees both with Boger's distance L_v and with Franzini and Finnemore (1998).

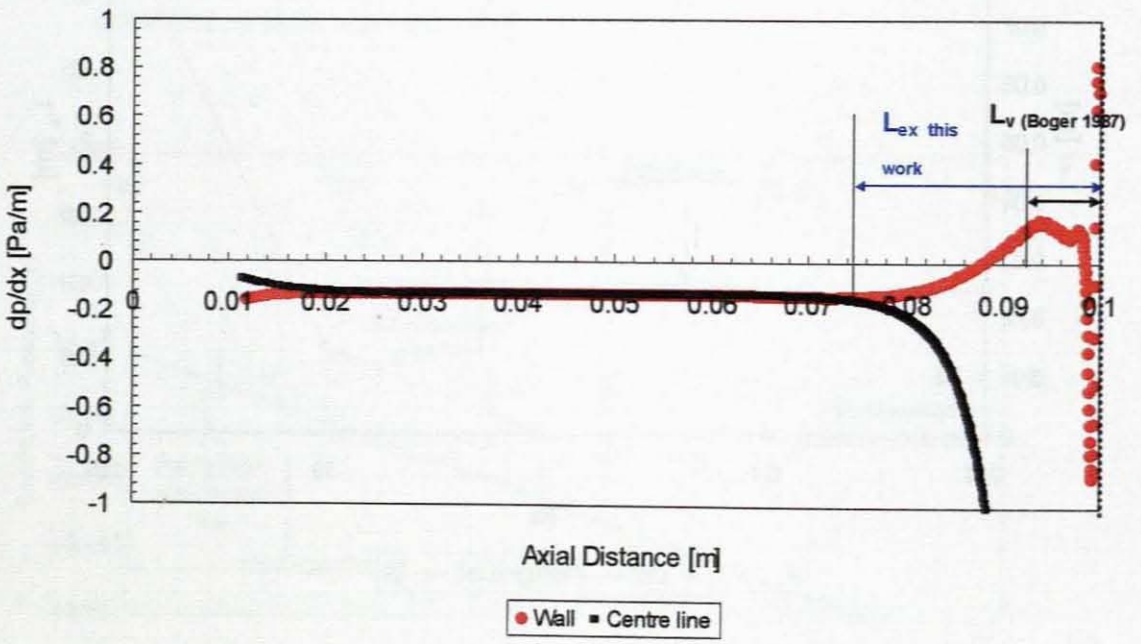

Figure 5.6 Comparison of Boger's L_v with this work L_{ex} at the wall and centre line

Further clarification is therefore required to support the contention that L_v and L_{ex} are not the same. This information is directly related to the new approximation that is discussed in the next chapter and it is therefore very important that it be validated. This is done in the sections below.

5.5 CONFIRMATION OF THE VALUE OF L_{ex}

The pressure grade line is a very robust method for determining the value of L_{ex}. It was therefore important to see if it could be verified in any other way. The pressure drop is associated with the change of the velocity profile from being fully developed to entering the smaller tube owing to secondary flow causing the streamline close to the wall to curve. Velocity profile, streamline and contour plots were produced to see if L_{ex} found in the previous section could be correlated with any of these.

5.5.1 Velocity Profile Development

To validate L_{ex}, the velocity profiles were observed at this distance to see if any deviation from the fully developed profile exists. The value of L_{ex} was found to be approximately 0.025 m for $Re \leq 1$. The contraction plane in this study was at 0.1 m, so the velocity profiles were evaluated at planes 0.05 m and 0.075 m before the contraction. Figure 5.7 shows a plot of u/u_{max} versus radius at various Reynolds numbers at a distance of 0.075 m compared with a theoretically perfect parabolic profile. The velocity profile was observed at a distance prior to L_{ex} at 0.05 m where the flow is supposed to be fully developed. At 0.075m, the velocity profile is

significantly different to fully developed flow. This is the point at which the pressure grade line starts to deviate from the fully developed flow as discussed in Section 5.4. Figure 5.7 shows that the velocity profile is indeed distorted at L_{ex} and also that the velocity profile development is independent of the Reynolds number at $Re < 1$. The magnitude of the change in velocity profile does not appear to be reflected in the pressure data. The shape of the velocity profile is the same at $Re < 1$ at a distance of 0.075 m.

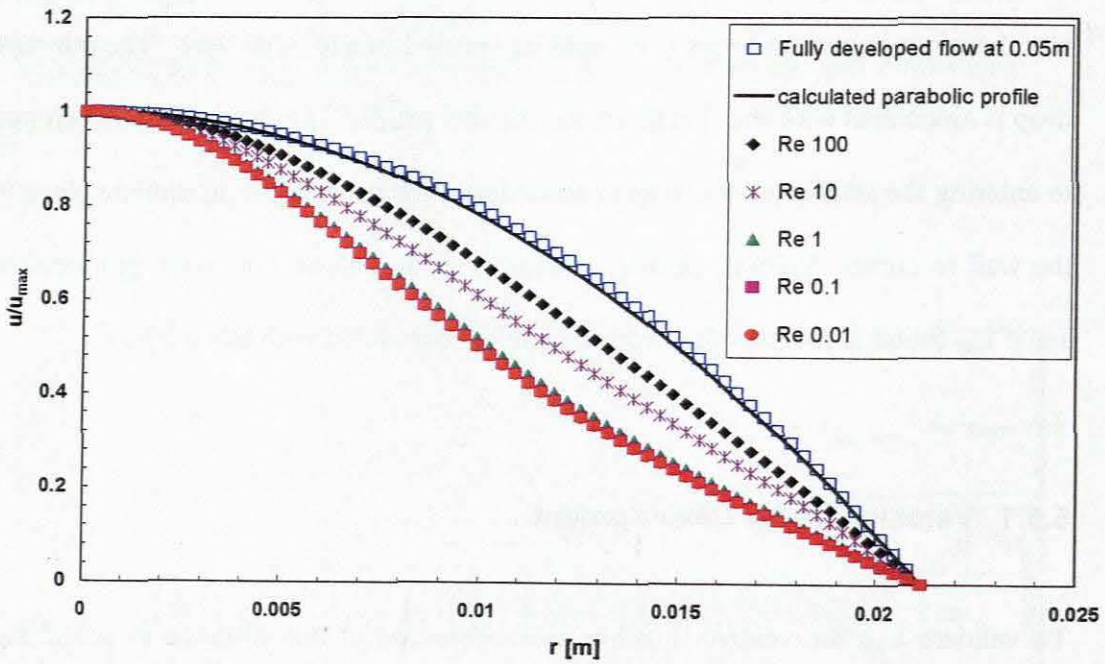

Figure 5.7: Comparison of velocity profiles at 0.05m and 0.075m

5.5.2 Streamlines

A plot of streamlines for Re 0.01 is given in Figure 5.8. The distance of L_{ex} is shown with a vertical line at X =0.075m. It is clear from the streamline shape that negligible curvature exists before this point, validating L_{ex} obtained in this work.

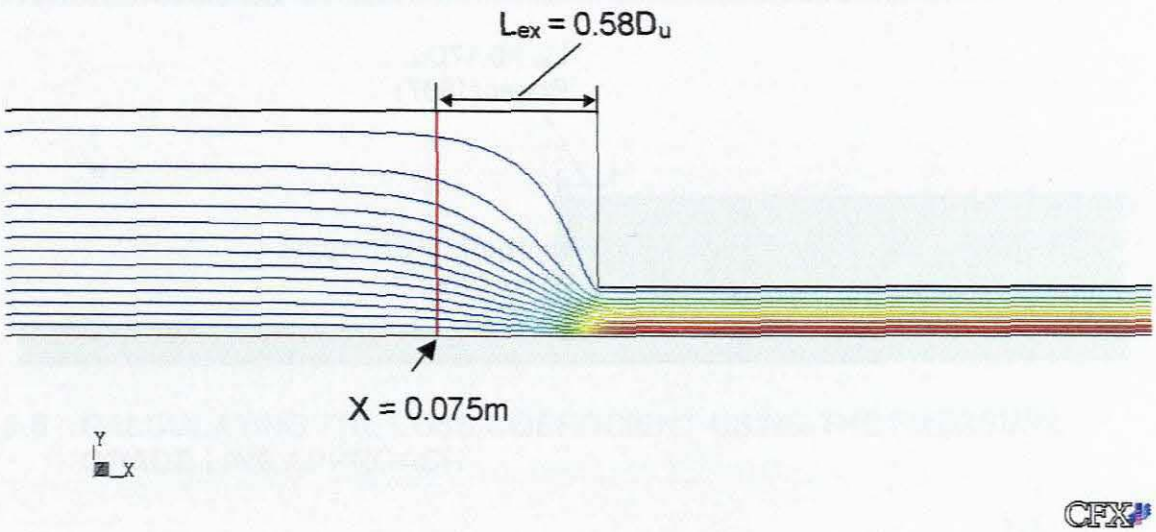

Figure 5.8: Streamlines at Re = 0.01

5.5.3 Contour Plots

A further method of evaluating the data was by means of contour plots. A contour plot of the u velocity in the XY plane is shown in Figure 5.9. The flow vortex can be observed in this case in the corner of the upstream tube. It agrees very well with the observations of Boger and Ramamurthy (1973) and the predictions of Boger (1987).

It is clear that the detachment plane is not at the same point as the start of the secondary flow vortex and that the prediction of Boger (1987) indicates the point at which the secondary flow vortex starts. This present work gives the onset of the detachment plane. In this case the flow detaches at a distance $0.58D_u$ and the secondary flow vortex can be observed at $0.17D_u$.

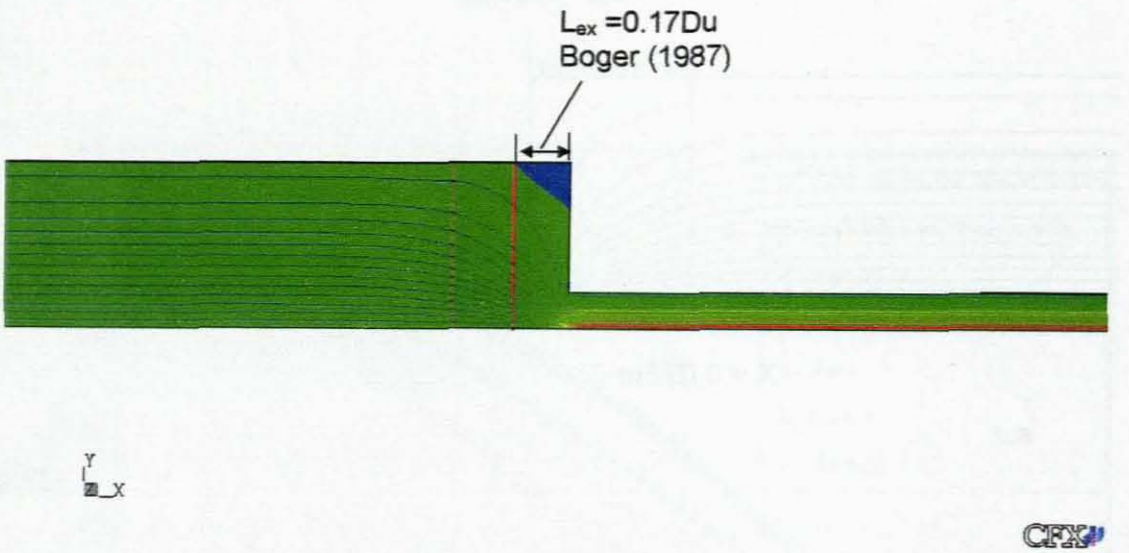

Figure 5.9: Contour plots at Re = 0.01

Figure 5.10 shows the disappearance of the flow vortex with increasing Reynolds number.

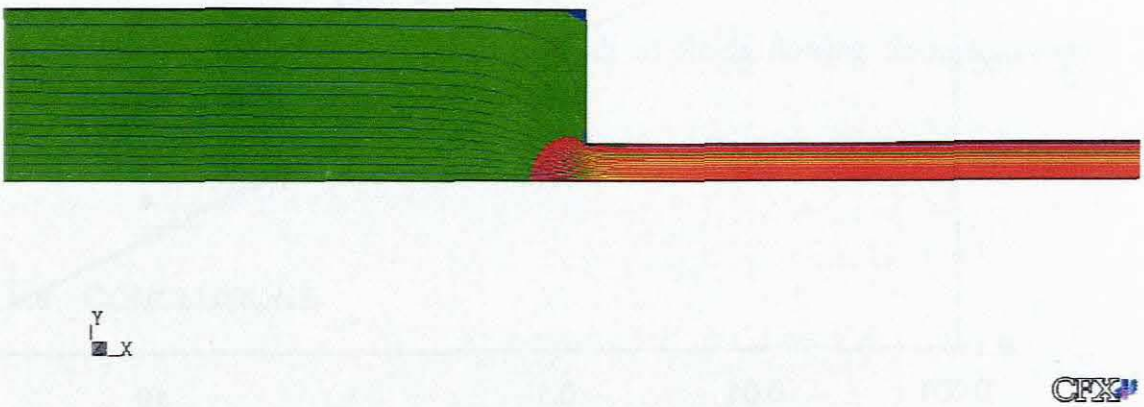

Figure 5.10: Contour plots at Re = 100

5.6 CALCULATING THE LOSS COEFFICIENT USING THE PRESSURE GRADE LINE APPROACH

The loss coefficient can be obtained by applying the Bernoulli equation as described in the previous chapter by extrapolating the pressure grade line to the contraction plane. The results are shown Figure 5.11 along with those of Sisavath *et al.* (2001) who did a similar study and there is good agreement between the results. There was, however, a significant discrepancy between the CFD study and the experimental results.

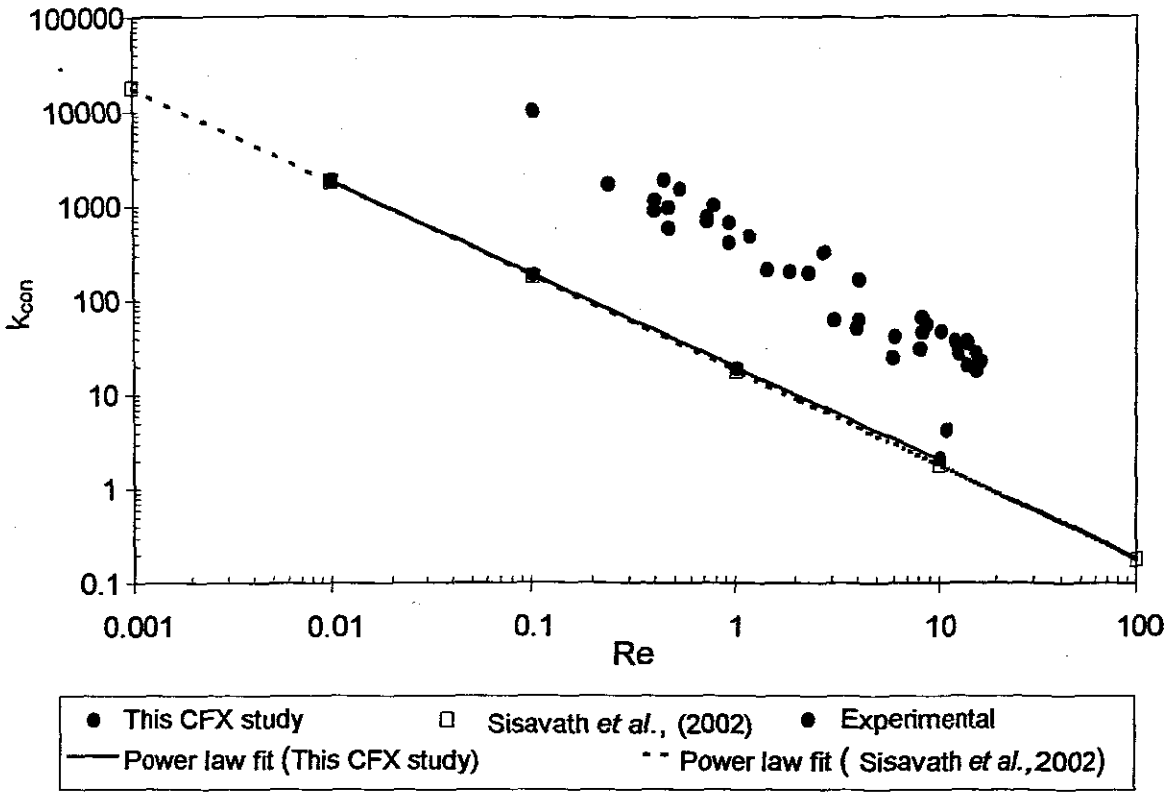

Figure 5.11: Comparison of this CFD work with Sisavath *et al.* (2001)

5.7 DISCUSSION

This work confirms that for a contraction ratio of $\beta \leq 0.25$, the flow phenomena at $Re < 1$ is independent of the Reynolds number and that the velocity profile is almost fully developed as the fluid enters the smaller tube. The size of the secondary flow vortex found in this work agrees with that of Boger (1987). It has been established that this is different from the point of detachment and an estimate for the point of detachment has been determined in this work.

The loss coefficient data obtained from this CFD work agrees with that of Sisavath *et al.* (2002). It did, however, not agree with the experimental work. The experimental work however agreed with the prediction of McNeil and Morris (1995). This work highlights the need for the further development of predictive techniques for the pressure drop as a result of fluids flowing through sudden contractions in laminar flow.

5.8 CONCLUSIONS

The operation of the CFD program, CFX, has been described. The geometry has been described and the details of the fluid properties given. It was shown that the result was grid independent. The analysis of the results was discussed. It was found that the entry length, $L_{ex} = 0.58D_u$, was 3.4 times of that given by Boger (1987). L_{ex} in this case is, in fact, the onset of the vortex detachment, where Boger's correlation describes the length of the secondary vortex flow (cell size) and that is not the full length (L_v) as shown in Figure 2.6. L_{ex} should therefore be used in any pressure drop calculations where the physical length of the vortex area is required, i.e., from the detachment plane.

The final results obtained for this work were within 6% of those obtained by Sisavath *et al.* (2002) even though two different CFD software packages were used. Unfortunately the results obtained using CFD did not agree with the experimental results, and this still needs to be investigated. The purpose of this work was not to determine why the discrepancies exist, but to generate detailed flow data not

possible with the available experimental apparatus, to enable the development of an approximation that is based on both the macro view (total pressure drop) and the micro view (detachment length) using both numerical and experimental results. The new approximation will be described in the following chapter.

CHAPTER 6

CHAPTER 6

PRESENTATION OF NEW ANALYSIS

6.1 INTRODUCTION

This chapter will describe the new approximation for predicting creeping flow through a sudden contraction of contraction ratio $\beta_{con} \leq 0.25$. The literature (Chapter 2) and the CFD study (Chapter 5) showed that the flow phenomena for this contraction ratio are simpler than those for larger contraction ratios. The proposed approximation will be based on this contraction ratio, but an attempt will be made to extrapolate it to other contraction ratios after the evaluation of this model in Chapter 7. This chapter will include

- Background to the analysis.
- Derivation of the conical approximation.
- Determination of the shape function, ϕ.
- Conclusions.

6.2 BACKGROUND TO ANALYSIS

Although much work has been done on sudden contractions, including both numerical solutions as well as experimental investigations, the literature shows that discrepancies exist amongst the experimental work of various researchers as well as numerical studies (Pienaar *et al.*, 2001). The focus of this study is strongly

experimental, but because of the scepticism that exists about the reliability of experimental studies (Sisavath *et al.*, 2002), it was decided to, simultaneously with the experimental study, also apply commercially available computational fluid dynamics software to investigate the problem.

The experimental procedure and analysis of results are presented elsewhere (Chapter 3 and 4) and will not be described in this chapter again. The detail of the computational investigation and analysis of results was discussed in Chapter 5, as this was central to determine some parameters required for the conical approximation. The results obtained and the approximation will only be compared with the experimental results that were conducted and analysed as explained in Chapters 3 and 4.

It was demonstrated that non-Newtonian behaviour in fluids could be accounted for by using the appropriate Reynolds number for each fluid (Edwards *et al.*, 1985; Ma, 1987; Pienaar, 1998; Pienaar & Slatter 1999). Based on this information it was decided to conduct the CFD investigations using a Newtonian fluid only, eliminating all questions regarding the ability of the software to accommodate non-Newtonian behaviour. It was also decided that the output data from CFD would be evaluated in the same way as the experimental data.

The experimental procedure is in brief that the pressure drop is measured along the length of the pipes; both upstream and downstream by means of a number of

pressure taps either side of the contraction. The fully developed friction gradient is extrapolated to the contraction plane (Edwards *et al.*, 1985) to determine Δp_{con}.

It was shown by Boger (1987) that in general the vortex reattachment length (refer to Fig. 2.6) is dependent on the Reynolds number. However, for $\beta_{con} \leq 0.25$, the reattachment length is independent of the Reynolds number for $Re \leq 1$ (Boger, 1987; Hammad & Vradis, 1996). This clearly suggests one less variable to consider in the analysis of the frictional losses across a sudden contraction.

It was also shown in the early work of Christiansen *et al.* (1972) that the velocity profile is not uniform when the fluid enters the smaller tube as Re tends to 0. Vrentas and Duda (1973) confirmed this work and went further by showing that substantial development of the axial velocity profile towards its final parabolic form occurs by the time the fluid reaches the entrance of the smaller tube. This statement eliminated another variable in the analysis of the frictional losses across a sudden contraction at low Reynolds numbers.

These ideas led to the conclusion that an approximate analytical approach based on creeping flow could be developed because the flow phenomena are simpler. This could provide a basis for deriving a simple correlation needed for engineering design purposes.

6.3 DERIVATION OF THE CONICAL APPROXIMATION

The pressure loss in a sudden contraction is the sum of the upstream and downstream pressure losses and the additional loss due to the presence of the contraction as shown in Eq. (6.1).

$$\Delta p_{tot} = \Delta p_{upstream} + \Delta p_{con} + \Delta p_{downstream}. \quad (6.1)$$

In the case of flow through the sudden contraction at low Reynolds numbers ($Re \leq 1$), the downstream pressure losses can be ignored and Eq. (6.1) can be rewritten as

$$\Delta p_{tot} = \Delta p_{upstream} + \Delta p_{con} \quad (6.2)$$

A conical frustrum-shaped solid conduit can approximate the upstream losses if the following assumptions are made that will ultimately have to be accounted for by calibrating the approximation with experimental results:

- The S-curve will be taken as a straight line.
- Since the approximation assumes fully developed flow, the viscous friction losses resulting from the change in the velocity profile as the fluid enters the smaller tube (over the length L_{ex}) must also be taken into account.

Equation (6.2) then becomes

$$\Delta p_{con} = \Delta p_{cone} * \phi, \quad (6.3)$$

and ϕ is the factor that accounts principally for simplifications in the approximation.

A schematic diagram is shown in Figure 6.1 and it can be integrated to obtain the frictional loss in the cone where

$$D_x = D_1 \text{ at } x = 0$$

and

$$D_x = D_2 \text{ at } x = L_{ex}.$$

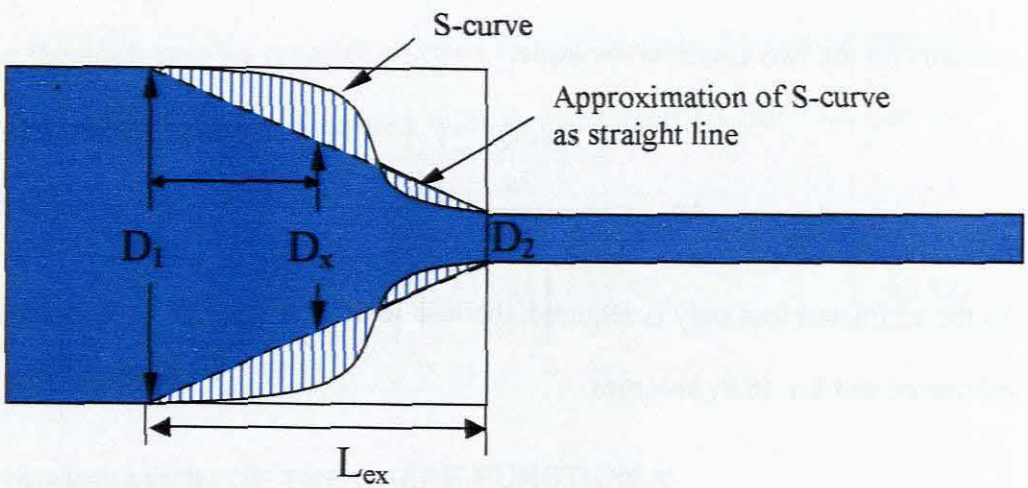

Figure 6.1: Conical approximation of low Reynolds number flows through a sudden contraction

The approximation is derived from the head loss in a straight pipe in laminar flow from Eq. (2.13) as

$$\frac{\Delta p}{L} = \frac{128\mu Q}{\pi D^4}. \tag{6.4}$$

For a differential element in the cone, Eq. (6.4) becomes

$$\frac{d\Delta p}{dx} = \frac{128\mu Q}{\pi (D_x)^4}, \tag{6.5}$$

where

$$D_x = D_1 - \frac{x(D_1 - D_2)}{L_{ex}}, \tag{6.6}$$

and Δp can be evaluated as

$$\Delta p = \int_0^{L-\alpha} \frac{128\mu Q}{\pi (D_x)^4} dx. \tag{6.7}$$

After integration, the following explicit equation is obtained, including ϕ that accounts for the two assumptions made,

$$\Delta p_{tot} = \frac{\phi \frac{128\mu Q L_{ex}}{3\pi}\left[\frac{1}{D_2^3} - \frac{1}{D_1^3}\right]}{[D_1 - D_2]}. \tag{6.8}$$

As the additional loss only is required, the loss in the straight pipe section should be subtracted and Eq. (6.8) becomes

$$\Delta p_{con} = \frac{128\mu Q L_{ex}}{\pi}\left[\frac{\phi}{3(D_1 - D_2)}\left(\frac{1}{D_2^3} - \frac{1}{D_1^3}\right) - \frac{1}{D_1^4}\right]. \tag{6.9}$$

The loss coefficient, k_{con}, can then be calculated from:

$$k_{con} = \left[\frac{2\Delta p_{con}}{\rho V_2^2}\right] + \theta, \tag{3.15}$$

where

$$\theta = \alpha_1 \beta^4 - \alpha_2,$$

but

$$C_{con} = k_{con} * Re. \tag{2.61}$$

Combining Eq. (6.9), Eq. (3.15) and Eq. (2.61) gives

$$C_{con} = \frac{64\beta L_{ex}}{D_2}\left[\frac{\phi\left(\beta^2+\beta+1\right)}{3}-\beta^3\right]+\theta \mathrm{Re}. \qquad (6.10)$$

As explained in Chapter 5, $L_{ex} = 0.58D_1$ and $D_2 = \beta D_1$, Equation (6.10) then becomes

$$C_{con} = 37\left[\frac{\phi\left(\beta^2+\beta+1\right)}{3}+\beta^3\right]+\theta\ \mathrm{Re}. \qquad (6.11)$$

For the low Reynolds number range considered for this analysis, the second term in Eq. (6.11) becomes negligible compared with the first term so that C_{con} can be approximated by

$$C_{con} = 37\left[\frac{\phi\left(\beta^2+\beta+1\right)}{3}+\beta^3\right]. \qquad (6.12)$$

6.4 DETERMINATION OF THE SHAPE FUNCTION, ϕ

Experiments were conducted in the Flow Process Research Centre as described in Chapters 3 and 4. The test section was made of an upstream section of 42.263mm and a downstream section of 9.28mm. Newtonian oil with a density of 887 kg/m3 and viscosity of 0.3534 Pa.s was tested. The experimental results were used to determine the value of ϕ. The value of L_{ex} used was 0.0246 and the resulting value of ϕ is 20 for $\beta_{con} = 0.22$. The results are shown in Figure 6.2.

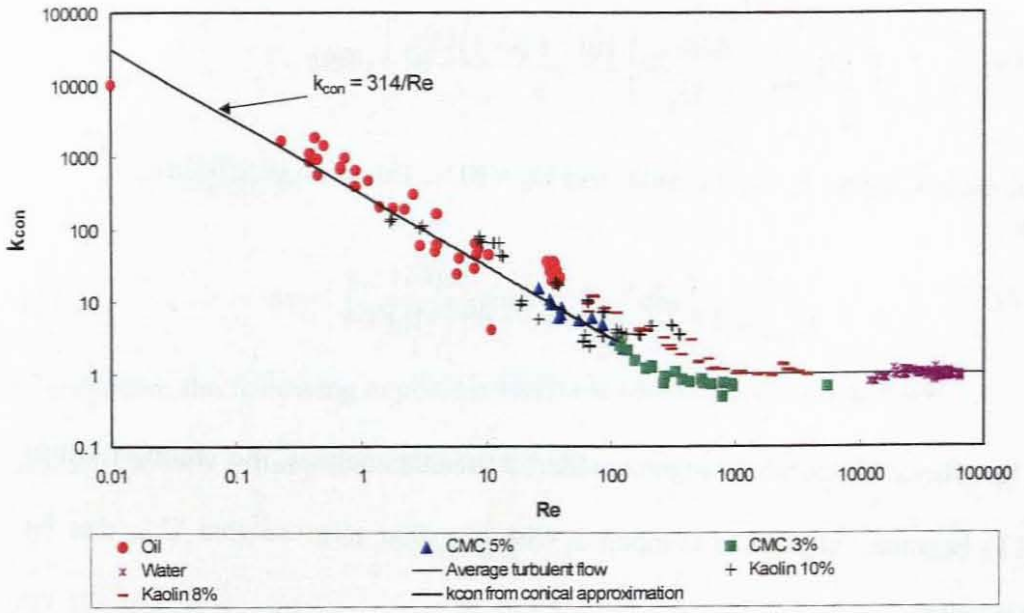

Figure 6.2: Fit of conical approximation to experimental data

6.5 CONCLUSIONS

The new analysis for modelling flow through a sharp-edged contraction of $\beta \leq 0.25$ was presented.

It was demonstrated that CFD, and in this case, the program CFX, was a useful tool to investigate flow through a sharp-edged contraction and allowed the determination of L_{ex} and L_e, not easily possible with experimental studies.

It was confirmed that L_e tends to zero with decreasing Reynolds number and that L_{ex} is independent of the Reynolds number at $Re < 10$.

The approximation was calibrated with experimental results and a value of 20 was determined for ϕ, to account for assumptions made. It was shown that laminar flow through a sharp-edged contraction of $\beta = 0.25$ can be approximated by this conical model.

CHAPTER 7

CHAPTER 7
EVALUATION AND DISCUSSION OF THE NEW ANALYSIS

7.1 INTRODUCTION

The main objective of this chapter is to compare the conical approximation with other engineering design models, more sophisticated fundamental models, as well as previous experimental results of various researchers, if available for $\beta = 0.25$ or less. If any agreement is obtained, it will not only validate the conical approximation, but also the experimental results obtained in the Flow Process Research Centre.

The second objective is to evaluate the extrapolation of this approximation to larger contraction ratios.

The models that will be used in this comparison are:

a) The engineering design approximation by ESDU (1989).
b) The mechanistic model based on the two-stream approach of McNeil and Morris (1995).
c) Approximation based on Sampson's rule by Sisavath *et al.*, (2002).

Fundamental aspects of these models were described in Chapter 2 and will not be repeated in this section.

7.2 COMPARISON WITH EXISTING MODELS

Three models were selected for comparison with the conical approximation. The models were selected based on the following criteria:

- A model widely used by industry (ESDU, 1989).
- A fundamentally sound and sophisticated model (McNeil and Morris, 1995).
- A model derived on a similar approach taken to that used in this study (Sisavath *et al.*, 2002).

A comparison of these models with the Conical Approximation will be given in this section.

7.2.1 The Engineering Design Approximation by ESDU (1989)

ESDU (1989) derived an expression for the prediction of the loss coefficient in laminar flow for Newtonian fluids that is valid for $Re < 10^4$. Equation 2.77 is only valid for $Re < 200$ for $\beta_{con} < 0.77$.

$$k_{con} = \left(0.32 + \frac{159}{Re}\right)\left(1 - \beta_{con}^{\ 2}\right). \qquad (2.77)$$

For $\beta = 0.22$ the loss coefficient, k_{con}, predicted from the Conical Approximation, was approximately 50% higher than that predicted by ESDU Eq. (2.77). The results are plotted on a graph of Reynolds number versus loss coefficient (k_{con}). The results and percentage difference in results are shown in Table 7.1.

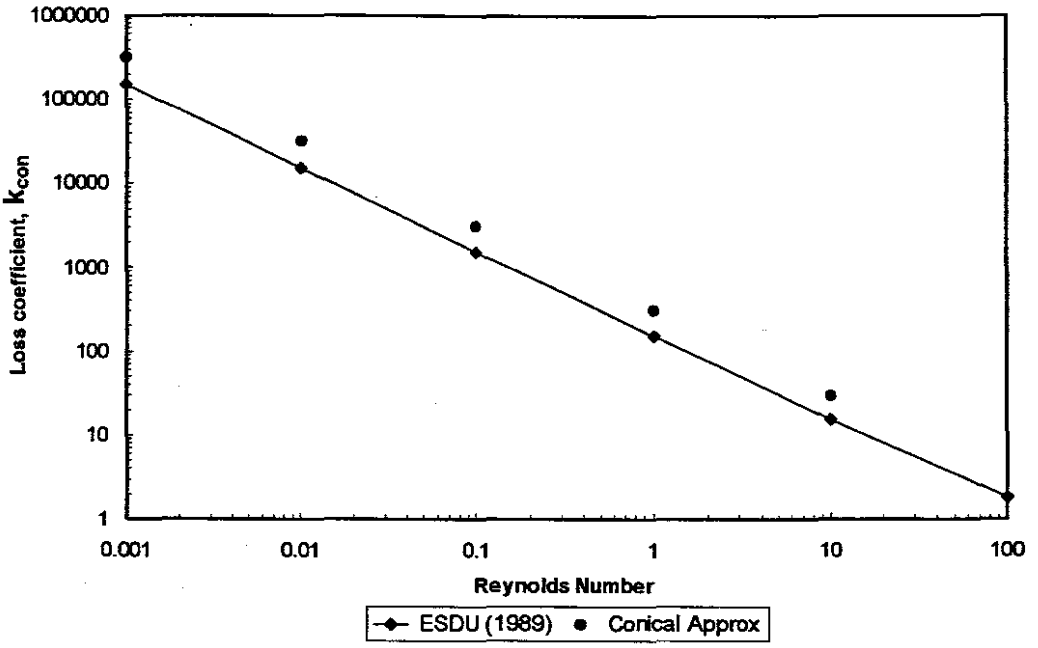

Figure 7.1: Comparison of loss coefficient predictions from ESDU (1989) and Conical Approximation

Table 7.1: Comparison of results for ESDU (1989) and Conical Approximation

Re	ESDU (1989)	CONICAL APPROXIMATION	%DIFF
0.001	151304	314459	51.88
0.01	15131	31444	51.88
0.1	1513	3143	51.84
1	152	312	51.48
10	15	29.5	47.59

This resulted in the following laminar flow loss coefficient constants (C_{con}) obtained from a power-law fit to the predicted results as shown in Table 7.2.

Table 7.2: Comparison of C_{con} from ESDU (1989) and Conical Approximation

METHOD	C_{con}
ESDU	152
CONICAL APPROXIMATION	314

The differences could lead to errors in final design estimates and are unacceptable.

7.2.2 The Mechanistic Model Based on Two-stream Approach by McNeil and Morris (1995)

This model by McNeil and Morris (1995) is one of the most sophisticated theoretical models developed for predicting flow through sudden contractions or nozzle flow. Originally developed for flows through sudden expansions, this model is based on a two-stream approach where the momentum and kinetic energy stored in the velocity profile of the fluid are altered by an area change of one stream relative to the other. The only problem with this model is that it does not converge to a simple equation for engineering design purposes. Although this work is based on sound theory, a geometry factor is introduced based on the experimental work of Edwards *et al.*, (1985).

Comparison with the conical approximation is shown in Figure 7.2.

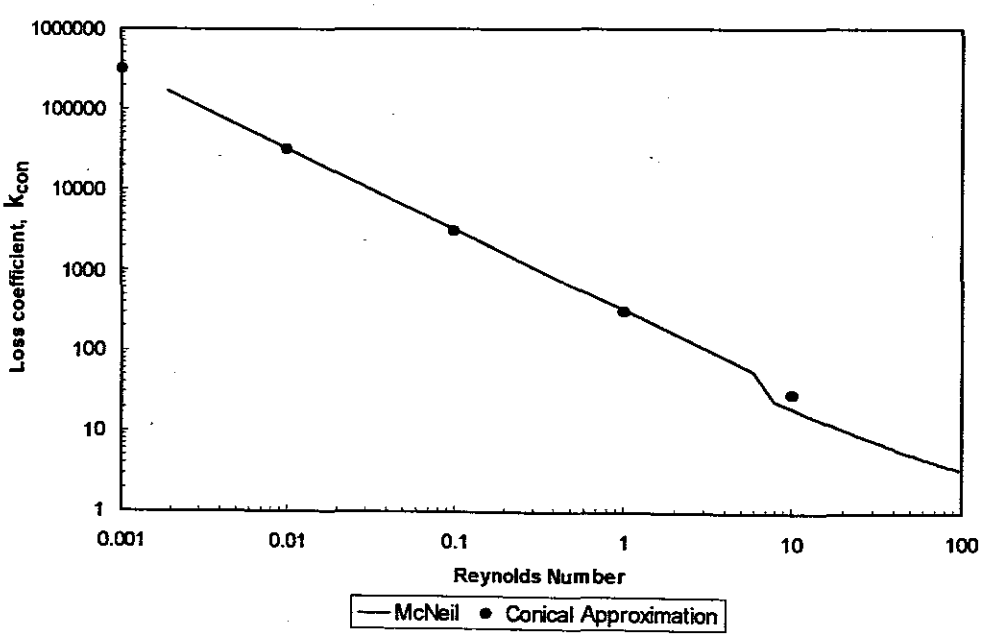

Figure 7.2: Comparison of loss coefficient predictions from McNeil and Morris (1995) and Conical Approximation

The results and percentage difference in results are shown in Table 7.3.

Table 7.3: Comparison of results for McNeil and Morris (1995) and Conical Approximation

Re	McNEIL (1995)	CONICAL APPROXIMATION	%DIFF
0.001	328000	314459	-4.31
0.01	32800	31444	-4.31
0.1	3280	3143	-4.37
1	328	312	-4.97
10	19	29.45	35.49

The following laminar flow loss coefficient constants (C_{con}) were obtained from a power-law fit to the predicted results as shown in Table 7.4.

Table 7.4: Comparison of C_{con} from McNeil and Morris (1995) and Conical Approximation

METHOD	C_{con}
McNEIL	328
CONICAL APPROXIMATION	314

There is excellent agreement between McNeil and Morris (1995) and the conical approximation with differences less than 5% for Re < 1, although the one model is very sophisticated (McNeil and Morris) and the other very simplistic (Conical Approximation). This is a good indication that the principle for deriving the conical approximation is sound as well as the results obtained in the Flow Process Research Centre.

7.2.3 Approximation Based on Sampson's Rule by Sisavath *et al.* (2002)

This study by Sisavath *et al.* (2002) is in many ways similar to the present study. It derives an analytical approximation for Newtonian flow through a sudden

contraction based on the creeping flow regime, i.e., as Re tends to 0. The two major differences are, however:

- A numerical investigation has been used to verify the analytical approximation.
- None of the results was calibrated or compared with experimental data.

Comparison with the conical approximation shows a difference of 95% as can be seen in Figure 7.3 and Table 7.5. The final form of the work of Sisavath *et al.* is an approximation for the calculation of the loss coefficient constant, C_{con} as described in this work. The results are shown in Table 7.6.

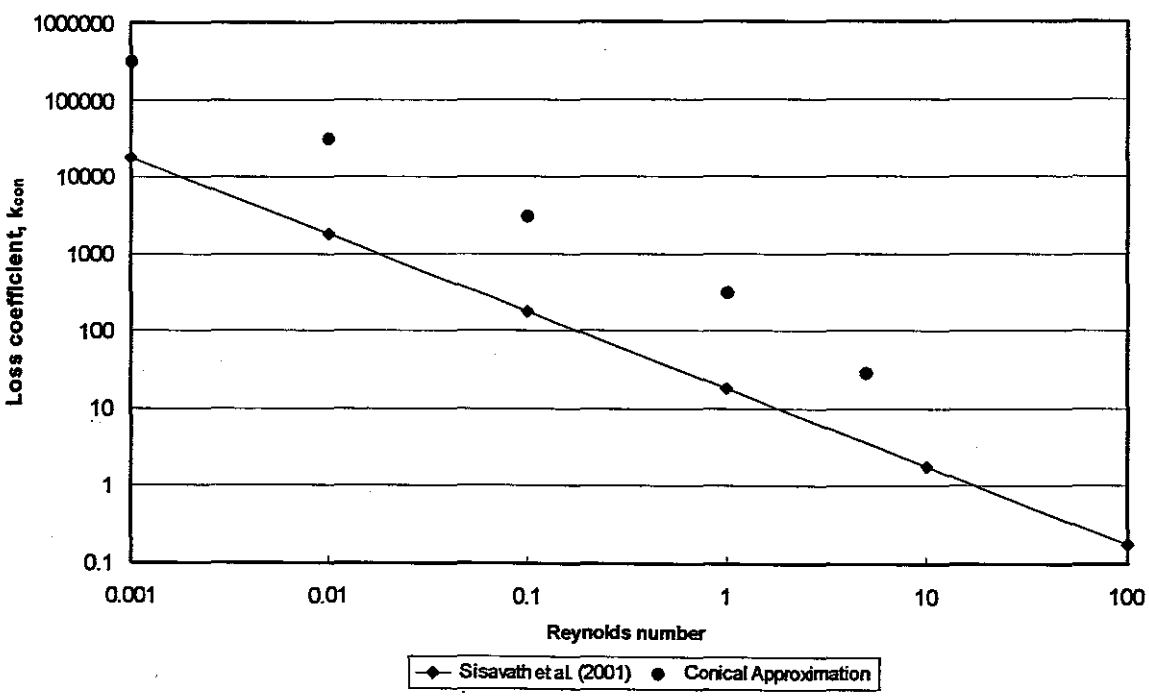

Figure 7.3: Comparison of loss coefficient predictions from Sisavath *et al.* (2002) and Conical Approximation

Table 7.5: Comparison of results for Sisavath *et al.* (2002) and Conical Approximation

Re	SISAVATH *et al.* (2002)	CONICAL APPROXIMATION	%DIFF
0.001	17671	314459	94.30
0.01	1767	31444	94.30
0.1	177	3143	94.29
1	18	312	94.26
10	2	29.45	93.91

Table 7.6: Comparison of C_{con} from Sisavath *et al.* (2002) and Conical Approximation

METHOD	C_{con}
SISAVATH *et al.* (2002)	18
CONICAL APPROXIMATION	314

If, however, the shape factor, ϕ, is not included, the conical approximation yields results within 10% of Sisavath *et al.*(2002) at the lowest Reynolds numbers. The results are shown in Figure 7.4 and Table 7.7.

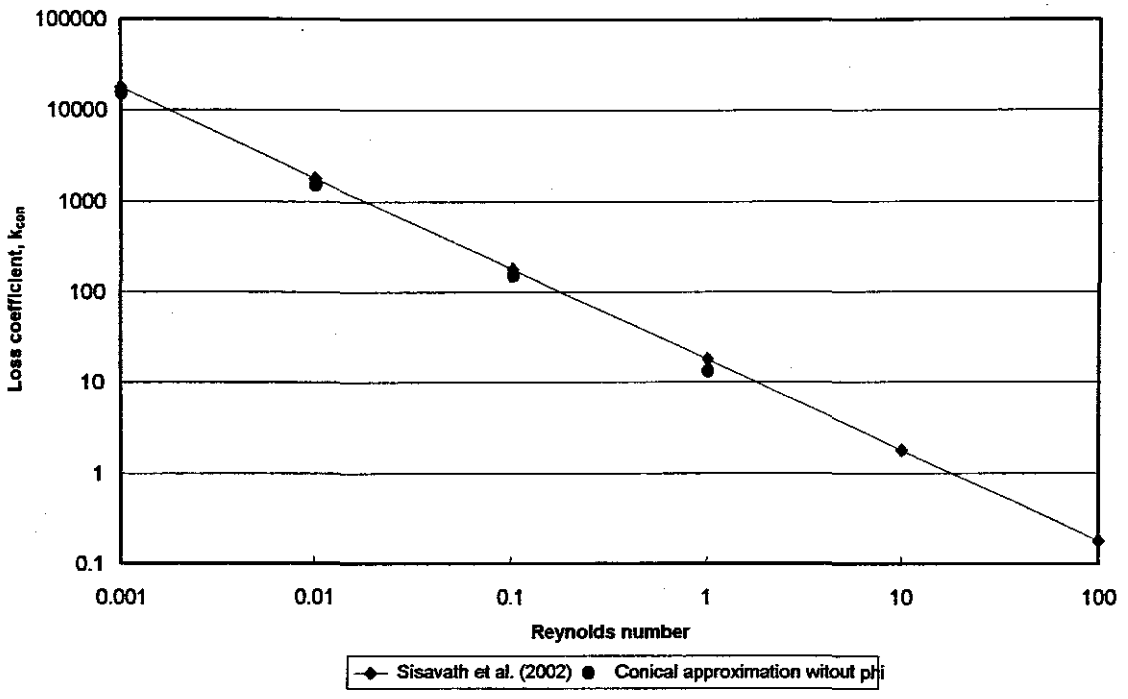

Figure 7.4: Comparison of Sisavath *et al.* (2002) with Conical Approximation without ϕ

Table 7.7: Comparison of Sisavath *et al.* (2002) with Conical Approximation without ϕ

Re	SISAVATH *et al.* (2002)	CONICAL APPROX WITHOUT ϕ	%DIFF
0.001	17937	17084.88	-4.99
0.01	1793	1706.797	-5.09
0.1	179	168.9883	-6.14

The discrepancies found in this work highlight the fact that numerical investigations are better suited to investigation of flow patterns, than actual pressure drop. It has not been established why discrepancies exist between numerical and experimental studies, and this is an issue that still needs to be addressed.

7.3 EXTRAPOLATION OF CONICAL APPROXIMATION TO $\beta > 0.25$

The conical approximation was extrapolated to $\beta > 0.25$. Contraction ratios were selected that was similar to experimental test sections, as it was clear that experimental studies are of utmost importance in the investigation of flow through sudden contractions. These ratios were $\beta = 0.5$ and $\beta = 0.875$. A similar approach was taken as described in Chapter 5. The results obtained from the conical approximation were calibrated with experimental results to obtain a value for the factor ϕ. The same value of L_{ex} was used, as any errors would be accounted for by ϕ. The reason for this is that the flow phenomena are not as simplistic as for $\beta = 0.25$, and the variables that were constant, now have to be accounted for. The value of ϕ should decrease with increasing contraction ratio as the S-curve will be less pronounced and the approximation of a straight line will be closer than for $\beta < 0.25$.

7.3.1 Contraction Ratio $\beta = 0.5$

The results obtained for $\beta = 0.5$ are given in this section. The value of ϕ is 10 and was obtained as explained in Section 6.4 using experimental results obtained in the contraction of $\beta = 0.5$. Comparison with the main models is given in Figure 7.5. There was good agreement between the conical approximation and the experimental data obtained. Comparison with other models showed differences of less than 30% from McNeil and Morris (1995), 43% difference from ESDU (1989) and 93% from Sisavath *et al.*(2002). The value of C_{con} was found to be approximately 214.

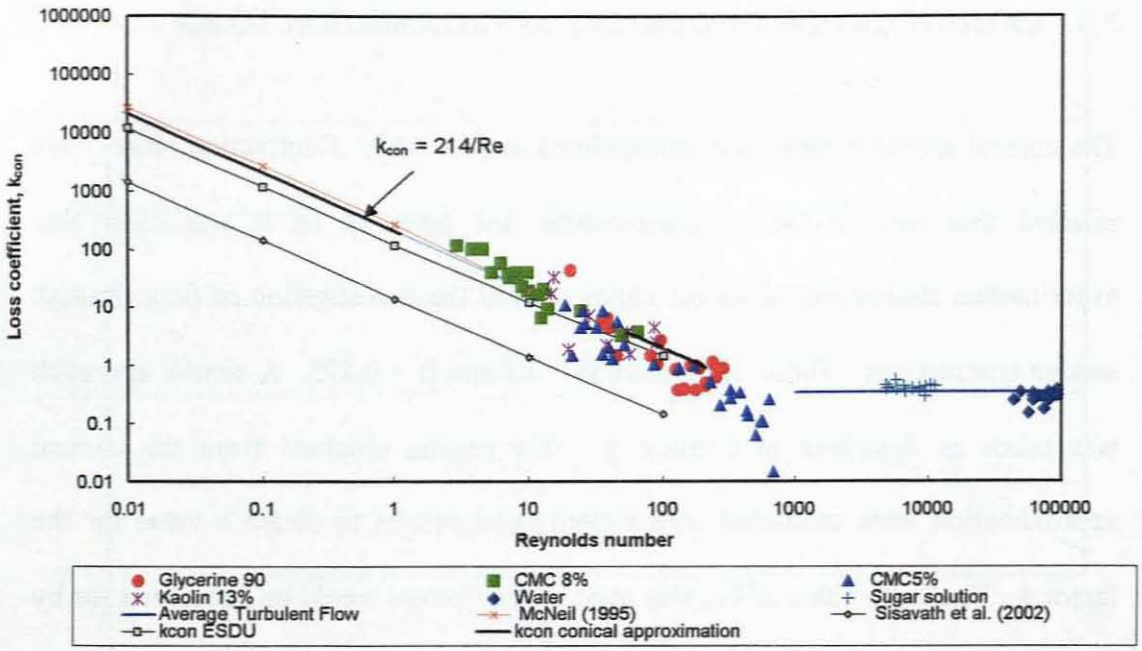

Figure 7.5: Comparison of experimental data for β = 0.5 with conical approximation and other models

7.3.2 Contraction ratio β = 0.85

The results obtained for β = 0.85 are given in this section. The value of ϕ is 10. Comparison with the main models showed good agreement with McNeil and Morris (43%), 71% difference from ESDU and 94% from Sisavath *et al.* The value of C_{con} was found to be approximately 155. These results are presented in Figure 7.6. Except for β = 0.85, very good agreement was found between McNeil's approximation and the conical approximation and experimental results. This could be because the geometry factors developed were based on the work of Kaye and Rosen (1971) and were limited to β = 0.797.

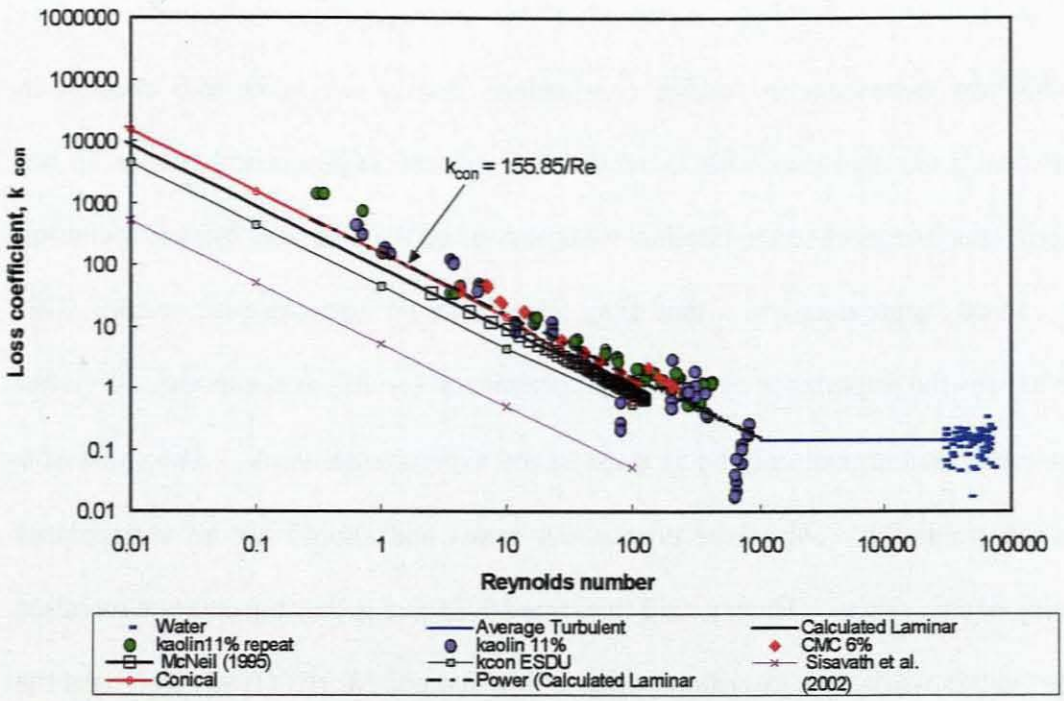

Figure 7.6: Comparison of experimental data for β = 0.85 with conical approximation and other models

7.4 DISCUSSION AND CONCLUSIONS

A simple engineering approximation has been developed that agrees with two other models that are based on two different approaches. It agrees with Mc Neil and Morris' (1995) mechanistic model that has a strong fundamental and analytical basis but includes a factor based on experimental results. However, if the shape factor that is determined based on experimental results, ϕ, is excluded, it agrees with the model developed by Sisavath *et al.* (2002) who took a similar approach. The pressure drop results calculated from these models that were not calibrated experimental results in turn agreed well with results obtained from CFD.

This work therefore highlights a possible fundamental problem in the understanding of the flow behaviour in sudden contractions that is not taken into account in numerical approaches and that is why numerical and experimental results do not agree. This brings us to the obvious weakness of all the available models including the conical approximation: that they dependent on experimental results. This emphasises the importance of credible experimental results, as the model, no matter how sophisticated, will only be as good as the experimental work. The value of ϕ was determined for only three contraction ratios and should not be extrapolated outside of this range. Having said this, one advantage is that the contraction ratios tested in this work is an extension to that of McNeil and Morris (1995) who used the data from Kaye *et al.* (1971) to develop geometry factors for contraction ratios β = 0.2 – 0.8. This work extends it to $\beta = 0.85$. The fact that approximations should not be extrapolated outside of these ranges of experimental results is clearly demonstrated in Section 7.3.4 where the difference in McNeil and Morris (1995) and the conical approximation increases from less than 5% when used with in the appropriate range, to 43% when extrapolated outside of this range.

In conclusion this work demonstrate the importance of credible experimental results to develop predictive models for losses in sudden pipe contractions in the absence of a definitive understanding of the detailed flow phenomena. It also offers a simple engineering design approximation to determine losses in sudden pipe contractions for contraction ratios between $\beta = 0.22 - 0.85$.

CHAPTER 8

CHAPTER 8
SUMMARY, SIGNIFICANT CONTRIBUTIONS AND RECOMMENDATIONS

8.1 INTRODUCTION

This thesis describes an experimental study of sudden contractions of three diameter ratios (β = 0.22, 0.5 and 0.85) and a numerical study of the flow through a sudden contraction at β = 0.22. It has resulted in the formulation of an approximation for predicting additional pressure losses that will arise from laminar flow through a sudden contraction for Newtonian fluids. It has offered an explanation as why different results were obtained by various researchers by scrutinising the experimental procedure and analysis of results. For the first time, qualitative and quantitative agreement was found among the work of various researchers.

8.2 SUMMARY

Fitting losses are important when total head losses across a pipeline system are to be estimated. The procedure to obtain an estimate of system head requirements is as follows (Miller 1978):

1. Define the geometric parameters of the system and fittings.
2. Define the flow parameters such as velocity and Reynolds number.
3. Select appropriate loss coefficients.
4. Calculate individual losses.

5. Add the individual system losses, plus the static or the pressure differential across the system to establish the required pump head.

When geometric and flow parameters are known, the selection of appropriate loss coefficients is the main task. It is thus clear that loss coefficients play an important role in practical design and that the information for non-Newtonian fluids is important.

It was established and confirmed that the loss coefficient is not independent of the Reynolds number in laminar flow as it is for turbulent flow (Edwards *et al.*, 1985). The loss coefficient increases hyperbolically with decreasing Reynolds number where

$$k_{con} = \frac{C_{con}}{Re}.$$

Experimentally determined values of C_{con} varied from researcher to researcher and little agreement was found with other theoretical studies (Edwards *et al.*, 1985; Ma, 1987; ESDU, 1989; McNeil and Morris, 1995; Pienaar, 1998; and Sisavath *et al.*, 2002).

Where agreement was found between theoretical studies and experimental studies, a factor was generally determined for the theoretical study using values from the experimental study (McNeil, 1995).

The only way to determine why variations existed and to ascertain quantitative agreement was to evaluate the various experimental techniques and the analysis of results as well as obtaining results using CFD to evaluate the flow phenomena and compare results obtained.

8.3 SIGNIFICANT CONTRIBUTIONS

A sudden pipe contraction – arguably geometrically the simplest pipe fitting – has been used to establish and validate a protocol for the experimental method and analysis of results for the determination of fitting losses in laminar flow. The main contribution of this work is in the experimental method, analysis of results, and modelling of flow through sudden contractions and actual values for C_{con} for three contraction ratios.

8.3.1 Reducing the Experimental Scatter

It has been demonstrated that the experimental scatter in results can be reduced by the implementation of multiple transducers.

8.3.2 The Use of Various Methods to Calculate the Loss Coefficient

It was demonstrated how different results could be obtained by evaluating the two methods used in literature, i.e., the extrapolation of the pressure grade line to the contraction plane and the total pressure drop approach. These methods both involved the application of Bernoulli, but it was further shown that different results could be obtained, depending on the method used to estimate the pipe friction losses

and the length of straight pipe. In the pressure grade line method, it was demonstrated that the selection of points used for determining the fully developed friction gradient also had a significant effect on the results obtained.

It is argued that these different approaches could explain the discrepancies found in the literature and a sound basis for further experimental investigation has been provided.

8.3.3 The Derivation of a Simple Engineering Design Approximation

A relatively simple engineering design approximation has been derived. The main difference between this method and other methods, is that it is based on the creeping flow regime $Re < 1$, where there is negligible pressure drop downstream of the contraction plane and only upstream losses need to be accounted for. Also for contraction ratios $\beta \leq 0.25$, the upstream vortex size is independent of the Reynolds number (Boger, 1987). The length of this vortex was determined using CFD, also termed the exit length, L_{ex}. It was also clear from CFD data that there was very little recirculation flow in the vortex area, and that the velocities of fluids in that area tended to zero. This stationary fluid reduced the flow area and acted as a boundary, which left the flow boundary geometry as a distorted conical frustrum, rather than a square as assumed by Sisavath *et al.* (2002). The assumptions were accounted for by a shape function. The shape function was determined as the difference between approximated results and experimental results. The approximation, with the shape function, was in agreement with McNeil and Morris's (1995) much more

sophisticated model. The advantage of the conical approximation is that it converged into a computationally simple equation.

8.3.4 Experimental Values of C_{con} and k_{con}

The actual values of C_{con} for β of 0.22, 0.50 and 0.85 are presented in Table 8.1.

Table 8.1: Loss coefficient data obtained in this work

β	C_{con}	k_{con}
0.22	364	1.003
0.50	288	0.346
0.85	155	0.145

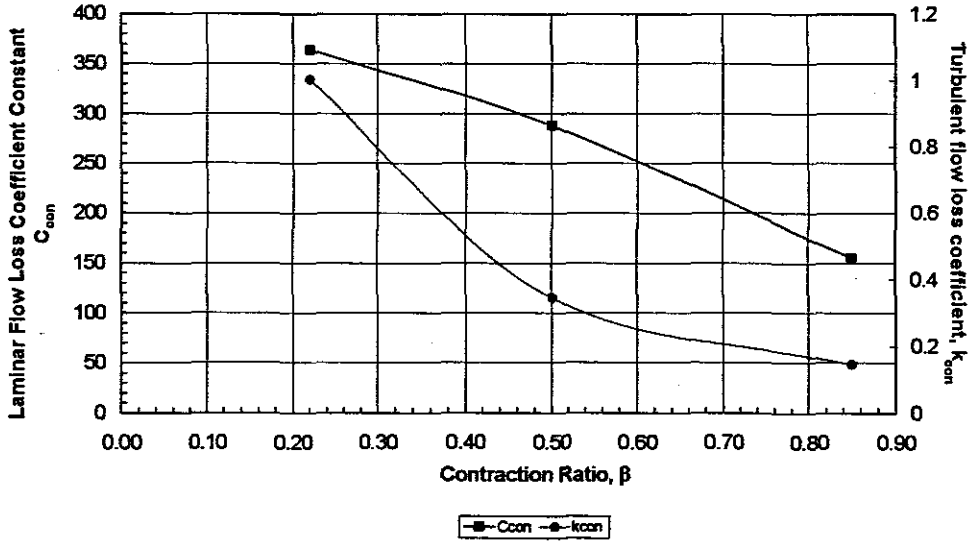

Figure 8.1: Loss coefficient data obtained in this work

8.4 FUTURE RESEARCH RECOMMENDATIONS

One of the greatest concerns raised throughout this work is the difference in pressure results obtained between experimental and numerical investigations. The conical approximation without the shape function yielded results similar to the work of Sisavath *et al.* (2002). Although the numerical studies were carried out on simple Newtonian flow, which the software should be able to handle with ease, the discrepancies in results is a cause for concern. More work should be carried out in this field.

Although several models (ESDU, 1989; McNeil and Morris, 1995) attempt to account for losses in the laminar/turbulent transition, more experimental results are required to improve predictions.

It is believed that a sound basis has been established for the examination of much larger and industrially relevant research projects, evaluating loss coefficients in laminar, transitional and turbulent flow for valves, bends, tees, etc. This project should be pursued with some urgency.

8.5 CONCLUSION

The following conclusions can be made from this study:

- A focused and in-depth experimental study has been conducted on hydraulic energy loss in pipe contractions with the emphasis on low Reynolds number laminar/creeping flow.
- A plausible explanation for the differences in results obtained by various researchers has been offered.
- A method of analysis with the appropriate level of complexity for design engineers has been developed.
- The experimental determination of fitting losses is extremely sensitive to both pressure drop and flow measurements and care should be taken to measure these as accurately as possible.
- When using the extrapolation of the pressure grade line method, care should be taken to ensure that only the points in the fully developed friction gradient are used for extrapolation of the pressure grade line to the contraction plane to obtain the actual pressure drop in the fitting.
- When using the total pressure drop method it is advised that if the full length of straight pipe of 50D or more is used, the experimentally determined friction factor should be used to obtain more accurate values of k_{con}. Furthermore, a length of 25D would result in k_{con} values that are similar when using either the experimental or calculated friction factor. Care should be taken that the length of pipe used should not fall within the distance of interference, as this can result in negative values of k_{con}.
- It was demonstrated that by using the appropriate Reynolds number to account for the rheology of the fluid, the results of both Newtonian and non-Newtonian fluids will collapse onto the same line and the same approximation can be used

to calculate the loss coefficient in laminar flow. It was also demonstrated how the incorrect value of C_{con} can be obtained when not accounting appropriately for the rheology of the fluid.

- A value of C_{con} for contraction ratios was found based on the conical approximation that is in agreement with other studies.
- When determining the loss coefficient constant, it is best to obtain results in the region of $Re < 10$ and to extrapolate this to $Re < 100$, than to do measurements in the higher Reynolds number range and extrapolate them to lower Reynolds numbers. Because it is more difficult to do measurements in the higher Reynolds number ranges, or to calculate them due to the number of variables and the complexity of the flow, the errors in extrapolated results will result in higher values of C_{con}.
- The experimental procedure should be applied when measuring losses through other types of pipe fittings as this work has laid a foundation for determining and eliminating experimental errors that have resulted in the discrepancies in the work of experimental researchers.
- This method will lend credibility to experimental results that will, it is hoped, be appreciated and trusted by the numerical investigators and that will enable them to understand differences between experimental and numerical studies in order to bring the two together, rather than to believe that the numerical investigation is correct and the experimental results are wrong.

REFERENCES

REFERENCES

Alderman, N.J. 1996. Non-Newtonian fluids: obtaining viscometric data for frictional pressure loss estimation for pipe flow. *ESDU 95012*, September.

Astarita, G. & Greco, G. 1968. Excess pressure drop in laminar flow through sudden contraction. *Ind. Eng. Chem. Fundam.*, 7: 27-31.

Baudouin, M.M. 2003. Contraction and expansion losses for non-Newtonian fluids. Unpublished M Tech thesis, Cape Technikon, Cape Town.

Boger, D.V. 1987. Viscoelastic flows through contractions. *Annu. Rev. Fluid Mech.*, 19: 157-181.

Boger, D.V. & Ramamurthy, A.V. 1970. Experimental measurements of loss coefficients in the entrance region of a pipe for viscous power law and viscoelastic fluids. *AIChE J.*, 1088-1092: November.

Bogue, D.C. 1959. Entrance effects and prediction of turbulence in non-Newtonian flow. *Ind. Eng. Chem.*, 51(7): 874-878, July.

Bojcic, P., Khan, M. M. K. & Broadfoot, R. 1997. Estimating pressure losses in pipe fittings at low Reynolds numbers. *Proc. of Austr. Soc. of Sugar Cane Technologist*, 479–484.

Brinkworth, B.J. 1968. *Introduction to experimentation.* London: English Universities Press.

Brooks, P.J. 1993. New ASHRAE local loss coefficients for HVAC fittings. *ASHRAE Trans. Res.*, 99(2): 169-193.

Bullen, P.R., Cheeseman, D.J. & Hussain, L.A. 1996. A study of turbulent flow in pipe contractions. *Proc. Inst. Mech. Eng.*, 210: 171-180.

Chadwick, A.J. & Morfett, J.C. 1993. *Hydraulics in civil and environmental engineering.* London: Taylor & Francis Books Ltd.

Chhabra, R. & Richardson, J.F. 1999. *Non-Newtonian flow in the process industries.* Oxford: Butterworth-Heinemann.

Christiansen, E.B., Kelsey, S.J. & Carter, T.R. 1972. Laminar tube flow through an abrupt contraction. *AIChE J.*, 18(2): 372-380, March.

Collins, M. & Schowalter, W.R. 1963. Behaviour of non-Newtonian fluids in the inlet region of a pipe. *AIChE J.*, 9(1): 804-809, November.

Coulson, J.M. & Richardson, J.F. 1990. *Chemical engineering, Volume 1.* 4th ed. Oxford: Pergamon Press.

Crane Co. 1965. Flow of fluids through valves, fittings and pipe. Technical paper No. 410. Chicago, IL: Crane Co.

Das, S.K., Biswas, M.N. & Mitra, A.K. 1991. Non-Newtonian liquid flow in bends. *Chem. Eng. J.*, 45: 165-171.

Dodge, D.W. & Metzner, A.B. 1959. Turbulent flow of non-Newtonian systems. *AIChE J.*, 5(2): 189-204.

Durst, F. & Loy, T. 1985. Investigations of laminar flow in a pipe with sudden contraction of cross-sectional area. *Computers & Fluids*, 13(1): 15-36.

Edwards, M.F., Jadallah, M.S.M. and Smith, R. 1985. Head losses in pipe fittings at low Reynolds numbers. *Chem. Eng. Res. Des.*, 63: 43-50, January.

Engineering Sciences Data Unit. 1989. Pressure losses in flow through a sudden contraction of duct area. Data Item 89040.

ESDU *see* Engineering Sciences Data Unit.

Finnemore, E.J. & Franzini, J.B. 2002. *Fluids mechanics with engineering applications.* 10th ed. Boston, MA: McGraw-Hill.

Goldstein, R.J. (ed). 1983. *Fluid mechanics measurements.* Washington, DC: Hemisphere.

Govier, G.W. & Aziz, K. 1972. T*he flow of complex mixtures in pipes.* Van Nostrand Reinhold Co.

Hammad, K.J. & Vradis, G.C. 1996. Creeping flow of a Bingham plastic through axisymmetric sudden contractions with viscous dissipation. *Int. J. Heat Mass Transf.*, 36(8): 1555-1567.

Hanks, R.W. 1975. Course Notes. Hydraulic design of flow of complex fluids. Orem, UT: Richard W Hanks Assoc. Inc.

Heywood, N. I. 1984. Comparison of methods for predicting head loss in turbulent pipe flow of non-Newtonian fluids. *Trans. Inst. M C.*, 6(1): 33-45.

Holland, F.A. and Bragg, R. 1995. *Fluid Flow for Chemical Engineers.* 2nd ed. London: Edward Arnold.

Hooper, W.B. 1981. The two-K method predicts head losses in pipe fittings. *Chem. Eng.*: 96-100, August.

Hwang, C.J. & Pal, R. 1997. Flow of two-phase oil/water mixtures through sudden expansions and contractions. *Chem. Eng. J.*, 68: 157-163.

Hwang, N.H.C. and Houghtalen, R.J. 1996. *Fundamentals of hydraulic engineering systems.* 3nd ed. New Jersey: Prentice-Hall.

Idelchik, I.E., Barouch, A. & Grunaer, D. 1966. *Handbook of hydraulic resistance: Coefficients of local resistance and friction.* Israel: Israel program for scientific translations Springfield.

Jacobs, B.E.A. 1993. Laminar/turbulent flow through an annulus with sudden constriction; as found in the Gannet project flow line bundles. *Proc of 12th International Conference on Slurry Handling and Pipeline Transport*: Hydrotransport 12, 28-30 September 1993, Brugge, Belgium, edited by C.A. Shook. London: Mechanical Engineering Publications.

Jadallah, M.S.M. 1980. Flow in pipe fittings at low Reynolds numbers. Unpublished PhD thesis, University of Bradford, UK.

Kaye, S.E. & Rosen, S.L. 1971. The dependence of laminar entrance loss coefficients on contraction ratio for Newtonian fluids. *AIChE J.*, 17(5): 1269-1270, September.

Kim-E, M.E., Brown, R.A. & Armstrong, R.C. 1983. The roles of inertia and shear-thinning in flow of an inelastic liquid through an axisymmetric sudden contraction. *J. Non Newton. Fluid. Mech.*, 13: 341-363.
King, R.P. 2002. *Introduction to practical fluid flow.* Oxford: Butterworth-Heinemann

Kittredge, C. P. & Rowley, D.S. 1957. Resistance coefficients for laminar and turbulent flow through one-half-inch valves and fittings. *Trans. ASME*, 79: 1759-1766.

La Nieve, H.L. 1968. Unpublished MSc Thesis, University of Tennessee, Knoxville.

Ma, T.W. 1987. Stability, rheology and flow in pipes, fittings and venturi meters of concentrated non-Newtonian suspensions. Unpublished PhD thesis, University of Illinois, Chicago.

Massey, B.S. 1970. *Mechanics of fluids.* 2nd ed. Van Nostrand Reinhold.

McNeil, D.A. & Morris, S.D. 1995. A mechanistic investigation of laminar flow through an abrupt enlargement and nozzle and its application to other pipe fittings. Report EUR 16348 EN.

McNeil, D.A., Addlesee, J. & Stuart, A. 1999. An experimental study of viscous flows in contractions, *J. of Loss Prevention in Proc. Ind.*, 12, 249 – 258.

Metzner, A.B. & Reed, J.C. 1955. Flow of non-Newtonian fluids – correlation of the laminar, transition and turbulent flow regions. *AIChE J.*, 1(9).

Miller, D.S. 1978. *Internal flow systems.* Cranfield: BHRA Fluid Engineering:

Muhktar, A., Singh, S.N. & Seshadri, V. 1995. Pressure drop in a long radius 90° horizontal bend for the flow of multisized heterogeneous slurries. *Int. J. Multiphas. Flow*, 21(2): 329-334.

Mumma, S.A., Mahank, T.A. & Ke, Yu-Pei. 1998. Analytical determination of duct fitting loss-coefficients. *Appl. Energ.*, 61: 229-247.

Mun, R. 1988. Turbulent pipe flow of yield stress fluids. Unpublished M Eng Science thesis, University of Melbourne.

Pal, R. & Hwang. C-Y. J. 1999. Loss coefficients for flow of surfactant-stabilised emulsions through pipe components. *Trans. IChemE*, 77 (Part A): 685-691.

Perry, R.H. & Chilton, C.H.(eds). 1973. *Chemical engineers' handbook.* 5th ed. New York: McGraw-Hill.

Phillippoff, W. & Gaskins, F.H. 1958. The Capillary Experiment in Rheology. *Trans. Soc. Rheology*, 2(1): 263-284, March.

Pienaar, V.G. 1998. Non-Newtonian fitting losses, Unpublished M Tech. thesis, Cape Technikon, Cape Town.

Potter, M.C. & Wiggert, D.C. 1997. *Mechanics of fluids.* Pearson Higher Education.

Ramamurthy, A.V. & Boger, D.V. 1971. Developing velocity profiles on the downstream side of a contraction for inelastic polymer solutions. *Trans. Soc. Rheology*, 15(4): 709-730.

Kasipati-Rao, K.V. 1986. Determine laminar-flow head losses for fittings. *Chem Eng.*, 93: 108–109, February 3.

Riffat, S.B. & Gan, G. 1997. CFD prediction of k-factors of duct elbows. *Int. J. Energy Res.*, 21: 675-681.

Shah, R.K. & London, A.L. 1978. *Laminar flow forced convection in ducts: a source book for compact heat exchanger analytical data.* New York: Academic Press.

Sisavath, S., Jing, X., Pain, C.C. & Zimmerman, R.W. 2002. Creeping flow through axisymmetric sudden contraction or expansion. *J. Fluids Eng. (Trans. ASME)*, 124(1): 273-278, March.

Slatter, P.T. 1994. Transitional and turbulent flow of non-Newtonian slurries in pipes. Unpublished PhD thesis, University of Cape Town.

Slatter, P.T. 1999. A new friction factor for yield stress fluids. *14th International Conference on Slurry Handling and Pipeline Transport Hydrotransport 14*, Maastricht, September 1999: 255-265.

Slatter, P.T. & Pienaar, V.G. 1999. Establishing dynamic similarity for non-Newtonian fittings losses. *14th International Conference on Slurry Handling and Pipeline Transport Hydrotransport 14*, Maastricht, September 1999: 245-254.

Slatter, P.T., Pienaar, V.G., & Petersen, F.W. 1997. Non-Newtonian fittings losses. *9th International Conference on Transport and Sedimentation of Solid Particles*, Cracow, 2-5 September 1997: 585-596.

Slatter, P. T. & Wasp, E. J. 2000. Laminar/turbulent transition in large pipes. *10th International Conference on Transport and Sedimentation of Solid Particles.* Wroclaw, 4-7 September 2000: 389-399.

Steffe, J.F., Mohammed, I.O. & Ford, E.W. 1984. Pressure drop across valves and fittings for pseudoplastic fluids in laminar flow. *Trans. ASAE*: 616–619.

Sylvester, N.D. & Rosen, S.L. 1970. Excess pressure drop in laminar flow through sudden contraction. *AIChE J.*, 16: 964-972.

Tanner, R.I. & Walters, K. 1998. *Rheology: an historical perspective*. Amsterdam: Elsevier Science Publishers.

Turian, R.M., Ma, T.W., Hsu, F.L.G., Sung, M.D.J. & Plackmann, G.W. 1998. Flow of concentrated slurries: 2. Friction losses in bends, fittings, valves and venturi meters. *Int. J. Multiphas. Flow*, 24(2): 243-269.

Vradis, G.C. & Hammad, K.J. 1996. Inertia effects on the flow of Bingham plastics through sudden contractions in a pipe. *Can. J. Chem. Eng.*, 74: 457-463, August.

Vrentas, J.S. & Duda, J.L. 1973. Flow of a Newtonian fluid through a sudden contraction. *Appl. Sci. Res.*, 28: 241-260, November.

Ward-Smith, A.J. 1976. Component interactions and their influence on the pressure losses in internal flow systems. *Heat and Fluid Flow © ImechE*, 6(2): 79-88.

White, S.A., Gotsis, A.D. & Baird, D.G. 1987. Review of the entry flow problem: experimental and numerical. *J. Non-Newton. Fluid Mech.*, 24: 121-160.

Wilson, K.C., Addie, G.R. & Clift, R. 1992. *Slurry transport using centrifugal pumps*. Essex: Elsevier Science Publishers.

APPENDICES

APPENDICES

INTRODUCTION

The experimental data obtained in this work such as the pressure drop along the length of the upstream and downstream pipes are presented in:

- Appendix A for contraction $\beta = 0.22$.
- Appendix B for contraction $\beta = 0.50$.
- Appendix C for contraction $\beta = 0.85$.

The pressure drop is given as measured at each pressure tap. The cumulative distances are given in centimeters [Distance (cm)] with 0 cm being at the first pressure tap (Pod No.5). The distances are also presented as the number of pipe diameters from the contraction plane. The contraction plane is at 397.71 cm.

The calculated variables such as the Reynolds numbers (Eq. 2.29, 2.30 and 2.32) and the loss coefficients (Eq. 2.57) are presented as well for all the pressure data sets. Loss coefficients are presented when all the data points were included for extrapolation to the contraction plane ($k_{con\ all\ data}$) and when some data close to the fitting was excluded ($k_{con\ selected\ data}$).

The pressure grade line is presented for each fluid at various velocities as plots of the pressure (Pa) versus the axial distance (diameters from the contraction plane).

INTRODUCTION

The experimental data obtained in this work such as the pressure drop along the length of the upstream and downstream pipes are presented in:

- Appendix A for contraction $\beta = 0.22$.
- Appendix B for contraction $\beta = 0.50$.
- Appendix C for contraction $\beta = 0.85$.

The pressure drop is given as measured at each pressure tap. The cumulative distances are given in centimeters [Distance (cm)] with 0 cm being at the first pressure tap (Pod No.5). The distances are also presented as the number of pipe diameters from the contraction plane. The contraction plane is at 397.71 cm.

The calculated variables such as the Reynolds numbers (Eq. 2.29, 2.30 and 2.32) and the loss coefficients (Eq. 2.57) are presented as well for all the pressure data sets. Loss coefficients are presented when all the data points were included for extrapolation to the contraction plane ($k_{con\ all\ data}$) and when some data close to the fitting was excluded ($k_{con\ selected\ data}$).

The pressure grade line is presented for each fluid at various velocities as plots of the pressure (Pa) versus the axial distance (diameters from the contraction plane).

APPENDIX A

Contraction β = 0.22

Contraction plane	397.71	cm																
Pod No.			5	6	7	8	9	10	11	12	13	14	15	16	17	18	19	20
Distance (diameters)			-94	-70	-49	-24	-12	-6	-3	-2	3	4	8	15	29	57	83	112
Distance (cm)			0	102	192	295	346	371	384	391	407	412	424	451	502	604	697	799
Pressure Drop		1	319130	319266	319399	320193	319571	319536	318871	320113	255005	240309	254334	233708	208085	152424	105220	51333
		2	208563	208029	207726	207752	207953	207830	207966	207668	166005	155857	164852	150470	134336	97436	66507	31107
Water		3	116821	116631	117289	116115	116667	117148	117901	119278	94791	89235	93953	86120	76937	54982	37731	16729
10/2/2003 Set 1		4	105554	105337	105087	104919	104743	104479	104299	104191	84032	78713	82886	78220	67087	48023	31958	13740
		5	56565	56467	56426	56417	56366	56464	56286	56277	46514	44087	45993	42548	37772	28052	19568	10001
		6	18622	18620	18609	18588	18595	18574	18582	18589	16025	15372	15759	14744	13266	10241	7569	4666
		7	8852	8829	8769	8717	8802	8838	8765	8738	8183	8096	8095	7864	7494	6730	6084	5354
		8	35267	35203	35190	35217	35215	35192	35196	35212	30033	28640	29529	27617	25009	19436	14573	9119
		9	60808	60943	60791	60822	60766	60826	60816	60854	51063	48443	50418	46999	42492	32405	23671	14377
		10	379070	379029	379198	379081	378875	378833	378813	378411	372960	371894	372897	370810	368329	362821	357794	352691
13/3/2002 Set 1		11	496769	497078	497073	496707	496831	497081	496996	497100	489727	488553	489764	487430	484215	476622	470792	464432
		12	430151	430105	430390	429862	429827	429855	429507	429840	423570	422367	423058	421143	418736	412084	407123	400993
		13	377870	377317	377066	377010	377591	377399	377203	377283	371848	370883	371731	369477	367105	361189	357161	351941

			Q (m^3/s)	Temp °C	$Re_{downstream}$	$V_{downstream}$	$P_{con\ all\ data}$	$P_{con\ selected\ data}$	$k_{con\ all\ data}$	$k_{con\ selected\ data}$
		1	5.07E-04	31.62	69579.44	7.50	60654	58809	1.110	1.045
		2	4.06E-04	32.04	55669.40	6.00	39759	38838	1.162	1.111
Water		3	3.03E-04	32.42	41511.48	4.47	22231	21871	1.175	1.138
10/2/2003 Set 1		4	2.83E-04	32.57	38844.63	4.19	19482	19260	1.176	1.151
		5	2.01E-04	32.37	27601.31	2.97	9228	8988	1.039	0.984
		6	1.05E-04	32.19	14424.87	1.55	2389	2355	0.930	0.902
		7	5.04E-05	32.07	6913.76	0.75	528	508	0.853	0.781
		8	1.48E-04	32.03	20261.54	2.18	30292	30412	1.010	0.959
		9	2.01E-04	31.86	27532.58	2.97	51604	8837	1.045	0.960
		10	1.41E-04	33.42	19314.82	2.08	5250	5456	1.376	1.472
13/3/2002 Set 1		11	1.61E-04	33.32	22080.75	2.38	6475	6198	1.240	1.142
		12	1.50E-04	33.42	20567.22	2.22	5709	5372	1.277	1.140
		13	1.40E-04	33.41	19261.08	2.08	5012	4587	1.279	1.082

Pod No.			5	6	7	8	9	10	11	12	13	14	15	16	17	18	19	20
Distance (diameters)			-94	-70	-49	-24	-12	-6	-3	-2	3	4	8	15	29	57	83	112
Distance (cm)			0	102	192	295	346	371	384	391	407	412	424	451	502	604	697	799
Pressure Drop		14	120752	120578	120446	120098	120010	119914	119877	119816	111907	108417	105113	98995	87213	63446	43266	19343
CMC 3 %		15	111798	111564	111354	111289	111085	111151	111103	111142	104197	101146	98102	92392	81262	58649	39871	17377
23/10/2002 Set 1		16	96741	96639	96570	96554	96477	96407	96360	96545	91125	88599	86166	81234	71376	51264	34185	14202
Density [kg/m^3]	1021	17	81558	81444	81390	81331	81248	81265	81225	81246	77172	75189	73033	68685	60198	42965	28148	10992
Viscosity [Pa.s]		18	70353	70171	70186	70094	70027	69965	70013	69997	66720	65153	63223	59442	51933	36796	23694	8593
Ty	0.00	19	54957	54850	54770	54696	54668	54665	54630	54628	52560	51563	50136	47165	41432	29917	19792	8332
K	0.111	20	43520	43476	43451	43328	43320	43321	43304	43264	41798	41152	40022	37527	32850	23616	15259	
n	0.805	21	37192	37148	37060	37070	37019	37068	37125	37082	35864	35341	34367	32280	28167	20259	13119	5144
		22	33848	33844	33646	33699	33664	33704	33642	33592	32667	32538	31768	30201	27244	21552	16323	10526
		23	30284	30234	30260	30264	30254	30139	30244	30227	29557	29173	28597	27189	24598	19359	14728	9539
23/10/2002 Set 2		24	47117	47040	47048	46933	46782	46946	46818	46881	45679	45059	44136	41873	37939	29796	22582	14482
		25	55505	55434	55375	55192	55138	55244	55249	55254	53731	52993	51800	49241	44525	35026	26515	16948
		26	61847	61777	61679	61681	61548	61693	61591	61643	59706	58787	57372	54423	48776	37566	27534	16315
		27	75773	75641	75635	75597	75478	75507	75453	75473	72817	71651	70035	66476	59748	46205	34163	20550
		28	89738	89690	89559	89482	89324	89355	89308	89328	85786	84214	82233	78200	70229	54329	40283	24225
		29	118926	118951	119067	118932	118935	118891	118818	118800	113164	110613	107861	102612	92073	71364	53130	32144
		30	135919	135784	135804	135626	135525	135482	135482	135558	128482	125155	122113	115999	104256	80726	60383	36821
CMC 5 %		31	131727	131439	131329	131161	130941	131041	131074	131148	127385	125772	122580	115634	102352	76144	52695	26476
22/10/2002 Set 1		32	118258	118137	117816	117674	117550	117522	117521	117590	114388	112838	109967	103543	91614	67858	46728	23091
Density [kg/m^3]	1025	33	103993	103775	103622	103401	103272	103239	103270	103171	100453	99222	96549	90945	80155	59096	40359	19469
Viscosity [Pa.s]		34	91854	91628	91470	91279	91194	91183	91103	91102	88709	87601	85260	80212	70611	51699	35138	16472
Ty	0.00	35	77974	77919	77794	77578	77635	77644	77598	77788	75621	74908	72730	68452	60052	43752	29175	13171
K	0.503	36	63570	63527	63389	63234	63275	63212	63205	63283	61613	60798	59164	55561	48635	34863	22603	9491
n	0.720	37	57527	57381	57341	57202	57228	57214	57188	57152	55782	55166	53645	50600	44632	32708	22216	10791
		38	49105	49050	48946	48829	48768	48731	48749	48818	47646	47047	45802	43105	37907	27689	18938	8905
		39	57123	56947	56885	56853	56769	56741	56728	56794	55426	54838	53410	50320	44375	32677	22277	11062
		40	63563	63477	63300	63250	63258	63236	63209	63251	61651	60929	59220	55672	48920	35331	23304	10183
22/10/2002 Set 2		41	68099	68029	67941	67958	67826	67849	67826	67885	66660	65918	64505	61515	45795	34186	23695	12380
		42	65046	64996	64966	64867	64780	64818	64794	64809	63310	62530	60882	57338	50541	37054	24999	11666
		43	73662	73558	73359	73335	73194	73227	73258	73188	71512	70574	68785	64860	57240	42307	28760	13910
		44	82561	82388	82254	82189	82066	82068	82074	82087	80090	79100	77021	72602	64278	47602	32740	16144
		45	89942	89781	89669	89513	89513	89460	89328	89327	87169	86075	83822	79085	70143	52156	35581	17982
		46	99358	99234	99133	98854	98866	98885	98823	98817	96372	95232	92796	87514	77625	57814	39490	20274
		47	107603	107410	107247	107083	107045	106966	106904	106986	104402	102979	100427	94739	84018	62744	43631	22274

CMC 3 % and CMC 5 %

			Q (m^3/s)	Temp °C	$Re_{downstream}$	$V_{downstream}$	$P_{ntt\ all\ data}$	$P_{ntt\ selected\ data}$	$K_{con\ all\ data}$	$K_{con\ selected\ data}$
		14	1.93E-04	24.26	1051.90	2.64	7832	9060	0.338	0.69
CMC 3 %		15	1.76E-04	23.65	941.61	2.41	6559	7646	0.356	0.73
23/10/2002 Set 1		16	1.52E-04	23.69	789.59	2.08	4653	5197	0.250	0.50
Density [kg/m^3]	1021	17	1.25E-04	23.61	628.40	1.72	3401	3695	0.403	0.74
Viscosity [Pa.s]		18	1.07E-04	23.48	518.67	1.46	2551	2946	0.482	0.85
Ty	0.00	19	7.85E-05	23.31	359.32	1.08	1364	1592	0.454	0.85
K	0.111	20	6.04E-05	23.06	262.41	0.83	782	977	0.383	0.98
n	0.805	21	4.99E-05	22.66	208.92	0.68	580	736	0.582	1.25
		22	3.41E-05	22.48	132.77	0.47	321	446	1.030	2.18
		23	3.05E-05	22.39	116.17	0.42	267	389	1.147	2.55
23/10/2002 Set 2		24	0.0000	22.00	207.61	0.68	597	746	0.682	1.326
		25	0.0001	21.98	261.18	0.82	825	905	0.528	0.765
		26	0.0001	22.03	318.61	0.97	1183	1429	0.598	1.116
		27	0.0001	22.08	419.73	1.23	1776	2025	0.464	0.795
		28	1.10E-04	22.13	537.28	1.51	2664	3022	0.445	0.780
		29	1.54E-04	22.21	803.05	2.11	5086	5905	0.384	0.752
		30	1.79E-04	22.30	960.64	2.45	6672	7761	0.320	0.683
CMC 5 %		31	7.11E-05	23.34	124.42	0.97	1507	1977	1.320	2.310
22/10/2002 Set 1		32	6.24E-05	23.55	105.28	0.85	1302	1831	1.706	3.154
Density [kg/m^3]	1025	33	5.32E-05	23.64	85.83	0.73	1097	1805	2.274	4.942
Viscosity [Pa.s]		34	4.57E-05	23.66	70.58	0.63	928	1574	2.885	6.187
Ty	0.00	35	3.78E-05	23.72	55.47	0.52	603	1034	2.633	5.847
K	0.503	36	2.99E-05	23.75	41.10	0.41	500	895	4.094	8.602
n	0.720	37	2.56E-05	23.79	33.64	0.35	408	714	4.780	9.761
		38	2.12E-05	23.80	26.44	0.29	325	761	5.863	18.182
		39	2.50E-05	23.86	32.70	0.34	332	762	3.794	11.109
		40	2.92E-05	23.96	39.90	0.40	442	708	3.658	6.985
22/10/2002 Set 2		41	2.55E-05	24.06	31.30	0.35	245	403	2.172	4.763
		42	3.00E-05	24.11	38.58	0.41	368	693	2.506	6.350
		43	3.48E-05	24.16	46.66	0.48	450	720	2.101	4.474
		44	4.01E-05	24.25	55.90	0.55	612	887	2.200	4.028
		45	4.50E-05	24.29	64.82	0.62	725	902	1.957	2.890
		46	5.11E-05	24.33	76.19	0.70	767	991	1.279	2.196
		47	5.66E-05	24.41	87.02	0.78	106082	105705	1.018	2.090

Pod No.			5	6	7	8	9	10	11	12	13	14	15	16	17	18	19	20
Distance (diameters)			-94	-70	-49	-24	-12	-6	-3	-2	3	4	8	15	29	57	83	112
Distance (cm)			0	102	192	295	346	371	384	391	407	412	424	451	502	604	697	799
Pressure Drop		48	125975	125837	125772	125632	125128	124777	124784	124844	101137	106265	103632	97829	85094	60803	40290	13886
Kaolin 5 %		49	103217	102948	102941	102571	102070	102003	101921	102178	82783	86446	84445	79550	69251	48743	31402	9383
4/10/2002 Set 1		50	84740	84169	84089	83878	83586	83372	83462	83396	67795	70342	68569	64598	55798	38695	24215	5830
Density [kg/m^3]	1075	51	68304	67915	67669	67599	67362	67002	67051	67243	54449	56661	55081	51800	44391	30110	17987	2654
Viscosity [Pa.s]		52	56179	55968	55843	55593	55406	55280	55201	55067	46173	46585	45561	42790	36985	25667	16091	4252
Ty	4.00	53	42309	42075	41664	41683	41069	41263	41241	41261	34375	34497	33584	31567	27070	18292	10665	1281
K	0.077	54	29502	29112	28881	28676	28581	28341	28374	28381	24352	23821	22778	21246	17825	11341	7154	1925
n	0.586	55	41749	41428	41257	41131	40718	40766	40726	40686	34291	34305	33286	31302	26822	18094	12714	6381
		56	57732	57553	57435	57382	56831	56855	56795	56777	47203	47925	46837	44252	38148	26581	16776	4734
		57	68973	68492	68482	68271	67995	68065	68042	67914	55331	56810	55614	52336	44995	30524	18386	3148

Kaolin 5 %

			Q (m^3/s)	Temp °C	$Re_{downstream}$	$V_{downstream}$	$P_{ntt\ all\ data}$	$P_{ntt\ selected\ data}$	$k_{con\ all\ data}$	$k_{con\ selected\ data}$
		48	3.00E-04	20.67	8605.79	4.11	16414	15278	1.753	1.619
Kaolin 5 %		49	2.76E-04	20.71	7300.67	3.78	13416	12063	1.303	1.113
4/10/2002 Set 1		50	2.50E-04	20.83	6028.08	3.43	11156	10114	1.101	0.923
Density [kg/m^3]	1075	51	2.26E-04	20.92	4931.30	3.09	8935	8155	1.228	1.063
Viscosity [Pa.s]		52	2.02E-04	21.51	4010.04	2.77	7052	6933	1.330	1.299
Ty	4.00	53	1.76E-04	21.54	3114.97	2.41	5398	5163	1.298	1.218
K	0.077	54	1.50E-04	21.56	2627.30	2.05	4057	5638	1.380	2.134
n	0.586	55	1.75E-04	21.59	3260.69	2.40	5773	7703	1.461	2.131
		56	2.06E-04	21.69	4146.36	2.82	7340	7361	1.647	1.652
		57	2.28E-04	21.95	5036.54	3.12	9237	8331	1.252	1.066

Kaolin 5 %

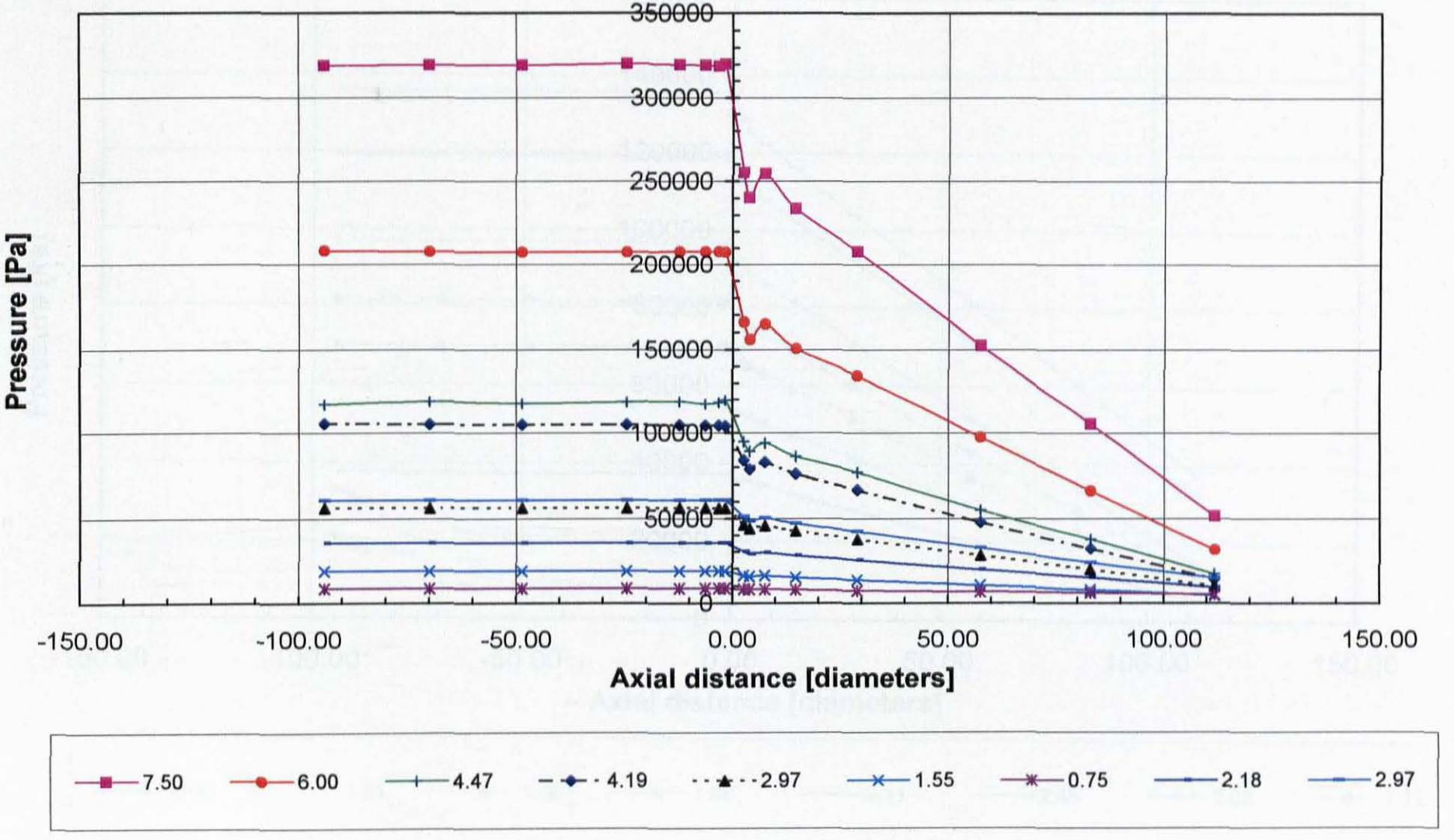

Pressure Grade Line for Water [Legend = Velocity in m/s]

Contraction β = 0.22

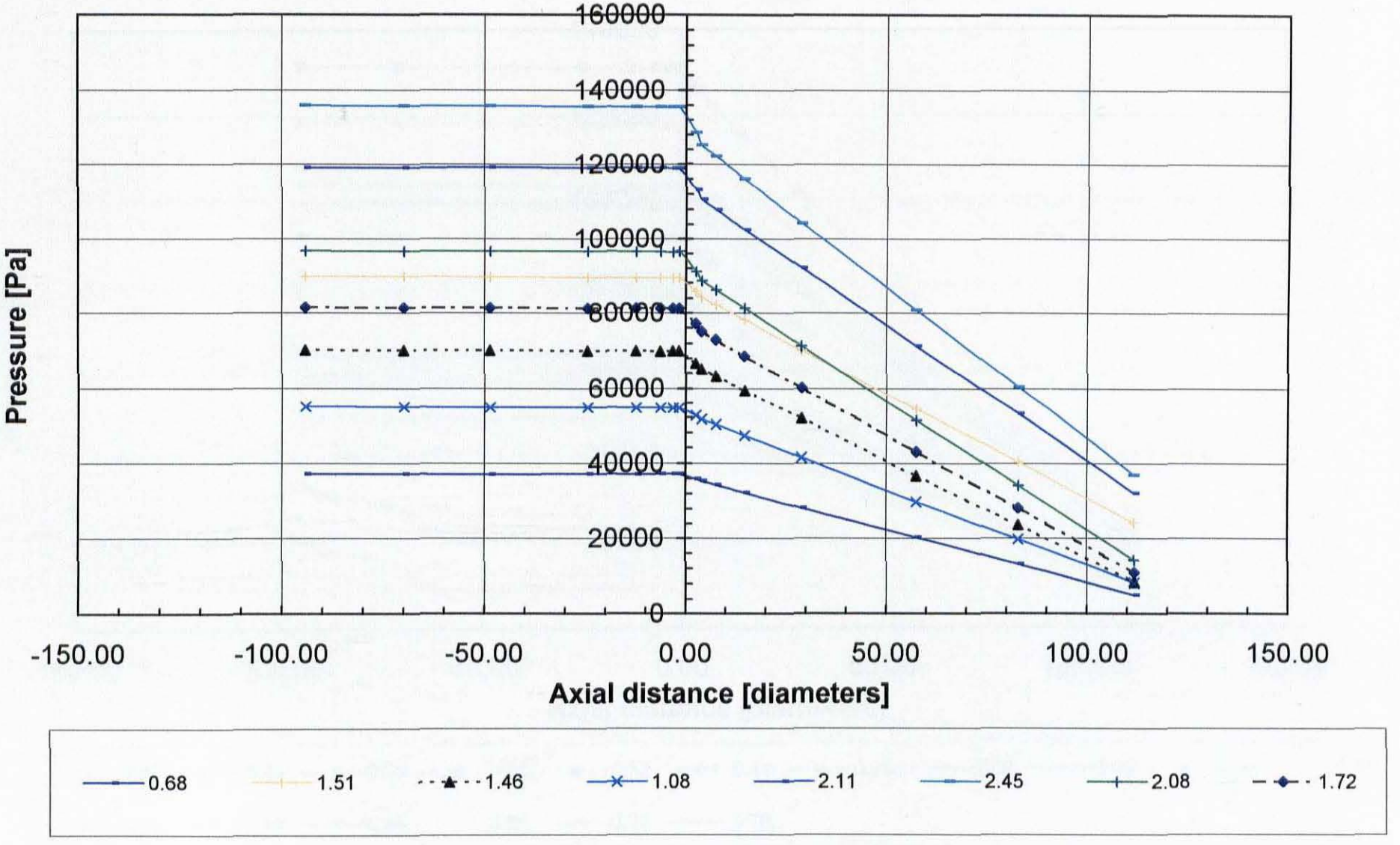

Pressure Grade Line for CMC 3 % at Various Velocities [Legend = Velocity in m/s]

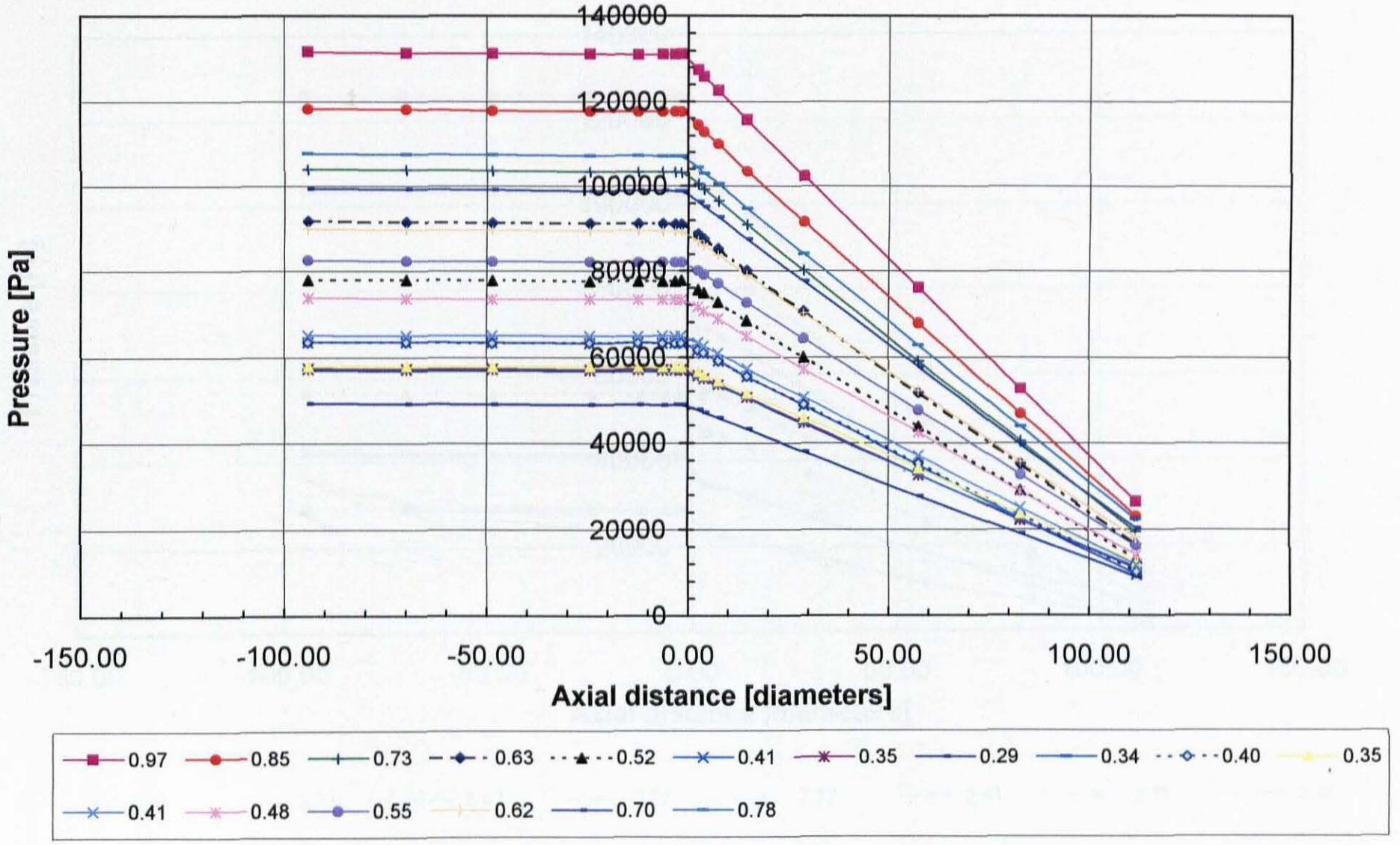

Pressure Grade Line for CMC 5 % at Various Velocities [Legend = Velocity in m/s]

Contraction β = 0.22

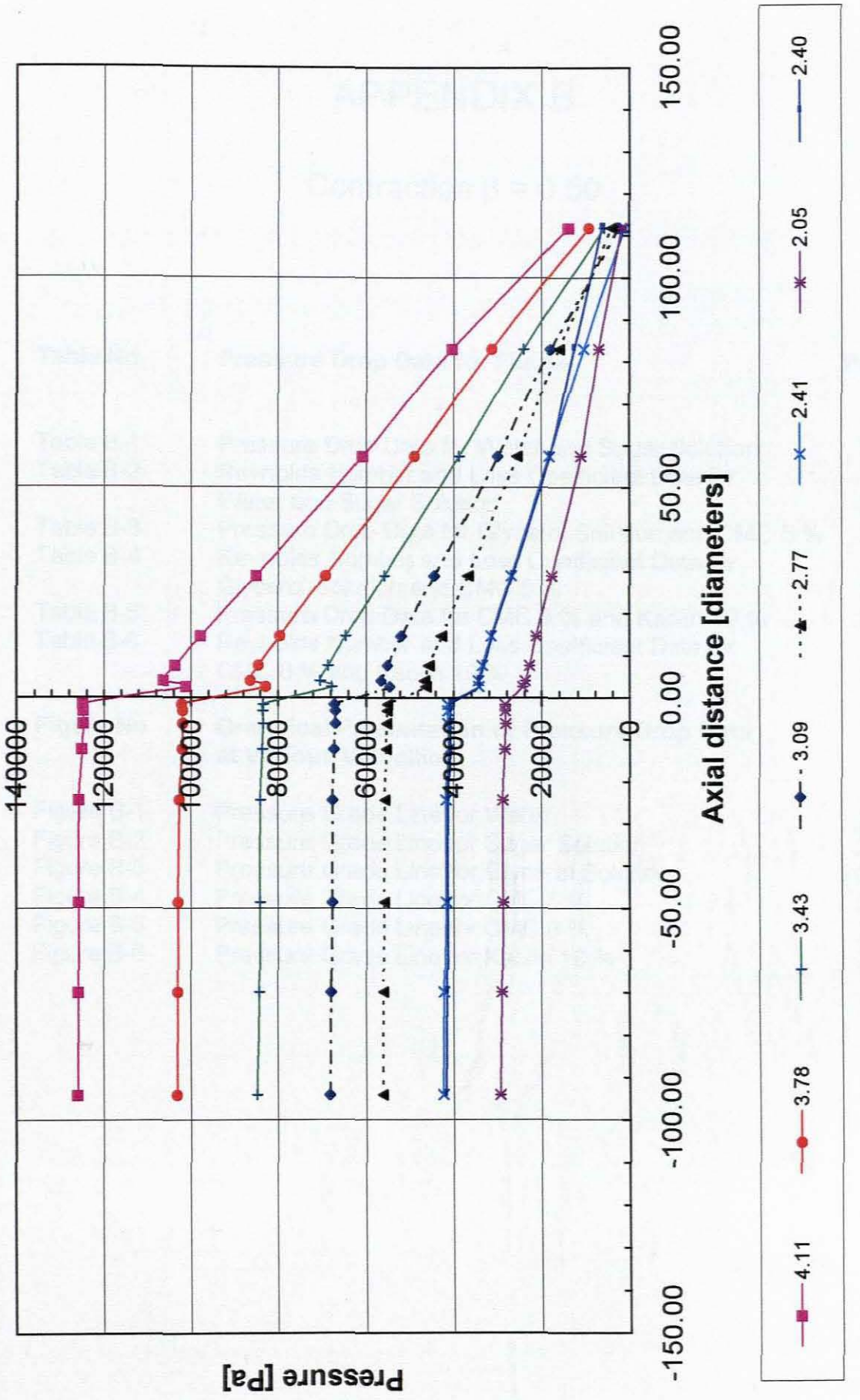

Pressure Grade Line for Kaolin 5 % at Various Velocities [Legend = Velocity in m/s]

APPENDIX B

Contraction β = 0.50

Contraction plane	397.71	cm																
Pod No.			5	6	7	8	9	10	11	12	13	14	15	16	17	18	19	20
Distance (diameters)			-94	-70	-49	-24	-12	-6	-3	-2	3	4	8	15	29	57	93	112
Distance (cm)			0	102	192	295	346	371	384	391	407	412	424	451	502	604	697	799
Pressure Drop		1	81140	80616	80322	80160	79916	80163	79796	79542	71190	68082	66938	65143	59905	54659	48519	42073
		2	80539	80301	79976	79853	79377	79252	79430	79119	68359	67462	66555	64647	59888	54494	48403	41726
Water		3	71425	71239	70824	70621	70387	70370	70334	70217	60082	59869	58972	57205	52713	47646	41733	35945
8/8/2002 Set 1		4	71157	70910	70714	70224	70234	70127	70162	69783	59913	59717	58869	56922	52482	47794	42177	36202
		5	60758	60649	60555	60440	60231	59564	59268	59080	50941	50921	50336	49152	45391	41358	36753	31860
		6	61304	60808	60358	60100	60090	60205	60286	60139	51688	51109	50367	48967	45279	41329	36703	31788
		7	49758	49672	49265	48837	48955	48939	48872	48871	41989	41880	41184	39857	36801	33378	29225	25064
		8	49865	49656	49498	49324	49239	49182	49203	49298	42201	41900	41180	39959	36919	33606	29596	25309
		9	33001	32924	32749	32703	32627	32532	32613	32563	27631	27477	26922	26054	23860	21386	18427	15254
		10	33176	33075	32995	32861	32719	32650	32404	32379	27382	27321	26870	25997	23749	21333	18398	15254
8/8/2002 Set 2		11	80394	80006	79689	79427	79249	79223	79327	78860	67659	67286	66331	64346	59681	54402	48016	41848
		12	68314	68102	67905	67528	67493	67518	67454	67402	57425	57322	56452	54619	50194	45770	40371	34435
		13	59135	59197	58846	58635	58414	58416	58358	58414	50147	49900	49164	47730	44146	40257	35624	30888
		14	49462	49463	49232	49206	49087	48927	48827	48916	41760	41680	41101	39728	36871	33299	29317	24991
		15	49621	49386	49302	49143	49092	49043	49013	48932	41948	41749	41164	39929	36736	33344	29326	25071
		16	40195	40103	39891	39879	39767	39688	39667	39646	33672	33541	33013	31976	29325	26517	23007	19415
		17	32309	32197	32075	31924	31914	31819	31709	31657	26892	26578	26162	25281	23070	20635	17777	14863
		18	25748	25485	25354	25005	24965	24946	25056	25096	21030	20951	20547	19821	17956	15879	13432	10796
		19	16466	16301	16173	16128	16095	16084	16031	16025	12670	12623	12314	11641	10043	8265	6176	3993
		20	9835	9760	9664	9577	9530	9539	9498	9508	6958	6907	6778	6260	5002	3525	1823	80
Sugar Solution		21	108950	108207	108377	107582	107229	107088	107331	107322	95876	95530	93944	91329	85412	75989	66648	56251
23/8/2002 Set 1		22	90345	89866	89670	89405	88903	88874	88826	88776	79626	79487	78122	75876	70762	62357	54433	45597
Density [kg/m^3]	1199.07	23	74808	74446	74238	73801	73352	73366	73379	73485	65436	65358	64429	62442	58107	51349	44466	36913
Viscosity [Pa.s]	0.008	24	61113	60350	60204	59995	59935	59951	60025	60006	53489	53420	52599	50893	47198	41341	35457	29011
		25	50555	50181	49968	49735	49651	49563	49579	49586	44348	44289	43568	42080	39207	34471	29678	24468
		26	39323	39128	38985	38905	38703	38682	38821	38692	34557	34483	34003	32875	30369	26391	22453	18124
		27	28289	28099	28001	27921	27705	27653	27804	27738	24509	24562	24063	23079	21263	18157	15056	11736
		28	18339	18172	18196	18175	17887	17974	18135	18000	15343	15368	15057	14212	12806	10258	7657	4834
		29	9878	9777	9768	9697	9594	9562	9722	9655	7848	7928	7725	7043	5969	4183	2276	333
23/8/2002 Set 2		30	10958	10799	10753	10763	10699	10628	10760	10811	8904	8925	8734	8110	6971	5236	3371	1324
		31	10873	10845	10793	10734	10599	10576	10717	10700	8890	8958	8748	8037	6987	5195	3355	1312
		32	13450	13386	13310	13230	13095	13106	13235	13248	11240	11224	10987	10319	9110	7088	5049	2822
		33	21524	21429	21311	21259	21111	21031	21209	21155	18631	18659	18301	17486	16057	13583	11102	8335
		34	30376	30141	30061	29939	29762	29730	29896	29802	26479	26504	26009	25061	23252	19926	16843	13274
		35	38684	38517	38354	38231	38093	37988	38139	38185	33950	33983	33496	32199	29943	26132	22352	18106
		36	50981	50790	50542	50482	50106	50106	50265	50103	44934	44834	44145	42625	39940	35122	30305	25123
		37	63657	63256	63049	62865	62632	62416	62521	62372	55754	55696	54770	52934	49285	43405	37410	30772

			Q (m^3/s)	Temp °C	$Re_{downstream}$	$V_{downstream}$	$P_{con\ all\ data}$	$P_{con\ selected\ data}$	$K_{con\ all\ data}$	$K_{con\ selected\ data}$
		1	1.52E-03	20.41	92315.71	4.41	10558	12038	0.101	0.253
		2	1.52E-03	21.13	92252.37	4.40	11021	11907	0.150	0.241
Water		3	1.44E-03	22.40	87540.68	4.18	9889	10561	0.146	0.223
8/8/2002 Set 1		4	1.44E-03	23.68	87346.06	4.17	9892	10583	0.116	0.231
		5	1.32E-03	24.40	80458.30	3.84	8137	9178	0.116	0.257
		6	1.33E-03	24.61	80604.31	3.85	8438	8599	0.153	0.175
		7	1.21E-03	24.75	73585.95	3.51	6639	6881	0.089	0.129
		8	1.21E-03	24.98	73794.65	3.52	6936	7350	0.131	0.198
		9	1.02E-03	25.07	61940.94	2.96	4837	5152	0.120	0.192
		10	1.02E-03	25.09	62003.51	2.96	4946	5442	0.142	0.256
8/8/2002 Set 2		11	1.53E-03	25.27	92930.50	4.44	11215	11882	0.153	0.221
		12	1.42E-03	25.46	86527.30	4.13	9694	10316	0.150	0.223
		13	1.32E-03	25.65	80150.48	3.83	8051	8677	0.113	0.199
		14	1.21E-03	25.73	73769.85	3.52	6915	7538	0.116	0.229
		15	1.21E-03	25.81	73848.79	3.53	6852	7281	0.116	0.185
		16	1.11E-03	25.85	67433.61	3.22	5816	6208	0.136	0.211
		17	1.01E-03	25.85	61567.94	2.94	4886	5213	0.145	0.220
		18	9.27E-04	25.83	56323.39	2.69	3780	3852	0.059	0.079
		19	8.10E-04	25.76	49226.60	2.35	3227	3400	0.182	0.245
		20	7.10E-04	25.67	43174.85	2.06	2370	2457	0.129	0.170
Sugar Solution		21	1.27E-03	22.15	11730.52	3.69	10525	10942	0.560	0.621
23/8/2002 Set 1		22	1.22E-03	22.51	11229.65	3.53	8403	8924	0.360	0.444
Density [kg/m^3]	1199.07	23	1.11E-03	22.83	10280.40	3.23	7146	7526	0.380	0.453
Viscosity [Pa.s]	0.01	24	1.01E-03	23.03	9339.60	2.94	5724	5506	0.340	0.289
		25	9.12E-04	23.16	8413.57	2.65	4693	4783	0.354	0.379
		26	8.16E-04	23.21	7531.17	2.37	3727	3894	0.342	0.401
		27	7.08E-04	23.22	6535.26	2.06	2840	3020	0.358	0.443
		28	6.12E-04	23.18	5647.85	1.78	2335	2437	0.493	0.558
		29	5.12E-04	23.11	4722.17	1.49	1506	1595	0.379	0.460
23/8/2002 Set 2		30	5.17E-04	23.32	4769.98	1.50	1558	1559	0.398	0.399
		31	5.17E-04	23.38	4768.20	1.50	1501	1637	0.348	0.469
		32	5.42E-04	23.41	4999.58	1.57	1680	1738	0.372	0.419
		33	6.28E-04	23.40	5790.62	1.82	2178	2285	0.327	0.391
		34	7.23E-04	23.41	6666.71	2.10	2894	2933	0.330	0.347
		35	8.05E-04	23.42	7429.74	2.34	3651	3777	0.351	0.397
		36	9.19E-04	23.47	8480.19	2.67	4708	4977	0.337	0.412
		37	1.03E-03	23.61	9507.51	2.99	6085	6381	0.370	0.441

Water and Sugar Solution

Pod No.			5	6	7	8	9	10	11	12	13	14	15	16	17	18	19	20
Distance (diameters)			-94	-70	-49	-24	-12	-6	-3	-2	3	4	8	15	29	57	83	112
Distance (cm)			0	102	192	295	346	371	384	391	407	412	424	451	502	604	697	799
Pressure Drop		38	113480	112417	111614	110555	109830	109735	109827	109261	108502	105924	103923	100679	94086	81155	69794	56893
		39	110136	109007	108096	107315	106348	105747	105910	106074	102634	102043	100764	97419	91221	78963	67797	55374
Glycerol Solution 90%		40	79898	79138	78606	78027	77426	77390	77367	77234	74988	74670	73472	70768	66081	56594	47957	38425
19/8/2002 Set 1		41	79933	79109	78566	78002	77485	77266	77435	77219	75194	74712	73685	70870	66201	56673	48104	38543
Density [kg/m^3]	1236.00	42	63180	62571	62069	61604	61254	61151	61211	61166	59610	59169	58156	55937	52023	44101	36952	28993
Viscosity [Pa.s]	0.140	43	63850	63039	62664	62045	61572	61475	61520	61487	59830	59461	58521	56300	52362	44413	37211	29213
		44	51539	51062	50692	50253	49912	49740	49772	49670	48452	48185	47431	45824	42544	36155	30418	24039
		45	51311	50874	50451	50036	49745	49589	49662	49547	48463	48144	47379	45583	42490	36145	30373	24026
		46	34185	33842	33529	33175	32936	32949	32860	32871	32141	31998	31345	30054	27729	23157	18888	14235
		47	34095	33740	33524	33195	32946	32805	32890	32847	32127	31953	31300	29986	27722	23081	18882	14189
20/8/2002 Set 1		48	63869	63294	62732	62178	61785	61604	61671	61640	59757	59307	58544	56240	52341	44268	37053	29063
Density [kg/m^3]	1236.00	49	38646	38197	37837	37605	37341	37220	37316	37134	36293	36021	35417	33973	31472	26370	21732	16613
Viscosity [Pa.s]	0.125	50	38292	37882	37585	37207	36974	36766	36863	36831	35983	35700	35069	33594	31174	26097	21504	16528
		51	15380	15197	15046	14877	14627	14713	14903	14775	14440	14291	13914	13142	11755	9074	6575	3884
		52	15317	15060	15011	14898	14685	14487	14696	14573	14295	14368	14005	13154	11853	9129	6717	4043
		53	14353	14426	14316	14372	14218	14143	14274	14355	14106	13949	13750	13154	12146	10095	8219	6339
		54	7515	7521	7451	7405	7308	7242	7329	7340	7216	7165	7048	6730	6289	5319	4436	3389
20/8/2002 Set 2		55	5299	5310	5263	5277	5164	5055	5237	5112	5019	4983	4891	4570	4169	3376	2630	1724
Density [kg/m^3]	1236.00	56	7274	7258	7135	7101	6971	6866	6981	6973	6865	6803	6676	6168	5457	4092	2766	1322
Viscosity [Pa.s]	0.120	57	7979	7948	7853	7824	7689	7577	7704	7686	7588	7482	7383	6871	6107	4696	3287	1784
		58	7942	7917	7815	7776	7637	7537	7642	7608	7503	7413	7271	6811	6057	4620	3241	1758
CMC 5 %		59	126289	124815	123562	121874	121122	120598	120581	120247	115940	115430	113668	110233	104079	91681	80459	68296
27/8/2002 Set 1		60	114188	112845	111449	110055	109118	108830	108689	108578	105084	104458	102936	99716	94059	82619	72327	60987
Density [kg/m^3]	1026.30	61	104263	102945	101820	100437	99641	99457	99251	99156	95958	95375	94113	91137	85892	75181	65583	54916
Viscosity [Pa.s]		62	94804	93539	92451	91225	90501	90275	90081	90055	87232	86816	85528	82820	77962	67992	59124	49321
Ty		63	85766	84770	83679	82536	82010	81705	81488	81422	78901	78493	77358	74851	70355	61082	52926	43810
K	0.756	64	76781	75765	74811	73835	73329	73003	72517	72739	70753	70328	69315	67019	62876	54450	46944	38668
n	0.650	65	67671	66722	65977	64891	64522	64323	64124	64128	62349	61932	61048	59060	55320	47616	40908	33358
		66	50759	50311	49681	48922	48596	48341	48276	48220	47143	46882	46157	44639	41858	36131	30980	25357
		67	42605	42011	41523	40955	40585	40428	40370	40324	39467	39182	38634	37394	34907	29974	25546	20844
		68	32068	31591	31228	30763	30520	30404	30377	30328	29734	29580	29050	28082	26106	22159	18867	14786
27/8/2002 Set 2		69	22832	22528	22246	21858	21676	21634	21555	21526	21095	20980	20577	19795	18331	15303	12615	9637
		70	20403	20283	20008	19655	19461	19411	19326	19302	18876	18765	18479	17722	16353	13587	11098	8348
		71	19365	19045	18783	18503	18333	18271	18195	18143	17788	17674	17382	16624	15360	12726	10300	7621
		72	17111	16863	16567	16281	16120	16053	16014	15997	15482	15440	15036	14315	13101	10427	7994	5239
		73	15682	15385	15127	14841	14694	14612	14523	14544	14071	13969	13740	13093	11895	9302	6959	4487
		74	14674	14370	14121	13877	13729	13671	13614	13594	13271	13178	12807	12191	11032	8663	6523	4159
		75	13601	13341	13099	12821	12721	12645	12607	12601	12282	12210	11925	11324	10194	7891	5850	3547
		76	12266	12012	11792	11539	11418	11369	11356	11329	11006	10848	10571	10002	8998	6846	4921	2795
		77	11298	11064	10867	10634	10511	10458	10448	10358	10126	10064	9790	9255	8241	6195	4347	2324
		78	9744	9550	9341	9132	9022	9002	8939	8938	8686	8624	8387	7867	6965	5076	3371	1499

			Q (m^3/s)	Temp °C	$Re_{downstream}$	$V_{downstream}$	$P_{fitt\ all\ data}$	$P_{fitt\ selected\ data}$	$K_{con\ all\ data}$	$K_{con\ selected\ data}$
Glycerol Solution 90%		38	4.40E-04	22.92	236.03	1.28	1999	2494	0.576	1.183
19/8/2002 Set 1		39	4.51E-04	23.78	242.20	1.31	2013	2406	0.469	0.926
Density [kg/m^3]	1236.00	40	3.58E-04	24.19	192.00	1.04	1355	1548	0.634	0.993
Viscosity [Pa.s]	0.14	41	3.62E-04	24.38	194.19	1.05	1209	1382	0.331	0.627
		42	3.04E-04	24.45	163.30	0.88	862	915	0.331	0.466
		43	3.05E-04	24.53	163.91	0.89	852	934	0.290	0.498
		44	2.52E-04	24.61	135.32	0.73	656	780	0.570	1.032
		45	2.53E-04	24.66	135.65	0.73	550	610	0.165	0.390
		46	1.86E-04	24.76	99.91	0.54	274	32494	-0.003	0.378
		47	2.07E-04	24.81	111.25	0.60	297	414	-0.235	0.410
20/8/2002 Set 1		48	3.05E-04	24.52	163.54	0.89	1068	1101	0.846	0.931
Density [kg/m^3]	1236.00	49	2.05E-04	24.96	123.57	0.60	457	491	0.693	0.883
Viscosity [Pa.s]	0.13	50	2.11E-04	25.29	126.66	0.61	429	539	0.418	1.010
		51	1.18E-04	25.46	70.87	0.34	97	172	-2.685	1.060
		52	1.07E-04	25.67	64.17	0.31	-39	163	-2.685	1.517
		53	1.01E-04	26.06	60.50	0.29	22	201	-1.366	2.844
		54	5.99E-05	25.86	36.04	0.17	7293	7319	-1.292	1.548
20/8/2002 Set 2		55	6.09E-05	25.42	0.00	0.09	3575	208	803.124	45.000
Density [kg/m^3]	1236.00	56	5.48E-05	25.02	0.00	0.16	5952	93	469.005	5.514
Viscosity [Pa.s]	0.12	57	5.98E-05	25.13	0.00	0.17	6195	7660	409.228	4.619
		58	5.87E-05	25.21	0.00	0.17	6183	125	423.965	6.700
CMC 5 %		59	6.80E-04	20.50	648.10	1.97	3389	3827	0.037	0.262
27/8/2002 Set 1		60	6.23E-04	21.21	576.39	1.81	2581	2968	-0.127	0.110
Density [kg/m^3]	1026.30	61	5.66E-04	21.45	508.49	1.65	2251	2401	-0.048	0.063
Viscosity [Pa.s]		62	5.10E-04	21.67	439.38	1.48	1919	2020	0.049	0.142
Ty		63	4.60E-04	21.95	382.60	1.33	1700	1827	0.203	0.345
K	0.76	64	4.09E-04	22.08	326.41	1.19	1220	1468	0.027	0.379
n	0.65	65	3.57E-04	22.24	272.03	1.04	1052	1031	0.251	0.213
		66	2.52E-04	22.34	169.92	0.73	583	724	0.472	0.998
		67	2.08E-04	22.42	130.74	0.60	399	481	0.490	0.942
		68	1.51E-04	22.33	84.87	0.44	216	263	0.549	1.037
27/8/2002 Set 2		69	1.06E-04	22.57	52.79	0.31	156	181	1.592	2.106
		70	9.52E-05	22.73	45.61	0.07	171	288	2.774	5.831
		71	9.02E-05	22.81	42.41	0.06	125	105	1.944	1.349
		72	8.54E-05	22.89	39.39	0.06	219	117	5.414	2.116
		73	7.93E-05	22.95	35.62	0.06	191	280	5.502	8.893
		74	7.33E-05	22.98	32.07	0.05	129	143	4.001	4.631
		75	6.92E-05	23.01	29.65	0.05	67	36	1.625	0.056
		76	6.36E-05	23.05	26.47	0.05	161	121	7.721	5.422
		77	5.94E-05	23.08	24.10	0.04	70	95	3.040	4.669
		78	5.40E-05	23.15	21.20	0.04	59	40	3.075	1.517

Glycerol Solution and CMC 5 %

Pod No.			5	6	7	8	9	10	11	12	13	14	15	16	17	18	19	20
Distance (diameters)			-94	-70	-49	-24	-12	-6	-3	-2	3	4	8	15	29	57	83	112
Distance (cm)			0	102	192	295	346	371	384	391	407	412	424	451	502	604	697	799
CMC 5 %		79	122648	121098	119923	118219	117796	117188	117035	116608	112262	111682	110141	106988	101262	89424	79169	67580
27/8/2002 Set 3		80	10266	10100	9980	9759	9720	9601	9585	9588	9316	9301	9088	8619	7765	6081	4559	2894
		81	102954	101798	100747	99376	98803	98427	98338	98152	94750	94163	92811	90053	85077	74961	65814	55807
		82	87053	85860	84954	83748	83381	82940	82791	82710	80014	79520	78474	76077	71616	62746	54736	45932
		83	71079	70095	69361	68388	67928	67597	67553	67471	65542	65178	64198	62126	58402	50759	43972	36394
		84	57676	56864	56433	55587	55366	54962	54875	54897	53513	53245	52470	50839	47868	41771	36243	30278
		85	40625	40102	39752	39206	38998	38686	38652	38644	37837	37594	37075	35898	33853	29121	24986	20483
		86	22387	22063	21884	21475	21388	21216	21174	21142	20735	20658	20322	19596	18253	15514	13073	10350
		87	16417	16146	15935	15653	15556	15428	15420	15398	15068	14989	14665	14044	12893	10530	8381	6014
		88	12742	12531	12450	12157	12089	11928	11938	11928	11663	11603	11348	10811	9866	7912	6181	4235
CMC 8 %		89	134440	132372	130794	128740	127702	127132	126178	126378	124319	123914	118236	118280	111381	97398	85033	71078
3/9/2002 Set 1		90		115458	114114	112234	111147	110828	110556	110320	108457	108138	106628	103446	97294	84981	73873	61715
Density [kg/m^3]	1045.00	91	93332	92134	91267	89715	89053	88427	88283	88174	86650	86396	85070	82367	77558	67381	58501	48520
Viscosity [Pa.s]		92	71061	70093	69441	68137	67754	67272	67193	67202	66067	65875	64787	62722	58891	51108	44121	36374
Ty		93	67027	65979	65240	64089	63774	63388	63293	63216	62250	62013	61003	58971	55409	48044	41433	34155
K	3.819	94	65643	64873	64205	63074	62494	62164	62077	62033	61055	60869	59783	57898	54363	47070	40601	33402
n	0.559	95	60098	59151	58547	57603	56946	56654	56568	56446	55663	55555	54397	52642	49425	42731	36795	30222
		96	58735	58050	57472	56530	56080	55796	55698	55620	54859	54750	53768	52040	49006	42795	37266	31103
		97	56259	55561	55138	54246	53743	53356	53241	53262	52463	52402	51482	49881	46912	40938	35613	29716
		98	52771	52092	51709	50842	50230	50082	50006	49957	49236	49184	48294	46772	44002	38372	33359	27813
Kaolin 10 %		99	90634	89374	87337	86048	83674	82856	82192	82235	75193	75558	75217	72884	69466	62695	56301	49529
4/10/2002 Set 1		100	93079	92043	89787	88558	85893	85681	85049	84828	77309	77155	76119	73866	70219	63435	56913	50352
Density [kg/m^3]	1159.00	101	83650	82616	80561	78726	76917	76723	75998	75895	70610	70286	70037	67431	64151	57708	51693	45113
Viscosity [Pa.s]		102	59324	57545	56535	53895	52532	52201	51478	51344	50028	49890	49691	48154	45102	39778	34821	29161
Ty	16.00	103	53906	52943	51934	49889	47963	47905	47043	46920	45864	45814	45734	44201	41605	36744	32144	26782
K	1.118	104	50075	49249	48237	46293	44535	44589	43948	43760	43089	42959	42929	40973	38571	33878	29722	24778
n	0.422	105	49353	48663	47868	45717	44322	44228	43510	43386	42724	42550	42460	41365	38541	33769	30016	25376
		106	44232	43993	42778	41493	40143	40045	39382	39252	38648	38615	38479	37684	35048	30551	27343	23175

			Q (m^3/s)	Temp °C	$Re_{downstream}$	$V_{downstream}$	$P_{fit\ all\ data}$	$P_{fit\ selected\ data}$	$k_{con\ all\ data}$	$k_{con\ selected\ data}$
CMC 5 %		79	7.23E-04	24.58	704.07	2.10	3616	3784	-0.061	0.015
27/8/2002 Set 3		80	4.93E-05	25.06	18.75	0.14	83	134	6.445	11.388
		81	6.12E-04	25.18	562.40	1.78	2670	2873	-0.012	0.117
		82	5.06E-04	25.33	434.89	1.47	1939	2016	0.095	0.166
		83	4.07E-04	25.43	324.37	1.18	1262	1383	0.104	0.277
		84	3.10E-04	25.55	224.69	0.90	820	904	0.320	0.526
		85	2.07E-04	25.51	130.43	0.60	394	467	0.474	0.878
		86	1.04E-04	25.24	51.63	0.30	148	187	1.521	2.372
		87	7.91E-05	25.14	35.51	0.23	15283	15306	2.223	1.616
		88	6.13E-05	25.14	25.17	0.18	11842	184	3.736	8.675
CMC 8 %		89	2.60E-04	21.99	64.83	0.75	1858	1328	3.422	3.776
3/9/2002 Set 1		90	2.14E-04	22.03	48.91	0.61	783	822	2.058	3.366
Density [kg/m^3]	1045.00	91	1.53E-04	22.05	24.48	0.44	589	1018	4.346	8.712
Viscosity [Pa.s]		92	1.03E-04	22.03	13.78	0.30	321	507	5.814	9.825
Ty		93	9.41E-05	22.02	12.18	0.27	269	317	5.554	6.840
K	3.82	94	9.16E-05	22.11	11.71	0.27	292	648	6.635	16.692
n	0.56	95	8.08E-05	22.18	9.77	0.23	240	582	7.090	19.540
		96	7.50E-05	22.23	8.79	0.22	241	605	8.521	23.849
		97	6.93E-05	22.28	7.84	0.20	234	703	9.936	33.105
		98	6.41E-05	22.34	7.01	0.19	178	610	8.609	33.611
Kaolin 10 %		99	1.06E-03	19.13	2477.14	3.08	6063	7803	-0.005	0.363
4/10/2002 Set 1		100	1.09E-03	20.68	2635.44	3.17	7319	9811	0.170	0.627
Density [kg/m^3]	1159.00	101	8.91E-04	22.21	1890.90	2.59	4835	6196	0.176	0.584
Viscosity [Pa.s]		102	2.98E-04	22.28	307.99	0.86	718	1594	0.716	3.061
Ty	16.00	103	2.03E-04	22.08	175.66	0.59	570	1886	2.090	9.650
K	1.12	104	9.98E-05	21.90	52.32	0.29	355	1850	7.296	42.918
n	0.42	105	5.94E-05	21.78	21.40	0.17	313	43038	19.910	123.049
		106	3.21E-05	21.59	11.75	0.09	244	1698	55.193	390.944

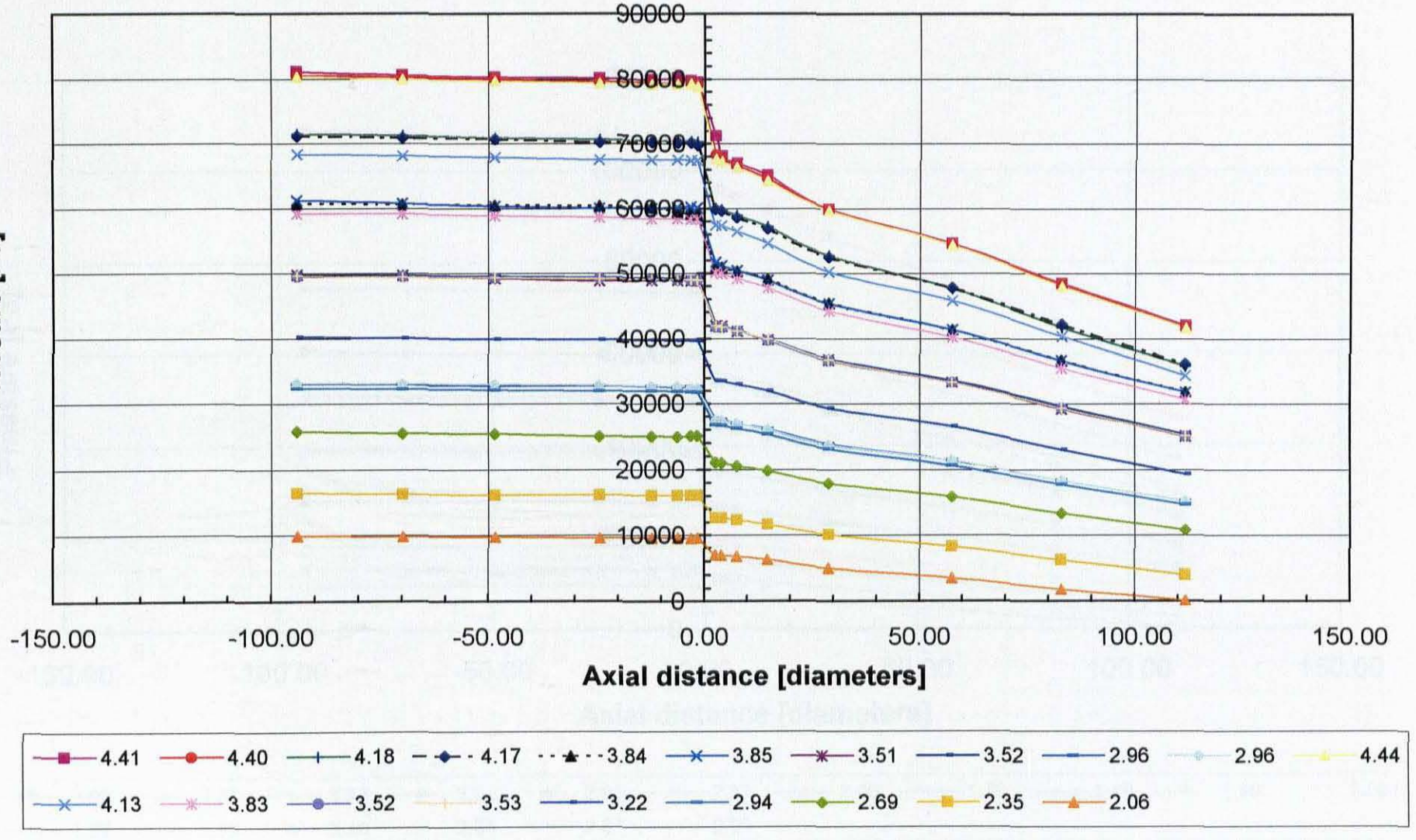

Pressure Grade Line for Water [Legend = Velocity in m/s]

Contraction β = 0.50

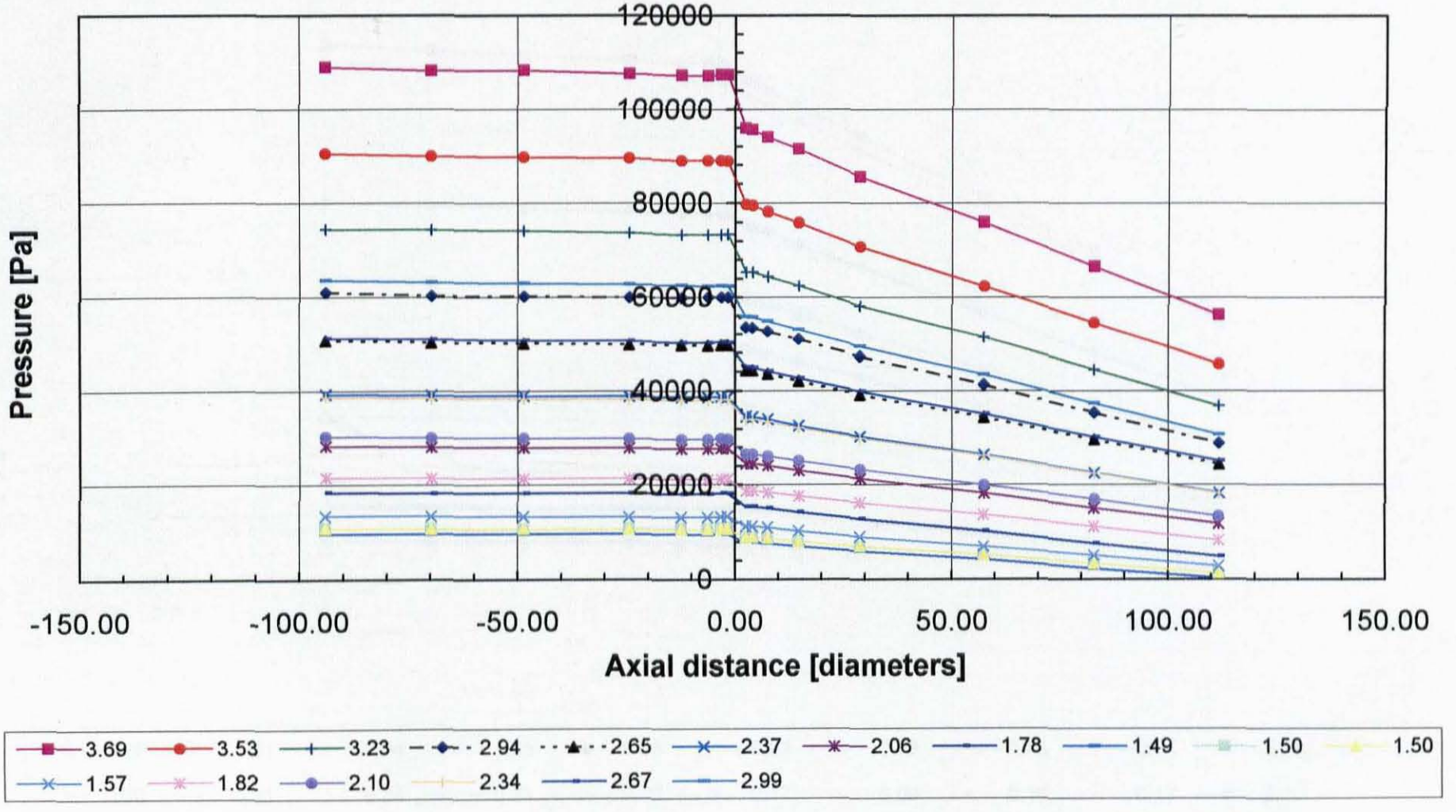

Pressure Grade Line for Sugar Solution [Legend = Velocity m/s]

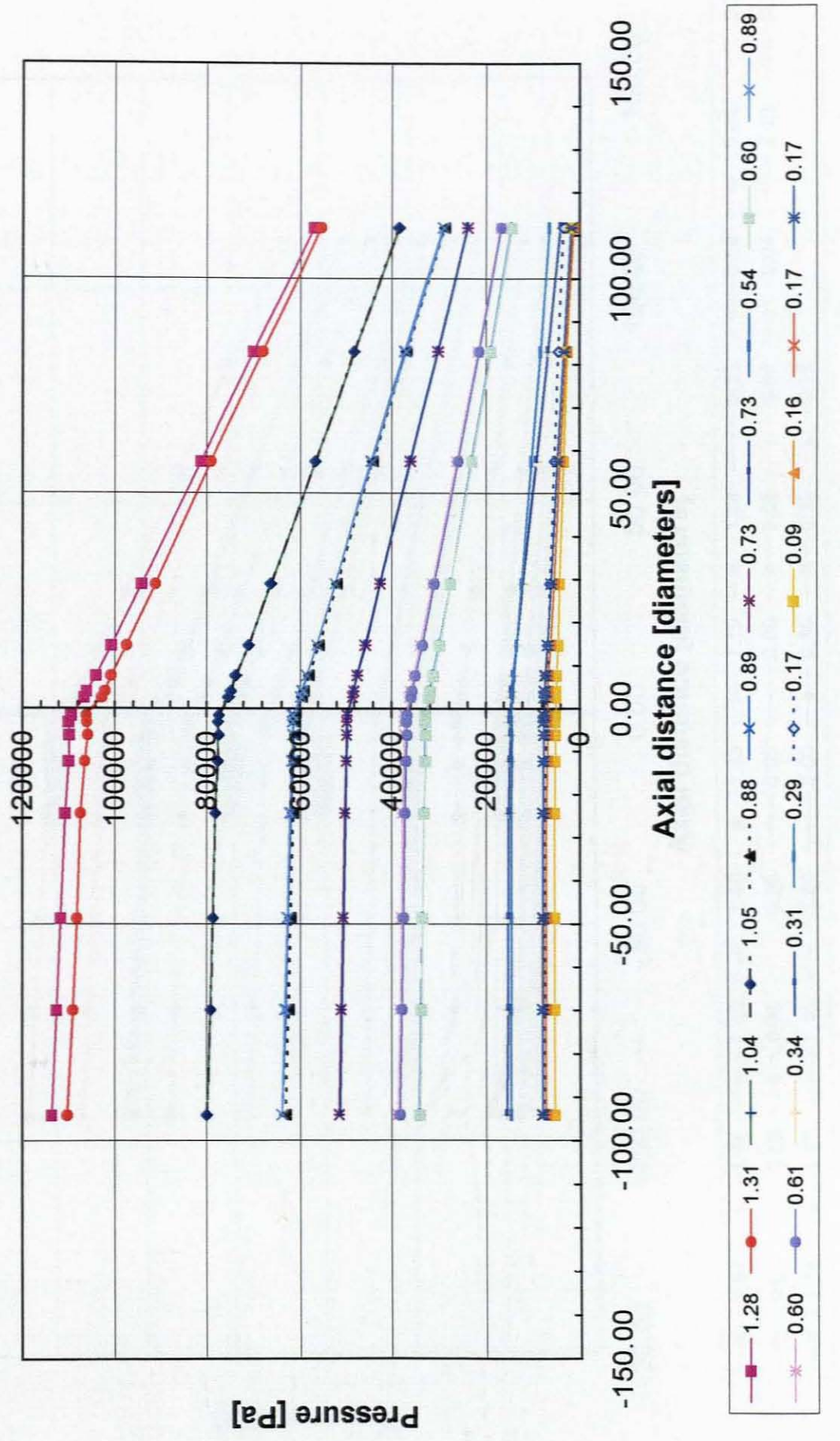
Pressure [Pa]
120000
100000
80000
60000
40000
20000
0
-150.00
-100.00
-50.00
0.00
50.00
100.00
150.00
Axial distance [diameters]
1.28
1.31
1.04
1.05
0.88
0.89
0.73
0.73
0.54
0.60
0.89
0.60
0.61
0.34
0.31
0.29
0.17
0.09
0.16
0.17
0.17
Pressure Grade Line for Glycerol Solution [Legend = Velocity in m/s]

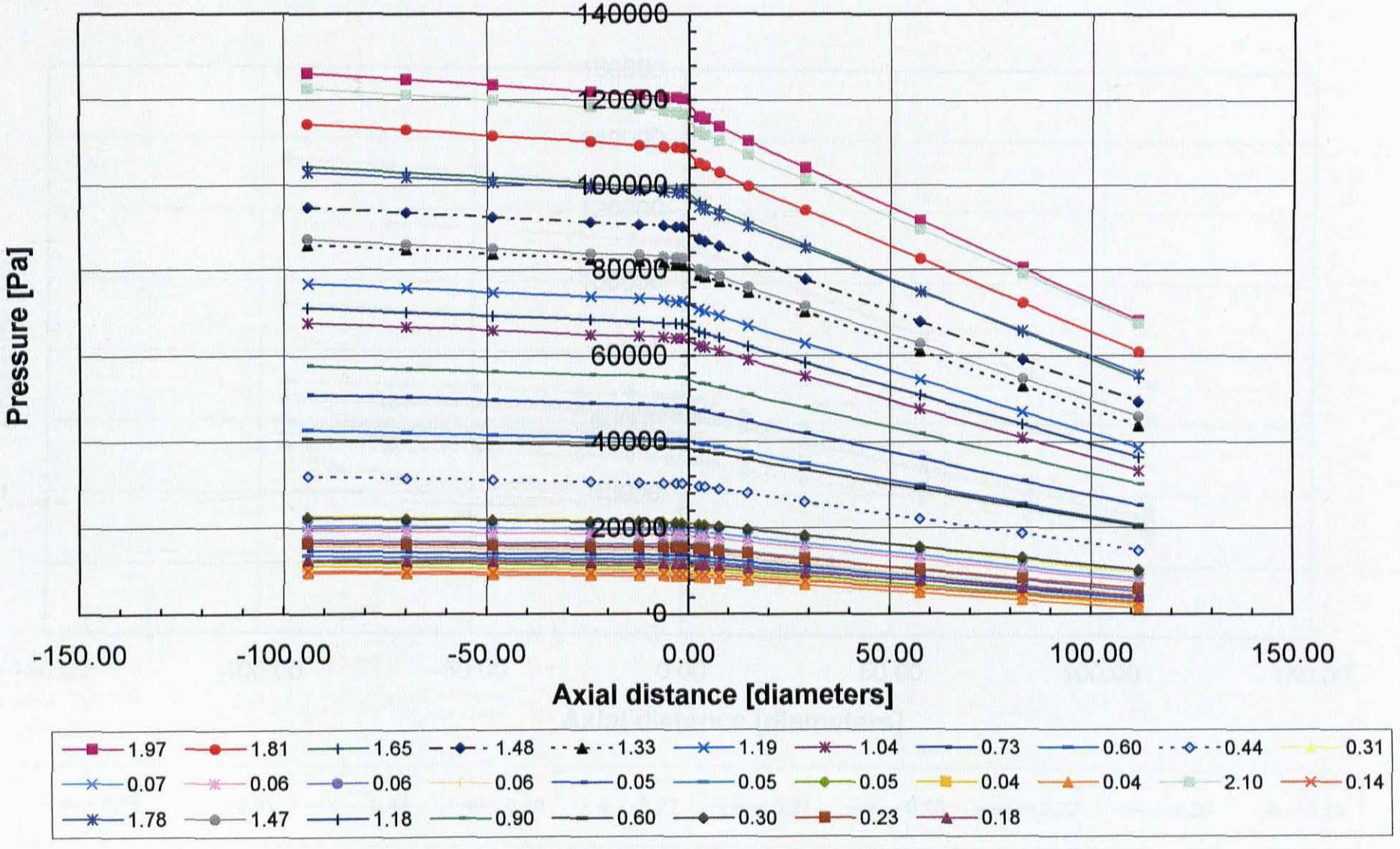

Pressure Grade Line for CMC 5 % at Various Velocities [Legend = Velocity in m/s]

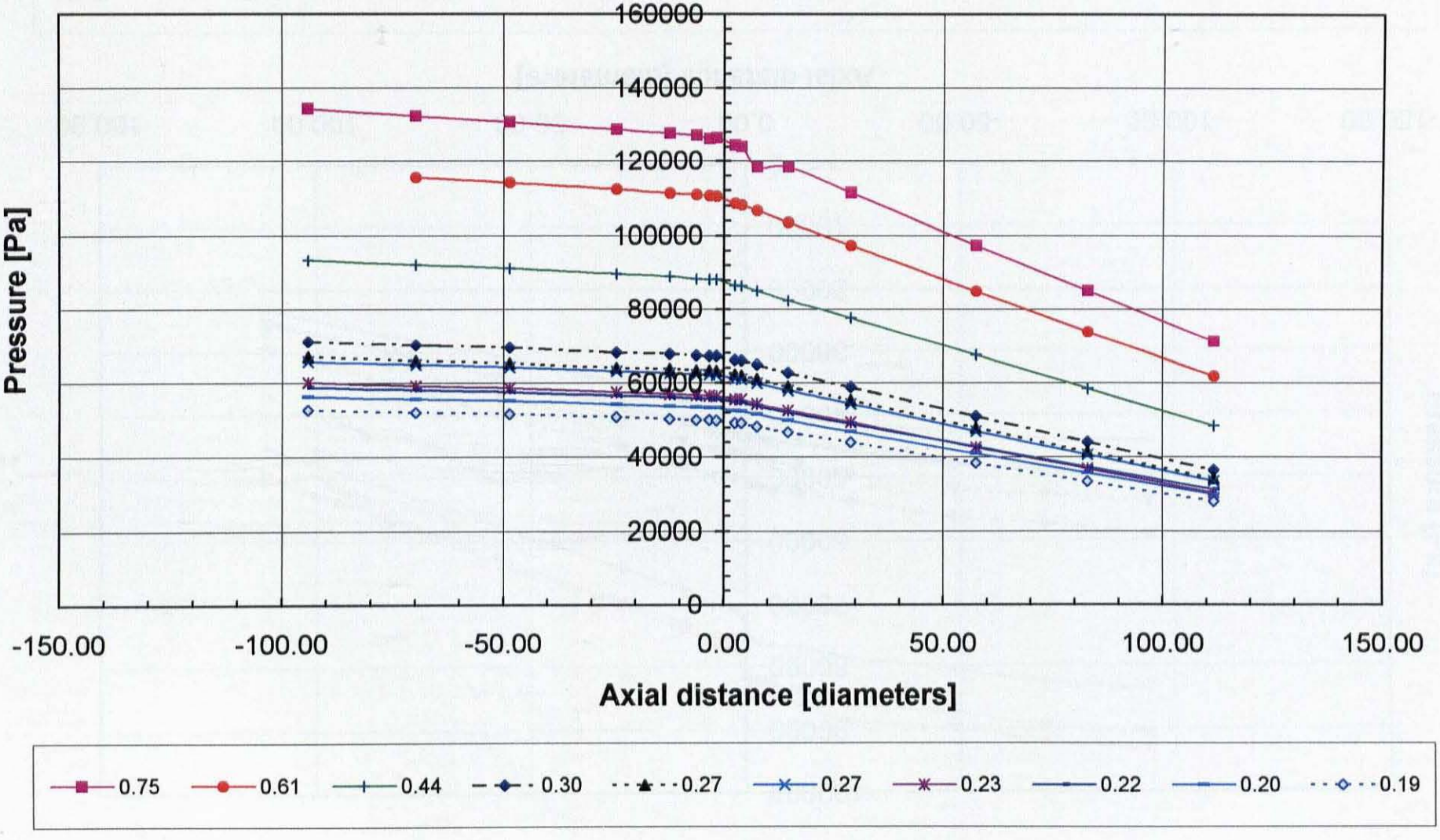

Pressure Grade Line for CMC 8 % at Various Velocities [Legend = Velocity in m/s]

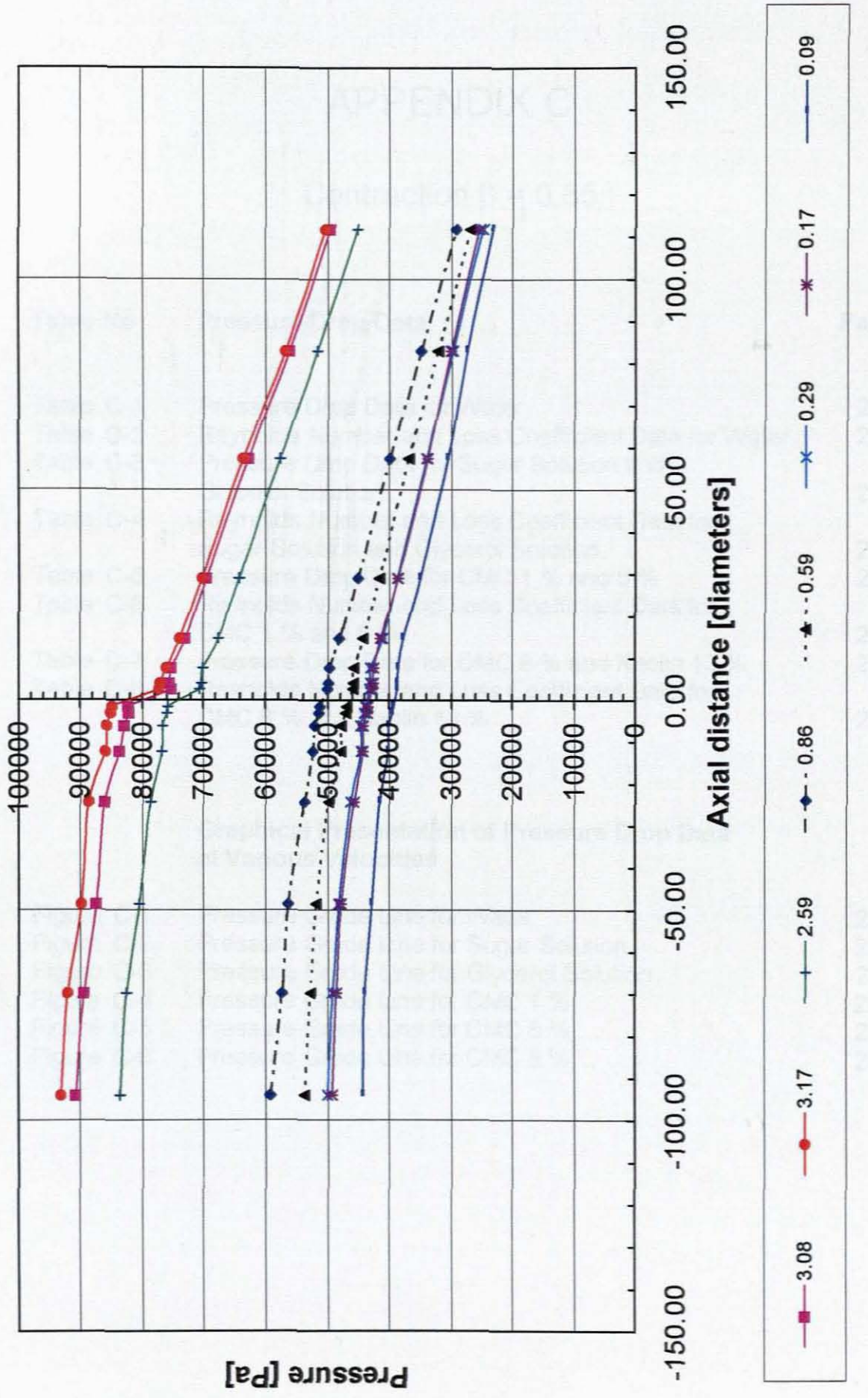

Pressure Grade Line for Kaolin 10 % at Various Velocities [Legend = Velocity in m/s]

APPENDIX C

Contraction β = 0.85

Contraction plane	397.71	cm																
Pod No.			5	6	7	8	9	10	11	12	13	14	15	16	17	18	19	20
Distance (diameters)			-94	-70	-49	-24	-12	-6	-3	-2	3	4	8	15	29	57	83	112
Distance (cm)			0	102	192	295	346	371	384	391	407	412	424	451	502	604	697	799
Pressure Drop		1	28466	28309	28004	27794	27620	27518	27501	27382	27083	26783	26695	26476	26186	25855	25156	24597
		2	47043	46880	46183	45898	45568	45506	45466	45277	44778	44515	44381	44159	43687	42886	42240	41458
Water		3	33295	33013	32634	32438	32215	32175	32073	31967	31639	31321	31256	31077	30672	30051	29495	28938
13/3/2002 Set 2		4	46794	46460	46068	45797	45557	45537	45386	45209	44877	44440	44379	44156	43704	43007	42383	41636
		5	53651	53260	52824	52490	52111	52162	51992	51791	51203	50642	50759	50473	49963	49046	48390	47500
		6	60260	59945	59215	58864	58492	58416	58354	58218	57708	57044	57044	56925	56354	55303	54455	53655
		7	61678	61148	60716	60117	59671	59701	59507	59274	58577	58032	57872	57549	56869	55790	54860	53997
		8	54941	54591	53988	53695	53355	53372	53231	52995	52277	51987	51900	51582	50913	50013	49256	48381
		9	48634	48360	47851	47593	47383	47230	47233	47077	46539	46160	46037	45795	45333	44420	43666	42904
		10	41394	41157	40799	40544	40207	40247	40202	40079	39574	39309	39252	39052	38572	37780	37200	36539
13/3/2002 Set 1		11	3417	3354	3257	3180	3133	3105	3091	3082	3162	3256	2886	2831	2720	2523	2366	2168
		12	8309	8197	8071	7961	7893	7868	7870	7848	7885	7834	7576	7491	7344	7088	6854	6607
		13	10399	10286	10150	10048	9968	9960	9904	9857	9883	9819	9563	9485	9315	9037	8789	8499
		14	12009	11871	11747	11630	11526	11484	11468	11433	11422	11324	11099	11012	10831	10524	10256	9957
		15	15724	15551	15383	15242	15133	15092	15088	15000	14968	14796	14631	14501	14305	13922	13613	13256
		16	20308	20090	19870	19732	19578	19557	19492	19402	19301	19105	18958	18861	18603	18169	17811	17368
		17	19130	18915	18651	18495	18367	18306	18261	18237	18028	17801	17712	17623	17380	16902	16492	16092
		18	16878	16698	16501	16340	16180	16161	16113	16028	17907	17670	17582	17436	17184	16736	16394	15919
		19	23785	23556	23354	23112	23002	22892	22888	22736	22568	22279	22187	22086	21753	21217	20809	20319
14/3/2002 Set 3		20	9702	9612	9462	9317	9241	9191	9174	9143	9037	8982	8805	8733	8547	8215	8000	7681
		21	13607	13481	13278	13175	13058	13037	12998	12978	12774	12684	12528	12458	12231	11886	11555	11249
		22	17831	17625	17418	17258	17115	17073	17053	16974	16799	16652	16551	16427	16193	15737	15414	14978
		23	18123	17941	17724	17547	17353	17315	17285	17224	16971	16821	16709	16581	16327	15881	15514	15079
		24	21693	21466	21226	21024	20874	20811	20749	20670	20369	20229	20092	19933	19640	19169	18758	18262
		25	26253	26006	25673	25446	25281	25255	25210	25070	24737	24525	24521	24264	23892	23352	22851	22323
		26	31160	30946	30636	30354	30190	30096	30037	29993	29402	29350	29255	29078	28701	28066	27530	26886
14/3/2002 Set 4		27	10103	10027	9894	9805	9721	9672	9676	9629	9400	9372	9308	9237	9059	8767	8500	8205
		28	10323	10209	10007	9942	9850	9803	9778	9735	9503	9432	9388	9347	9159	8834	8569	8253
		29	4740	4664	4547	4487	4406	4393	4374	4346	4170	4132	4092	4043	3914	3668	3460	3251
		30	6704	6559	6422	6293	6189	6194	6164	6129	5912	5773	5827	5775	5620	5360	5129	4868
		31	*3116*	*3019*	*2882*	*2822*	*2757*	*2726*	*2702*	*2678*	*2527*	*2382*	*2449*	*2396*	*2267*	*2065*	*1885*	*1677*
		32	3057	2966	2854	2763	2711	2704	2679	2664	2495	2372	2423	2380	2267	2038	1886	1661
		33	3021	2924	2809	2728	2691	2661	2635	2629	2447	2330	2354	2323	2214	1989	1813	1602
		34	3114	3015	2891	2848	2749	2720	2709	2674	2527	2386	2443	2413	2281	2068	1886	1644
		35	3043	2935	2846	2733	2704	2682	2660	2632	2450	2333	2369	2317	2191	1992	1815	1597
		36	2946	2839	2767	2655	2584	2590	2547	2519	2362	2264	2289	2225	2113	1902	1686	1503

			Q (m^3/s)	Temp °C	$Re_{downstream}$	$V_{downstream}$	$p_{con\ all\ data}$	$p_{con\ selected\ data}$	$k_{con\ all\ data}$	$k_{con\ selected\ data}$
		1	1.51E-03	27.05	53414.01	1.48	566	793	0.016	0.222
		2	1.70E-03	23.80	60292.50	1.66	722	930	0.016	0.164
Water		3	1.60E-03	27.47	56620.34	1.57	574	749	-0.035	0.107
13/3/2002 Set 2		4	1.70E-03	28.02	60308.52	1.66	709	924	0.006	0.159
		5	1.81E-03	28.30	64031.28	1.78	956	1190	0.106	0.253
		6	1.91E-03	28.67	67584.05	1.85	1176	1580	0.119	0.331
		7	1.99E-03	29.27	70246.30	1.88	848	973	-0.017	0.053
		8	1.91E-03	29.66	67503.82	1.88	1007	1256	0.074	0.215
		9	1.82E-03	29.93	64446.09	1.79	812	992	0.008	0.120
		10	1.71E-03	30.18	60549.37	1.66	666	884	-0.028	0.126
13/3/2002 Set 1		11	7.71E-04	25.79	27297.32	0.76	9	186	-0.467	0.149
		12	9.09E-04	25.85	32159.87	0.89	91	235	-0.271	0.089
		13	9.66E-04	25.91	34246.15	0.95	141	314	-0.186	0.195
		14	1.01E-03	25.98	35683.66	0.99	166	358	-0.161	0.229
		15	1.10E-03	26.06	42657.52	1.19	303	470	-0.066	0.171
		16	1.21E-03	26.16	42657.52	1.09	225	401	-0.116	0.183
		17	1.31E-03	26.38	46402.60	1.29	343	429	-0.086	0.018
		18	1.31E-03	26.58	46378.32	1.29	328	518	-0.103	0.126
		19	1.41E-03	26.71	50023.60	1.39	437	648	-0.048	0.173
14/3/2002 Set 3		20	1.02E-03	30.77	35944.62	1.00	198	318	-0.101	0.140
		21	1.11E-03	30.68	39362.55	1.09	292	392	-0.011	0.157
		22	1.21E-03	30.62	47387.52	1.32	381	551	-0.059	0.137
		23	1.34E-03	30.62	42887.60	1.19	302	415	-0.074	0.085
		24	1.41E-03	30.67	50013.01	1.39	455	619	-0.027	0.142
		25	1.50E-03	30.74	53220.03	1.48	499	635	-0.042	0.082
		26	1.60E-03	31.03	56652.32	1.57	593	701	-0.020	0.067
14/3/2002 Set 4		27	1.04E-03	33.32	36748.42	1.02	251	318	-0.016	0.111
		28	1.04E-03	33.18	36606.66	1.02	264	284	0.007	0.045
		29	8.96E-04	33.03	31711.91	0.88	192	213	-0.003	0.051
		30	9.05E-04	23.20	32028.28	0.89	249	245	0.130	0.120
		31	8.04E-04	23.32	28448.22	0.79	202	213	0.148	0.182
		32	8.03E-04	23.36	28427.42	0.79	195	177	0.125	0.068
		33	8.04E-04	23.41	28432.25	0.79	211	189	0.178	0.107
		34	8.09E-04	23.51	28618.70	0.80	195	213	0.120	0.174
		35	8.09E-04	23.57	28618.54	0.80	224	213	0.211	0.174
		36	8.09E-04	23.65	28635.21	0.80	200	227	0.132	0.219

Pod No.			5	6	7	8	9	10	11	12	13	14	15	16	17	18	19	20
Distance (diameters)			-94	-70	-49	-24	-12	-6	-3	-2	3	4	8	15	29	57	83	112
Distance (cm)			0	102	192	295	346	371	384	391	407	412	424	451	502	604	697	799
Pressure Drop		37	9554	9440	9324	9266	9018	8944	8985	8961	8901	8787	8587	8465	8295	7847	7500	7000
Sugar Solution		38	14994	14862	14670	14551	14373	14236	14269	14289	14126	13945	13791	13664	13440	12954	12501	11953
19/3/2002 Set 1		39	21822	21649	21385	21207	20960	20871	20917	20883	20648	20463	20359	20165	19906	19293	18751	18179
Density [kg/m^3]	1200	40	28544	28259	27952	27719	27448	27351	27461	27381	27023	26773	26710	26516	26131	25404	24768	24347
Viscosity [Pa.s]	0.01	41	35480	35136	34785	34470	34183	34077	34056	33988	33666	33319	33259	33040	32601	31800	31084	30231
		42	43224	42793	42284	41870	41556	41413	41415	41311	40793	40431	40410	40106	39667	38708	37855	36958
		43	50958	50195	49635	49107	48686	48696	48649	48584	47991	47573	47517	47194	46691	45707	44869	43470
		44	49284	48772	48296	47908	47676	47479	47493	47435	46826	46498	46507	46140	45617	44605	43578	42524
		45	56946	56222	57578	57110	56788	56590	56526	56458	55879	55403	55154	55069	54372	53196	52185	50850
		46	50259	49809	49278	48963	48645	48428	48501	48218	47842	47280	47308	46972	46345	45315	44436	43385
19/3/2002 Set 2	1130	47	60320	60128	59503	58969	58477	58432	58330	58097	57458	57168	57007	56550	55932	54877	53946	52700
	0.013	48	56179	55577	55078	54793	54347	54265	54254	54104	53487	53165	53025	52784	52216	51140	50199	49111
		49	51918	51561	51025	50876	50420	50305	50415	50145	49768	49467	49085	48920	48517	47565	46550	45534
		50	47860	47615	47140	46886	46628	46562	46599	46345	46155	45869	45374	45235	44715	43924	43117	42181
		51	44480	44225	43881	43555	43399	43302	43299	43144	42534	42443	42141	42032	41597	40754	39960	39116
		52	37669	37445	37103	36883	36556	36556	36530	36387	36057	35815	35719	35607	35160	34327	33691	32949
		53	31406	31219	30902	30670	30362	30267	30396	30234	29920	29776	29585	29427	29050	28464	27831	27237
		54	25139	25106	24763	24666	24423	24329	24477	24329	24039	23926	23775	23553	23299	22756	22203	21633
		55	18968	18765	18511	18425	18166	18143	18246	18099	17805	17774	17560	17378	17116	16684	16118	15640
Glycerol Solution 98%		56	69899	68831	67906	66925	66322						65244	64813	63769	61735	59938	57924
12/7/2002 Set 1		57	69805	68803	67798	66825	66274						65206	64702	63713	61702	59936	57927
Density [kg/m^3]	1246.00	58	48123	47471	46900	46338	45977						45263	44954	44367	43153	42056	40820
Viscosity [Pa.s]	1.000	59	46867	46169	47573	46973	46594	46340					45734	45390	44743	43451	42337	41042
		60	30103	29712	29382	29087	28854						28425	28239	27897	27190	26560	25862
		61	30318	29935	29662	29417	29207						28843	28672	28331	27624	26987	26279
11/7/2002 Set 1		62	80744	79435	78313	77115	76462	76115	75899	75748	75615	75460	74916	74331	73153	70838	68701	66331
Density [kg/m^3]	1235	63	78184	76970	75876	74527	74120	73834					72781	72280	71118	68875	66883	64558
Viscosity [Pa.s]	1.050	64	54883	54109	53433	52666	52263	52045	51995	51909			51416	51117	50401	48927	47643	46171
16/7/2002 Set 1	0.800	65	83357	82000	80815	79742	79115	78590					77620	76817	75703	73479	71251	68843
Viscosity [Pa.s]	0.900	66	82264	81037	79861	78721	78065	77665					76468	76017	74801	72563	70401	68122
	0.800	67	66400	65487	64555	63750	63228	62879					62205	61772	60847	59039	57486	55595
	0.800	68	66504	65636	64721	63841	63352	63010					62327	61894	60924	58971	57410	55589
	1.236	69	57004	56354	55537	54669	54414	54127					53497	53107	52345	50940	49676	48191

			Q (m^3/s)	Temp °C	$Re_{downstream}$	$V_{downstream}$	$P_{frict\ all\ data}$	$P_{frict\ selected\ data}$	$k_{con\ all\ data}$	$k_{con\ selected\ data}$
		37	8.06E-04	23.94	3423.95	0.79	167	432	0.033	0.877
Sugar Solution		38	9.08E-04	24.00	3854.06	0.89	252	434	0.133	0.592
19/3/2002 Set 1		39	1.01E-03	24.16	4282.33	0.99	308	493	0.127	0.505
Density [kg/m^3]	1200	40	1.11E-03	24.31	4717.92	1.09	450	621	0.255	0.543
Viscosity [Pa.s]	0.01	41	1.21E-03	24.52	5134.07	1.19	477	650	0.176	0.421
		42	1.31E-03	24.80	5565.32	1.29	644	768	0.277	0.427
		43	*1.40E-03*	*25.13*	*5965.69*	*1.38*	*679*	*593*	*0.213*	*0.123*
		44	1.39E-03	25.78	5916.29	1.37	639	679	0.183	0.225
		45	1.51E-03	26.06	6400.08	1.48	751	721	0.185	0.158
		46	1.61E-03	27.09	4973.79	1.58	799	994	0.142	0.299
19/3/2002 Set 2	1130	47	1.71E-03	27.67	5297.90	1.68	928	1424	0.157	0.507
	0.013	48	1.66E-03	28.05	5134.54	1.63	752	891	0.067	0.171
		49	1.61E-03	28.91	4989.47	1.58	663	901	0.029	0.220
		50	1.56E-03	29.11	4824.18	1.53	629	837	0.036	0.215
		51	1.51E-03	29.25	4680.64	1.49	704	764	0.139	0.193
		52	1.41E-03	29.36	4377.87	1.39	466	624	-0.014	0.147
		53	1.32E-03	29.45	4076.45	1.29	436	669	0.021	0.300
		54	1.21E-03	29.51	3760.43	1.19	389	602	0.047	0.345
		55	1.12E-03	29.51	3460.91	1.10	366	530	0.108	0.379
Glycerol Solution 98%		56	1.00E-04	22.16	5.53	0.10	12	61	1.547	11.656
12/7/2002 Set 1		57	1.00E-04	22.37	5.53	0.10	19	31	2.938	5.334
Density [kg/m^3]	1246.00	58	5.20E-05	22.30	2.49	0.05	60	76	60.151	57.059
Viscosity [Pa.s]	1.000	59	5.20E-05	22.34	2.29	0.05	173	255	131.546	193.990
		60	2.61E-05	22.23	1.24	0.03	*80*	*99*	*206.464*	*258.260*
		61	2.61E-05	22.24	1.24	0.03	24	31	62.052	79.266
11/7/2002 Set 1		62	9.45E-05	21.93	3.93	0.09	88	270	19.337	61.658
Density [kg/m^3]	1235	63	9.32E-05	22.05	3.86	0.09	51	-144	11.259	-35.208
Viscosity [Pa.s]	1.050	64	6.07E-05	21.84	2.52	0.06	30	22	16.196	11.613
16/7/2002 Set 1	0.800	65	9.86E-05	20.55	4.47	0.10	216	223	44.845	46.269
Viscosity [Pa.s]	0.900	66	1.02E-04	21.01	5.05	0.10	254	276	49.578	53.990
	0.800	67	8.71E-05	22.41	4.84	0.09	19	86	4.125	22.444
	0.800	68	9.08E-05	22.82	5.13	0.09	26	150	-	36.576
	1.236	69	4.64E-05	17.89	1.70	0.05	155	300	148.062	287.425

Pod No.			5	6	7	8	9	10	11	12	13	14	15	16	17	18	19	20
Distance (diameters)			-94	-70	-49	-24	-12	-6	-3	-2	3	4	8	15	29	57	83	112
Distance (cm)			0	102	192	295	346	371	384	391	407	412	424	451	502	604	697	799
Pressure Drop		70	33266	32945	32567	32276	32093	31926	31909	31845	31231	31232	31146	30923	30505	29686	29061	28236
CMC 1 %		71	24826	24612	24243	23988	23827	23760	23742	23633	23212	23183	23103	22950	22552	21939	21421	20761
26/4/2002 Set 1		72	19670	19465	19209	18948	18786	18740	18698	18622	18218	18265	18118	17993	17692	17135	16672	16145
Density [kg/m^3]	1007	73	26446	26184	25921	25680	25505	25454	25397	25346	24985	25006	24827	24719	24416	23795	23302	
Viscosity [Pa.s]	0.005	74	21486	21229	21051	20807	20679	20630	20598	20546	20218	20260	20141	20046	19752	19222	18785	18328
Ty		75	17053	16856	16619	16425	16290	16211	16198	16179	16197	15906	15748	15631	15380	14925	14491	14001
K		76	17054	16873	16635	16427	16312	16236	16241	16203	15871	15972	15771	15669	15395	14924	14501	13976
n		77	11514	11382	11214	11061	10882	10896	10843	10830	10601	10669	10517	10451	10237	9857	9567	9170
		78	7587	7465	7321	7180	7118	7052	7055	7008	6808	6887	6756	6683	6528	6184	5928	5610
		79	3575	3461	3344	3243	3189	3151	3122	3098	2957	3059	2921	2858	2711	2493	2275	2026
26/4/2002 Set 2		80	3735	3648	3541	3450	3370	3353	3340	3319	3182	3228	3134	3081	2911	2686	2482	2233
		81	3745	3685	3583	3471	3385	3374	3354	3313	3204	3230	3143	3054	2954	2700	2481	2237
		82	7459	7349	7268	7103	7033	6986	6979	6917	6751	6771	6700	6618	6450	6137	5889	5542
		83	11775	11610	11477	11314	11210	11157	11150	11082	10849	10868	10797	10681	10488	10108	9799	9399
		84	12190	12039	11920	11772	11657	11634	11609	11563	11335	11335	11264	11173	11000	10636	10394	10005
		85	15953	15782	15597	15419	15302	15255	15241	15202	14944	14923	14871	14769	14539	14152	13795	13403
		86	21661	21435	21185	20994	20880	20827	20794	20719	20384	20367	20272	20138	19877	19393	18939	18422
		87	27440	27172	26871	26645	26465	26379	26360	26291	25843	25876	25769	25623	25259	24663	24198	23586
CMC 5 %		88	45842	44969	44261	43443	43139	42849	42759	42669	42390	42787	42039	41673	40981	39840	38459	37077
6/5/2002 Set 1		89	39393	38583	37971	37223	36850	36612	36493	36420	36017	36573	35764	35417	34726	33547	32453	31341
Density [kg/m^3]	1027	90	39078	38456	37877	37237	36891	36724	36683	36946	35735	35422	35387	35111	34602	33428	32422	31229
Viscosity [Pa.s]		91	31990	31407	30884	30294	30111	30020	29951	29785	29564	29453	29295	28905	28450	27543	26546	25472
Ty	0	92	26888	26562	26069	25512	25331	25183	25117	24928	24808	24708	24620	24370	23849	22942	22066	21203
K	0.26698	93	28503	28070	27403	26988	26764	26558	26507	26387	26242	26076	26020	25767	25244	24289	23471	22525
n	0.684	94	21795	21346	20857	20494	20299	20132	20061	19986	19873	19750	19613	19419	19058	18272	17528	16737
		95	51695	50922	50095	49357	48976	48660	48558	48443	47889	47738	47915	47522	46825	45358	44207	42574
		96	57036	56201	55297	54525	54101	53901	53827	53677	53373	53122	52843	52435	51711	50308	48974	47401
		97	67853	66887	65990	65169	64817	64544	64359	64237	63794	63504	63011	62595	61881	60188	58818	57404
10/5/2002 Set 1		98	62374	61509	60597	59816	59368	59110	59053	59059	58502	58442	58089	57641	56889	55332	53982	52592
		99	62430	61484	60711	60037	59383	59171	59064	58873	58394	58342	57954	57562	56749	55326	53911	52527
		100	55993	55155	54394	53704	53243	53087	52948	52859	52400	52326	52035	51715	50979	49573	48448	47222
		101	50191	49364	48606	47788	47343	47110	47007	46843	46449	46410	46087	45667	44981	43650	42564	41189
		102	43486	42790	42205	41523	41158	41017	41015	40949	40824	40597	40320	40003	39381	38175	37100	35928
		103	43802	43082	42509	41831	41454	41223	41165	41071	40749	40654	40336	40105	39504	38231	37214	36041
		104	37457	36737	36295	35605	35273	35167	35095	35158	34854	34840	34557	34146	33569	32497	31524	30392
		105	37230	36555	35998	35320	34989	34786	34740	34690	34439	34334	34119	33771	33216	32246	31254	30222
		106	31578	30969	30479	29959	29664	29484	29419	29352	29185	29100	28904	28620	28167	27198	26358	25409

			Q (m^3/s)	Temp °C	$Re_{downstream}$	$V_{downstream}$	$p_{fit\ all\ data}$	$p_{fit\ selected\ data}$	$k_{con\ all\ data}$	$k_{con\ selected\ data}$
		70	0.0015	21.65	10022.42	1.44	537	599	0.020	0.081
CMC 1 %		71	0.0013	21.94	8955.24	1.29	413	446	0.002-	0.041
26/4/2002 Set 1		72	0.0012	22.14	8473.70	1.18	372	452	0.032	0.146
Density [kg/m^3]	1007	73	0.0012	22.30	8263.70	1.19	329	383	-0.030	0.046
Viscosity [Pa.s]	0.005	74	0.0011	22.43	7584.02	1.09	274	302	-0.036	0.011
Ty		75	0.0010	22.67	7089.64	1.02	181	320	-0.149	0.120
K		76	0.0010	22.73	7092.12	1.02	254	291	-0.008	0.064
n		77	0.0009	22.83	6219.88	0.89	179	276	-0.049	0.195
		78	0.0008	23.12	5540.70	0.80	163	197	0.017	0.125
		79	0.0007	23.19	5018.25	0.69	-959	162	0.946	0.200
26/4/2002 Set 2		80	0.0007	23.26	4861.01	0.70	113	164	-0.034	0.174
		81	0.0007	23.27	4862.06	0.70	117	195	-0.017	0.303
		82	0.0008	23.29	5519.23	0.79	166	226	0.032	0.221
		83	0.0009	23.33	6239.59	0.90	223	264	0.058	0.211
		84	1.01E-03	23.42	6910.60	0.99	225	265	-0.042	0.081
		85	1.11E-03	23.59	7612.91	1.09	235	271	-0.105	-0.045
		86	1.11E-03	23.75	7608.68	1.09	329	335	0.053	0.064
		87	1.23E-03	23.82	8395.30	1.20	394	458	0.044	0.132
CMC 5 %		88	8.11E-04	19.54	507.84	0.80	96	249	-0.570	-0.089
8/5/2002 Set 1		89	7.10E-04	19.54	426.59	0.70	192	486	-0.085	1.120
Density [kg/m^3]	1027	90	7.29E-04	20.37	441.20	0.72	704	863	1.872	2.488
Viscosity [Pa.s]		91	6.04E-04	20.44	344.67	0.59	245	223	0.514	0.390
Ty	0	92	5.16E-04	20.45	279.94	0.51	173	255	0.470	1.113
K	0.26898	93	5.35E-04	20.46	293.96	0.53	159	161	0.274	0.289
n	0.684	94	4.35E-04	20.46	223.76	0.43	136	146	0.614	0.742
		95	9.21E-04	20.57	600.17	0.91	374	221	0.041	-0.333
		96	1.01E-03	20.77	681.89	1.00	339	378	-0.191	-0.113
		97	1.30E-03	23.18	940.46	1.27	646	808	-0.075	0.124
10/5/2002 Set 1		98	1.23E-03	23.33	877.38	1.21	395	521	-0.331	-0.159
		99	1.23E-03	23.51	879.54	1.21	515	686	-0.169	0.337
		100	1.12E-03	23.66	773.09	1.10	411	618	-0.190	0.154
		101	*1.02E-03*	*23.90*	*687.50*	*1.00*	*408*	*647*	*-0.065*	*0.412*
		102	9.17E-04	23.97	597.53	0.90	190	260	-0.405	-0.234
		103	9.19E-04	24.02	598.92	0.90	313	465	-0.107	0.266
		104	8.13E-04	24.03	509.82	0.80	155	290	-0.388	0.035
		105	8.13E-04	23.99	510.02	0.80	222	368	-0.179	0.277
		106	7.11E-04	23.90	426.88	0.70	156	252	-0.232	0.159

CMC 1 % and 5 %

Pod No.			5	6	7	8	9	10	11	12	13	14	15	16	17	18	19	20
Distance (diameters)			-94	-70	-49	-24	-12	-6	-3	-2	3	4	8	15	29	57	83	112
Distance (cm)			0	102	192	295	346	371	384	391	407	412	424	451	502	604	697	799
Pressure Drop		107	103393	101612	99999	97167	95603	96311	95123	94886	94795	94577	93344	91342	90272	87169	85298	80148
CMC 8 %		108	89942	87794	86214	84271	83091	82629	82516	82376	81712	81692	81389	80598	78979	75864	73123	70492
3/9/2002 Set 1		109	79292	77590	76152	74391	73501	73172	72981	72887	72355	72147	71786	71163	69754	66989	64576	61836
Density [kg/m^3]	1040.00	110	78985	77351	75803	74088	73290	72812	72555	72326	71986	71850	71448	70851	69399	66764	64306	61566
Viscosity [Pa.s]		111	70720	69052	67536	66398	65892	65477	65151	65042	64619	64470	64194	63520	62327	59977	57805	55432
Ty	0.00	112	70453	68931	67681	66159	65403	65058	64810	64742	64346	64220	63860	63318	62107	59745	57518	55145
K	1.454	113	59281	58180	57137	55887	55298	55011	54811	54787	54484	54387	54125	53702	52843	50679	48889	46904
n	0.584	114	60012	58830	57804	56578	55960	55659	55506	55454	55126	55014	54788	54300	53270	51299	49540	47566
Kaolin 13 %		115	130538	128697	128067	120475	117239	116434	115355	115322	113274	113048	111592	108219	102659	90445	80690	70922
4/10/2002 Set 1		116	134226			120981	116964	115898					111373	108092	102271	90503	80716	70469
Density [kg/m^3]	1195.00	117	128802			116348	114075	113019					108542	105383	99877	88763	78967	68052
Viscosity [Pa.s]		118	128181			116077	113648	112421					109034	105227	99662	87736	78558	67718
Ty	16.50	119	126823	120910	120910	112371	109618	108445	107901	107498	105648	105904	104882	101267	95815	84499	75509	64758
K	13.160	120	119247			109820	107380	106369					102883	99625	93811	82770	73587	63041
n	0.164	121	114818			103343	101029	99488					97078	93583	88744	78008	69520	59748
		122	110905	108531		100815	98770	97723					93399	91638	86881	76268	68101	58247
		123	109442			101979	99647	98355					94463	91883	86346	75872	67649	58141

			Q (m^3/s)	Temp °C	$Re_{downstream}$	$V_{downstream}$	$P_{fitt\ all\ data}$	$P_{fitt\ selected\ data}$	$K_{con\ all\ data}$	$K_{con\ selected\ data}$
		107	8.19E-04	19.88	162.82	0.81	623	1913	1.079	5.053
CMC 8 %		108	7.04E-04	20.07	131.45	0.69	128	284	-0.307	0.262
3/9/2002 Set 1		109	6.05E-04	20.17	105.92	0.59	181	166	0.186	0.101
Density [kg/m^3]	1040.00	110	6.04E-04	20.25	105.80	0.59	125	182	-0.133	0.193
Viscosity [Pa.s]		111	5.11E-04	20.28	83.48	0.50	193	-39	0.686	-1.147
Ty	0.00	112	5.12E-04	20.30	83.62	0.50	102	118	-0.034	0.095
K	*1.454*	113	*4.08E-04*	*20.25*	*60.63*	*0.40*	*20*	*42*	*-0.596*	*-0.321*
n	0.584	114	4.09E-04	20.25	60.83	0.40	83	103	-0.063	0.436
Kaolin 13 %		115	2.39E-04	25.84	86.07	0.69	1423	5849	4.790	23.253
4/10/2002 Set 1		116	2.43E-04	25.97	88.78	0.70	1136	3339	3.442	12.333
Density [kg/m^3]	*1195.00*	117	*1.92E-04*	*26.12*	*53.51*	*0.56*	*777*	*1108*	*3.874*	*8.000*
Viscosity [Pa.s]		118	1.96E-04	26.79	55.70	0.57	288	1441	0.635	7.754
Ty	16.50	119	1.59E-04	27.02	37.66	0.46	379	2628	2.425	23.570
K	13.160	120	1.37E-04	27.20	27.85	0.40	588	2147	6.293	25.990
n	0.164	121	1.10E-04	27.30	19.80	0.32	-254	795	-6.156	14.597
		122	9.36E-05	27.39	14.51	0.27	656	1046	16.658	27.235
		123	9.45E-05	27.57	15.35	0.27	1519	3613	39.315	95.040

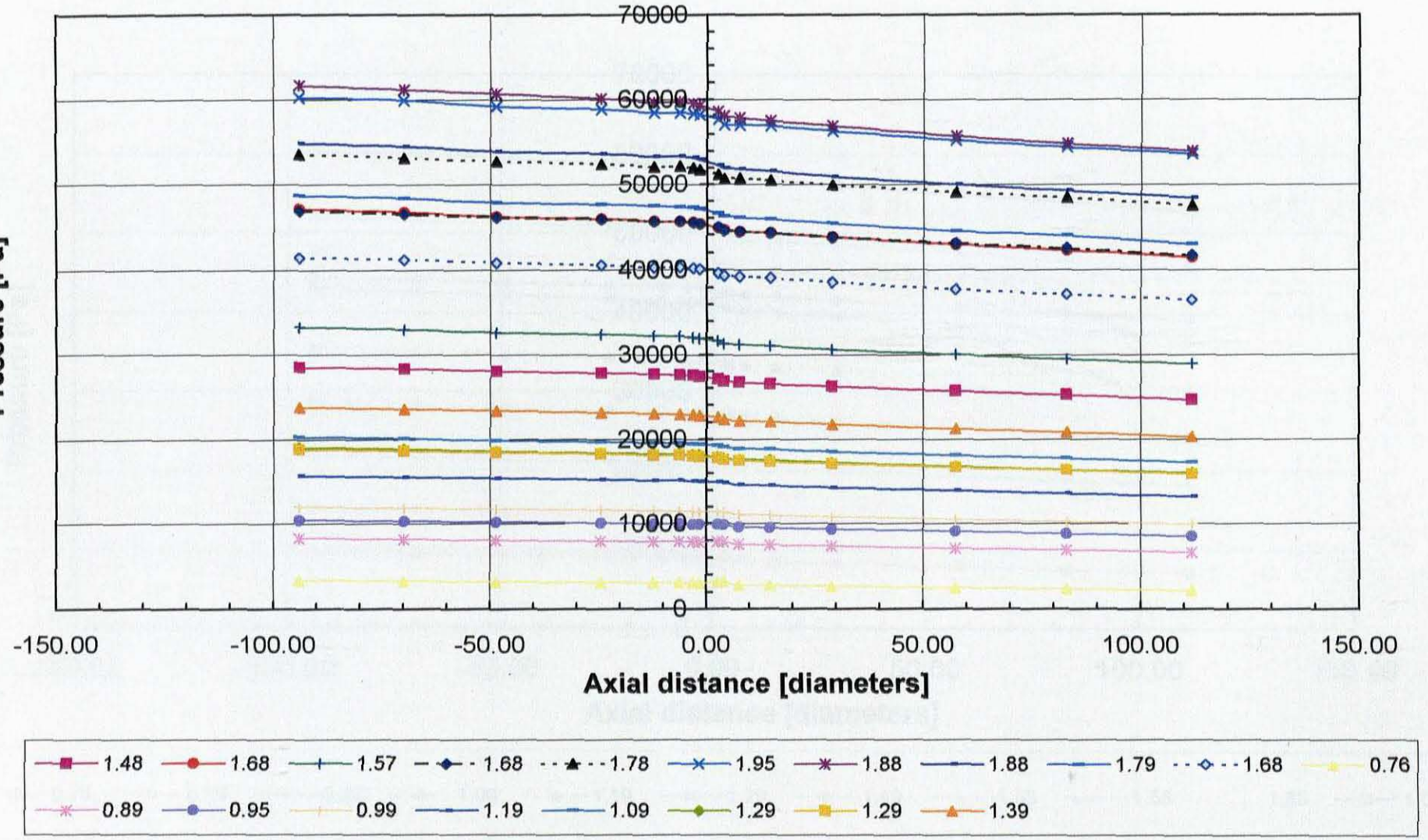

Contraction $\beta = 0.85$

Pressure Grade Line for Water [Legend = Velocity in m/s]

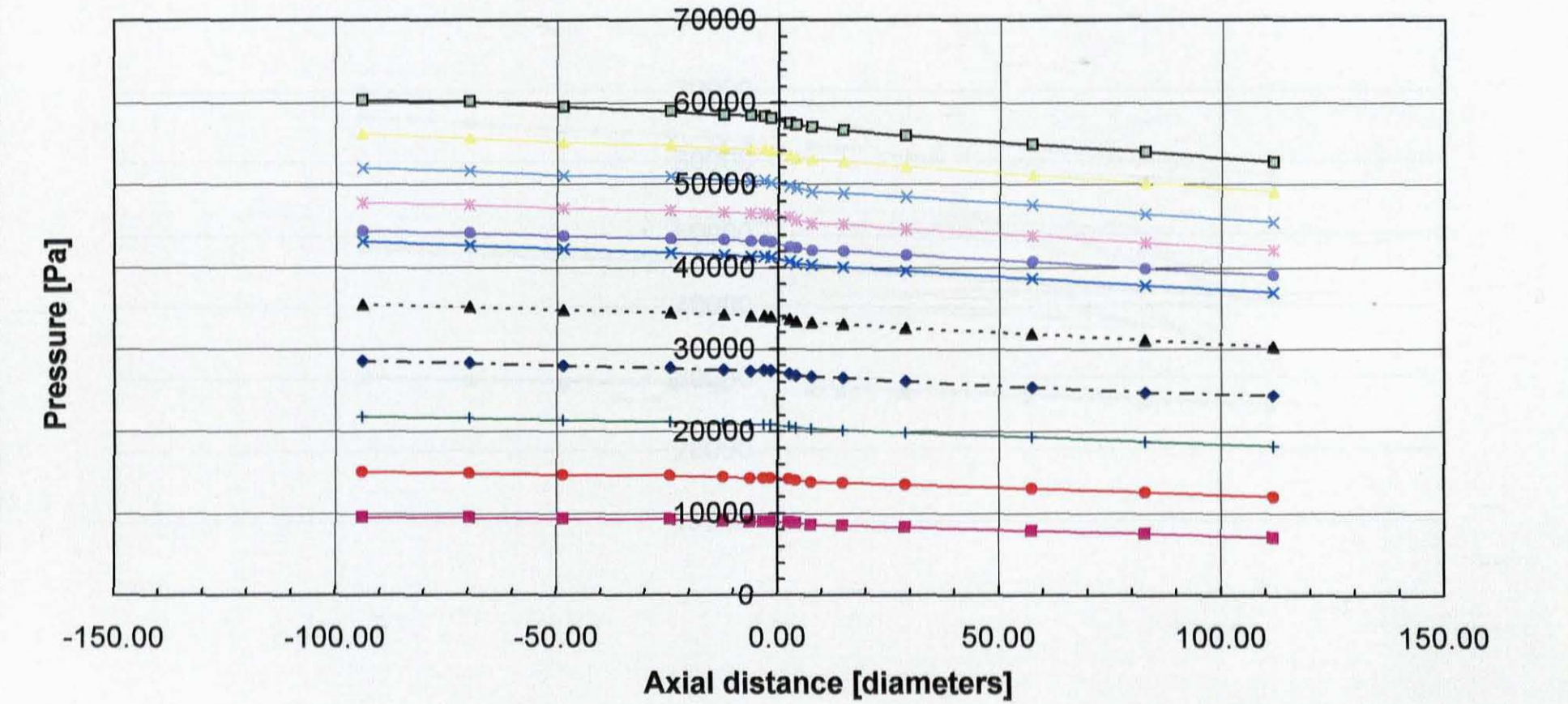

Contraction β = 0.85

Pressure Grade Line for Sugar Solution [Legend = Velocity m/s]

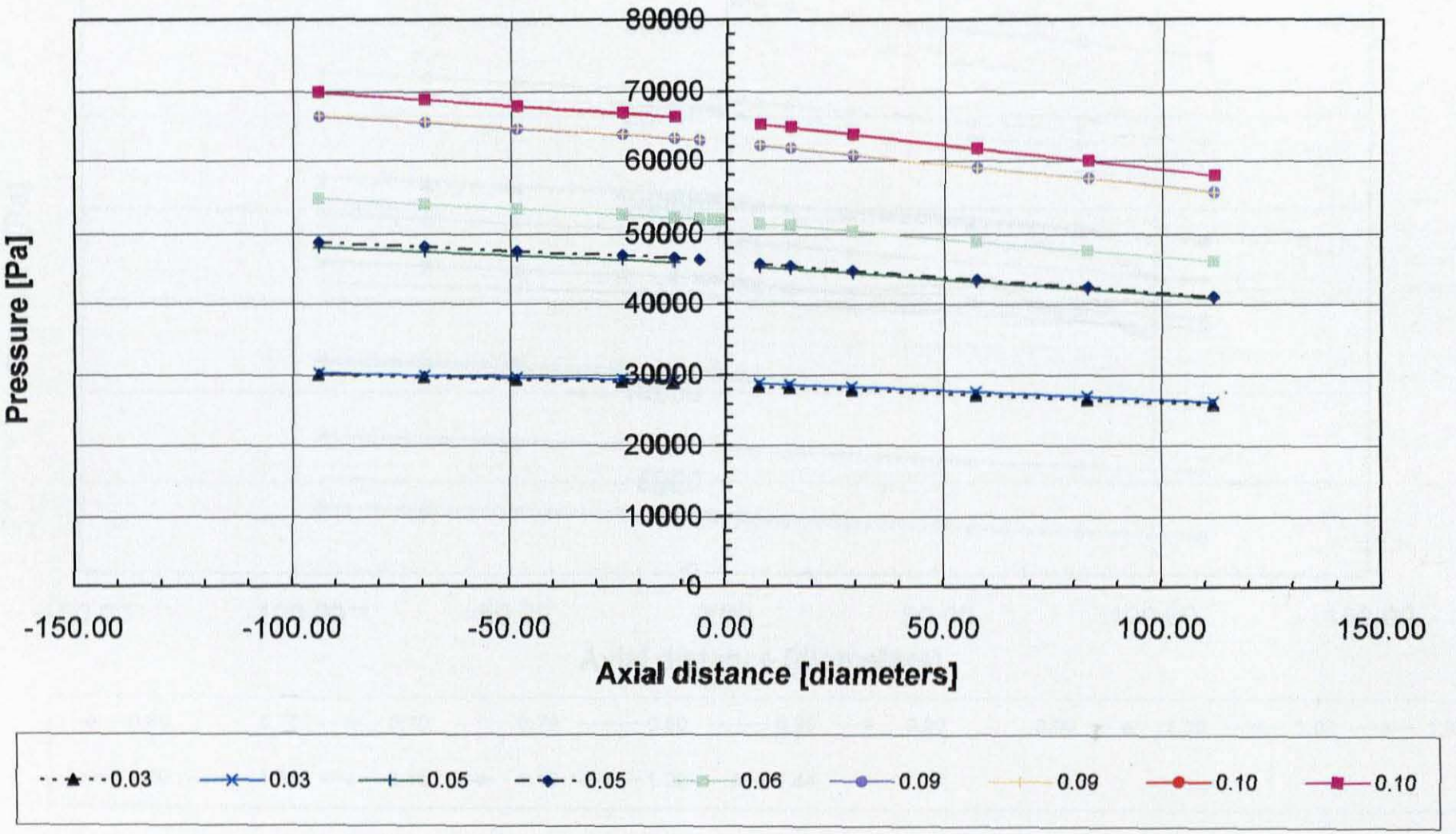

Pressure Grade Line for Glycerol Solution [Legend = Velocity in m/s]

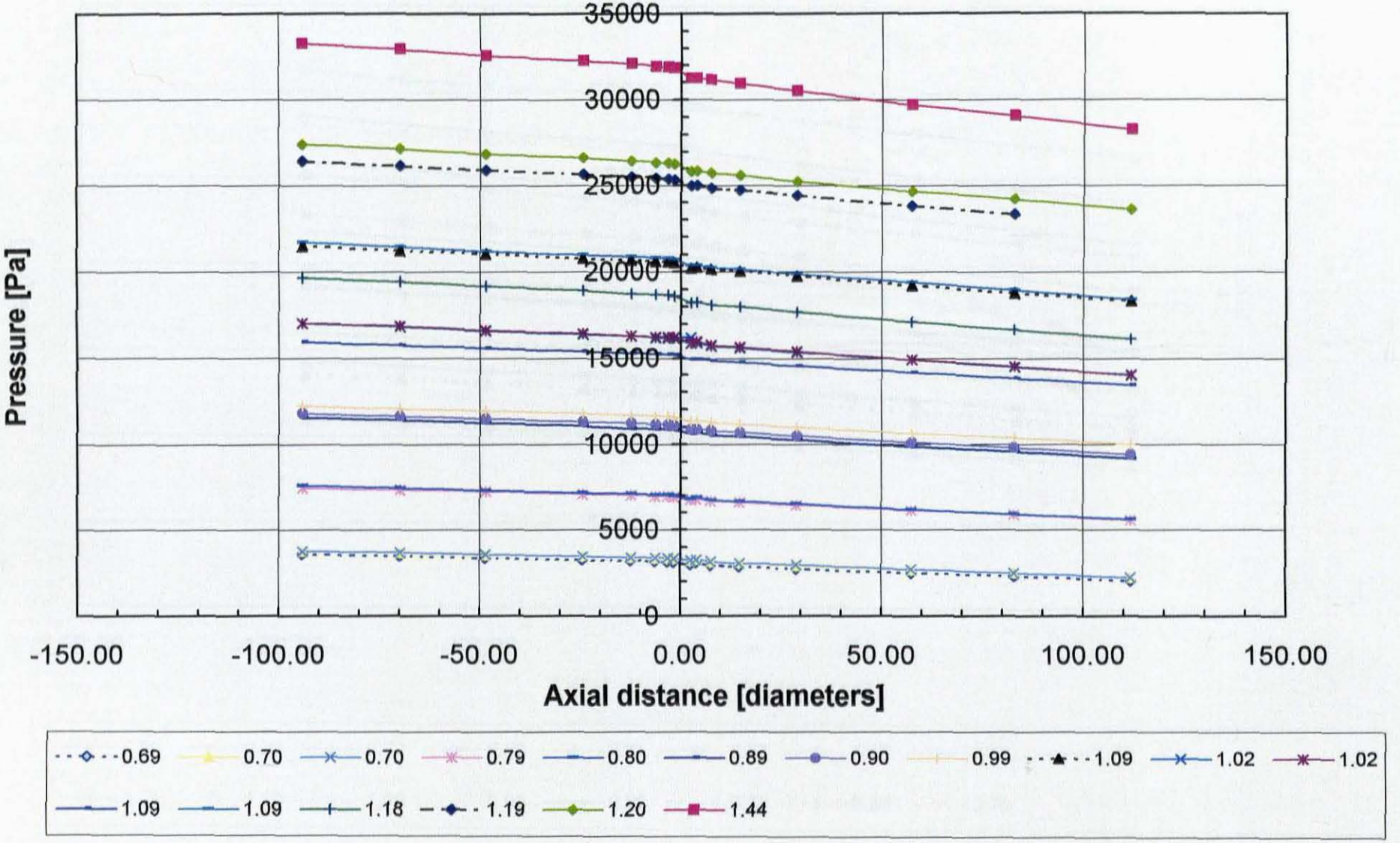

Pressure Grade Line for CMC 1 % at Various Velocities [Legend = Velocity in m/s]

Contraction β = 0.85

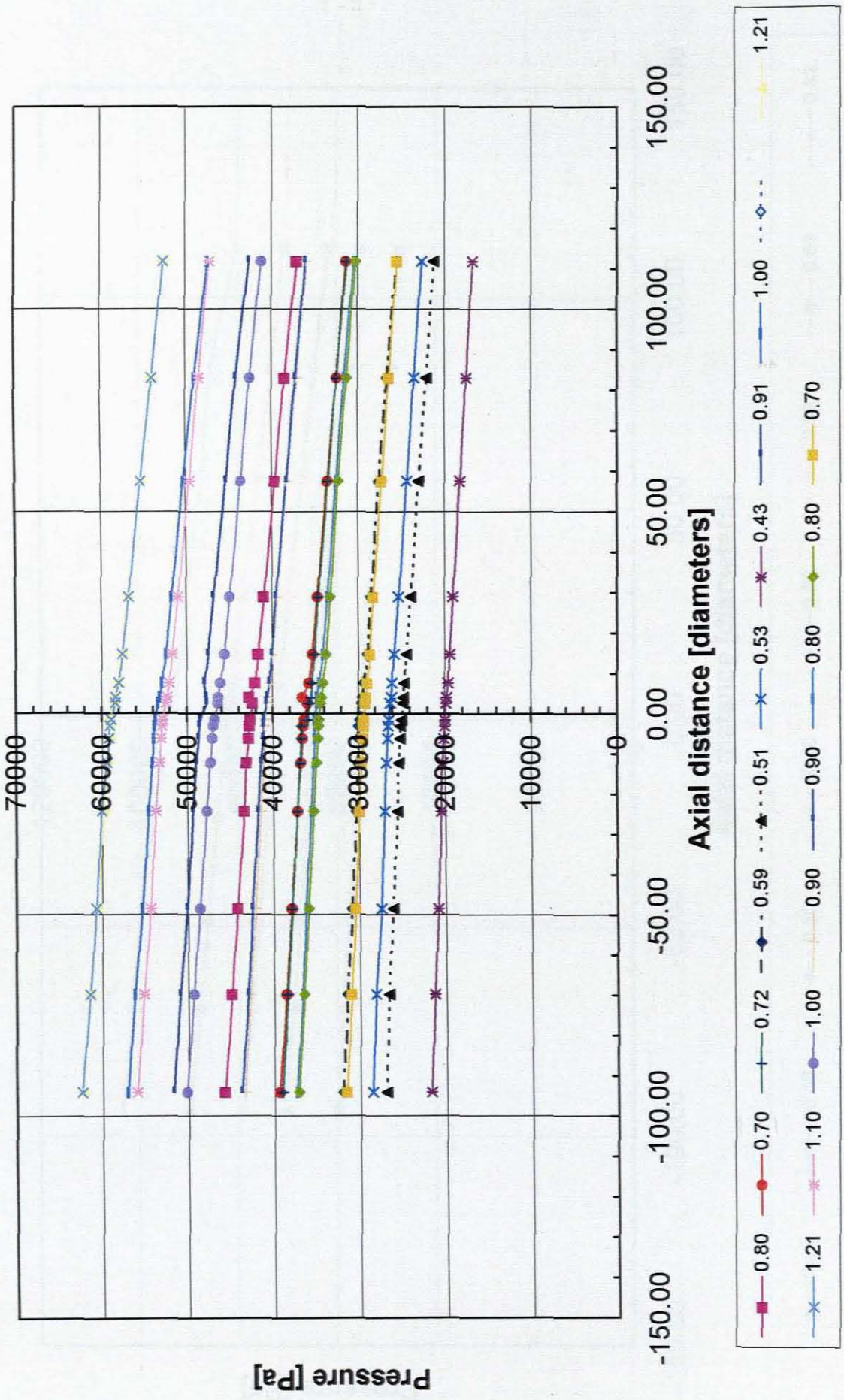

Pressure Grade Line for CMC 5 % at Various Velocities [Legend = Velocity in m/s]

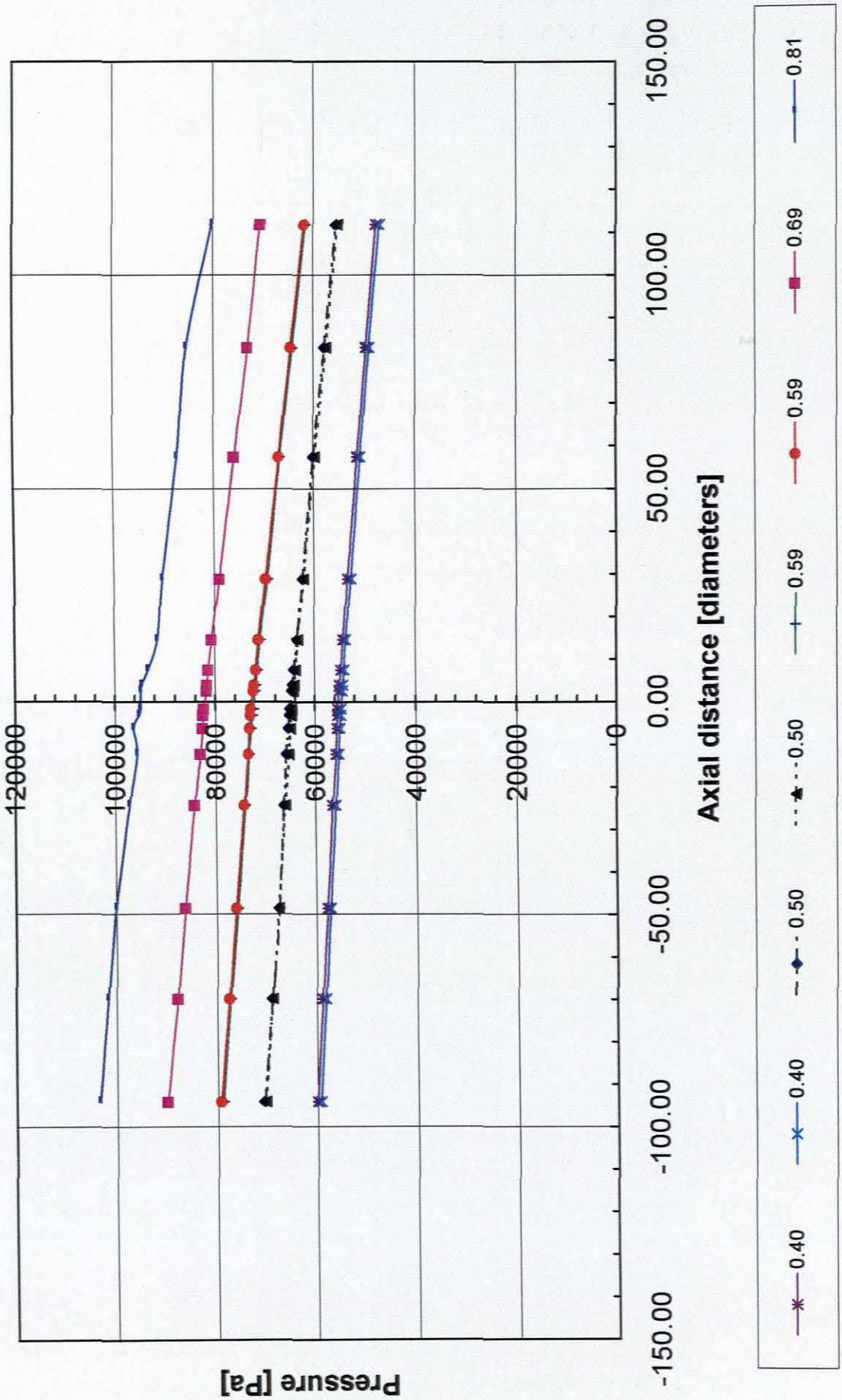

Pressure Grade Line for CMC 8 % at Various Velocities [Legend = Velocity in m/s]